



UNIVERSIDAD AUTÓNOMA CHAPINGO

POSTGRADO EN
INGENIERIA AGRÍCOLA Y USO INTEGRAL DEL AGUA

**“DESIGN OF AUTOMATIC FOOD DOSING AND
OXYGENATION FOR A CARP RECIRCULATING
AQUACULTURE SYSTEM (RAS)”**

TESIS

**QUE COMO REQUISITO PARCIAL
PARA OBTENER EL GRADO DE:**

**DOCTOR EN INGENIERÍA AGRÍCOLA
Y USO INTEGRAL DEL AGUA**

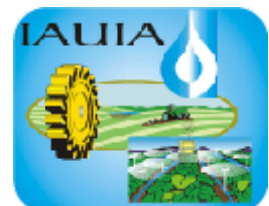
PRESENTA:

M.SC. WAEL MOHAMED ALY EL-MESSERY

Chapingo, México; Noviembre de 2011



DIRECCION GENERAL ACADÉMICA/
DEPTO. DE SERVICIOS ESCOLARES
Y DE EXÁMENES PROFESIONALES



**DESIGN OF AUTOMATIC FOOD DOSING AND OXYGENATION FOR
A CARP RECIRCULATING AQUACULTURE SYSTEM (RAS)**

Tesis realizada por el **Wael Mohamed Aly El-Messery**, bajo la dirección del Comité Asesor indicado, aprobada por el mismo y aceptada como requisito parcial para obtener el grado de:

DOCTOR EN INGENIERÍA AGRÍCOLA Y USO INTEGRAL DEL AGUA

DIRECTOR:

DR. FEDERICO FÉLIX HAHN SCHLAM

ASESOR:

DR. IRINEO LORENZO LÓPEZ CRUZ



ASESOR:

DRA. GUADALUPE HERNÁNDEZ EUGENIO

DIRECCION GENERAL ACADÉMICA/
DEPTO. DE SERVICIOS ESCOLARES
OFICINA DE EXAMENES PROFESIONALES

ASESOR:

DR. GERARDO FIGUEROA LUCERO

Agradecimientos

Mi más profundo agradecimiento a la Universidad Autónoma Chapingo y al postgrado en Ingeniería Agrícola y Uso integral del Agua por darme la oportunidad de realizar los estudios de Doctorado en Ingeniería Agrícola y Uso Integral del Agua.

Doy gracias a la Dirección de Intercambio Académico, Unidad de Relaciones Económicas y Cooperación Internacional, Secretaria de Relaciones Exteriores, por el apoyo económico y felicitar los servicios de seguridad de salud, las renovaciones de beca y visa etc., durante los tres años y por la paciencia en los trámites administrativos y su agradable atención.

Doy gracias al Consejo Nacional de Ciencia y Tecnología (CONACyT), al Departamento de Ingeniería Mecánica Agrícola y al Departamento de Irrigación por el apoyo brindado durante los estudios de postgrado.

Al Ing. Ignacio Ramírez del campo Tlapeaxco, así como a las personas que laboran en este campo experimental, por su apoyo invaluable durante la realización de este trabajo.

Al Dr. Federico Hahn Schlam por compartirme sus conocimientos y darme su apoyo al inicio, durante y en la conclusión de este trabajo de investigación. Al Dr. Ramón Arteaga Ramírez y al Dr. Eugenio Romantchik Kriuchkova por el apoyo brindado en la gestión administrativa como coordinador del IAUIA para el buen término de esta tesis, así como las observaciones realizadas a la misma. No puedo terminar sin antes dar gracias a esos grandes países que son Egipto y México y externar mi gusto.

DESIGN OF AUTOMATIC FOOD DOSING AND OXYGENATION FOR A CARP RECIRCULATING AQUACULTURE SYSTEM (RAS)

Wael El-messery¹; Federico F. Hahn Schlam²

ABSTRACT

During the past years the trend to move from conventional open systems to high density and highly productive recirculation aquaculture systems (RAS) was observed for its advantages. Recirculating aquaculture systems was poorly applied in Mexico, and the majority of its components were imported. The main objectives of the present study was to design and evaluate each component of a recirculating aquaculture system under local Mexican conditions, solids separator was evaluated obtaining optimum operations factors of water level in fish tank 90 cm and 2.54 cm of tank base diameter. Four suitable aerators locally designed for RAS was evaluated for choosing the maximum aeration efficiency (AAE). Spray column aerator records the highest AAE of 1.075 kgO₂/kW and oxygen transfer rate of 23.04 gO₂/h. Tezontle (Volcanic sand) as an alternative media for the biostrata for its higher cost in biofilters was studied. Total ammonia nitrogen removal efficiency was 64.5 % and 73.4 % for the Tezontle and Bio-strata respectively, so the Tezontle can substitute the biostrata as an alternative media for the biofilter for its lower cost. The oxygen budgets in RAS was studied realizing one model to calculate aeration requirements and aerator size for whatever RAS producing mirror carp. Recirculating aquaculture system to preserve water; the total water used during the growing season to produce 18 kg/tank was 4666.55 liter of water. An automatic feeder was designed to provide predetermined amounts of food at controlled feeding times; food conveying was studied optimizing energy consumption. An intelligent instrumentation system monitoring and control three fish tanks with one galvanic dissolved oxygen probe and its transmitter. Peristaltic pumps extracted water from each tank without adding oxygen to the sample and dissolved oxygen measurements were auto-calibrated and statistically diagnosed.

Keywords. Recirculating aquaculture system, automatic feeder, oxygenation, monitoring and control.

¹ Thesis author.

² Thesis advisor.

CONTENTS

1. INTRODUCTION	1
1.1. General introduction	2
1.2. Solid wastes removal	3
1.3. Removal of dissolved inorganic wastes	3
1.4. Dissolved oxygen control and aeration	4
2. REVIEW OF LITERATURE	7
2.1. Aquaculture system	7
2.1.1. Types of aquaculture systems	7
2.2. Recirculating Aquaculture systems (RAS) components	8
2.2.1. Waste solids removal.	11
2.2.1.1. Solids types in the RAS	11
2.2.1.2. Removal Mechanisms	13
2.2.2. Removal of dissolved inorganic wastes.	19
2.2.2.1. Nitrification processes	20
2.2.2.2. Biofiltration in RAS	23
2.2.3. Aeration process	36
2.2.3.1. Aerators for aquaculture systems	38
2.2.3.2. Aeration management	45
2.2.3.3. Impact of aeration on fish farms productivity	47
2.3. Dissolved oxygen budgets in aquaculture systems	48
2.4. Recirculating aquaculture system automation	54
2.4.1. Dissolved oxygen sensors	56
2.4.1.1. Polarographic sensors	56
2.4.1.2. Galvanic sensors	58
2.4.1.3. Luminescence-based dissolved oxygen sensor	60
2.4.2. Sensor auto calibration	61
2.4.3. Aeration automation	62
2.4.4. LabView in Recirculating aquaculture system	64

CONTENTS

2.4.5. Dosing automation system	65
3. MATERIALS AND METHODS	71
3.1. Recirculating aquaculture system design(RAS)	71
3.1.1. Fish tank	72
3.1.2. Separator	73
3.1.3. Emergent biofilter	74
3.1.4. Spray column aerator	74
3.2. Characterization of each RAS system element	75
3.2.1. Separator theory and design	75
3.2.1.1. Separator removal efficiency evaluation	78
3.2.1.2. Effect of tank base diameter and water level in the tank on bottom cleanliness	81
3.2.2. Biofilters design	82
3.2.2.1. Design of the second re-circulating trickling biofilter	83
3.2.2.2. Submerged packed biofilter design for the first re-circulating fish system	85
3.2.3. Biofilter initialization	88
3.2.4. Biofilter measurements	90
3.2.5. Biofilter performance indicators	91
3.2.6. Aerators used in the RAS system	91
3.2.6.1. Air lift pump	91
3.2.6.2. Diffused aerator	92
3.2.6.3. Venturi aerator	94
3.2.6.4. Spray column aerator	95
3.2.7. Aerators evaluation calculations	96
3.3. Recirculating aquaculture system operation performance	99
3.4. Dissolved oxygen budget monitoring and sampling system	102
3.4.1. Dissolved oxygen mass balance in RAS.	102

CONTENTS

3.4.2. Dissolved oxygen sampling system	103
3.5. Oxygenation system automation	107
3.5.1. Data acquisition system installation.	108
3.5.2. LabView coding.	110
3.5.2.1. The user interface (front panel)	111
3.5.2.2. Compiled code algorithm	113
3.5.2.3. Environment and dissolved oxygen sensor	117
3.5.2.4. Signal filtering using LabView for temperature and dissolved oxygen measurements	117
3.6. Water mass balance in RAS	119
3.7. Dosing system automation	120
3.8. Growth rate indicators	123
4. RESULTS AND DISCUSSIONS	126
4.1. Separator evaluation	127
4.1.1. The effect of water level in fish tank on separator removal efficiency and tank bottom cleanliness efficiency	127
4.1.2. The effect of tank base diameter on tank bottom cleanliness and separator removal efficiency	129
4.2. Biofilter performance.	132
4.2.1. Biofilters initialization	132
4.2.2. Comparative performance between the biofilters	133
4.2.2.1. Total ammonia nitrogen conversion rate	134
4.2.2.2. Total ammonia nitrogen removal efficiency percentage and index.	137
4.2.2.3. Total ammonia nitrogen conversion rate and volumetric oxygen consumption rate as indicators for nitrifying bacteria growth rate.	138
4.3. Aeration experiments	143
4.3.1. The effect of air inlet pressure on airlift pump aerator performance.	144
4.3.2. Effect of air bubbles raising velocity diffused aerator.	144

CONTENTS

4.3.3. Effect of differential pressure on venturi aerator performance.	147
4.3.4. Spray column aerator performance.	148
4.4. Dissolved oxygen transfer analysis	151
4.4.1. Effect of water temperature and oxygen deficit on oxygen transfer rate.	151
4.4.2. The effect of oxygen transfer rate on tank water temperature.	152
4.4.3. Dissolved oxygen mass balance in RAS	155
4.4.3.1. The effect of algae on dissolved oxygen demand	155
4.4.3.2. Carp dissolved oxygen demand	158
4.4.3.3. Biofilter dissolved oxygen demand	160
4.4.3.4. Sediments dissolved oxygen demand	162
4.4.3.5. Overall dissolved oxygen demand	163
4.4.3.6. Model Expectations	163
4.4.4. Effect of three different aeration levels on carp growth rate	167
4.4.5. Carp sorting based on their size as a percent	169
4.5. Dissolved oxygen automation	169
4.6. Water mass study	179
5. Conclusions	182
6. References	187
7. AppendixI	213
8. AppendixII	228
9. AppendixIII	247

CONTENTS

LIST OF TABLES

Table 2.1	Representative net production (Kg/ha) for Channel Catfish, Tilapia, and Marine Shrimp with different levels of management.	8
Table 2.2	Water and land use per kg of production of aquaculture products and a relative comparison to an intensive RAS Tilapia farm (RAS assumed to discharge 5% of system volume per day)	9
Table 2.3	Culture unit volume, flow and required clarifier diameter when operated at 15% and 5% underflow rates.	17
Table 2.4	Tezontle characteristics.	33
Table 2.5	Relative efficiencies of various aeration devices.	46
Table 2.6	Clark cell reaction	56
Table 2.7	Galvanic cell reaction	59
Table 3.1	Particle weight category	78
Table 3.2	Toxic (un-ionized) ammonia Fraction in aqueous solutions at different pH values and temperature	87
Table 3.3	Oxygen mass balance equations in RAS.	103
Table 3.4	Parameter definitions for carp oxygen consumption calculation.	103
Table 3.5	Hand meter (HI 9146) specifications	105
Table 3.6	Dissolved oxygen analyzer (HI 8410) specifications.	105
Table 3.7	NI-USB 6008 port configuration	110
Table 3.8	RAS system aeration requirement in hours during the day and the night at different water temperatures for 50 organisms per m ³ .	115
Table 3.9	Aeration requirements equation constants	116
Table 3.10	Filters characteristics.	119
Table 3.11	Monthly feeding for each tank containing 100 organisms three meals daily.	121
Table 3.12	Port configuration	122
Table 4.1	Tank bottom removal efficiency	129
Table 4.2	Effect of hydraulic loading rate and sprayers' number on spray column aerator performance.	149
Table 4.3	Temperature measurements for three tanks at December	155
Table 4.4	Food supply for different carp sizes under three different aeration levels.	168

CONTENTS

Table 4.5	Aeration requirements (hours) when RAS system has algae at period (1:00 am to 1:00 pm.	173
Table 4.6	Aeration requirements (hours) when RAS system has algae at period (1:00 am to 1:00 pm.	174
Table 4.7	Oxygen requirements when RAS system has not algae.	176
Table 4.8	Aeration requirements (hours) when RAS system has not algae based on DO set point 3.5-5 ppm.	177
Table 4.9	Aeration requirements (hours) when RAS system has not algae based on DO set point 4-6 ppm.	178
Table 4.10	Aeration requirements (hours) when RAS system has not algae based on DO set point 2-4 ppm.	204
Table 4.11	water exchange strategy that applied during the growing season	180
Table 4.12	Monthly water loss in the system.	180
Table 4.13	Water and land use per kg of production of aquaculture products and a relative comparison to an intensive RAS Tilapia farm (RAS assumed to discharge 5% of system volume per day).	181

LIST OF FIGURES

Fig. 2.1	Required unit processes and some typical components used in recirculating aquaculture production systems	11
Fig. 2.2	Particle trap is an advanced double drain design that concentrates much of the settleable solids in only 5 percent of the water flow leaving the fish culture tank (B).	12
Fig. 2.3	Typical drum screen filter (shown with a cut-away and expanded midsection) for waste solids removal from aquacultural recycle flow streams	18
Fig. 2.4	Pump driven by venturi type foam fractionator.	19
Fig. 2.5	Fish excrete dissolved wastes convert to cell tissue by bacteria.	24
Fig. 2.6	Heterotrophs exist on the surface because of their higher growth rates while the slower growing nitrifiers become embedded in the biofilm.	25
Fig. 2.7	An organizational tree of Biofilters.	28
Fig. 2.8	Trickling filter.	29
Fig. 2.9	Rotating Biological Contactor	30
Fig. 2.10	Rock packed bed biofilter	32
Fig. 2.11	Bead filters are distinguished by the way the beads are washed. The bubble washed unit is cleaned by draining and the propeller-washed units are intermittently cleaned by a propeller and The PolyGeysler Bead Filter is the next generation in Bead Filter technologies primarily through its automatic pneumatic backwash mechanism. Microbead Biofilter.	36
Fig. 2.12	The four-step gas transfer process	37
Fig. 2.13	A vertical pump aerator and A pump sprayer aerator	39
Fig. 2.14	(A) floating electric paddlewheel aerator (B) triangular paddles (135° interior angle) spiraled on the hub (C) Taiwan paddle wheel aerator.	40
Fig. 2.15	(A) Simple diffused-air aerator (B) diffused-air aeration system with diffuser mounted in a bore hole in the pond bottom	41
Fig. 2.16	An air lift pump	42
Fig. 2.17	Propeller-aspirator-pump aerator (A) designed to propel water horizontal to the pond surface (B and C) to propel water with angle.	43

CONTENTS

Fig.2-18	Various types of gravity aerators, (A) simple weir, (B) weir with splashboard, (C) corrugated sheet, (D) corrugated sheet with holes, (E) lattice, and (F) cascade. (Soderberg, 1982) Examples of gravity aeration combined with other device (G) weir with paddlewheel ;(H) weir with rotating brush (Wheaton, 1993).	44
Fig. 2.19	Microcontrolled aquaculture system (Fowler, et al., 1994)	56
Fig. 2.20	Polarographic dissolved Oxygen sensor OOS 4 / OOS 4HD.	57
Fig. 2.21	Luminescence-based dissolved oxygen sensor photo by YSI, 2008.	60
Fig.2.22	Luminophor reaction with oxygen molecules with blue light excitation Photo by (Jackson and Craig, 2004)	60
Fig. 2.23	Novel dissolved oxygen sensor with auto assesses.	62
Fig. 2.24	Design of the emergency aeration system. 1, Press-differential switch (PDS); 2, emergency air pump; 3, batteries; 4, 5, diodes; 6, battery charger; 7, resistors; 8, air diffusers; 9, fish tanks; 10, 11, control lamps; 12, air valves; 13, relay; 14, normal aeration; 15, emergency aeration.	63
Fig 2.25	Diagram of recirculating aquaria system	64
Fig. 2.26	Rotifers counter system.	65
Fig.2.27	Timed automatic feeder.	66
Fig. 2.28	Schematic view of a self-feeding system (Touch-Feed, manufactured by Sterner Products, Leksand, Sweden).	67
Fig. 2.29	Schematic diagram of the control and data acquisition systems.	67
Fig. 2.30	Automatic feed system with an airlift pump	69
Fig. 2.31	The hydroacoustic food detector mounted in the sea cage.	69
Fig. 2.32	(A), fish feeding behavior in the sea (Don, 2008), and (B) underwater Camera mounted in sea cage.	70
Fig.3.1	Full recirculating aquaculture system that were used in the study.	71
Fig.3.2.	Recirculating aquaculture system (RAS).	72
Fig.3.3	Fish Tank	72
Fig. 3.4	.Algae found in the re-circulating system (RAS) (a) <i>Scenedesmus sp.</i> (b) <i>Chlorella sp.</i> (c) filamentous microalgae.	73
Fig. 3.5	Separator with two inlets one from the tank bottom to the separator center and the other from the upper part of the tank to the lateral side	74

CONTENTS

	of the separator.	
Fig. 3.6.	The separator schematic design (A) centrifugal water inlet (B) Radial inlet, the arrows indicate water flow directions inside the separator (C) central galvanic cylinder.	76
Fig. 3.7.	(a)Sieves used to determine particle size (b) water tank level.	79
Fig. 3.8	Solids analysis for the Tezontle that was used for all the experiment	79
Fig 3.9.	Samples vision microscopy I, bottom discharged (II)and Channel captured (III) separation and by naked eye (IV).	80
Fig. 3.10	The solids that captured in the channel of the separator and that discharged from the bottom.	81
Fig.3.11.	Tank base of 2.54 cm diameter, under the effect of water level in the tank (A and B) at water level 90 cm and (C) water level 80 cm	81
Fig. 3.12	The Bio-strata used in the nitrification process.	85
Fig. 3.13.	The biofilter of Tank 2	85
Fig. 3.14.	First submerged biofilter and its water distributor mounted above the biofilter media, Tezontle used as a media for the submerged biofilter with mean diameter 1 cm.	88
Fig. 3.15	The biofilter of Tank 3	88
Fig. 3.16	Stress Zyme Trade marks of Mars Fishcare North America, Inc.	89
Fig. 3.17.	Tezontle (Volcanic sand) biofilm development (A) first biofilter after 25 days and (B) after 45 days and the third biofilter after 25 days and 45 days.	89
Fig. 3.18	TAN sampling points on RAS system	90
Fig 3.19	Air lift pump aerator A air lift pump at the moment of compressor tank filling (A), and evacuating (B), air compressor (C), air bubbles raising inside raiser tube (D), cruciform base (E), and lateral view of airlift pump (F).	92
Fig 3.20	Diffused aerator, diffuser tube (A), compressor hose connection with two PVC valves controlling air inlet pressure (B) tank bottom photo (C), air bubbles in movement in the water (D) and (E).	93

CONTENTS

Fig 3.21.	Venturi aerator, showing (A) venturi; (B) 200 liter tank; (C) lateral view; (D) isometric view; (E) aeration by venturi.	94
Fig. 3.22	Spray column aerator, (A) Water sprayer SURTEK 130027; (B) Isometric view; (C) Spray column aerator photo.	95
Fig. 3.23.	The three different aeration techniques that were used (1) spray column aerator (i.e. water pump with air fan), (2) Gravity aerator, and (3) spray column aerator with water pump only.	99
Fig. 3.24.	Algae growth developing in the Tank 3 was 45, 56, 95, 150 and 420 NTU respectively.	101
Fig. 3.25	Three different forms of gravity aeration through the biofilters.	101
Fig. 3.26.	Dissolved oxygen budget in RAS.	102
Fig. 3.27	Dissolved oxygen meters (A) hand meter (HI 9146), (B) controller and data logger, (C) DO sensor HI 76410/4, (D) DO analyzer HI 8410 and (E) electronic data logger LOGBOX-AAIP65 and its wireless interface with USB cable.	104
Fig. 3.28.	polarographic probe HI 76407/4F	104
Fig.3.29.	DO sampling points on RAS system.	106
Fig. 3.30.	Overview of the peristaltic pumps mounted over the tanks and the hydraulic head system.	108
Fig. 3.31.	Acquisition system connection.	108
Fig.3.32	A central controller PC for dissolved oxygen controller with dissolved oxygen analyzer (HI 8410)	109
Fig. 3.33.	Close loop control	111
Fig.3.34.	Front panel-User Interface with dissolved oxygen control.	113
Fig. 3.35.	Timing signals during system operation	114
Fig.3.36.	Open-loop control system.	116
Fig. 3.37.	Block diagram for thermocouples.	118
Fig. 3.38.	Filtered and unfiltered DO signal using a) low pass filter (red line), band stop (blue line), high pass filter (green line) and smooth filter (exponential based method) (white line)	118
Fig. 3.39.	Dosing system (1) lateral view, (2) top view, (3) feeder photo, (4) fan, and (5) feeder parts.	120
Fig.3.40.	Gate (a) general view and (b) opening or closure	122

CONTENTS

Fig. 3.41.	Weight carp sorting at the moment of initial tanks stocking.	125
Fig. 3.42.	Sampling process.	125
Fig. 4.1.	Closed loop control diagram.	126
Fig. 4.2.	Separator Removal Efficiency	128
Fig. 4.3.	Tank bottom cleanliness efficiency	128
Fig. 4.4.	Solids distribution in the (a)discharged water and (b) separator channel using a tank base of 5 cm.	130
Fig. 4.5.	Solids distribution in the (a)discharged water and (b) separator channel using tank base of 3.81 cm.	131
Fig. 4.6.	Solids distribution in the (a)discharged water and (b) separator channel using tank base of 2.54 cm.	131
Fig. 4.7.	Biofilter initialization for the first (a), second (b) and third (c) biofilter and the nitrate accumulation in biofilter 3 (d).	132
Fig. 4.8.	(a) Diurnal changes in TAN removal rates (b) the relationship between water temperature and TAN removal rates.	134
Fig. 4.9	Air and water temperatures for the three tanks at March.	135
Fig. 4.10.	Volumetric TAN conversion rate ($\text{mg TAN}/\text{m}^3\cdot\text{day}$) for three biofilters.	136
Fig. 4.11.	Surface TAN conversion rate ($\text{mg TAN}/\text{m}^2\cdot\text{day}$) for the biofilters.	137
Fig. 4.12.	Total ammonia nitrogen removal efficiency (%) for the biofilters.	137
Fig. 4.13.	Total ammonia nitrogen removal efficiency ($\text{mg TAN}/\text{kW}\cdot\text{h}$) for the biofilters.	138
Fig. 4.14	Total ammonia nitrogen consumed by nitrifying bacteria and algae in the 1 st biofilter (a) the overall growth of nitrifying bacteria during biofilter initialization (b) the nitrifying bacteria growth behavior in the first 15 days and (c) The nitrifying bacteria growth behavior aftermath (d) The relationship between the TAN conversion rate and volumetric oxygen consumption rate $\text{mg O}_2/\text{m}^3\cdot\text{day}$ for biofilter1.	139
Fig. 4.15	Nitrifying bacterial biomass per stone of Tezontle (mg) for the first biofilter.	141

CONTENTS

Fig. 4.16	(a) Overall growth rate for the nitrifying as TAN consumption in the tank 2 (b) Overall growths of heterotrophic and autotrophic bacteria during biofilter initialization expressed as volumetric oxygen consumption rate (c) The relationship between the TAN conversion rate and volumetric oxygen consumption rate for biofilter2 (d) Nitrifying bacterial biomass growth per panel (mg).	142
Fig 4.17	(a) Overall TAN consumption for biofilter 3 (b) The relationship between Volumetric TAN conversion rate (mg TAN/m ³ .day) and Volumetric oxygen consumption rate mg O ₂ /m ³ .day for the third biofilter (c) Nitrifying bacterial biomass per stone of Tezontle (mg) for the third biofilter.	143
Fig. 4.18.	Effect of air injection pressure on (a) oxygen transfer rate and change rate in DO and (b) Aeration efficiency index and outlet dissolved oxygen percentage (%) for the air lift pump aerator.	145
Fig. 4.19.	Effect of air bubbles raising velocity on (a) oxygen transfer rate and change rate in DO and (b) aeration efficiency index for the diffused aerator.	146
Fig. 4.20.	Effect of differential pressure (kPa) on DO change rate, oxygen transfer rate, outlet dissolved oxygen percentage (%) and aeration efficiency index.	147
Fig. 4.21	Effect of superficial air velocity on DO change rate and OTR with two sprayers (a) and three sprayers (c) and on %DO and AAE for two sprayers (b) and three sprayers (d) at hydraulic loading rate of 0.0013 m ³ /m ² .s.	150
Fig. 4.22.	Effect of superficial air velocity on DO change rate and OTR with two sprayers (a) and three sprayers (c) and on %DO and AAE for two sprayers (b) and three sprayers (d) at hydraulic loading rate of 0.0021 m ³ /m ² .s.	150
Fig. 4.23.	Effect of temperature on oxygen transfer rate at dissolved oxygen of 2PPM.	151
Fig. 4.24.	Effect of oxygen deficit on oxygen transfer rate at 20°C.	152

CONTENTS

Fig. 4.25.	The effect of air temperature on water temperature and dissolved oxygen concentrations at OTR of 26 gO ₂ /day.	152
Fig. 4.26.	The effect of air temperature on water tanks temperature at December, January and February.	153
Fig. 4.27.	The effect of air temperature on water tanks temperature at March, April and May.	154
Fig. 4.28.	The effect of algae density on dissolved oxygen concentration(A)and its effect on the amount of oxygen that produced(B) or consumed (C) per hour.	156
Fig. 4.29.	The effect of algae density on the accumulated oxygen production (A) or consumption (B) per day.	157
Fig. 4.30	Diurnal fish oxygen consumption (mgO ₂ /hr) for carp mean weight (A) 200 grams and (B) 150 grams.	158
Fig. 4.31.	The effect of water temperature on carp oxygen consumption at different carp mean weight.	159
Fig. 4.32	Effect of the carp mean weight on nitrifying bacteria oxygen consumption.	161
Fig. 4.33.	Diurnal oxygen consumption by the sediments	162
Fig. 4.34.	Effect of algae turbidity on overall dissolved oxygen demand at 20°C and 0.001 m ³ sediments using tezontle of 0.2 m ³ as biofilter media.	164
Fig. 4.35.	The effect of algae on overall oxygen demand during day and night.	164
Fig. 4.36.	The effect of water temperatures on (A) specific oxygen consumption (mgO ₂ /kg fish.hr) and (B) Overall dissolved oxygen demand at without algae and 0.001 sediments (gO ₂ /h).	165
Fig. 4.37.	(A) The effect of sediments volume on overall dissolved oxygen demand at without algae and 20°C. (B) The overall dissolved oxygen demand expected and measured according to the diurnal change in temperature at carp mean weight of 70 grams.	165
Fig. 4.38	(A) Aeration requirements at different temperatures for different carp sizes; (B) Aeration energy consumption per each 10 grams of carp growth.	166

CONTENTS

Fig. 4.39.	Weekly carp growth rate for three different aeration techniques (AE) and carp growth rate under a reduced stocking density of 50 organisms per m ³ (SDE).	167
Fig. 4.40.	Carp sorting for first, second and third tank at the 140 th day, for 100 organisms per m ³ water.	169
Fig. 4.41.	Carp physiological changes during the growing season.	169
Fig. 4.42	. Dissolved oxygen concentrations for the three tanks under three DO levels.	170
Fig. 4.43.	Filtered and unfiltered dissolved oxygen measurements.	171
Fig. 4.44	Aeration requirements levels during the day in the case with algae and without algae.	172

CONTENTS

NOMENCLATURE

dc/dt	Gas transfer rate, mg/L h;
D	Diffusion coefficient;
Δ	Liquid film thickness;
A	Area of gas-liquid interface;
V	Volume of liquid into which the gas is diffusing;
C_s	Saturation concentration of the gas; and
C_m	Measured gas concentration at time t .
K_La	Overall oxygen transfer coefficient, h^{-1}
OD_1	Oxygen deficit at time 1,
OD_2	Oxygen deficit at time 2,
t	Time.
E	Efficiency (%),
DO_b	Dissolved oxygen concentration below the aerator (mg/l),
DO_a	Dissolved oxygen concentration above the aerator (mg/l),
DO_s	Dissolved oxygen concentration at saturation (mg/l).
DO_t	Solubility of oxygen at 760 mm Hg
DO_c	Corrected solubility of oxygen
DO_i	Dissolved oxygen at one tap point (mg/l),
DO_{i+1}	Dissolved oxygen at another tap point (mg/l),
DO_{s20}	Dissolved oxygen concentration saturation at 20 ⁰ C (mg/l),
DO_f	Dissolved oxygen concentration in pond water (mg l ⁻¹).
OTR	oxygen transfer rate in pond water (kg O ₂ h ⁻¹),
SAE	Standard aeration efficiency kgO ₂ /kW.h
AAE	Actual aeration efficiency kgO ₂ /kW.h
BP	Total brake power (kW) for the bump and blower
u_L	Hydraulic loading rate (m/s),
h_i	Distance between the i th and the $i+1$ th sampling location (m),
N	The total number of sampling-points along the column.
$SOTR$	Standard oxygen transfer rate (Kg oxygen/ h),

CONTENTS

$\frac{P_A}{760}$	Pressure correction factor
F	<i>ponds of food per day</i>
DO_{inf}	DO in mg/L at the pond influent
DO_{eff}	DO in mg/L at the pond effluent
Q_H	Pond discharge in gpm for a diet containing 1200 Cal./lb
SOC_B	Specific oxygen consumption mg l^{-1} per pound of fish per gallon per minute (gpm) of flow,
SOC_R	Specific oxygen consumption rate in weight units of DO per 100 weight units of fish per day,
OC	Oxygen consumption(mgO_2/h)
SOC_I	Specific oxygen consumption ($\text{mgO}_2 / \text{kgfish} / \text{h}$)
W_g	Average individual fish weight in g,
W_{lb}	Average individual fish weight in lb,
T_B	Temperature in °F.
T_I	Temperature in °C.
k	Rate constant,
W_{kg}	Body weight kg
U	Swimming speed (body length s^{-1})
C	Constant depending up on water temperature
COD	Chemical oxygen demand mg/l
$f(t)$	Temperature dependence (unitless),
$SphOC$	specific reference phytoplankton respiration rate at 20°C (1/h),
$PhOC$	phytoplankton respiration rate (1/h)
SOC	Half saturation constant of oxygen respiration (mg l^{-1}).
$PhOP_{20}$	Photosynthetic oxygen production at 20°C ($\text{mg O}_2/\text{mg TSS}$ per hour),
$PhOP_{\text{max } 20}$	Maximum photosynthetic oxygen production at 20°C ($\text{mg O}_2/\text{mg TSS}$ per hour),
I_{opt}	Optimal or saturating effective light intensity (W/m^2).
I	Effective light intensity (W/m^2),
DO_e	Equilibrium concentration of dissolved oxygen

CONTENTS

K	Ratio of molecular weight to molecular volume (mg/ml)
β	Bunsen coefficient (liter/liter atm)
x	Mole fraction (%) (dimensionless)
P	Pressure (mmHg)
P_w	Vapor pressure of water (mmHg)
DO_m	Measured concentration of dissolved oxygen in water (mg l ⁻¹)
S	The percentage saturation (%).
P_{O_2}	DO pressure in water (mmHg).
W_{t1}	Initial mean weight of fish at time T1
W_{t2}	Final mean weight of fish at time T2
W_f	Final average weight at the end of the experiment
W_i	Initial, average weight at the beginning of the experiment.
VTR	Volumetric TAN conversion rate (mg TAN/(m ³ d))
STA	Surface TAN conversion rate (mg TAN/(m ² d))
$VOCR_{tot}$	Volumetric oxygen consumption rate (mg oxygen/(m ³ d))
$VOCR$	Volumetric oxygen consumption rate for heterotrophic bacteria (mg oxygen/(m ³ d))
NBOC	biofilter oxygen consumption gO ₂ /hour

1. INTRODUCTION

1.1. General introduction

The aquaculture industry that began developing in the late 1960s has exploded into a major global industry of 60 million tons a year, with huge annual revenues in excess of US\$ 70 billion (FAO, 2006). With the current increase in environmental awareness and the consequent stringency in environmental legislation, a new approach to dealing with the ecological problems associated with aquaculture has been developed—recirculating aquaculture systems. This approach was originally developed to provide a solution to the environmental problems generated by the traditional pond and flow-through aquaculture systems, since it enables the treatment of polluted water within a closed loop, offers improved control of effluent discharge, and allows complete environmental control (van Gorder, 1994 and Shnel et al., 2002).

Commercial Recirculating fish culture systems have been developing for decades for various purposes in many parts of the world, but the development has largely been delayed due to many constraints, including economic setback to produce food fish and technical problems yet to be innovated. Nevertheless, feeding aquaculture in inland waters and in the protected coastal seas in the culture should be practiced with waste treatment for the reduction of pollution in the environment. We therefore need to develop the technology of environmentally friendly aquaculture systems as completely as possible not only to preserve our natural environment but also to sustain aquaculture production.

For the success of aquaculture the attainment of profit against invested capital is an absolute must like any other business. For the recirculating aquaculture system capital investment for the construction of the farm is normally much higher than that of conventional production system,

INTRODUCTION

therefore the system should be designed and constructed so as to be able to manage at less running cost to compensate the initial capital investment. One must also expect better production than that from conventional systems, provided that optimum stable conditions in water quality parameters for fish growth is maintained through controlled system management.

For the growing of fish at high densities some critical factors must be met for the well-being of the fish in the system. There are a variety of factors that affect the health of fish leading to the performance of fish production business. To meet these factors the strategy must contain both hardware structure design and software management technology.

The following factors are absolutely essential for the management of intensively stocked fish ponds either in closed system or in open-air ponds.

- (a) Solid wastes removal
- (b) Removal of dissolved inorganic wastes (ammonia and others)
- (c) Oxygenation to add oxygen and aeration to strip CO₂
- (d) Pumping or water movement
- (e) pH correction (for completely closed system especially where make-up water is soft).

1.2. Solid wastes removal

Innovative solutions to solids capture can further the expansion of recirculating aquaculture worldwide, through the reduction of both capital and operating costs. The continuous removal of solids is a key factor in the design of any recirculating aquaculture system(RAS) (McMillan et al., 2003; Timmons et al., 2001). Suspended solids are generally detrimental as they negatively impact the components in a RAS: clogging biofilters, increasing system biological oxygen demand (BOD) and, eventually, mineralization and ammonia production. Additionally, fine

INTRODUCTION

solids may impact fish health by causing gill damage or harboring pathogens (McMillan et al., 2003; Timmons et al., 2001; Chen et al., 1993). The rapid and efficient removal of large particles (>100 μm) is very important, as large particles will become small particles over time, which are much more difficult and costly to remove (McMillan et al., 2003; Timmons et al., 2001). McMillan et al. (2003) found pumping to have a significant negative effect on particle size ($P < 0.05$) based on differential volume. Therefore, capturing and removing large solids quickly (prior to passing through pumps) can reduce the overall effort required for filtration (McMillan et al., 2003).

1.3. Removal of dissolved inorganic wastes

Ammonia is toxic, not only to fish but also to all aquatic animals, especially in pond aquaculture at low concentrations of dissolved oxygen. The toxic levels of un-ionized ammonia for short-term exposure usually are reported to lie between 0.6 and 2 mg/L, while some consider the maximum tolerable concentration to be 0.1 mg L⁻¹. Feed efficiency and body composition of fish are negatively affected by ambient ammonia concentration. The production of un-ionized ammonia is related to the quantity of nitrogen supplied by dietary protein.

Controlling the concentration of un-ionized ammonia-nitrogen (NH₃) in the culture tank is a primary design consideration in recirculating systems. Ammonia-nitrogen (a by-product of the metabolism of protein in feeds) must be removed from the culture tank at a rate equal to the rate it is produced to maintain a stable and acceptable concentration. In systems with external ammonia-nitrogen treatment processes, the efficiency of the ammonia-nitrogen removal process will dictate the recirculating flow rate (e.g., a less efficient removal system will require a higher recycle flow rate from the tank through the filter). There are a number of methods for removing

INTRODUCTION

ammonia-nitrogen from water: air stripping, ion exchange, and Biological filtration. Air stripping of ammonia-nitrogen through non-flooded (no standing water in the reactor) packed columns require that the pH of the water be adjusted to above 10 and readjusted to safe levels (7 to 8) before the water reenters the culture tank. Ion exchange technology is costly and requires a mechanism for “wasting” ammonia-laden salt water. A salt-brine is used to “regenerate” the filter by removing ammonia-nitrogen from the resin (filter medium) once it becomes saturated with ammonia-nitrogen. Biological filtration is the most widely used method. In biological filtration (or biofiltration), there is a substrate with a high specific surface area (large surface area per unit volume) on which the nitrifying bacteria can attach and grow. Ammonia and nitrite-nitrogen in the recycled water are oxidized (converted) to nitrite and nitrate by *Nitrosomonas* and *Nitrobacter* bacteria, respectively the nitrification process will discuss in the section 4.2.

Commonly used biofilter substrates include gravel, sand, plastic beads, plastic rings, and plastic plates. The most common biofiltration technologies were discussed in the section 4.3.

1.4. Dissolved oxygen control and aeration

Dissolved oxygen is the most critical water quality variable and depends on water temperatures, stocking and feeding rates and the effectiveness of the aeration installed within the recirculation system. Dissolved oxygen concentrations should be kept above 50% saturation to ensure the survival and growth of the culture species. The activity of the bacteria within the biofilter also depends on the level of dissolved oxygen within the water column and usually become inefficient when oxygen levels fall below 2 ppm. Declining oxygen levels can be caused by a number of factors such as high stocking rates that occur within the recirculation system and the decomposition of organic matter including feces and uneaten food.

INTRODUCTION

Low dissolved oxygen can be lethal to the aquaculture species. Some effects include stress which brings behavioral (e.g., gasping) and morphological (marked melanin pigment in the skin) changes in the fish, increased susceptibility to disease, poor feed conversion, poor growth and cause mass mortalities in extreme cases. Signs of low dissolved oxygen can be detected when fish are observed rising to the surface and gulping air or gathering around the water inlet. Oxygen depletions are often caused by an imbalance in oxygen budgets between the organisms in RAS and the aeration equipment. Although oxygen depletion can sometimes be predicted before it occurs, it can develop suddenly without warning.

Phytoplankton produces oxygen by photosynthesis during the day but are the major consumers of oxygen at night. The magnitude of daily changes in DO is influenced primarily by light intensity and phytoplankton density.

There is no net transfer of oxygen between air and water if the water is at equilibrium with atmospheric oxygen. When water is under-saturated with oxygen, oxygen will transfer from air to water, and the reverse is true when water is supersaturated with oxygen. The driving force causing oxygen transfer is the difference in oxygen tension in the air and water. At equilibrium, the oxygen tension in air and are the same, and there is no oxygen transfer. (Boyd and Watten 1989; Soderberg, 1982) reported that the net oxygen transfer depends upon oxygen deficit (OD) or oxygen surplus (OS), the area of contact of the air-water interface, the temperature, and the time of contact. Oxygen enters or leaves water at the interface between the air and water. Therefore, for the thin film of water in contact with the air, the greater (OD) or (OS), the faster oxygen will diffuse through this interface. Turbulence increases the rate of transfer by increasing the contact area of the air and water. Aerators work by increasing the area of contact between air and water and let the oxygen to transfer.

INTRODUCTION

The objectives of the present study are:

1. Design recirculating aquaculture system under local Mexican conditions by
 - a. Choose the aerator (locally designed) that has the highest performance between four different aerators that can use in RAS.
 - b. Test the performance of Tezontl as an alternative media for the bio-strata for its higher cost in biofilters.
 - c. Design and study the ideal operating factors for the separator.
2. Design recirculating aquaculture system to preserve water.
3. Model to calculate aeration requirements and oxygen budget in RAS.
4. Study three different oxygen ranges on carp growth rate to choose the lower level that do not affect carp growth rate, consequently lower energy consumption.
5. Design and evaluate the performance of automatic feeder
6. Intelligent dissolved oxygen control with autocalibration.

2. REVIEW OF LITERATURE

2.1 Aquaculture system:

Aquaculture is the rearing of aquatic organisms under controlled or semi controlled conditions, (Pillay, 1990). The word of "Aquaculture" through used rather widely for over a decade to denote all forms of culture of aquatic animals and plants in fresh, brackish and marine environments, is still used by many in a more restrictive sense, (Stickney, 1994). Aquaculture is the cultivation of aquatic animals and plants, (Enga et al., 1999). Aquaculture is the science and technology of producing aquatic plants and animals (Lawson, 1995). Jhingran and Gopalakrishnam, (1974) listed more than 400 aquaculture species. (Pillay, 1990) named 95 finfish, 32 crustaceans, 35 mollusks, and 19 aquatic plants commonly used in aquaculture.

2.1.1 Types of aquaculture systems:

Pond aquaculture is generally the most profitable approach to growing aquatic animals because nature provides many of the resources need to grow the crop (Boyd, 1998). Pond aquaculture may be classified as species, pond characteristics, and intensity of culture. The culture systems may be classified by type of grow-out units (i.e., ponds, cages, pens, raceways, tanks, silos, etc). Ponds may be classified according to construction methods as watershed ponds, excavated ponds, and levee ponds (Yoo and Boyd, 1994). Ponds can also be utilized for both aquaculture and agriculture (rice culture cultivated with fish).

Egna et al., (1997) classified aquaculture ponds depending upon the intensity of management inputs and the amount of production. In extensive aquaculture there are few inputs of nutrients, and production is quite low. Larger nutrient inputs are provided and greater production is obtained in semi-intensive aquaculture. The greatest inputs of nutrients are provided in intensive

REVIEW OF LITERATURE

aquaculture to achieve very high production. Table (2.1) summarizes the different levels of management and amounts of net production that are typical in the culture of marine shrimp, tilapia and channel catfish. There are no standard definitions of extensive, semi intensive and intensive aquaculture, but reasonable divisions between the three levels of management and are as follows:

- 1- Extensive-production is enhanced only by manures or chemical fertilizers.
- 2- Semi-intensive feeds are used to increase production, manures and chemical fertilizers also may be used.
- 3- Intensive-large amounts of feed are applied, manures and fertilizers may be used, and ponds are aerated by mechanical means.

Table 2.1: Representative net production (kg/ha) for Channel Catfish, Tilapia and Marine Shrimp with different levels of management.

Management	Channel Catfish	Tilapia	Marine shrimp
Stocking only	50-100	200-500	100-200
Stocking and fertilization	200-300	1000-3000	400-600
Stocking and feeding	1500-2500	3000-6000	---
Stocking-feeding and water exchange	----	----	1000-2000
Stocking-feeding and aeration	2500-5000	6000-10000	----
Stocking-feeding-aeration and water exchange	5000-10000	10000-20000	3000-10000

2.2. Recirculating Aquaculture systems (RAS) components

Indoor RAS offers the advantage of raising fish in a controlled environment, permitting controlled product growth rates and predictable harvesting schedules. RAS conserve heat and

REVIEW OF LITERATURE

water through water reuse after reconditioning by biological filtration using biofilters. RAS allow effective economics of scale, which results in the highest production per unit area and per unit worker of any aquaculture system. RAS are environmentally sustainable using 90-99% less water than conventional aquaculture systems and providing environmentally safe waste management treatment. Table 2.2 provides a comparison of water used per kg of fish produced. The RAS assumes a tilapia culture system with a density of 100 kg/m³, 1% feeding rate, and a feed conversion of 1 to 1 with a system volume discharge rate of 5% per day. Some current commercial RAS are using less water (2 or 3% system discharge per day), higher densities and similar feed conversion. RAS allow year-round production of consistent volumes of product, and complete climate control of the environment (Timmons and Ebeling, 2007).

Table 2.2 Water and land use per kg of production of aquaculture products and a relative comparison to an intensive RAS Tilapia farm (RAS assumed to discharge 5% of system volume per day)

System	Species	Production intensity (kg/ha/y)	Water required (L/kg)	Ratio	
				Land	Water
RAS Produced	<i>O. niloticus</i> (Nile tilapia)	1,340,000 ^a	500	1	1
Ponds	<i>O. niloticus</i> (Nile tilapia)	17,400	21,000	154	420
Ponds	<i>I. punctatus</i> (Channel catfish)	3,000	3,000-5,000	896	800
Raceways	<i>S. gairdneri</i> (Rainbow trout)	150,000	210,000	18	4,200
Ponds	Panaeid Shrimp	4,200-11,000	11,000-21,340	354	320

^a does not account for land used external to building space

Indoor aquaculture is probably the only potential method that could be used to ensure a 100% safe source of sea food, free from chemicals and heavy metals. The challenge to designers of recirculating systems is to maximize production capacity per dollar of capital invested. Components should be designed and integrated into the complete system to reduce cost while maintaining or even improving reliability. Research and development in recirculating systems has been going on for nearly three decades. There are many alternative technologies for each process and operation. The selection of a particular technology depends upon the species being reared, production site infrastructure, production management expertise, and other factors. Prospective users of recirculating aquaculture production systems need to know about the required water treatment processes, the components available for each process, and the technology behind each component.

The by-products of fish metabolism include carbon dioxide, ammonia-nitrogen, and particulate and dissolved fecal solids. Water treatment components (Fig. 2.1) must be designed to eliminate the adverse effects of these waste products. In recirculating tank systems, proper water quality is maintained by pumping tank water through special filtration and aeration or oxygenation equipment. Each component must be designed to work in conjunction with other components of the system.

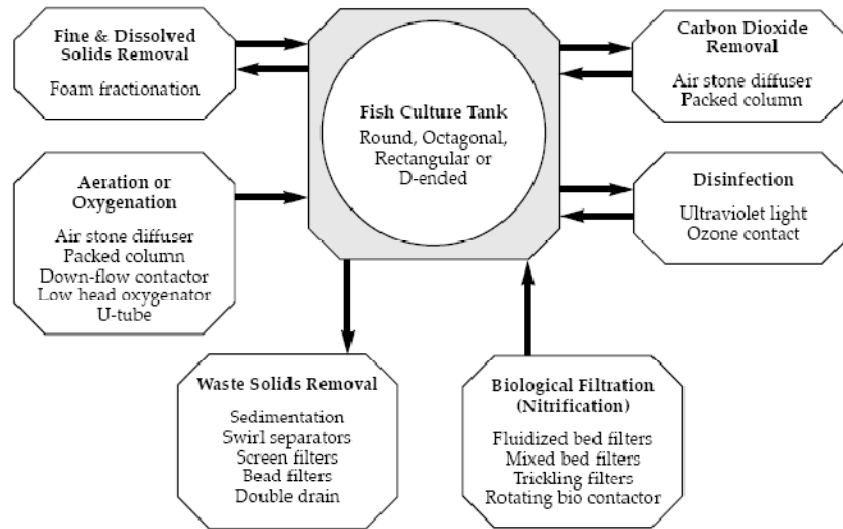


Fig. 2.1. Required unit processes and some typical components used in recirculating aquaculture production systems (Losordo et al., 1998).

So the major RAS components that were applied in this study;

1. Waste solids removal
2. Biological filtration
3. Spray column aerator
4. Automatic feeder
5. Dissolved oxygen controller

2.2.1. Waste solids removal.

2.2.1.1. Solids types in the RAS

There are three categories of waste solids-settable, suspended, and fine or dissolved solids (Losordo et al., 1999). Large particles than 100 μ m can be effectively removed by settling basins or mechanical screen filtration. However, fine particles cannot be removed effectively by either

gravity separation or granular filtration methods. Granular filters are effective only in the removal of particles larger than 20 μm (Task committee, 1986).

Settleable solids are generally the easiest to deal with and should be removed from the culture tank water as rapidly as possible. This is easiest when bottom drains are properly placed. In tanks with circular flow patterns (round, octagonal, hexagonal, square with rounded corners) and minimal agitation, settleable solids can be removed as they accumulate in the bottom center of the tank, in a separate, small flow-stream of water, or together with the entire flow leaving the tank. Center drains with two outlets are often used for the small flow-stream process. This double drain divides the flow leaving the tank into a small pipe carrying the settleable solids, and a larger pipe with a higher flow rate carrying the suspended solids from the upper water column of the tank (Fig. 2.2)

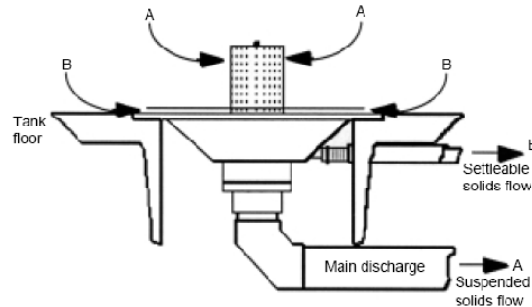


Fig. 2.2. Particle trap is an advanced double drain design that concentrates much of the settleable solids in only 5 percent of the water flow leaving the fish culture tank (B). (after Hobbs et al., 1997).

Settled solids should be removed from the center of the tank on a continuous or semi-continuous basis. The settleable solids flow rate will determine the method used to collect and concentrate them for further treatment or disposal. In systems with high settleable solids flow rate (20 to 50 percent of the total tank flow), swirl separators, settling basins, or drum screen filters are used to collect these solids.

Suspended solids will not easily settle out of the water column in the fish culture tank. Suspended solids are not always dealt adequately in recirculating systems. Most current technologies for removing suspended solids generally involve some form of mechanical filtration.

Many of the fine suspended solids and dissolved organic solids that build up within intensive re-circulating systems cannot be removed with traditional mechanisms. A process called foam fractionation (also referred to as air-stripping or protein skimming) is often employed to remove and control the build-up of these solids. Foam fractionation is a general term for a process in which air is introduced into the bottom of a closed column of water and creates foam at the surface of the column.

2.2.1.2. Removal Mechanisms

There are three primary methods that are used to remove suspended solids from fish culture waters. These are:

1. Gravity separation (sedimentation).
2. Mechanical Filtration.
3. Foam fractionator.

Gravity separation works on the principle of sedimentation and settling velocities. Unit processes in this category include clarifiers (settling tanks), tube settler, and hydro cyclones. Sedimentation (e.g., settling basins) is an effective method of solids removal and has been applied to aquaculture systems with varying degrees of success (Timmons et al., 2001; Metcalf and Eddy, 1991). Sedimentation basin design in aquaculture systems depend upon: (1) flow rate, (2) particles specific gravity (density) and (3) the size of particle one wishes to remove. Traditional settling basin design from wastewater treatment uses hydraulic retention time to

determine the basin volume (Timmons et al., 2001; Metcalf and Eddy, 1991). However, Stechey and Trudell (1990) reported an overflow rate (V_o) method, which provides more consistent total suspended solids (TSS) removal in aquaculture systems. When applying this method, the overflow velocity of the settling basin determines the size of particles that will settle in the basin. Any particle with a settling velocity greater than the overflow rate of the basin ($V_s > V_o$) will theoretically settle out of suspension. Settling velocities can be theoretically determined for small particles with a low Reynolds number using Stoke's Law. However, it is best to obtain a sample of waste particles to determine settling velocities, as most aquaculture solids are not homogeneous and do not meet the assumption of perfect spheres.

Empirically, a wide variety of derived settling velocities have been reported for fish feces. The V_s range for tilapia feces has been reported as 1.7–4.3 cm/s (Timmons et al., 2001). By comparison, trout feces have a much lower specific gravity (1.005) and exhibit lower V_s (True et al., 2004; Timmons et al., 2001). Settling velocities for solids in flow through commercial rainbow trout facilities were reported as 0.16 cm/s and 2.31 cm/s for particles less than and greater than 815 μm , respectively (True et al., 2004). Wong and Piedrahita (2000) determined the median settling velocity, on a mass basis, for manually stripped rainbow trout waste to be 1.7 cm/s. Stechey and Trudell (1990) recommended an off-line settling basin overflow rate between 40 and 80 $\text{m}^3/(\text{m}^2.\text{d})$ for salmonid culture, which translates to settling velocities between 0.046 cm/s and 0.092 cm/s, respectively (Timmons et al., 2001). Removal of settable solids was found by Mudrak (1981) to be greater than 90% for intensive trout culture off-line settling basins with a design overflow rate of 60 $\text{m}^3/(\text{m}^2.\text{d})$ (0.069 cm/s) (Timmons et al., 2001). It has been estimated that 97% of solids loading could be captured in settling basins if re-suspension is not a problem (i.e., good design) (Henderson and Bromage, 1988). The Freshwater Institute (Shepherdstown,

WV) successfully applied this technique to solids thickening of drum filter effluents (97% removal of solids) using a radial flow clarifier (Timmons et al., 2001). However, traditional limitations associated with sedimentation, such as inefficient removal of particles <100 µm, difficulty in the removal of settled solids (including high water loss) and large space requirements, remain (Timmons et al., 2001).

Static separators, based on swirling flow, are simple and relatively inexpensive to manufacture and operate, which accounts for their widespread use, in a wide spectrum of industries. These include: storm water treatment (U.S. E.P.A., 1999; Koní'e`ek et al., 1996; Villeneuve and Gaume, 1994; Sullivan et al., 1978, 1982), industrial dedusting (Hoffmann et al., 2001; Hoekstra et al., 1999), powder coating (Thorn, 1998). Much research has been done on the solid–liquid hydrocyclone. In the aquaculture industry, swirl separators are sometimes referred to as hydro cyclones. However, the swirl separator operated in the aquaculture industry is significantly different from conventional hydro cyclones. Though both have a similar structure with a cono-cylindrical body, a tangential inlet and bottom and top outlets, they differ in dimension.

Hydrocyclones tend to have a diameter of the order of a few centimeters (Chen et al., 2000; Svarovsky, 1984) while swirl separators generally have diameters on the order of a meter. The pressure drop across hydro cyclones is also much larger than across swirl separators. The high pressure drops in hydro cyclones are achieved by high inlet velocities which give rise to large shearing forces. These should be avoided in swirl separators because they break wastes into smaller particles that are more difficult to remove. Though the design of hydro cyclones has been the subject of several studies (Castilho and Medronho, 2000; Chen et al., 2000 and Svarovsky, 1984), the differences between conventional hydro cyclones and swirl separators makes it

impractical to apply these results to a swirl separator. In particular, swirl separators as considered here are dilute systems (<1% volume fraction solids) with more moderate flows than conventional hydro cyclones.

Radial-flow settling units, also called circular center-feed sedimentation basins, are the most common settling tank design used in municipal wastewater treatment plants ([Metcalf and Eddy Inc., 1991](#)). A radial-flow settler is only similar to a swirl separator in that they are both cylindrical settling tanks with effluent launders located around the top perimeter of the vessels and sometimes with cone bottoms. However, radial-flow settlers have completely different flow hydraulics from swirl separators. A radial-flow settler introduces water into the center of the vessel, inside a ‘turbulence-dampening’ cylinder, and the water injected into the center of the tank then flows outward (in the vessel’s radial direction) to the overflow collection launder that surrounds the perimeter of the settler. Radial flow away from the center of the circular tank produces a progressively decreasing water velocity along the settling path. In addition, the circumference of the circular vessels produces a substantial outlet weir length, providing a low weir-loading rate. According to [Metcalf and Eddy Inc., \(1991\)](#), the design of the flow injection point within the center of the radial-flow settler is critical to dampen the turbulence created by the flow injection at the center of the tank. Therefore, the turbulence-dampening cylinder, located at the center of the circular settling tank, should be designed with a minimum diameter that is 25% of the tank diameter and should be located well above the maximum depth of sludge to minimize re-suspension of captured solids ([Metcalf and Eddy Inc., 1991](#)). [Johnson and Chen, \(2011\)](#) studied culture tank underflow rates of 5% and 15% to investigate size-up and commercial suitability of the design over a range of total culture tank flow rates as shown in the Table 2.3.

REVIEW OF LITERATURE

Table 2.3. Culture unit volume, flow and required clarifier diameter when operated at 15% and 5% underflow rates.

15% Underflow		5% Underflow		Underflow rate (LPM)	Clarifier diameter ^b (m)
Culture unit volume (L)	Culture unit flow rate ^a (LPM)	Culture unit volume (L)	Culture unit flow rate ^b (LPM)		
600	20	1800	60		
2601	87	7800	260	13	1.0
16208	540	48600	1620	81	2.5
64632	2154	193800	6460	323	5.0
145273	4842	435600	14520	726	7.5
258329	8611	774600	25820	1291	10.0

^a One turnover/30min.

^b Test conditions of $V_s = 0.0274$ cm/s (loading rate = 0.40 gpm/ft²).

There are two types of mechanical filtration are

1. Screen filtration, and
2. Expandable granular media filtration.

Screen filters use some form of fine mesh material (stainless steel or polyester) through which effluent passes while the suspended solids are retained on the screen. Solids are usually removed from the screen by rotating the clogged screen surface inside high pressure jets of water. The solids are carried away from the screen in a small stream of waste water, Fig. 2.3. The feature that makes each screen filter different and the challenge in designing these units is the process of collecting the solids on the mesh surface.

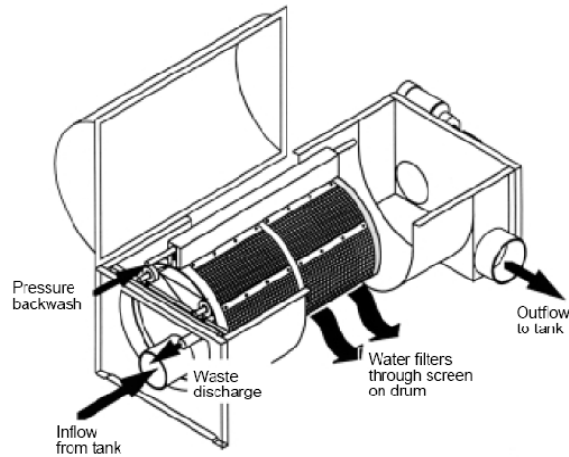


Fig. 2.3. Typical drum screen filter (shown with a cut-away and expanded midsection) for waste solids removal from aquacultural recycle flow streams (after [Losordo et al., 1999](#)).

Expandable granular media filters remove solids by passing water through a bed of granular medium (sand or plastic beads). The solids either adhere to the medium or are trapped within the open spaces between the medium particles. Over time, the filters will become clogged with solids and require cleaning, or backwashing. Backwashing these filters require that the filter bed be expanded (from a compacted state) to release the solids. Floating plastic beds have low density trapping and removing suspended solids from the flow-stream as water passes up.

Foam fractionation removes dissolved organic compounds (DOC) from the water column by physically adsorbing DOC on the rising bubbles. Fine particulate solids are trapped within the foam at the top of the column, which can be collected and removed. The main factors affected by the operational design of the foam fractionator are bubble size and contact time between the air bubbles and DOC. A counter-current design (bubbles rising against a downward flow of water) improves its efficiency by lengthening the contact time between the water and the air bubbles, (Fig. 2.4). In this design, water is injected into the foam fractionator through a venturi or by air

compression using an air lift pump. The venturi mixes air with the water and the air/water mixture enters the body of the foam fractionator tangentially.

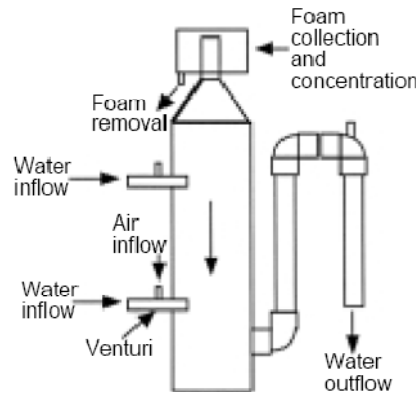


Fig. 2.4. Pump driven by venturi type foam fractionator (Losordo, 1997).

2.2.2. Removal of dissolved inorganic wastes

There are a number of methods for removing ammonia-nitrogen from water: air stripping, ion exchange, and biological filtration. Air stripping of ammonia-nitrogen through non-flooded (no standing water in the reactor) packed columns require that the pH of the water be adjusted to above 10 and readjusted to safe levels (7 to 8) before the water reenters the culture tank (Losordo et al., 1999). Ion exchange technology is costly and requires a mechanism for “wasting” ammonia-laden salt water. A salt-brine is used to “regenerate” the filter by removing ammonia-nitrogen from the resin (filter medium) once it becomes saturated with ammonia-nitrogen (Losordo et al., 1992). Biological filtration is the most widely used method. In biological filtration (or biofiltration), there is a substrate with a high specific surface area (large surface areaper unit volume) on which the nitrifying bacteria can attach and grow. Ammonia and nitrite-nitrogen in the recycled water are oxidized (converted) to nitrite and nitrate by *Nitrosomonas* and *Nitrobacter* bacteria, respectively the nitrification process will discuss in the section below.

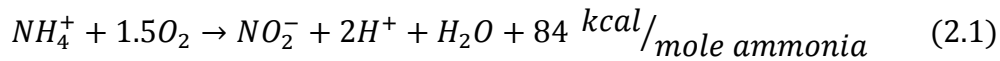
Commonly used biofilter substrates include gravel, sand, plastic beads, plastic rings, and plastic plates (Malone and Pfeiffer, 2006)

2.2.2.1. Nitrification processes

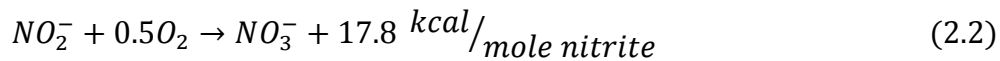
Ammonia is produced as the major end product of the metabolism of protein catabolism and is excreted by fish as unionized ammonia from their gills. Ammonia, nitrite, and nitrate are all highly soluble in water. Ammonia exists in two forms: un-ionized NH_3 and ionized NH_4^+ . The relative concentration of each of these forms of ammonia in the water column is primarily a function of pH, temperature and salinity. The sum of the two ($\text{NH}_4^+ + \text{NH}_3$) is called total ammonia or simply ammonia. It is common in chemistry to express inorganic nitrogen compounds in terms of the nitrogen they contain, i.e., $\text{NH}_4^+\text{-N}$ (ionized ammonia nitrogen), $\text{NH}_3\text{-N}$ (un-ionized ammonia nitrogen), $\text{NO}_2\text{-N}$ (nitrite nitrogen) and $\text{NO}_3\text{-N}$ (nitrate nitrogen). It permits an easier computation of total ammonia-nitrogen ($\text{TAN} = \text{NH}_4^+\text{-N} + \text{NH}_3\text{-N}$) and easy conversion between the various stages of nitrification. Biological filtration can be an effective means of controlling ammonia; opposed to water flushing control of ammonia levels. There are two phyto-genetically distinct groups of bacteria that collectively perform nitrification. These are generally categorized as chemosynthetic autotrophic bacteria because they derive their energy from inorganic compounds as opposed to heterotrophic bacteria that derive energy from organic compounds (Hagopian and Riley, 1998). Ammonia oxidizing bacteria obtain their energy by catabolizing un-ionized ammonia to nitrite and include bacteria of the genera *Nitrosomonas*, *Nitrosococcus*, *Nitrosospira*, *Nitrosolobus* and *Nitrosovibrio*. Nitrite oxidizing bacteria oxidize nitrite to nitrate, and include bacteria of the genera *Nitrobacter*, *Nitrococcus*, *Nitrospira* and *Nitrospina*. Nitrifying bacteria consume carbon dioxide as their primary carbon source, and obligate aerobes, which require oxygen to grow (Hagopian and Riley, 1998).

Nitrification is a two-step process, where ammonia is first oxidized to nitrite and then nitrite is oxidized to nitrate. The two steps in the reaction are normally carried out sequentially. Since the first step has a higher kinetic reaction rate than the second step, the overall kinetics is usually controlled by ammonia oxidation and as a result there is no appreciable amount of nitrite accumulation. Equations 2.1, 2.2 and 2.3 (EPA 1993; Ebling et al., 2006) show the basic chemical conversions occurring during oxidation by *Nitrosomonas* and *Nitrobacter*.

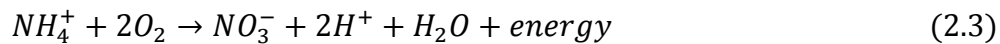
For *Nitrosomonas*:



For *Nitrobacter*:

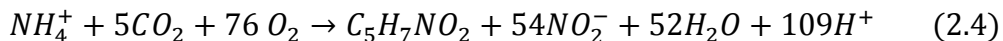


Overall:

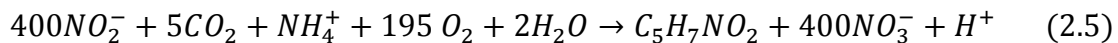


The reaction of nitrification and cell biomass formation can also be written as (Haug and McCarty, 1972):

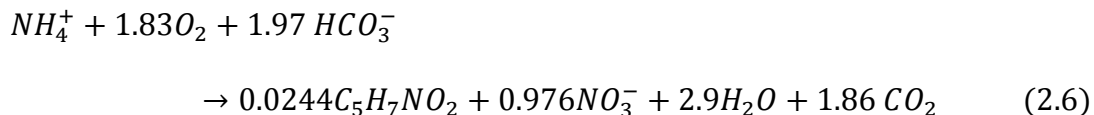
For *Nitrosomonas*



For *Nitrobacter*



Overall reaction (Ebling et al., 2006)



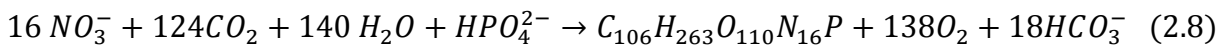
Two major categories of microbial flocculation systems are found in aquaculture. Photoautotrophic systems often referred as green systems, use natural blooms of algae to control

nitrogen. The second microbial flocculation system consists of heterotrophic bacteria, where their growth is stimulated through the addition of a carbonaceous substrate. At high carbon to nitrogen (C/N) feed ratios, heterotrophic bacteria will assimilate ammonia-nitrogen directly into cellular protein.

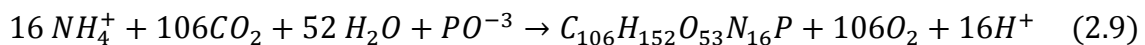
Conventional aquaculture ponds rely on the use of algal biosynthesis for the removal of the majority of the inorganic nitrogen. The major disadvantage of algal based systems is the wide diurnal variations in dissolved oxygen, pH and ammonia-nitrogen. Other disadvantages are long term changes in algal density and frequent die-offs, (Burford, et al., 2003). Undamaged algal populations in conventional ponds typically can fix 2-3g carbon/m² day. High rate mixed ponds that are well managed can yield higher rates of 10-12 g carbon/m²day, (Brune, et al., 2003). The biosynthesis of algae was described by Stumm and Morgan (1996). For ammonia as the nitrogen source:



or, for nitrate as the nitrogen source:

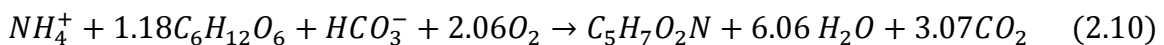


Algalbiosynthesis (Brune et al., 2003)



C/N = 5.7/1 mg/mg, VS = 50% carbon 8.7% nitrogen

Ammonia removal by heterotrophic bacteria can be described in general by equation 2.10 being ammonia the nitrogen source, (Ebling, et al., 2006):



This equation predicts that for every gram of ammonia-nitrogen converted to microbial biomass 4.71 g of dissolved oxygen, 3.57 g of alkalinity (0.86 g inorganic carbon) and 15.17 g of

carbohydrates (6.07 g organic carbon) are consumed (Ebling, et al., 2006). A microbial biomass of 8.07 g (2.63 g inorganic carbon) is produced. Oxygen demand is slightly higher being the alkalinity requirement about half and the CO₂ production almost 75% greater than the corresponding reaction for nitrification.

2.2.2.2. Biofiltration in RAS

Biological treatment in the RAS is the use of bacteria to convert those fish dissolved wastes to cell mass and other stable end products. This section will discuss several key issues in biological treatment: (1) how wastes, bacteria, and feed are related; (2) why fixed film is the predominant biological treatment method in recirculating systems; (3) how biofilter design guidelines are derived from the needs of bacteria; and (4) how biofilter reliability is affected by the strategy employed to fulfill the design requirements.

Wastes and bacteria have a complementary relationship. Dissolved wastes generated by the fish belong to one of two major categories: organic carbon or ammonia, which are used as energy and food by bacteria, Fig. 2.5. Organic carbon is both energy and food for heterotrophic bacteria which consume oxygen for respiration. The amount of oxygen used to convert the organic waste to cell material is referred to as biochemical oxygen demand (BOD). If the organic wastes are not removed by a filter, the BOD can cause that the oxygen concentration in the fish tank declines rapidly killing the fish (Golz, 1995). Ammonia is an energy source for autotrophic bacteria which use alkalinity to build cell material. Ammonia is first converted to nitrite by one group of bacteria *Nitrosomonas* and then to nitrate by yet another bacterial group *Nitrobacter*. Nitrate is a stable end product with low toxicity and does not harm the fish in the concentrations present, but ammonia and nitrite are both highly toxic at low concentrations.

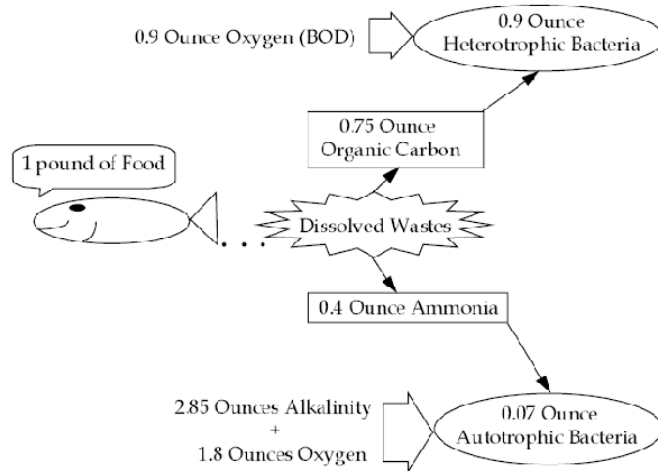


Fig. 2.5. Fish excrete dissolved wastes convert to cell tissue by bacteria (Golz, 1995).

In biofilters, the nitrifying bacteria usually coexist with heterotrophic microorganisms such as heterotrophic bacteria, protozoa and micro-metazoa, which metabolize biologically degradable organic compounds. Heterotrophic bacteria grow significantly faster than nitrifying bacteria and will prevail over nitrifying bacteria in competition for space and oxygen in biofilters, when concentrations of dissolved and particulate organic matter are high. For this reason, it is imperative that the source water for biofilters be as clean as possible with minimal concentration of total solids.

Heterotrophic bacteria grow very efficiently doubling in population about every 8 hours (Golz, 1995). As Fig. 2.5 shows that for one pound of feed, 9/10 of an ounce of heterotrophic bacteria is produced, using 3/4 of an ounce of dissolved carbon. Aeration must be sufficient to supply the heterotrophs with 9/10 of an ounce of oxygen per pound of feed. Comparatively nitrifiers are less efficient requiring 24 hours doubling in population (Golz, 1995). As a result of the one-pound feeding (Fig. 2.5), the fish excretes 4/10 ounces of ammonia, which yields only 7/100 of an ounce of nitrifying bacteria. To perform the conversion of ammonia to nitrate, the nitrifiers require nearly 3 ounces of alkalinity and 2 ounces of oxygen per pound of feed. When water quality is sufficient to meet their environmental needs and they are given enough time to

reproduce, the nitrifying bacteria will flourish, producing nitrate as their final end product, Fig. 2.5. However, if the water quality is allowed to decline or the ammonia loading is suddenly increased, ammonia and nitrite levels can raise rapidly. In summary, as with nitrifiers water quality demands are stricter and their growth is less efficient than heterotrophs, selecting biological treatment on the basis of nitrification will ensure that organic carbon is also removed.

Biological treatment processes are classified as either suspended growth or fixed film. In suspended growth processes, the waste is added to a large aerated tank where it is converted to cellular material by suspended bacteria. These suspended bacteria must be removed by a solid separation device before recirculation water is returned to the culture tank. Autotrophic bacteria time to reproduce requires that a portion of the separated solids is continually monitored and recycled to the aeration tank. Because the operational requirements of suspended growth make it a large-scale intensive process, it is infrequently employed in aquaculture systems. In contrast, fixed-film processes require much less management or maintenance, and bacterial attachment (Fig. 2.6) provides sufficient time for the slow-growing nitrifiers to reproduce. Because of its advantages biofilm nitrification has become the standard treatment method for re-circulating aquaculture systems.

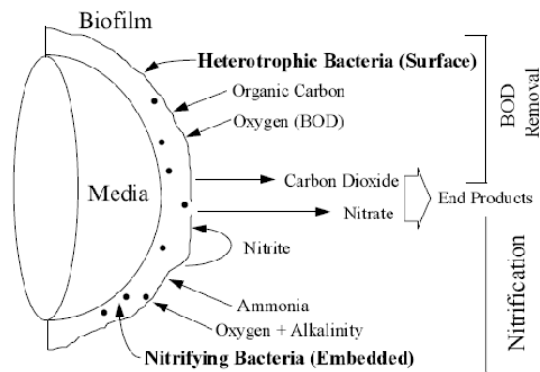


Fig.2.6. Heterotrophs exist on the surface because of their higher growth rates while the slower growing nitrifiers become embedded in the biofilm (Golz, 1995).

The first juncture separates the two fundamental approaches to bacterial culture: suspended growth or fixed film. Suspended growth systems were rarely found in production aquaculture with the increased utilization of microbial flocculation systems for the production of tilapia and marine shrimp. In these systems heterotrophic bacterial growth is stimulated through the addition of organic carbonaceous substrate as molasses, sugar, wheat, cassava, etc. At high organic carbon to nitrogen (C/N) feed ratios heterotrophic bacteria assimilate ammonia-nitrogen directly from the water replacing the need for an external fixed film biofilter (Avnimelech, 1999; McIntosh, 2001).

In traditional intensive recirculating aquaculture production systems, large fixed-film bioreactors are used; nitrification of ammonia-nitrogen to nitrate-nitrogen is carried out by ammonia oxidizing bacteria (AOB) and nitrite oxidizing bacteria (NOB).

A common problem in freshwater production systems is nitrite poisoning. This typically occurs in newly established tanks systems where the nitrifying bacteria, *Nitrobacter*, has not become established, in tanks that are overcrowded and overfed, and after treating the fish tank with antibiotics or chemicals that kill the bacteria. In all of these situations ammonia from metabolic wastes from the fish and from organic matter (uneaten food, dead plants, etc.) builds up. The bacteria *Nitrosomonas* oxidizes the ammonia to nitrite which is usually further oxidized to nitrate which has a low toxicity for fish. The nitrates are then removed through water changes. If the *Nitrobacter* bacteria is not established or becomes overwhelmed by the amount of nitrite present, nitrite levels quickly reach toxic levels.

If nitrite enters as ions primarily through chloride cells, then expected role of pH is considerably smaller. This matter will be considered be low in connection with pH. From the blood plasma, nitrite diffuses into red blood cells, where it oxidizes the iron in hemoglobin to the +3 oxidation state. Hemoglobin that is changed in this way is called methemoglobin or

ferrihemoglobin (Kiese 1974), which lacks the capacity to bind oxygen reversibly (Bodansky, 1951). As nitrite raises the fraction of methemoglobin in the blood, it reduces the total oxygen-carrying capacity of the blood (Cameron 1971) results in hypoxia severe enough to cause sudden death but often the fish will live until they exert themselves. A visible symptom of high methemoglobin levels is a brown color in the blood or gills.

Treatment not only includes decreasing the population to decrease ammonia levels, but also adding a chloride salt (in the form of sodium chloride or calcium chloride) to the water. The level of salt needed to treat (<50 mg/l) is not toxic to freshwater fish. The chloride ion competes with the nitrite ion at the gills. When the chloride ion is present at least three times and not more than six times the level of the nitrite ion, it is preferentially transported across the gills. Thus transport of the nitrite ion is reduced. Keeping the chloride levels in the water at least 20 mg/l can prevent nitrite toxicities. Additional treatments can include emergency water changes to dilute the nitrite problem (Greely, 1994).

In intensive recirculating systems heterotrophic bacteria growth and organic carbon accumulation are minimized intentionally through rapid removal of solids from the system and through water exchange. In general fixed film bioreactors are more stable than suspended growth systems (Malone and Pfeiffer, 2006). In a fixed film biofilter, a thin bacterial biomass coats the filter media and the dissolved nutrients and oxygen are transported by diffusion into the biofilm. Numerous types of media have been employed to support this biofilm, including rock, shells, sand, plastic, etc. Anything that supports a biofilm having a reasonable specific surface area has been used over the years.

The major drawback to these types of filters is that they can be quickly ‘smothered’ by heterotrophic bacteria degrading its performance. Malone and Pfeiffer (2006) subdivided fixed film biofilters into four fundamental blocks distinguished by the strategy used to provide oxygen

and the techniques used to handle excess biofilm growth (Fig. 2.7). Biofilters employ different strategies to fulfill their design guidelines for nitrification. Malone and Pfeiffer (2006) established a decision tree with the numerous options available for providing oxygen and bio-film growth handling.

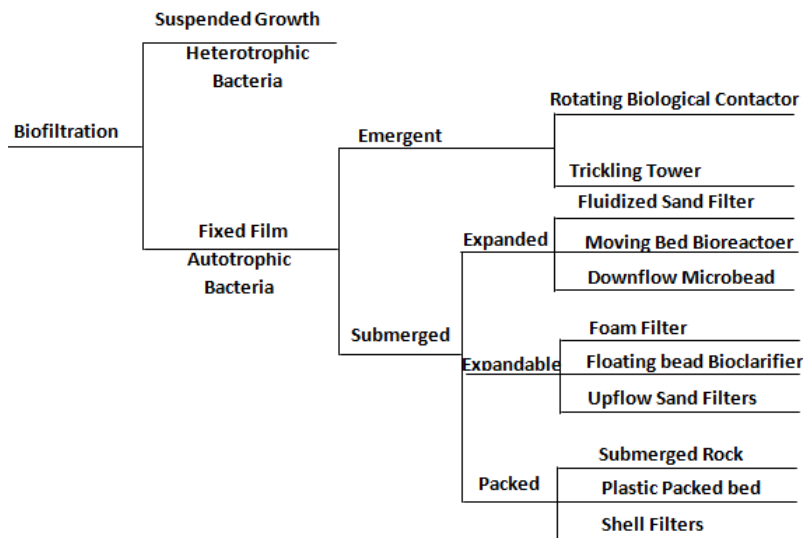


Fig. 2.7. An organizational tree of Biofilters (Malone and Pfeiffer, 2006).

An ideal biofilter would maximize the media specific surface area and remove 100% of the inlet ammonia concentration, generate very little nitrite and maximize oxygen transfer. It will also use a small footprint, inexpensive media, and present minimum head loss; require very little maintenance without capturing solids. Unfortunately there is no biofilter that meets all of these properties. Each biofilter will present its own advantages and weaknesses for a given application. Currently large scale commercial re-circulating systems have been moving towards using granular filters (expanded beds, fluidized beds and floating bead beds). However, there are many types of bio-filters that are commonly used in intensive RAS: submerged bio-filters, trickling bio-filters, rotating biological contactors (RBC), floating bead bio-filters, moving bed bioreactors, fluidized-bed bio-filters and countless others.

Emergent biofilters provide biofilm aeration taking advantage of the oxygen in the air. Rotating biological contactors (RBC) rotate the media slowly in and out of the water, providing both nutrients and aeration. Trickling biofilters allow the water to cascade over the media in a column, transporting both nutrients and oxygen towards the media having biofilm growth. These types of biofilters are capable of high aerial ammonia conversion rates, but are limited by low specific surface area.

These types of filters also provide some carbon dioxide stripping and reduced system aeration requirements. Trickling biofilters consist of a fixed media bed through which a pre-filtered wastewater trickles down the filter height, Fig. 2.8. Like RBCs, the media is never completely submerged so bacteria can get oxygen from both exposures to air and extraction from water. Trickling filters like RBCs rely on passive biofilm shedding, so they can become clogged with excess heterotrophic growth; it reduces substrate transport and depress nitrification. RBCs and trickling filters have very similar nitrification rates.

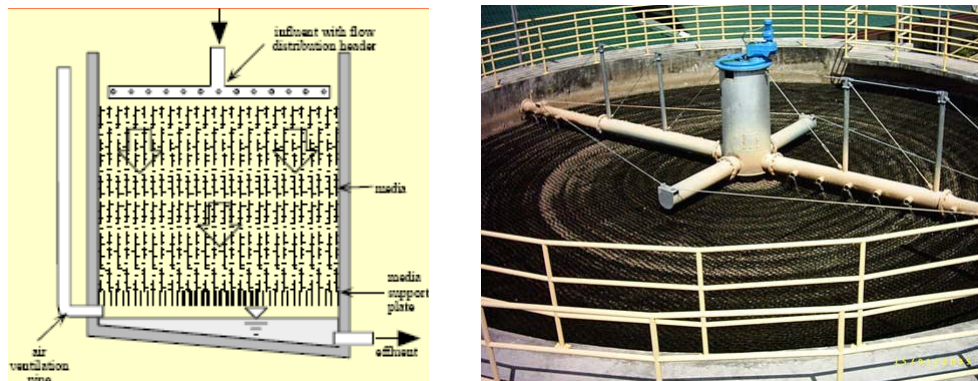


Fig. 2.8 Trickling filter.

The wastewater flows downwards over a thin aerobic biofilm diffusing the dissolved substrates into the biofilm where they are consumed by the nitrifying bacteria. As it trickles over the media, the water is continuously oxygenated and carbon dioxide is removed by the ventilated air. Trickling filters have been widely used in aquaculture, because they have a moderate cost, are

easy to construct and operate, are self-aerating and very effective at off gassing carbon dioxide. [Eding et al., \(2006\)](#) has published an excellent review on the design and operation of trickling towers.

In municipal waste water treatment systems, trickling filters were traditionally constructed of rocks, but today most filters use plastic media, because of its low weight, high specific surface area ($100\text{--}300\text{ m}^2/\text{m}^3$) and high void ratio ($>90\%$). A specific surface area of $150\text{--}200\text{ m}^2/\text{m}^3$ is the most suitable for corrugated plastic media applied in wastewater treatment, ([Eding et al., 2006](#); [Boller and Gudjer, 1986](#)). Bionet, Filterpac and Munters specific surface areas for plastic media are $160\text{ m}^2/\text{m}^3$, $200\text{ m}^2/\text{m}^3$ and $234\text{ m}^2/\text{m}^3$, respectively ([Kamstra et al., 1998](#)). Rotating biological contactors (RBC, Fig. 2.9) have been used in the treatment of domestic wastewater for decades ([Van Gorder and Jug-Dugakovic, 2005](#); [Brazil, 2006](#)). Rotating biological contactors are widely used as nitrifying filters in aquaculture applications. RBC technology is based on the rotation of a biofilter medium (bio-discs) attached to a shaft which is partially submerged in water.

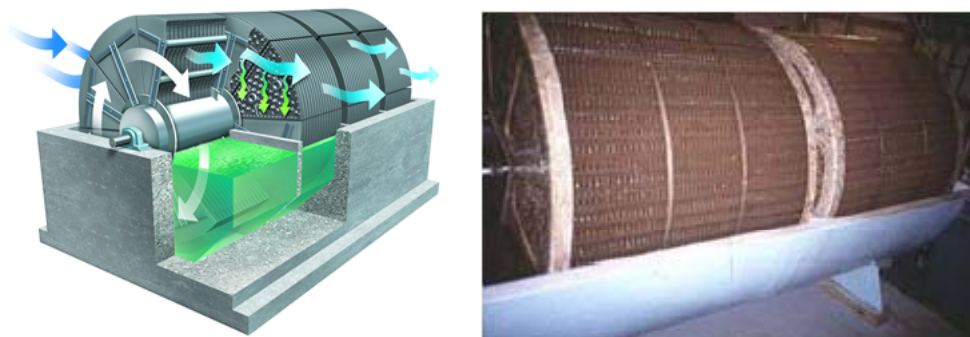


Fig. 2.9. Rotating Biological Contactor.

Approximately 40% of the substrate is submerged in the recycled water. In aquaculture applications, volumetric nitrification rates of approximately $76\text{ g TAN}/\text{m}^3$ per day can be expected with this type of biological filter ([Wheaton et al., 1994](#)). The discs are rotated slowly at 1.5- 2.0 rpm to expose the biologically active media to the nutrient recirculated water and to the

air providing oxygen to the biofilm. Early RBC designs were fabricated from discs of corrugated fiberglass with low specific surface area ($164 \text{ m}^2/\text{m}^3$). On average, they convert about 1,250 mg of ammonia per cubic foot of media per day to nitrate (Golz, 1995). Media with higher specific surface area ($258 \text{ m}^2/\text{m}^3$) are utilized in RBC construction, reducing physical size and increasing ammonia and nitrite removal capacity. Hochheimer and Wheaton (1998) recommended a maximum hydraulic loading design limit for RBCs of $300 \text{ m}^3/\text{m}^2 \text{ day}$. Brazil (2006) determined an average total ammonia nitrogen areal removal rate of $0.43 \pm 0.16 \text{ g}/\text{m}^2 \text{ day}$ for an industrial-scale, air-driven RBC used to rear tilapia at $28 \text{ }^\circ\text{C}$. Van Gorder and Jug-Dugakovic (2005) reported higher rates for multiple commercial scale systems of $1.2 \text{ g}/\text{m}^2 \cdot \text{day}$.

Rotating biological contactors have inherent advantages for aquaculture, because they are self-aerating, require little hydraulic head, have low operating costs, provide gas stripping, and can maintain an aerobic environment. In addition, they tend to be self cleaning due to the shearing of loose biofilm caused by the rotation of the media through the water. The main disadvantages of these systems has been the mechanical nature of its operation, the substantial weight gain due to biomass loading of the media and the resultant load on the shaft and bearings.

The first major category of submerged biofilters employ a fixed, static packed bed of media that has no active management of either biofilm or solids accumulation. Examples of fixed, static packed beds are submerged rock biofilters, plastic packed beds and shell filters. Submerged packed beds rely entirely upon endogenous respiration to control biofilm accumulation (Manthe et al., 1988). The water can flow either from the bottom up (up-flow) or from the top down (down-flow). Hydraulic retention time can be controlled by adjusting the water flow rate. Solids from the culture tank can accumulate within the submerged filter, along with cell mass from nitrifying and heterotrophic bacteria.

This process can eventually block void spaces, requiring a mechanism to flush solids from the filter for successful long term operation. Large void spaces prevent filter clogging requiring of large size media, such as uniform crushed rock over 5 cm in diameter or plastic media over 2.5 cm in diameter, Fig 2.10. However, 5 cm diameter crushed rock would only have a specific surface area of $75 \text{ m}^2/\text{m}^3$ and a void fraction of only 40 to 50%. Random packed plastic media would also have a relatively low specific surface area of $100\text{--}200 \text{ m}^2/\text{m}^3$, but a much higher void fraction, greater than 95%. These filter drawbacks are low dissolved oxygen and solids accumulation, resulting from heavy organic matter (feed) loading and back flushing difficulty.



Fig. 2.10. Rock packed bed biofilter.

The Tezontle is an original stone material of igneous rocks formed by solidification of molten magma originating from eruptions. Its type is Extrusive or that solidified on the surface quickly. Its composition is $\text{CaO} \cdot \text{Al}_2\text{O}_3 \cdot (\text{SiO}_2)_2$ (Vargas Tapia et al., 2008), the Structure of Tezontle present the oxide of Fe giving the red or black color, its characteristics depend on the presence of Hematite or magnetite. Table 2.4 shows some of the most important characteristics of Tezontle:

Table 2.4. Tezontle characteristics.

Group:	Oxides	Brightness:	Matt
Chemical formula:	CaO AlO ₃ (SiO ₂) ₂	Specific weight:	2.41 g/MI
Origin:	Volcanic	Porosity:	75.9%
Hardness:	5 Mohs	Loss by ignition:	0.49%
Texture:	Vesicular, Porous	Solubility in HCl 30%:	0.47%
Density:	From 1.2 to 1.6 kg/m ³	Solubility in NaOH 30%:	0.55%
Color:	Red or black	Abrasion loss:	0.60%

The volcanic rock has been tested as filter material for removing suspended solids ([Valdivia Soto et al., 2000](#); [Vaca Mier et al., 2001](#), [Navia et al., 2005](#)) in wastewater. In a pilot-filter domestic type ([Valdivia Soto et al., 2000](#)) reduce chemical oxygen demand, total suspended solids, ammonia and nitrates concentration and separation efficiencies of suspended organic matter up to 74% and a reduction of turbidity, with total elimination of coliform bacteria. ([Vaca Mier et al., 2001](#)). TSS removals of up to 95% and 80% COD ([Navia et al., 2005](#)).

Recently tested the removal of uranium very low concentrations and ratios have been reported for two species Langmuir stable in different pH, even without recommending appropriate application or report the removal efficiency obtained ([López Muñoz et al., 2009](#)). ([Ortiz Polo et al., 2007,2009](#)) reported that Tezontle has a very high removal efficiency of Cu(II), Cd (II), Co (II), Hg (II), Mn (II), Ni (II), Pb(II) and Zn (II) in water, without showing selectivity.

Medium sized fluidized sand biofilters (Fig. 2.11) have a surface area to volume ratio of 2297m²/m³ and will typically convert 17,500 milligrams of nitrogen per cubic foot of media per day which is 14 times higher than a RBC or trickling filter. The sand filter has two operational modes: filtration and washing. In the filtration mode, the flow rate is controlled to expand the bed

by 50%. Flow must be provided at high rates to prevent clogging, but taking care that it will not cause media scouring. Over time, when bacterial growth begins to clog the filter, a washing mode is initiated by increasing the flow rate to scour the sand. The fluidized-bed biofilter can easily be scaled to large sizes, and are relatively inexpensive to construct per unit treatment capacity (Summerfelt and Wade, 1997, Timmons, 2000).

Since this biofilter cost is roughly proportional to its surface area, fluidized-bed biofilters are cost competitive and small in size compared to other biofilter types (Summerfelt, 1999). Fluidized-bed biofilters are efficient for removing ammonia; typically removing 50-90% of the ammonia during each pass in cold- and cool-water aquaculture systems (Summerfelt et al., 2001). Nitrification rates for coldwater systems range from 0.2 to 0.4 kg TAN removal per day per cubic meter of expanded bed volume (Timmons and Summerfelt, 1998). In warmwater systems, TAN removal rates range from 0.6 to 1.0 kg per day per cubic meter expanded bed volume (Timmons et al., 1998).

The main disadvantages of fluidized-bed biofilters are the high pumping water cost through the biofilter and lack of water aeration, as do trickling towers and RBC's. Additional disadvantages are that they can be more difficult to operate and can have serious maintenance problems, usually due to poor suspended solids control and bio-fouling.

Microbead biofilteris distinctly different than the more commonly used floating bead filters, (Fig 2.11) (Timmons et al., 2006). Floating bead filters work in pressured vessels and use a media that is slightly buoyant. The required beads mass for the required volume (~700 kg per cubic meter) make the media relatively expensive; Sand or microbead media are less expensive on a per volume basis. Microbead filters use a polystyrene bead (microbead, density of 16 kg per cubic meter) that has a diameter of 1-3 mm compared to floating bead filters media of approximately 3 mm in diameter (Greiner and Timmons, 1998).

Microbead filters are considered a low-cost design alternative similar to fluidized sand filters because of their ability to be scaled to large production systems. A key advantage of microbead filters is that their operation cost will be 50% of conventional fluidized sand beds due to their ability to use low head high volume pumps (Timmons and Ebeling, 2007). For design purposes having influent ammonia-nitrogen levels from 2 to 3 mg/l, microbead filters can be assumed to nitrify approximately 1.2 kg of TAN per cubic meter of media daily for warm water systems. For cool water applications, rates should be assumed to be 50% lower than warm water rates (Timmons and Ebeling, 2007). These rates are similar to those used for fluidized sand beds.

Floating bead bioclarifiers are fixed expandable beds which utilize floating polyethylene beads that have a specific surface area of $350 \text{ ft}^2/\text{ft}^3$, and convert about 8,750 milligrams of nitrogen per cubic foot of media per day, (Fig 2.11). When the filter is used for both biological treatment and solids capture (Malone and Beecher, 2000) during the filtration mode, water flows up through the media where solids, soluble carbon, and ammonia are removed. Bead filters are often referred to as bio-clarifiers for their ability to perform both bio-filtration and clarification in a single unit. Clarification is the process of removing suspended solids from the water. Suspended solids in aquaculture are generally small particles (< 100 micron) of undigested or partially digested food, bacteria, algae, clay, and silt, suspended in the water column. The beads used are food-grade polyethylene 3-5 mm in diameter with a specific gravity of 0.91; its specific surface area is of $1150\text{-}1475 \text{ m}^2/\text{m}^3$ (Malone et al., 1993). Floating bead filters are resistant to bio-fouling and generally require little water for backwash.

The bead filter is typically either bubble-washed or propeller-washed during the backwash procedure. In this procedure bed expands and separates trapped solids from the beads. Bead filters advantages include their modular and compact design, ease of installation, and operation (Timmons and Ebeling, 2007). In addition, they can be used as a hybrid filter for both solids

removal and nitrification. The propeller-washed bio-clarifiers are operated in the filtration mode most of the time, (Fig. 2.11). The disadvantage is that solids are held in a place where they can degrade and affect system's water quality. In general, using these filters will require the designer to provide for more oxygenation and biofiltration capacity.



Fig. 2.11. Bead filters are distinguished by the way the beads are washed. The bubble washed unit is cleaned by draining and the propeller-washed units are intermittently cleaned by a propeller and The Poly Geyser Bead Filter is the next generation in Bead Filter technologies primarily through its automatic pneumatic backwash mechanism Microbead Biofilter.

2.2.3. Aeration process

Gas dissolution in water involves four major steps, and each has the potential of being rate limiting, (Fig. 2.12) (Boyd and Watten, 1989). In step 1, oxygen moves from the bulk gaseous phase into the gas-liquid interface. In step 2 and 3, the oxygen diffuses through laminar gas and laminar liquid films, respectively. In step 4, the oxygen enters the bulk liquid phase. Under normal conditions, gas transfer resistance occurs primarily in step 2 and 3. The transfer of highly soluble gases, such as ammonia, is restricted to the gas film while the transfer of less soluble gases, such as oxygen and nitrogen are restricted within the liquid film. In the latter case, the transfer rate is proportional to the differential between existing and saturated of a gas in solution.

This relationship can be expressed by the Lewis-Whitman gas transfer model (Lewis and Whitman, 1924):

$$\frac{dc}{dt} = \frac{D}{\Delta} \frac{A}{V} (C_s - C_m) \quad 2.11$$

When $(C_s - C_m)$ is positive (under-saturation), gas will transfer from the atmosphere into the bulk liquid. If $(C_s - C_m)$ is negative (super-saturation) gas will transfer from the liquid to the atmosphere. It's difficult to measure interface film Δ and A , therefore the ratios A/V and D/Δ are usually combined into a composite term called the *overall gas transfer coefficient* ($K_L a$) such that

$$\frac{dc}{dt} = K_L a (C_s - C_m) \quad 2.12$$

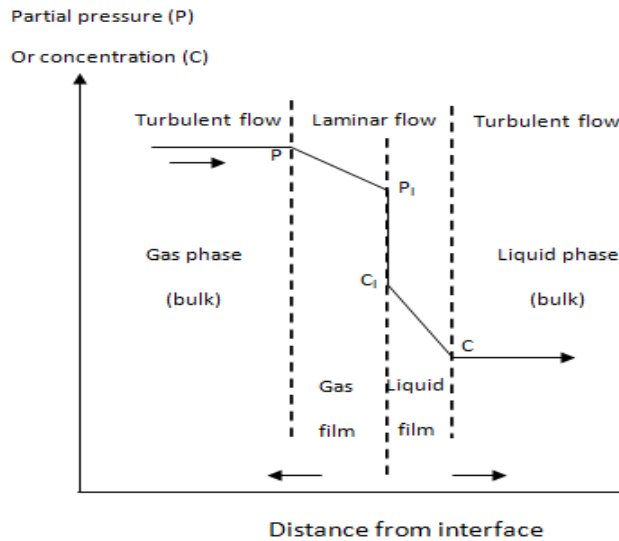


Fig. 2.12. The four-step gas transfer process.

The overall gas transfer coefficient represents conditions in a specific gas-liquid contact system (Boyd 1990). The rate of gas transfer can be increased by reducing the thickness of the interface film (Δ), by increasing the surface area of contact (A) or by increasing the value of $(C_s - C_m)$. Turbulence and/or mixing are required for rapid transfer of oxygen to or from the atmosphere. All aerators (except for some pure oxygen aeration systems) increase the rate at

which oxygen is transferred to water after creating turbulence and/or mixing. Turbulence is difficult to estimate, but it's possible to obtain the K_La value empirically between two points.

Integration of the previous equation:

$$K_La = \frac{\ln(OD)_1 - \ln(OD)_2}{t_2 - t_1} \quad 2.13$$

2.2.3.1. Aerators for aquaculture systems

There are many different types of aerating devices that are used in aquaculture. These fall into the broad categories of mechanical aerators, gravity aerators, and air diffusion systems. Mechanical aeration is achieved imparting mechanical energy to water in order to break it up into droplets. Oxygen transfer is enhanced by increasing the air-water interface area. Mechanical aerator is driven by electric motors or internal combustion engines. Surface aerators are devices that break up or agitate the water surface such that larger oxygen transfer rates are achieved. Water drawn into the vertical tube by a propeller, is pumped upward, deflected radially, and sprayed in an umbrella pattern over the water surface (Fig. 2.13A). [Boyd and Martinson \(1984\)](#) stated that in comparison tests, spray type-surface aerator transferred 1.34 to 1.91 kg O₂/kW-h. [Wheaton \(1993\)](#) reported that the oxygen transfer rate (kgO₂/h) depends on different variables as (1) depth of submergence, (2) rotor speed, (3) rotor diameter, (4) unit volume of liquid being aerated, (5) oxygen concentration gradient, and (6) aerator design. [Cancino \(2004\)](#) designed and tested a small surface aerator with propeller having a diameter of 94 mm, an inlet angle of 11° and an exit angle of 25° which yielded standard aeration efficiency (SAE) of 1.805 kg O₂/kW-h.

A vertical pump aerator consists of a submersible, electric motor with an impeller attached to its shaft. The motor is suspended by floats, and the impeller pushes water into the air to apply the aeration. A vertical pump aerator is shown in Fig. 2.13. These aerators are manufactured in sizes ranging from less than one kW to over 50 kW, but those used for aquaculture are seldom larger

than 2 kW. Units for aquaculture have high speed impellers, which rotate at 1730 or 3450 rpm. Vertical pump aerators cause a water circulation pattern similar to that of diffused air systems (Boyd and Tucker, 1998). Losordo et al., (1992) reported that vertical pump aerators on average are 50 percent more efficient at transferring oxygen than air stones diffusers based on the analysis of data listed by (Boyd, 1990). A pump sprayer aerator consists of a high-pressure pump that discharges water through a series of orifices or slots in a pipe manifold (Fig. 2.13C and D). Many different orifice designs are used. Sizes typically range from about 2 to 15 kW and the impeller speeds range from 500 to 1000 rpm (Boyd and Tucker, 1998).

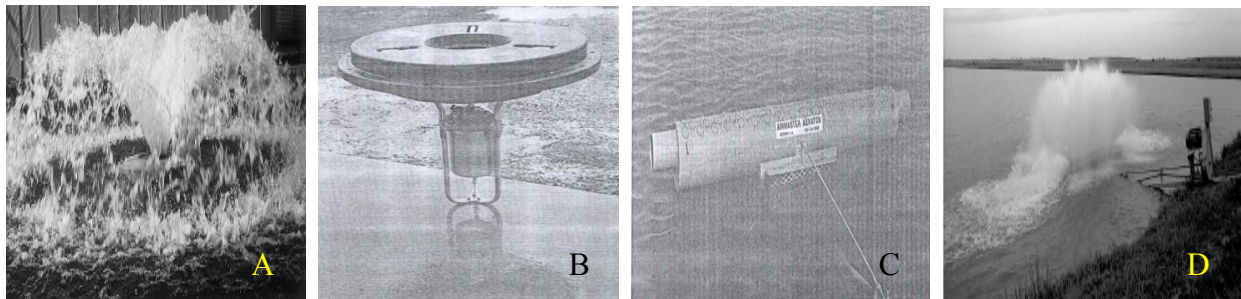


Fig. 2.13. A vertical pump aerator and a pump sprayer aerator (Boyd, 1998) and (Lawson, 1995).

The paddlewheel aerator is at present the most efficient aerator due to the combined way in which it rapidly destratifies a pond through strong water circulation and aeration spraying water into the air. As well, it drags air into the water creating large surface areas of air/water interface allowing an efficient gaseous exchange (oxygen in and harmful gas out). Paddle-wheel aerator consists of a rotating hub with attached paddles. The rotating paddlewheel splashes water into the air to affect aeration. The device consists of floats, motor, speed reduction mechanism, coupling, paddlewheel, and bearings. The paddles can be set deeper into the water to increase water circulation while sacrificing oxygen exchange. Moore and Whitis (1999) used a 7.5 kW paddlewheel aerator for a 2.7 ha pond surface as a vertical aerator and they measured dissolved oxygen profiles at a 3.6 m depth during daylight hours. Boyd and Watten (1989) mentioned that

power requirements are on order of 1 kW for each 50 cm of paddle length, (Fig. 2.14A). [Ahmad and Boyd \(1988\)](#) stated that the highest oxygen transfer efficiency was achieved with a paddlewheel 91cm in diameter with triangular paddles (120 to 135° interior angle) spiraled on the hub, (Fig. 2.14B). ([Chen et al., 1988](#); [Wyban et al., 1989](#)) used Taiwanese paddle-wheel aerators in intensive shrimp culture ponds, (Fig. 2.14C).

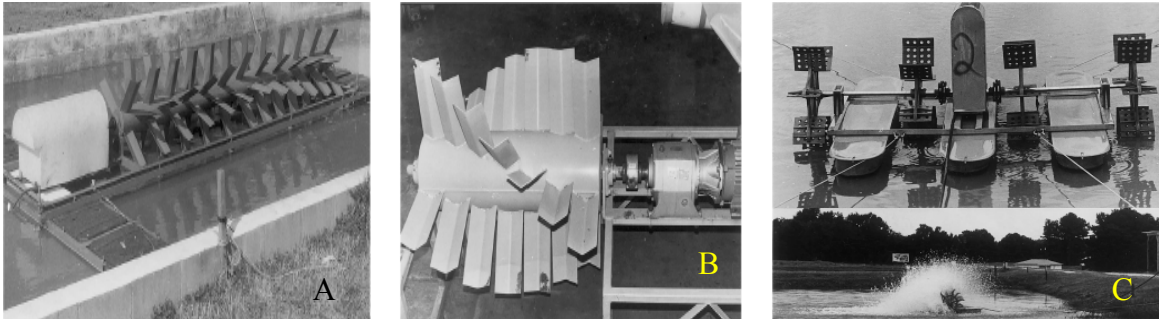


Fig. 2.14. (A) floating electric paddlewheel aerator (B) triangular paddles (135° interior angle) spiraled on the hub (C) Taiwan paddle wheel aerator.

Diffuser aerators inject air into a body of water in the form of bubbles, and oxygen is transferred from the bubbles to the water by diffusion across the liquid film. Bubbles rise in a water column being a relative motion between water and bubbles. This causes water circulation and a renewing of the surface area in contact with the bubble, increasing oxygen transfer. Simple diffused-air aerators use an air compressor or an air blower to provide air to diffusers positioned on the pond bottom or suspended in the water, (Fig. 2-15A). A variety of types of diffusers have been used, including ceramic domes, porous ceramic tubing, porous paper tubing, perforated rubber tubing, perforated plastic pipe, packed columns, and carborundum air stones. The minimum operating pressure increases with increasing water depth above the diffuser, since enough pressure must be provided to force air from the diffuser against the total pressure (atmospheric plus hydrostatic) at the discharge point ([Boyd, 1990](#)). [Boyd and Ahmad \(1987\)](#) stated that simple diffused aeration is not efficient in shallow ponds commonly used for fish

REVIEW OF LITERATURE

production (depth = 1.0-1.5 m) because the contact time of the air bubbles with the water is not great enough for sufficient oxygen transfer. With diffuser depths about 0.9 – 1.2m average (standard aeration efficiency) SAE values are around 0.5 kgO₂/kW-h. Lawson (1995) reported average operating costs for diffused-air systems of \$0.095/kg O₂ compared to \$0.053/kg O₂ for paddle wheels, \$0.059/kg O₂ for propeller-aspirator pumps, \$0.079/kg O₂ for vertical pumps, and \$0.079/kg O₂ for pump sprays. The diffuser pores also clog easily in fish ponds and culture tanks, requiring frequent maintenance. Boyd (1995) placed the diffuser in a bore hole drilled about 3 m within the pond bottom (Fig.2-15B). The unit consists of an outer casing and an inner riser pipe, being the air diffuser suspended beneath the riser pipe. In operation, fine air bubbles released by the diffuser ascend the riser pipe creating an air lift to pump water upward. Water from the pond bottom descends in the space between the casing and the riser pipe to replace the rising water. The bore hole provides depth to increase hydrostatic pressure on the rising bubbles. Greater pressure facilitates the dissolution of oxygen into water from the rising air bubbles. This device has an extremely high efficiency for transferring oxygen from air bubbles to water. The individual units are small, so several units must be placed in a pond to cause uniform aeration and mixing.

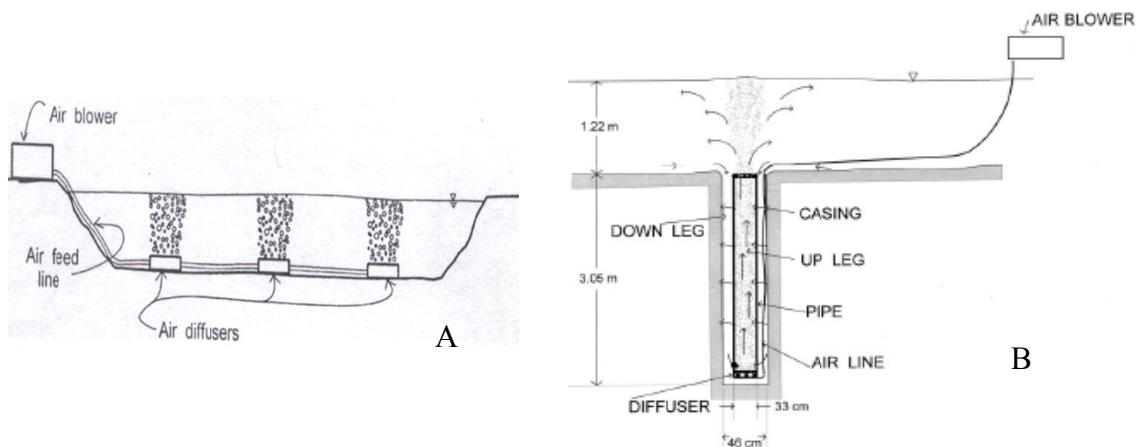


Fig. 2.15. (A) Simple diffused-air aerator (B) diffused-air aeration system with diffuser mounted in a bore hole in the pond bottom.

Parker (1983) designed an air-lift pump which is illustrated in (Fig. 2.16A). The pump is constructed with a PVC pipe, termed the eductor and a PVC elbow. Air from an air blower is released through a 90° hose adaptor into the PVC pipe. If desired, an air diffuser that releases smaller bubbles of air can be placed in the pipe. The rising air bubbles lift water through the eductor and discharge it at the surface. A pump holder is attached between the anchor post and the pump. This holder contains a flotation device and it permits the pump to pivot. Ballast must be provided at the bottom of the pump. Loyless and Malone (1998) developed and evaluated air lift-pump capabilities for water circulation, aeration, and degasification (for stripping carbon dioxide) for recirculating aquaculture systems. The air-lift was constructed from 2" PVC with a double 'way' inlet and a combination 90 and 45° outlet. The air was injected through 3/8" tubing, either terminating into 6" air stones or open-ended (Fig. 2-16B).

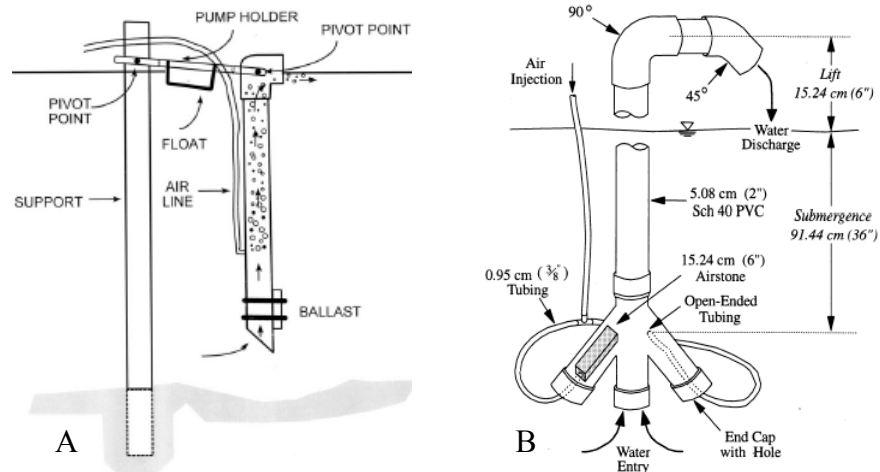


Fig. 2.16. An air lift pump

Propeller-aspirator aerators function according to the Venturi principle. The primary parts of a propeller-aspirator-pump aerator are an electric motor, a hollow shaft which usually rotates at 3450 rpm, a hollow housing inside which the rotating shaft fits, a diffuser, and an impeller attached to the end of the rotating shaft (Fig. 2.17). In operation the impeller accelerates the water sufficiently to cause a pressure drop within the hollow tube to force atmospheric air into the tube.

The air passes through the diffuser and enters as fine bubbles that are mixed by the impeller. These aerators provide water circulation in addition to aeration.

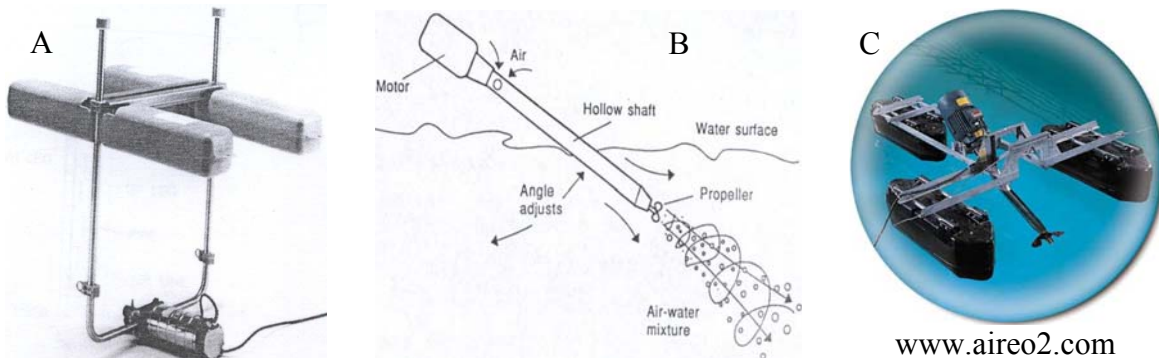


Fig. 2.17. Propeller-aspirator-pump aerator (A) designed to propel water horizontal to the pond surface (B and C) to propel water with angle.

Propeller-aspirators are manufactured with motor sizes varying from 0.37 to over 11 kW. In practice the float supports the motor and shaft at an angle with the water surface and the angle can be adjusted to operate in either deep or shallow water conditions. [Boyd and Martinson \(1984\)](#) found that 30° was the best angle for maximum oxygen exchange, give SAE averages of 1.73 to 1.91 kg O₂/kW-h. The other type has the entire aerator assembly suspended beneath the water; water is directed horizontally to the surface, (Fig. 2.17A). [Ruttanagosrigit et al., \(1991\)](#) indicated that the propeller aspirator pump aerator was more efficient than the Taiwan-style paddlewheel aerator at salinities of 10-30 PPT (aeration efficiencies averaged 1.2 and 0.85 kg O₂/kW-h respectively).

Gravity aerator is the simplest way to aerate in flowing water aquaculture systems like race way ponds, if a sufficient gradient exists. Man-made gravity aerators utilize the energy released when water loses altitude to transfer oxygen. Gravity aerators consist of weirs, splashboards, lattices, and screens. To evaluate the efficiency of a gravity aerator ([Chesness and Stephens,](#)

1971; Tebbutt, 1972) dissolved oxygen concentration is measured in water above and below the aerator.

$$E = \frac{DO_b - DO_a}{DO_s - DO_a} \times 100 \quad (2.14)$$

Water may pass over a simple weir, fall onto a splashboard, flow across a screen or an expanded metal sheet, flow down an inclined corrugated sheet (with or without holes), flow down a stair-step surface with holes called lattice, or pass down a stair-step surface without holes that is known as a cascade, Fig. 2-18. They are used individually, or in combination with other devices to enhance aeration, such rotors or brushes Fig. (2-18 B).

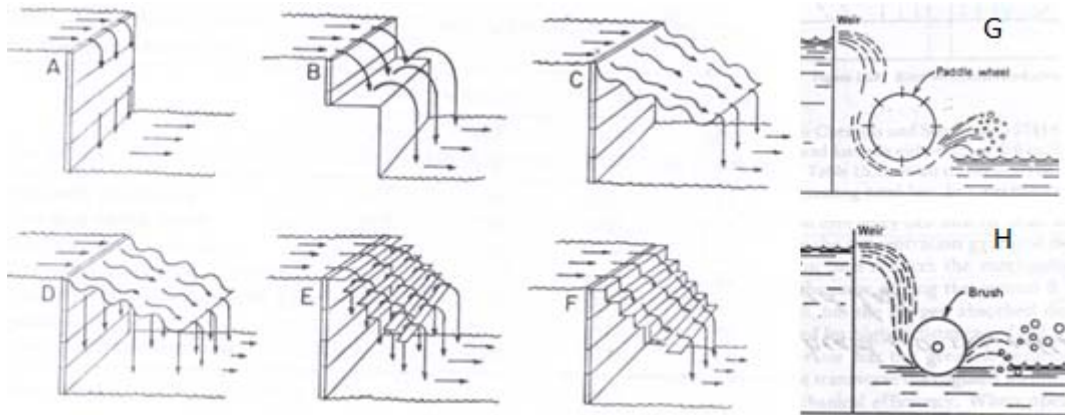


Fig. 2.18. Various types of gravity aerators, (A) simple weir, (B) weir with splashboard, (C) corrugated sheet, (D) corrugated sheet with holes, (E) lattice, and (F) cascade (Soderberg, 1982). Examples of gravity aeration combined with other device (G) weir with paddlewheel; (H) weir with rotating brush (Wheaton, 1993).

Simple weirs were the least efficient of the aerators tested. A series of screens, perforated trays, or expanded metal sheets can be stacked one above the other in a box (Wheaton, 1993). Typical spacing between trays is 10-25 cm and 4-10 trays are commonly used. An aerator with a height of 1m usually can provide at least 70-80% saturation of water with oxygen.

2.2.3.2. Aeration management

Emergency aeration is commonly practiced in larger ponds of 3 to 20 acres and involves the use of splash or spray type aerators typically powered by tractors or electric/fuel driven motors. This aeration is used only when dissolved oxygen drops to levels stressful to fish. Inherent in this approach is the need to frequently monitor oxygen in the pond to anticipate when crises may arise. Maintenance aeration systems are intended to prevent critical low oxygen levels from occurring. Aeration systems of this type typically include a low-pressure high-volume blower, PVC and/or polyethylene distribution pipe, and air releasers. Often small bubble diffusers are used to maximize oxygen transfer from the air stream. Air is released near the pond bottom, aerating and mixing water as it rises to the surface. These systems are relatively energy efficient and when operated continuously create and sustain an improved environment for fish production. Total operating costs may be higher for the maintenance systems, but labor cost of oxygen monitoring is reduced. Risk due to low oxygen kills is minimized, and higher production per acre realized. Oxygen maintenance systems usually entail higher purchase and installation costs, but again the benefits realized can offset the initial expense over a relatively short period of time.

Standard aerator efficiencies (SAE) for several types of aerators commonly used in aquaculture systems are listed in table 2.4. The SAE for all aerators shown ranges from 0.6 to 3.0 kg O₂/kW-h. Paddlewheels, in general, are more efficient at transferring oxygen and circulating water than other types of aerators, based on performance in clean water tanks (Boyd and Ahmad, 1987).

Table 2.5. Relative efficiencies of various aeration devices.

Aeration device	Standard aerator efficiency (Kg O ₂ /kW h)	Reference
<i>Gravity aerators</i>		
Cascade weir (45°)	1.5 – 1.8	Colt and Orwicz (1991)
Corrugated incline plane	1.0 – 1.9	Colt and Orwicz (1991)
Horizontal screen	1.2 – 2.6	Colt and Orwicz (1991)
Lattice	1.8 – 2.6	Colt and Orwicz (1991)
Average transfer efficiencies	1.2 – 2.3	Chesness and Stephens (1971)
<i>Packed column</i>		
Zero head	1.2 – 2.4	Colt and Orwicz (1991)
0.5 – 1 m head	10 – 80 ^a	Colt and Orwicz (1991)
<i>Surface aerators</i>		
Low speed surface	1.2 – 2.4	Colt and Orwicz (1991)
Low speed surface with draft tube	1.2 – 2.4	Colt and Orwicz (1991)
High speed surface	1.2 – 2.4	Colt and Orwicz (1991)
Vertical pump	0.7 – 1.8	Colt and Orwicz (1991)
Pump sprayer	0.9 – 1.9	Colt and Orwicz (1991)
Paddle wheel	1.1 – 3.0	Colt and Orwicz (1991)
<i>Subsurface aerators</i>		
Aeration cone	2.5	Colt and Orwicz (1991)
Air-lift pump	2.0 – 2.1	Colt and Orwicz (1991)
Air diffuser	0.6 – 3.9	Boyd (1990)
Air diffuser Fine bubbles	1.2 – 2.0	Colt and Orwicz (1991)
Air diffuser Medium bubbles	1.0 – 1.6	Colt and Orwicz (1991)
Air diffuser Coarse bubbles	0.6 – 1.2	Colt and Orwicz (1991)
Propeller aspirator	1.7 – 1.9	Colt and Orwicz (1991)
Propeller aspirator	1.3 – 1.8	Boyd (1990)
Nozzle	1.3 – 2.6	Colt and Orwicz (1991)
Static tube	1.8 – 2.4	Colt and Orwicz (1991)
U-tube	0.7 – 2.3	Colt and Orwicz (1991)
Venturi	2.0 – 3.3	Colt and Orwicz (1991)

^a = doesn't include power to the pump.

2.2.3.3. Impact of aeration on fish farms productivity

In most pond culture operations, aeration offers the most immediate and practical solution to water quality problems encountered at higher stocking and feeding rates. The aeration has higher effect on fish growth rate than other parameters. [Loyacano \(1974\)](#) reported that channel catfish production was increased from 2700 kg/ha in control ponds to 5500 kg/ha in aerated ponds with continuous diffused aeration. [Parker \(1979\)](#) used several types of aeration and water exchange to increase channel catfish production from 3000 kg/ha in control ponds to 15000 kg/ha in aerated ponds. [Plemmons and Avault \(1980\)](#) used a combination of continuous aeration with floating electric aerators, emergency aeration with PTO aerators and water exchange producing a channel catfish yield of 12800 kg/ha. Maximum net production of 6000 kg/ha, when feeding rates rose to 168 and 224 kg/ha, feed conversion ratio was 2.5 and 16.5kg fish biomass/kg food, respectively. [Sandifer et al., \(1987\)](#) stocked 45 post-larval *P. vannanei* /m² having paddlewheel 7.5 kW/ha aerators with an average water exchange of 17.5% per day. The production increased to 7500 kg/ha in 169 days. [Chen et al. \(1988\)](#) indicated that shrimp can be reared in intensive systems with aeration producing 12000 kg/ha (*Penaeus penicillatus*) in 141 days. Ponds were stocked initially with 286 post-larval/m². They used aeration with paddlewheel aerators at 11.7 kW/ha and water exchange up to 30% of pond volume per week. Dissolved oxygen concentration remained above 3.5 mg/L and the feed conversion factor was 1.7. [Wyban et al., \(1989\)](#) stocked six earthen ponds with area of 0.4 ha for each with *P. vannanei* of 25 post-larval /m². Three ponds were aerated at 3.7 kW/ha with Taiwanese paddlewheel aerators and three ponds were not aerated. Water was exchange of 0.8 and 2.2% of pond volume per day in aerated and unaerated ponds, respectively. All other management procedures were identical between treatments. Average shrimp production was 2852 kg/ha in aerated ponds and 2061 kg/ha in unaerated ponds. Feed conversion ratios were 3.2 and 3.8 in aerated and unaerated ponds, respectively. The net

value of the shrimp crop of aerated ponds was 42% greater than that of the unaerated ponds. [Rockey and McGinty \(1989\)](#) indicated that with continuous use of two to four, one horse power paddlewheel aerators per pond at stocking rates of tilapia 12000 to 20000/acre have been used in 1.2 to 2.5 acre, yields for a single crop range from 6 to 10 ton/acre.

[\(Diana et al., 1994; Diana et al., 1995\)](#) reported that Tilapia yields of 11,000-15,000 kg/ha in 5-8 months were achieved in Thailand ponds in aerated, fertilized and fed ponds stocked with 3 fish/m². [Yi and Lin \(2001\)](#) stated that nighttime aeration for 5 h enhanced the growth of tilapia in the integrated cage-cum-pond system with 4 cages/pond, and increased the carrying capacity. Net yield of caged tilapia in aerated ponds averaged 6.92 ± 0.60 t/ha/crop, which was significantly ($P < 0.05$) higher than that (3.65 ± 0.22 t/ha/crop) in unaerated ponds with four cages each.

2.3. Dissolved oxygen budgets in aquaculture systems

The oxygen demand varies with fish species, life stage, size, stock health, water temperature, feeding regime (time after feeding), ambient dissolved oxygen concentrations, activity or swimming. [Marvine and Heath \(1968\)](#) stated that fish also consume less oxygen when exposed to low oxygen concentrations for a prolonged period. Channel Catfish subjected to gradual hypoxia reduced oxygen consumption from about 100 mgO₂/kg/h at 100% oxygen saturation to about 30 mgO₂/kg/h at about 25% oxygen saturation. [Willoughby \(1968\)](#) related oxygen consumption to the amount of food fed to trout in hatcheries with the following expression:

$$(DO_{inf} - DO_{eff}) \times 0.0545 \times Q_H = F \quad (2.15)$$

[Farmer and Beamish \(1969\)](#) mentioned that the oxygen consumption increases substantially with activity. Nile Tilapia (*Tilapia nilotica*) forced to swim against a current of 30 cm/s consumed 220 mgO₂/kg fish/h, and 460 mgO₂/kg fish/h swimming at 60 cm/s. [Elliot \(1969\)](#) studied the oxygen consumption rate for Chinook Salmon between 1.85 and 17.5g in weight. He

REVIEW OF LITERATURE

measured the DO concentrations above and below groups of fish under hatchery conditions and developed an empirical method for estimating their rate of oxygen consumption.

1- For fish from 1.85 to 5.90 g

$$SOC_B = (0.02420T - 0.7718) - [(0.001242T_B - 0.04544)(Wg - 1.85)] \quad (2.16)$$

2- For fish from 5.90 to 17.50 g

$$SOC_B = (0.01917T - 0.5877) - [(0.0003676T_B - 0.011601)(Wg - 5.90)] \quad (2.17)$$

Liao (1971) collected oxygen consumption data for trout and Pacific Salmon in hatcheries and developed an equation that predicts oxygen uptake when water temperature and average fish size are known:

$$SOC_R = kT_B^n W_{lb}^m \quad (2.18)$$

where m and n are slopes, the following constants were provided:

Species	T, °F	k	m	n
Salmon	≤50	7.20x10 ⁻⁷	- 0.194	3.200
Salmon	>50	4.90x10 ⁻⁵	- 0.194	2.120
Trout	≤50	1.90x10 ⁻⁶	- 0.138	3.130
Trout	>50	3.05x10 ⁻⁴	- 0.138	1.855

Andrews and Matsuda (1975) Reported that catfish held under constant environmental conditions decreased in respiration rate after feeding as follows:

Time after feeding	Oxygen consumption (mgO ₂ /kg/h)
Immediately after feeding	520
1 h after feeding	680
Fasted overnight	380
Fasted 3 days	290
Fasted 9 days	290

The increase of oxygen consumption is due to the metabolic demands associated with digestion and assimilation of food. [Schroeder \(1975\)](#) gave a general equation for calculating fish respiration at 20 - 30°C,

$$OC = W_g^{0.82} \quad (2.19)$$

[Boyd et al. \(1978\)](#) used data from [Andrews and Mastuda \(1975\)](#) to develop the following equation for estimating channel catfish respiration.

$$SOC_I = 1000 \left[\text{antilog}(-0.999 - 0.000957W_g + 0.0000006W_g^2 + 0.0327T_I + 0.000008T_I^2 + 0.0000003W_gT_I) \right] \quad (2.20)$$

[Muller-Fuega et al. \(1978\)](#) presented an equation for estimating oxygen consumption by rainbow trout:

$$SOC_I = \alpha W_g^\beta 10^\gamma \quad (2.21)$$

The constants α , γ and β values are as follows:

Constant	4-10, °C	12-22, °C
α	75	2.49
γ	- 0.196	- 0.142
β	0.055	0.024

[\(Jobling, 1981; Wells et al., 1983\)](#) indicated that oxygen consumed faster by fish that have recently eaten than by fasted fish. The increase in oxygen consumption following the ingestion of food (commonly termed specific dynamic action) is greater as feeding rate (FR) rises. [Grottum and Sigholt \(1998\)](#) developed a model for estimate oxygen consumption as a function to body weight, temperature and swimming speed for Atlantic Salmon (*Salmosalar*):

$$SOC_I = 61.6(\pm 6.6)BW_{kg}^{-0.33(\pm 0.11)} 1.03(\pm 0.10)^{T_I} 1.79(\pm 0.10)^U \quad (2.22)$$

Ali (1999) presented the following equation to estimate oxygen consumption by tilapia,

$$SOC_I = 1892.0 + 4.33W_g - 161.3T_I - 0.0017W_g^2 + 3.89T_I^2 - 0.20W_gT_I \quad (2.23)$$

at following constraints

- Water temperature 24 to 32°C,
- Tilapia 19 to 203 g average individual fish weight,
- Feeding rate was according to [Rockey, 1989](#)

[Valverde and Garcia \(2004\)](#) estimated oxygen consumption for *Octopus vulgaris* with body weights between 0.22 and 3.26 kg at temperature of 13.75 – 22.23 °C;

$$\ln Mo_{2routine} = -0.726 + 0.702 \ln W_{kg} + 10876 \ln T_I \quad (2.24)$$

$$\ln Mo_{2sda} = 0.045 + 0.713 \ln W_{kg} + 1.769 \ln T_I \quad (2.25)$$

where, $Mo_{2routine}$ is the routine oxygen consumption, defined as the mean value of individual hourly oxygen consumption excluding the specific dynamic action period.

This represents an estimate of the energy needed for standard metabolism, and Mo_{2sda} is the post – prandial oxygen consumption, the value of individual hourly oxygen consumption in the specific dynamic action. Respiratory oxygen used in the aerobic decomposition of organic matter by heterotrophic bacteria, oxygen used in the oxidation of reduced inorganic substances by autotrophic bacteria (such as oxygen consumed in the oxidation of ammonia to nitrate by nitrifying bacteria), also oxygen consumed in various chemical reactions in pond soils. ([Wang 1980](#); [Barcelona, 1983](#)) indicated that oxygen used in chemical oxidation reactions may represent a significant fraction of the total oxygen used by sediment, such as the sediment at anaerobic conditions may contain a high concentrations of sulfides and consequently oxygen use in chemical reactions. [Boyd \(1979\)](#) named the amount of oxygen required by microorganisms to decompose the organic matter in the water under a specific set of conditions the biochemical

oxygen demand. (Sawyer and Mc Carty, 1967; Boyd, 1973) called that is the amount of oxygen required to completely oxidize all of the organic matter in a sample to carbon dioxide and water chemical oxygen demand. To reduce chemical or biochemical oxygen demand, farmers sometimes add calcium hydroxide or potassium permanganate to oxidize the organic matter and lower the demand for the dissolved oxygen. Bertholson (1992) Measured oxygen use in Mississippi Delta catfish ponds usually ranged between 100 and 200 mg O₂/m²/h.(Schroeder 1975; Boyd et al., 1978; Costa-Pierce et al., 1987; Teichert - Coddington and Green, 1993) Found that sediment oxygen up take in fresh water ponds usually yield lower values, usually between 50 and 125 mg O₂/m²/h. Phytoplankton is the most photosynthetic organism in freshwater ponds. Phytoplankton dynamics tend to dominate the oxygen cycle in most aquaculture ponds. Accurate prediction of the rates of phytoplankton growth and respiration is essential to obtain water quality in aquaculture ponds. The rates of oxygen production and consumption by phytoplankton vary as functions of environmental conditions and other parameters. The phytoplankton primary production rate takes into account the effects of light intensity, ammonia nitrogen concentration (as a source of inorganic nitrogen), water temperature, and the concentration of chlorophyll *a*., in presence of sunlight phytoplankton tends to release oxygen into pond water by photosynthesis, and otherwise at night or on cloudy days, phytoplankton remove oxygen from the water for respiration. Normally, phytoplankton produce more oxygen than they consume, thus providing oxygen for the fish and other organisms in the pond (Lu and Piedrahita, 1997).

Low oxygen depletions are often caused by an imbalance in the phytoplankton community. Although oxygen depletion can sometimes be predicted before it occurs, it can develop suddenly without warning. So Boyd et al., (1978) presented a convenient equation to determine the oxygen consumption by planktonic community based on chemical oxygen demand and water temperature:

$$POC = 1.006 - 0.00148 (COD) - 0.0000125(COD)^2 + 0.0766T_I - 0.00144T_I^2 + 0.000253 CT_I \quad (2.26)$$

Lu and Piedrohita (1997) used this equation to simulate the phytoplankton respiration rate:

$$PhOC = SphOC \times f(t) \times \frac{DO}{SOC + DO} \quad (2.27)$$

Phytoplankton produces oxygen by photosynthesis during the day but are the major consumers of oxygen at night. The magnitude of daily changes in DO is influenced primarily by light intensity and phytoplankton density. (Brune et al., 2003) studied photosynthetic intensification techniques to use algae for add more oxygen beyond the commonplace practice of supplemental aeration for intensive aquaculture ponds. (Steele, 1962; Lehman et al., 1975; Welch, 1980; Drapcho and Brune, 2000) Measured algae oxygen production based on Total suspended solids (TSS) concentration of the culture water by using the following equation.

$$PhOP_{20} = PhOP_{\max 20} \frac{I}{I_{opt}} e^{-I/I_{opt}} \quad (2.28)$$

Some farmers add Copper sulfate crystals Copper sulfate liquid to make a control on the phytoplankton.

The Solubility of Oxygen

If air is in contact with water, oxygen will enter the water from the air until the pressure of oxygen in the water is equal to the pressure of oxygen in the air. Rather than dealing with the pressure of dissolved oxygen depends on its temperature, salinity, gas composition, and total pressure as related by Henry's law (Colt, 1984);

$$DO_e = 1000 K\beta (P - P_w) / 760 \quad (2.29)$$

The values of water vapor pressure (P_w) and dissolved oxygen solubility $1000\beta k$ can be obtained from table 7.1 (Appendix 1) as a function of water temperature to calculate equilibrium dissolved oxygen. The solubility of dissolved oxygen in water at different temperatures and salinities is presented in table 7.2 (Appendix 1). If water contains the amount of dissolved oxygen that it should theoretically hold at a given temperature, pressure, and salinity, it is said to be saturated with oxygen. The percent saturation of water with oxygen is calculated as (Lawson, 1995);

$$S = \frac{DO_m}{DO_s} \times 100 \quad (2.30)$$

The oxygen deficit is the difference between the measured DO concentration and the DO concentration at saturation. That is

$$OD = DO_s - DO_m \quad (2.31)$$

The solubility of oxygen in water also may be expressed as oxygen tension, the oxygen tension represents the partial pressure of oxygen in the atmosphere required to hold a certain concentration of oxygen in the water. The pressure or tension of DO in water can be estimated as (Boyd, 1998);

$$P_{O_2} = \frac{DO_m}{DO_s} \times 0.2095 \times 760 \quad (2.32)$$

2.4. Recirculating aquaculture system automation

The most important parameters to be monitored and controlled in an aquaculture system are related to water quality, since they directly affect animal health, feed utilization, growth rates and carrying capacities.

The primary water quality parameters include temperature, dissolved oxygen (DO), pH, ammonia, nitrites, nitrates, suspended solids, salinity, alkalinity, biochemical oxygen demand (BOD) and water flowrate. Water levels, availability of electric power, means of detecting fire, smoke and the intrusion of vandals should also be monitored.

Due to the cost and/or unreliability of sensors and associated equipment, most automated aquaculture systems do not attempt to monitor and control all of these parameters. It is recommended that temperature, DO, pH and water flow rate be monitored directly on a continuous basis since they tend to change rapidly and have a significant adverse effect on the system if allowed to operate out-of range. Other parameters change slowly and tend to stay in range if proper flow rate is maintained. For example, ammonia is usually not a problem if the biological filters are properly sized for the loading rate and if adequate flow is maintained. In this case, flow rate is the critical parameter that should be monitored continuously, taking only periodic measurements of ammonia.

Recirculating aquaculture systems commonly include controls to monitor the water quality parameters of temperature, dissolved oxygen, pH and water flow rate either directly or by monitoring equipment which maintains the parameter. In the past, only the most sophisticated and expensive instruments were adequate for monitoring and controlling aquaculture systems. However, today there are many new developments in solid state electronics which are bringing down the cost and increasing the reliability of sensors and instruments. The following is a review of several of the sensors and instruments used to monitor some of the parameters of an aquacultural system.

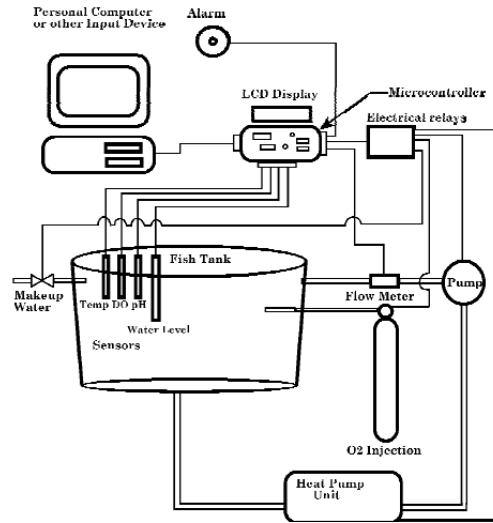


Fig. 2.19. Microcontrolled aquaculture system (Fowler, et al., 1994)

2.4.1. Dissolved oxygen sensors

Three different technologies available to measure dissolved oxygen (1) galvanic cell, (2) Clark (Polarographic) cell and (3) luminescence based sensing.

2.4.1.1. Clark Cell (Polarographic)

The Clark cell was discovered by Dr. Clark in 1956. And the amperometric cell is polarized with 800 mV which is provided externally by a battery source. Reduction of oxygen is achieved between 400 to 1200 mV. The Clark cell is built around the popular Ag/AgCl half-cell and a noble metal such as gold, platinum or palladium (Eutech Instruments, 1997), Table 2.5.

Table 2.5. Clark cell reaction

Anode (Ag) reaction (with Electrolyte KCl or KBr)	$2\text{Ag} + 2\text{Cl}^- \rightarrow 2\text{AgCl} + 2\text{e}^-$ (800mV)
Cathode reaction (Platinum, gold, palladium)	$2\text{e}^- + \frac{1}{2}\text{O}_2 + \text{H}_2\text{O} \rightarrow 2\text{OH}^-$
Net result:	$2\text{Ag} + 2\text{e}^- + \frac{1}{2}\text{O}_2 + \text{H}_2\text{O} + 2\text{Cl}^- \rightarrow 2\text{AgCl} + 2\text{OH}^- + 2\text{e}^-$

Every time O_2 is reduced at the cathode, you get 4 electrons i.e. a current is generated as the oxygen is reduced (consumed) at the cathode.

Assuming a measurement system without any interference i.e. only dissolved oxygen in water, the Clark cell has four major problems that limit its use in continuous operation (Eutech Instruments, 1997). These four problems are Anode Isolation, Zero Shift, Depletion of Chloride and Warm-up Time.

Anode Isolation

Since the net result of the chemical reaction is $AgCl$, cover the anode; stopping the reaction and its operation. A simple, impractical solution is to clean the anode to remove the $AgCl$ deposit and reactivate the probe.

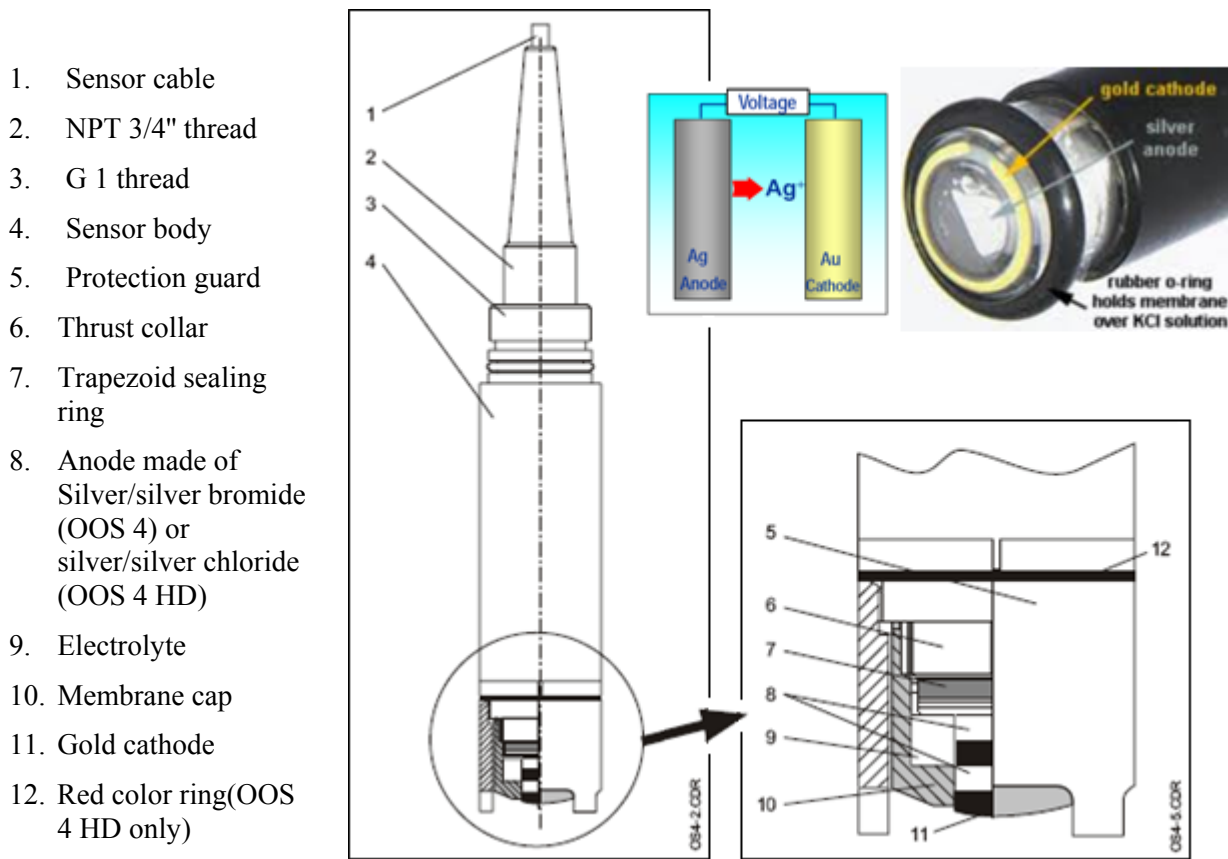


Fig. 2.20. Polarographic dissolved Oxygen sensor OOS 4 / OOS 4HD (<http://www.hobeco.com>)

The OH⁻ ions produced move the pH value of the electrolyte towards the alkaline area. The internal electrolyte (normally KCl) at neutral pH value moves into the alkaline range. This shifts the electrolyte potential into the negative range and causes a zero shift. This shift is always present over time, the electrolyte needs to be changed.

The net reaction also consumes Cl⁻ ions. With time, the chloride ions are consumed and the electrolyte has to be replenished.

When the probe is disconnected, the power supply is cut off. After connecting the probe again, the user must wait for the probe to be polarized i.e. for the current loop to be stabilized. This warm up time is approximately 10 minutes. If you measure during this time, there is normally a higher value displayed.

2.4.1.2. Galvanic Cell

The galvanic probe principle was discovered by Macreth in 1964. Since then, there have been a few changes. Eutech Instruments is using a modified probe designed by Hoeffner in 1985 ([Eutech Instruments, 1997](#)).

The idea of the galvanic probe is to avoid the external polarization required by the Clark cell. Even though the cell is an amperometric cell and a 800 mV potential difference is required to reduce the oxygen at the cathode, this can be accomplished by using two dissimilar metals. In the presence of an electrolyte, there is an electromotive voltage produced between 2 metals. If a comparison is made between lead and gold or lead and silver, the differential voltage is approximately 800 mV.

Hence, a galvanic probe is really a self-polarizing amperometric cell. The single biggest advantage is the fact that the cell is now always ready and there is no warm up time. The cell is

also a corrosion cell with the corrosion rate determined by the rate of oxygen consumed at the cathode.

Table 2.7. Galvanic cell reaction.

Anode reaction (material: Zinc or Lead)	$Zn \rightarrow Zn^{2+} + 2 e^{-}$
Cathode reaction	$2 e^{-} + (\frac{1}{2})O_2 + H_2O \rightarrow 2OH^{-}$
Net reaction:	$Zn + 2 e^{-} + \frac{1}{2} O_2 + H_2O \rightarrow 2 OH^{-} + Zn^{2+} + 2e^{-}$ $Zn + \frac{1}{2} O_2 + H_2O \rightarrow Zn(OH)_2$ (heavily soluble and stable, transparent) $\rightarrow ZnO$ (white precipitate) + H_2O
In summary	$Zn + \frac{1}{2} O_2 \rightarrow ZnO$

One molecule of oxygen produces 4 electrons; there is a direct relationship between the oxygen consumed at the cathode and the current produced by the cell, Table 2.6.

H₂O is recreated in a galvanic cell as the electrolyte volume is not consumed. Water molecule is replenished and electrolyte will go on forever and there is no need to change unless there is a problem with the membrane. Typical YSI probes need to be replenishing the electrolyte and rinse the anode every 2 weeks.

Two systems are available. The Macreth electrode uses the lead anode and the Hoeffner system the zinc anode. The net result is the formation of either PbO or ZnO. Both are reasonably stable but flake off the anode instead of coating it. This increases the life of the anode and reduces the anode. If ZnO covers the anode, the process is stopped. There are various oxides formed in addition to Zn, so the layer is not uniform and is porous; oxide falls off and exposes new Zn metal.

Theoretical life time of the anode is of 10 years and depends on O₂ level and temperature; at 10 ppm and 25 °C, Probe life is of 5 years. In the Hoeffner cell, the electrolyte is 2M NaCl; The Macreth cells use NaOH as the electrolyte.

2.4.1.3. Luminescence-based dissolved oxygen sensor

As shown in Figures (2.21 and 22), the luminescent dissolved oxygen sensor’s active optical components consist of a pair of blue and red light-emitting diodes (LEDs) and a silicon photodetector. The sensor cap has a coating of a platinum based luminophor that is excited by the light from the blue LED.

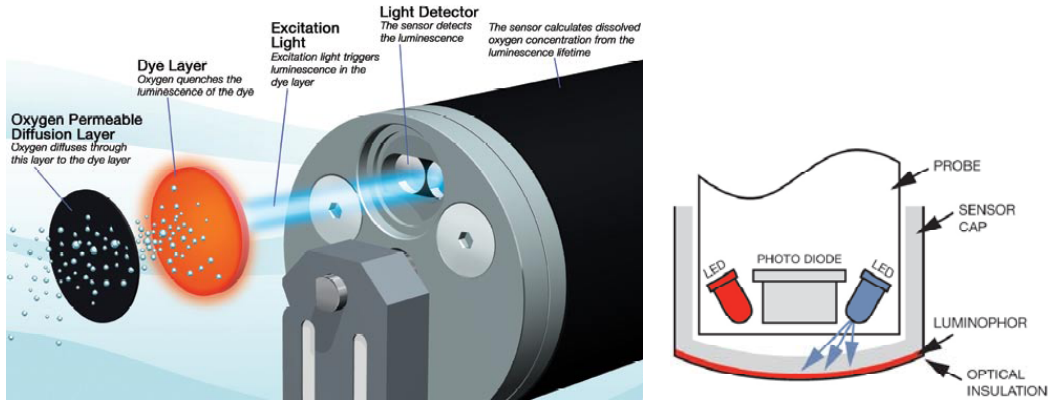


Fig. 2.21. Luminescence-based dissolved oxygen sensor. Photo by YSI (2008).

The luminophor is coated at the outside layer with carbon black polystyrene for optical insulation, providing excellent protection against photobleaching from external light sources when the sensor cap is attached to the sensor (Mitchell, 2006).

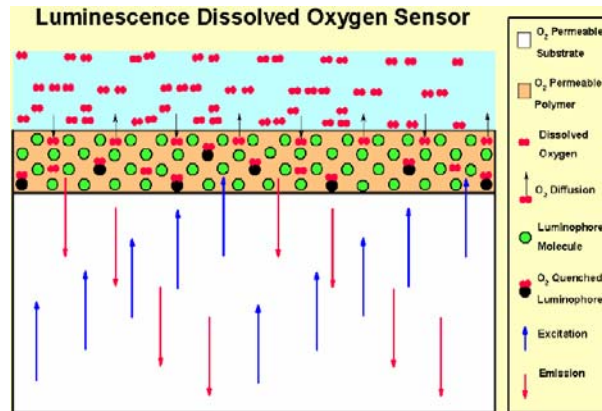


Fig. 2.22. Luminophor reaction with oxygen molecules with blue light excitation. Photo by Jackson and Craig, (2004)

The blue excitation LED is sinusoidally modulated at a frequency related to the luminophor's luminescence lifetime and the upper and lower lifetimes of analytical interest. The parameter measured from the opted is the phase delay between the exciting blue LED signal and the detected red emission from the luminophor. The phase delay is inversely related to the amount of dissolved oxygen near the luminophor.

This phase-modulation technique is used to measure the lifetime of the oxygen-dependent quenching of luminescence. The use of the phase-modulation technique means that intensity fluctuations of the blue LED or bleaching effects of the luminophor have no discernable impact on the lifetime measurement throughout the life of the sensor. In addition, because of the inverse relationship between oxygen concentration and phase delay of the emitted red light, the signal-to-noise ratio is particularly advantageous for measuring very low dissolved oxygen concentrations. Finally, the blue and red LEDs are alternatively switched between measurement cycles, allowing the red LED to provide an internal reference for the optical and electronic signal paths. This internal reference provides measurement stability by correcting for temperature or time induced changes in the phase measurement electronics.

2.4.2. Sensor auto calibration

(Bryan and Cushman, 1991) developed a system having real time, on-line capability for continuously monitoring galvanic dissolved oxygen sensor membrane impedance. The sensor system response to oxygen was tested by two external electrodes [Fig. 2.23\(17 and 18\)](#). When the system is used the two additional electrodes function as an anode and a cathode. A small current is passed from anode to cathode through the water.

The resulting electrolytic action produces a small amount of extra oxygen, so the anode is placed so that the oxygen generated will reach the sensor. The test current results in the

electrolysis of the process where H_2O molecules produce a repeatable quantity of hydrogen and oxygen gases. The hydrogen gas is exhausted by the process system and is ignored by the oxygen sensor. The effect of the additional generated oxygen of the sensor is monitored and compared with previous behavior; the additional oxygen level signal is subtracted from the normal level of oxygen. System computer algorithms compare the amplitude response, initial speed of response, and decay response to the additional oxygen to detect sensor and system performance (Fig. 2.23).

Chuang and Arnold, (1998) introduced a mathematical model as a calibration function for various optical oxygen sensors based on quenching of ruthenium fluorescence.

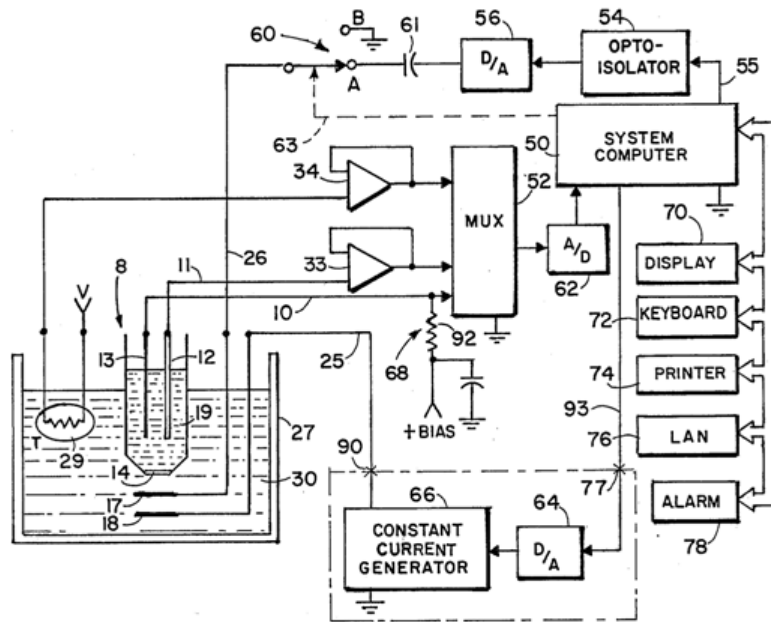


Fig. 2.23. Novel dissolved oxygen sensor with auto assesses.

2.4.3. Aeration automation

After meeting the culture animal's food requirements, low concentration of dissolved oxygen is the next major variable limiting the production of fish in intensive and semi-intensive aquaculture operations becoming critical in minutes. In addition, the managers of these intensive production facilities need accurate, real time information on system status and performance, in

order to maximize their production potential. At high production densities, failure of a circulation pump or aeration system can result in severe stress to the fish or even significant losses within minutes. Appelbaum et al., (1999) constructed an automatic emergency aeration device for use in aquaculture facilities. The device consists of a differential switch emergency air pump operated from standard vehicle batteries (Fig. 2.24).

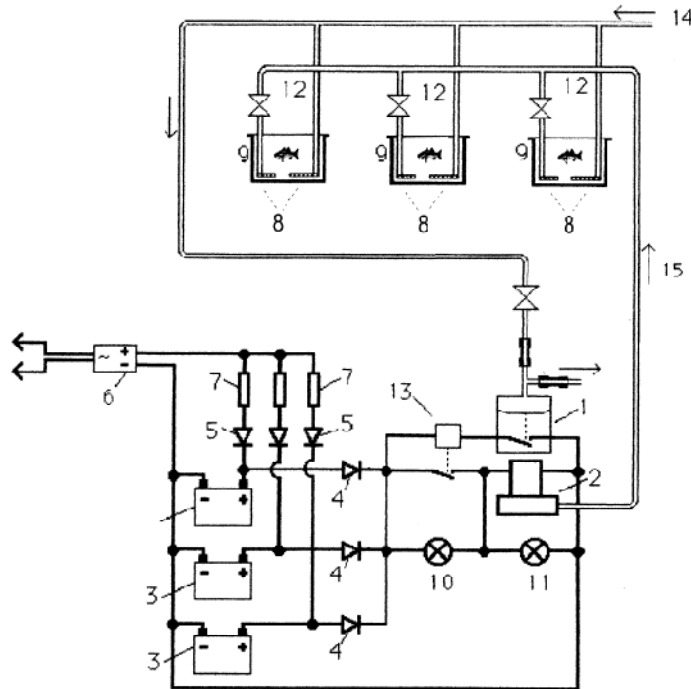


Fig. 2.24. Design of the emergency aeration system. 1, Press-differential switch (PDS); 2, emergency air pump; 3, batteries; 4, 5, diodes; 6, battery charger; 7, resistors; 8, air diffusers; 9, fish tanks; 10, 11, control lamps; 12, air valves; 13, relay; 14, normal aeration; 15, emergency aeration.

Peterson and Ardahl, (1992) presented an electronically controlled system to reduce the variation in oxygen concentration to maintain oxygen set point in a flow-through aquarium unit. Traoré et al., (2005) applied DO control based on a fuzzy logic strategy, taking into account the step and the difference between the measured DO and the setpoint in a sequencing batch reactor pilot plant.

2.4.4. LabView in Recirculating aquaculture system

Widmer et al., (2006) built a recirculating aquarium system with computerized temperature control to maintain static temperatures, using a LabView program to compare the temperature recorded by thermocouples in fish tanks to a desired set temperature and then calculate the amount of hot or cold water to add to tanks to reach or maintain the desired temperature. Intellifaucet three-way mixing valves controlled temperature of the input water and ensured that all fish tanks had the same turnover rate (Fig. 2.25).

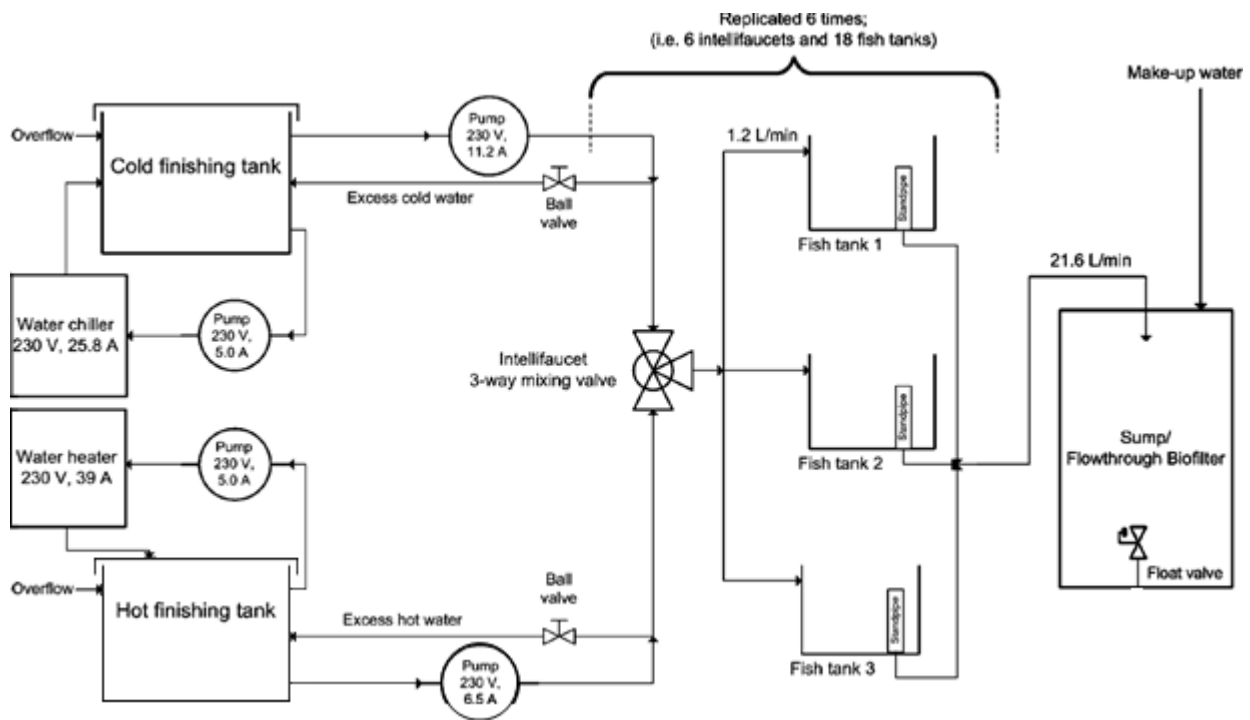


Fig. 2.25. Diagram of recirculating aquaria system

Alver et al., (2007) designed a rotifer counter where the instrument extracted samples automatically relying on a digital camera and image processing to measure the rotifer density. Due to its autonomous nature, the instrument is suited for use as a component in a process monitoring and control system. The imaging box is drawn without its front wall to indicate the lights and object glass inside (Fig. 2.26).

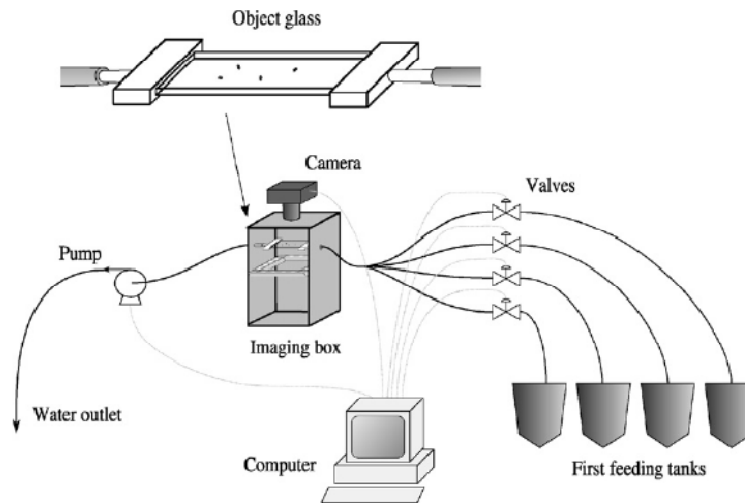


Fig. 2.26. Rotifers counter system.

2.4.5. Dosing automation system.

Feed wastage affects fish farm production cost, profits, appropriate additive delivery. The feed conversion ratio FCR is used as a measure of feed usage and is defined as the ratio of the mass of the food ration delivered to the mass gained by fishes, over a given time period. The daily ration is judged by observing fish feeding activity at the surface. Feeding is usually discontinued when the fish feeding activity greatly diminishes. The optimal feed conversion would be the one which produces the biggest fish using the least amount of feed in the shortest time period (Foster, 1993). Maximum fish growth cannot be achieved using classic methods of feed administration by personnel due to human and logistic limitations as lack of night-shift workers.

There are different techniques used for assuring proper dose delivery according to the control system. Different time-automatic feeders design are available as belt feeders that work on wind-up springs, and electric vibrating feeders that can be programmed to feed hourly for extended periods (Saravanan and Santhanam, 2008). Other automatic feeders have been reported for

feeding within predetermined time schedules for a certain feeding rate, without a food outlet weighting process (Juell et al., 1993, Fast et al., 1997, Fang and Chang, 1999, Fang et al., 2002 and Yeoh et al., 2010). Timer-controlled automatic feeders with a rotating plate and scrubber are widely used in indoor re-circulating eel culturing (Chang et al., 2005), Fig. 2.27.

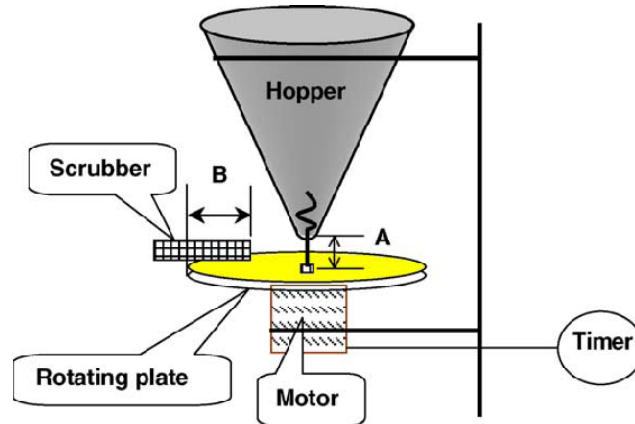


Fig. 2.27. Timed automatic feeder.

There are several close loop dosing systems in close loop and demand self feeders depend upon the ability of fish to press a lever to obtain food. An electronically controlled self-feeding system (Fig. 2.28) consists of a trigger rubber knob, a control unit and a feeder. As the fish stretches the knob to eat it, pressure changes are monitored by the microphone which sends a signal to the control unit. However, the majority of the fish do not trigger the mechanism and food delivery is lost (Alanära, 1992). Self feeder consists of (Fig. 2.28A) Power source (e.g. car battery or transformer), (Fig. 2.28B) Control unit. This unit regulates the running time of the feeder, the sensitivity of the trigger, and the hours during which the system operates. The control unit also includes a timer function that can be used separately, (Fig. 2.28C) Feeder hopper. Various types of feeders are suitable for this system (e.g. large holders that spread the food or small holders that give precise food portions) and (Fig. 2.28D) Trigger. The trigger includes a rubber knob ended pendulum or a pendulum with a string that ends in a plastic, pellet-like knob.

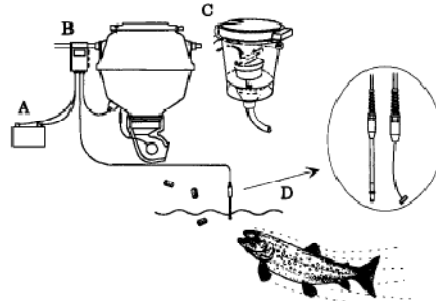


Fig. 2.28. Schematic view of a self-feeding system (Touch-Feed, manufactured by Sterner Products, Leksand, Sweden).

In a comparative study between predetermined automatic feeders and self feeder fish growth using self feeders was within those fed with low and high energy diets by means of predetermined automatic feeders (Paspatis and Boujard, 1996). Some fishes could not learn the behavior experience affecting fishing feeding. Manual self-feeders are simple and cheap, but the gate mechanism often gets jammed; feeding can easily be induced by accident by fish swimming through the gate or by wave action (Shepherd and Bromage, 1989). Food portions are difficult to adjust, and it is not possible to spread food over the water surface, (Alanärä, 1996). Chang et al., (2005) used an infrared photoelectric sensor for starting and stopping feeding depending on the gathering behavior under the feeder; this method does not work properly with distributed food or with intensive fish tanks (Fig. 2.29).

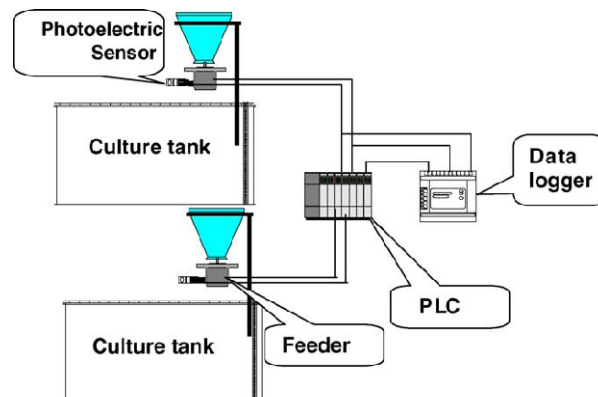


Fig. 2.29. Schematic diagram of the control and data acquisition systems (Chang et al., 2005).

Papandroulakis et al., (2002) implemented an automated feeding system for larvae computing the plankton organisms required according to feeding tables; a programmable logic controller (PLC) activated a peristaltic pump and a solenoid valves for food distribution to the tanks.

Appelbaum and Birkan, (1999) developed an automated feeding system with a conical feed hopper, a control unit and an air-lift pump Fig. 2.30. A plastic funnel with an 18-cm opening, tapering to 1.8 cm at the apex, is used as a feed hopper (1). The height of the funnel is 10 cm and the volume 1.0 liter. An opening of 0.7 cm is drilled in the wall of the funnel at a height of 1 cm from the apex, into which a plastic elbow joint (2) is placed and fixed by hot glue. A U-formed pipe (3), 0.8 cm diameter, assembled from a standard elbow (4, 5) and tee joints (6, 7) is connected to the elbow (2). The tee connector (6) is connected by a flexible plastic pipe (8) to the small, standard, air pump widely used for aeration of aquariums (9). An adjustable air-flow restrictor (10) is installed on the pipe (8). The air pump (9) is connected by electric wires (11) to the control unit (12). The control unit (12) contains two timing devices: a programmable clock switch (13), and an electronic timer (14), (RTB MP 1NU, Izumi, used on electric control boards). The device is supported by a wooden bracket (16), resting on the side of the tank containing larvae (15). The horizontal part of the tee joint (7) is turned towards the tank (15). A piece of open pipe is placed on the top part of the tee joint (7) to prevent water from splashing while the device is working, A plastic drain valve (17) is glued by hot glue to the bottom end of the funnel (1). An air-diffuser (18) is submerged into the apex of the funnel (1) to provide compressed air and also to create gentle water motion, allowing distribution of the nauplii in the water.

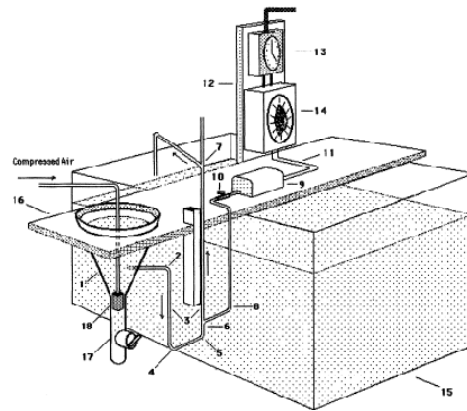


Fig. 2.30. Automatic feed system with an airlift pump.

Juell et al., (1993) used a food detector that consist of a cylindrical, steel framed net cage ($r = 60$ cm, $h = 35$ cm, mesh size = 32 mm/stretched mesh) with a 670 kHz acoustic transducer mounted in the centre. The transducer emits a 360° horizontal sound beam and the echo energy obtained between 10 and 50 cm from the transducer was measured, where the net cage prevents fish from entering the detection volume. The transducer is connected to a receiver that analyses the echo signals and controls the feeder. If the accumulated echo energy corrected for background noise measured prior to feeding exceeds a preset threshold, the feeder is turned off. The observation period ranged between 10-140 s, while the time interval between meals was 15-360 min. The echo energy threshold was set on an operating panel (Fig. 2.31).

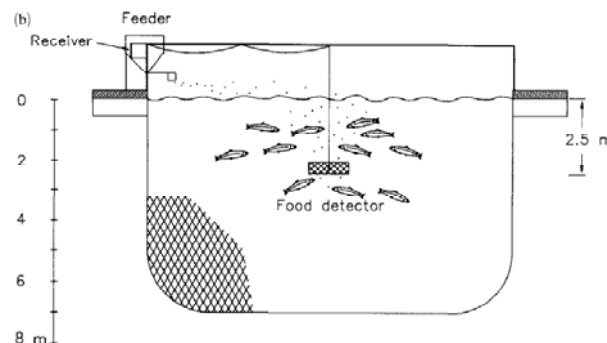


Fig. 2.31. The hydro acoustic food detector mounted in the sea cage.

Foster et al. (1995) used an underwater camera with an image analysis tool to detect and count left over pellets (Fig. 2.32). Similar system is now commercially available for sea cage

applications, sensors used including a doppler pellet sensor, CAS pellet sensor and camera sensor (Akvasmart, Norway).

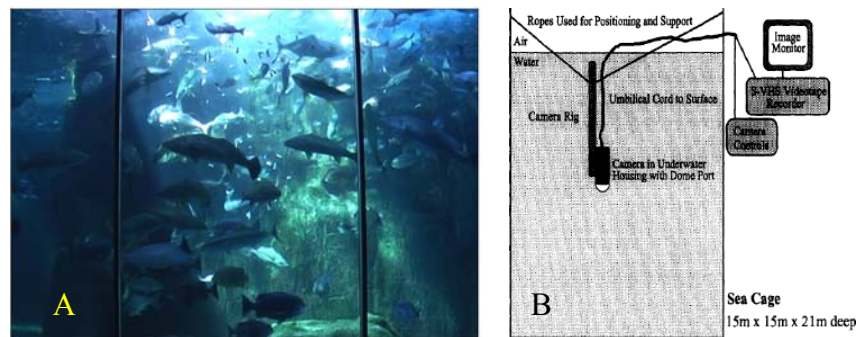


Fig. 2.32. (A) fish feeding behavior in the sea (Don, 2008), and (B) underwater Camera mounted in sea cage.

Kevin and Royann (2003) used the accuracy of a new machine-vision system for the identification of feed wastage and the response times were reported. Without using a feedback mechanism, an ultrasonic telemetric system was also used for automatic positioning of individual salmon in a sea cage (Juell and Westerberg, 1993); Kimura et al., (1993) indicated that one of the biggest problems in these farming systems was the problem in transmitting high- quality signals from fish finders within the signal transmission band width allowed by the radio wave laws of the country. Therefore sizes of schools of fish are over estimated because of significant reduction in the signal received. At present, in fish farms, visual observation of fish appetite is often impeded by high fish density and water turbidity (Mallekh et al., 2003).

Fang and Chang (1999) used other method to stop feeding before the water became polluted. Fang et al. (2002) used the reflective type photoelectric sensor to detect the gathering behavior of the eels, which is incorporated in the feedback concept. Their results showed that stopping a feeding cycle before polluting the water is possible using floating feed for eels. Based on their previous study, an intelligent feeding controller based on gathering behavior has been evaluated in a pilot scale commercial fish farm.

3. MATERIALS AND METHODS

3.1. Recirculating aquaculture system design (RAS).

The recirculation system aquaculture is located in the experimental facilities of UACH used three different biofilters (Fig. 3.1).

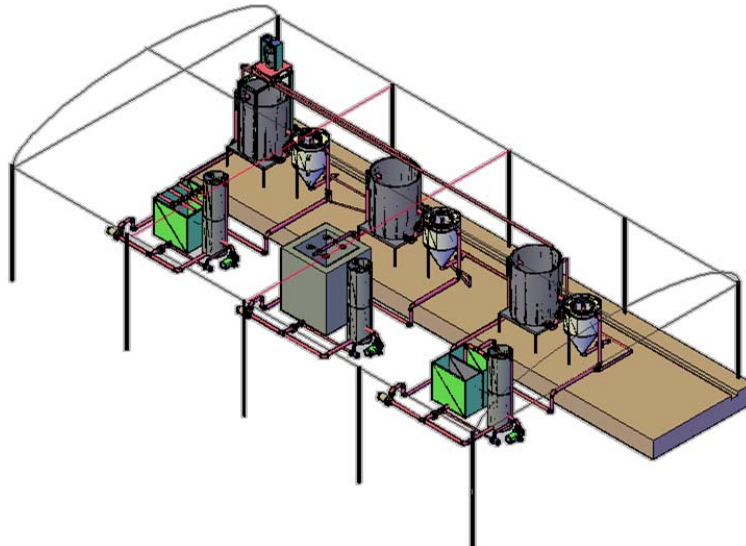


Fig. 3.1. Full recirculating aquaculture system that were used in the study.

The re-circulating aquaculture system consists of a plastic circular tank 1.1 m diameter with three water inputs and two outputs. The culture volume is approximately 1100L with two centrifugal pumps which re-circulates 20-35 l/min of water depending on carp size. The first pump (0.75 Hp) returns water to the tank and the second pump (0.5 Hp) is used with the aerator. The water is forced by gravity to the separator which extracts the solids generated by the fish greater than 80 micrometers. The water from the top of the separator flows by gravity to the distributor pushing the water to the bio-strata surface at the biofilter (Fig. 3.2). The water is pumped to three fine jet sprayers (SURTEK 130327) mounted at the top of the aerator; an air blower is connected at the bottom of the column introducing the air in counter current to the water flow aerating it.

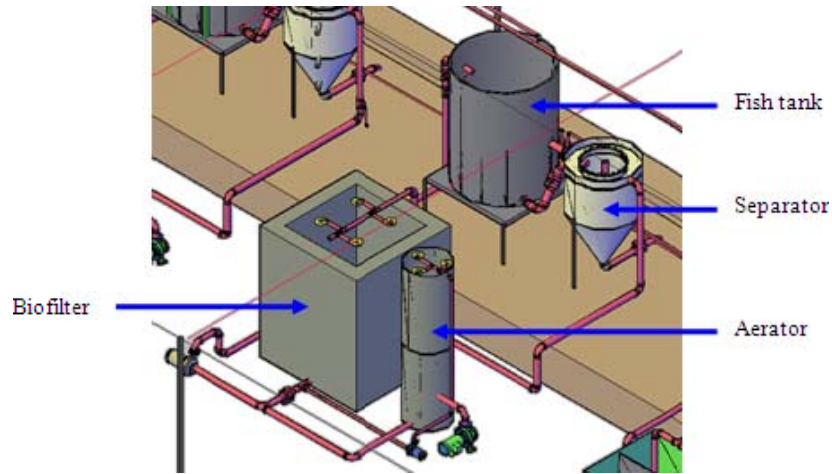


Fig. 3.2. Recirculating aquaculture system (RAS).

3.1.1. Fish Tank

Low cost polyethylene tanks (Fig. 3.3) are used to cultivate mirror carp var. *Cyprinus carpio*. Their smooth surface makes it easy for cleaning, but because they are very soft and malleable, they need to be well supported. Circular tanks have been widely used for fish culture because they provide a uniform water quality, and waste water is easily removed. Treated water is injected through three elbows located inside the tank lateral wall. The elbows inject a uniform water flow at an average speed of 15-20 cm/s of the tank perimeter. Each tank was cultivated with 100 fishes with an average initial weight of 20 g. In the first three weeks, some species of algae were found accidentally in the system (Fig.3.4).



Fig.3.3. Fish Tank.

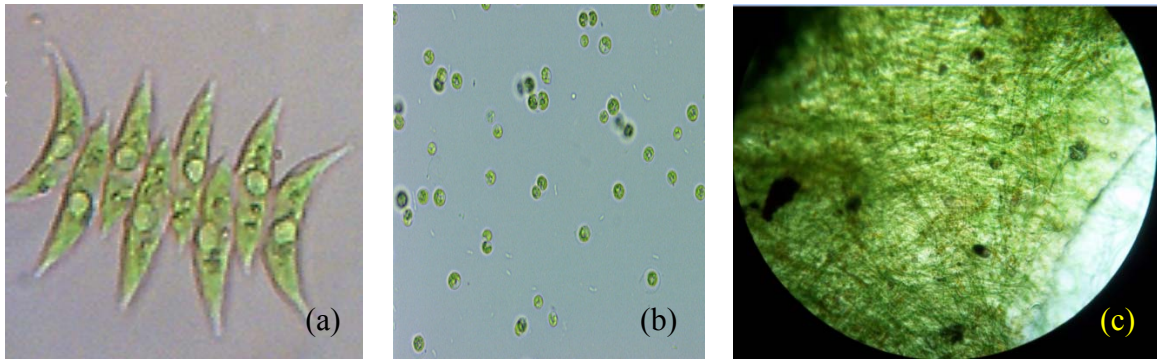


Fig. 3.4. Algae found in the re-circulating system (RAS) (a) *Scenedesmus sp.* (b) *Chlorella sp.* (c) *Filamentous microalgae.*

3.1.2. Separator

A combination of swirl separator and radial flow settler was developed to maximize the sedimentation efficiency. Swirl separators employ the principle of centrifugal sedimentation, i.e., the suspended solid particles are subjected to centrifugal acceleration, separating them from the water (Timmons and Ebeling, 2007). The suspended particles were concentrated at the center of the water and collected along the inside wall of the separator; these particles are yielded by the effect of the gravitational forces and then settle at the bottom of the clarifier cone (Veerapen et al., 2005). The separator has two inlets, Fig. 3.5: the centrifugal inlet connected at the upper 25 cm which corresponds to the play area of the fishes, and the center inlet (as radial flow settler) is connected to the bottom of the tank to suck all the solids at the bottom inlet.



Fig. 3.5. Separator with two inlets one from the tank bottom to the separator center and the other from the upper part of the tank to the lateral side of the separator.

3.1.3. Emergent Biofilter

The biofilter consists of a fixed support (packing material) and water enters the culture media through a water distributor mounted above the packing material in an open tank. Water movement through the biofilter provides additional aeration giving good support nitrifying bacteria. Three different biofilters were designed in this study and all of them have a certain level of water depending on its retention time, two different materials were used Tezontle (volcanic sand) and biostrata (polyethylene) to sustain the nitrifying bacteria on their superficial areas forming a suitable biofilm for the nitrification process.

3.1.4. Spray column aerator

The spray column aerator consists of plastic shells having a volume of 0.4276 m^3 (0.55 m diameter x 1.80 m height) with two mass transfer units (each 0.9 m long). The two units were separated by a water distributor plate having 65 holes (diameter 0.02 m) to allow that air and water passes through it. As water flows through the top of the spray tower, three sprays reform

the wafer. Three delicate cones increase the solubility of oxygen in water increasing the contact surface area between air and water. The distributor plate causes great turbulences between air and water enhancing the solubility of oxygen in the water.

3.2. Characterization of each RAS system element.

3.2.1. Separator theory and design:

The separator was designed for removing of particles greater than 80 μm when operated in conjunction with the culture tank. It connects the bottom drain of the fish tank to the separator and allows particles to be quickly transported to the separator before pumping breaking them into small, hard-to-settle sizes. This provides a reduced flow compared to the system flow, requiring a smaller unit. The clarifier was designed with a 60° cone bottom in order to concentrate the solids at the bottom of the cone for easy removal with minimal water use.

The modified settler employs the principle of centrifugal sedimentation, i.e., the suspended solid particles are subject to centrifugal acceleration, and separates them from the liquid more rapidly by increasing their density. The principle of sedimentation that occurs is due to the density difference between the solid particles and water, a V-notch weir of 60° and effluent launder circumscribing the tank top perimeter of the tank (Fig. 3.6). The settling tank contained a 60° cone bottom with an overall height of 0.7 m and a 3.8 cm. diameter drain at its base (Fig. 3.6). The separator was operated as a swirl separator by introducing the water flow through a 3.8 cm diameter tube with tangential inlet located 0.25 m below the top (Fig.3.6 A). The other separator inlet worked as radial flow settler, where it turned up at a 90° angle at separator's center and spilled the waste water out just below the water surface (Fig. 3.6B). A galvanic cylinder (0.1 m diameter and 0.15 m height) was installed around the radial flow settler inlet tube (Fig. 3.6C) to dampen water turbulence at the point of water injection. As waste water entered the separator,

it was forced to flow downward the dampening cylinder; after the water returned to flow radially to the V-notch weir (separator channel) (Fig. 3.6B and C). The treated water passed through a V-notch to the separator channel leaving the separator.

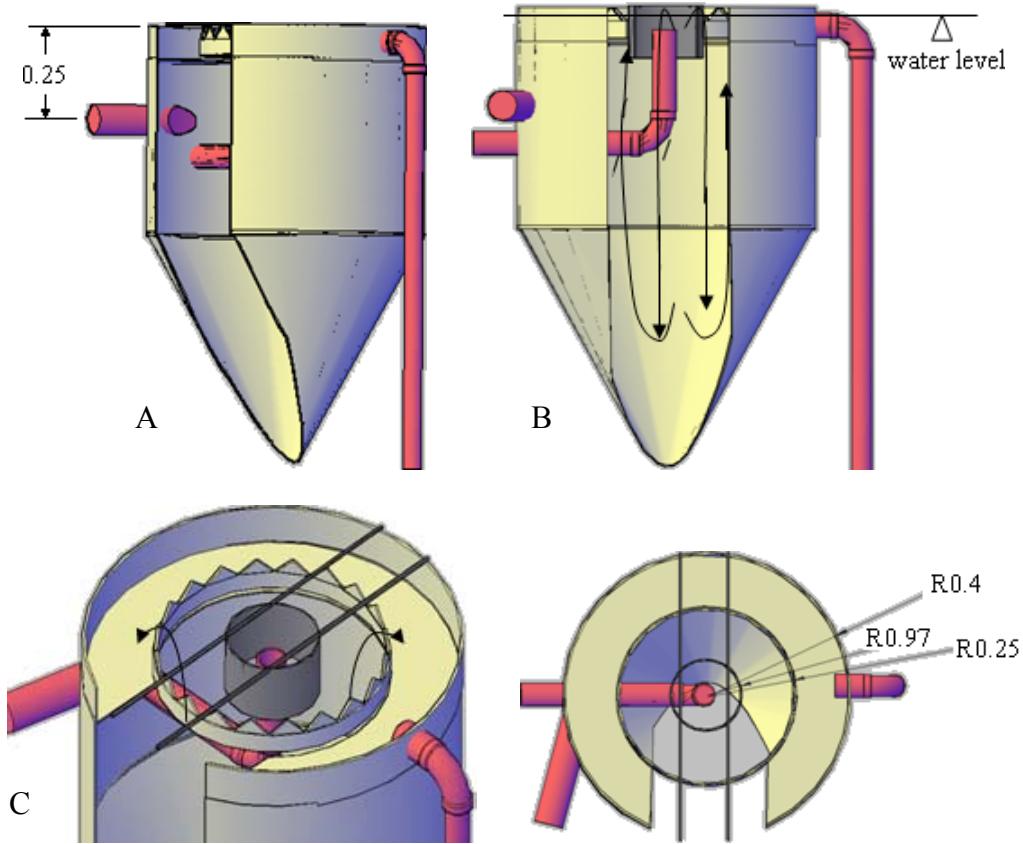


Fig. 3.6. The separator schematic design (A) centrifugal water inlet (B) Radial inlet, the arrows indicate water flow directions inside the separator (C) central galvanic cylinder.

Assuming particles are heavier than water, they will fall through the water with increasing speed until reaching its settling velocity. Each discrete particle has an equilibrium settling velocity. Assuming spherical particles, the settling velocity can be calculated by the following equation (Montgomery, 1985)

$$V_s = \sqrt{\frac{4g(\rho_p - \rho)D_p}{3C_D\rho}} \quad (3.1)$$

For a small particle having a Reynolds number lower than one, Stocke's law applies, and Eq. 3.1 can be written as

$$V_s = \frac{g(\rho_p - \rho)D_p^2}{18\mu} \quad (3.2)$$

Both Eqs. 3.1 and 3.2 indicate that denser and larger particles will settle faster than smaller less dense particles. The best technique for maintaining large particles sizes is to remove the particles as quickly as possible from the fish culture vessel and before pumping. Turbulence/falling water situations should be minimized prior to the primary total suspended solids (TSS) capture event.

Settling column of 10 cm diameter and 1.5 m long was utilized to determine the terminal settling velocity (V_s) solids. Fresh samples (<24 h) were collected from an existing fish pond, by gently siphoning from the center portion of a culture tank. Samples were immediately passed, serially, through sieves of 250, 125, 62.5, and 42 μ m (Fig. 3.7a). Samples of particles collected on the 62.5 mm sieve ($62.5 \mu\text{m} < d < 125 \mu\text{m}$) were rinsed from the sieve to deionized water and used for V_s determination.

Clarifier size was calculated from clarified water production rate, or by influent flow rate to the unit, Eq. (3.3).

$$Q = AV_0 \quad (3.3)$$

where Q is the influent flow rate, A the surface area of the unit and V_0 the overflow velocity. Equation 3.3 was manipulated to provide the area, and therefore the clarifier diameter, required for any flow rate and solids settling velocity.

Applying V_s 0.0829 cm/s as V_0 in Eq. (3.3), the diameter of the separator was obtained. The resulting surface loading rate on the clarifier was 0.00082 m/s of settling area. The separator presented a 60° cone bottom a circular tank with a diameter of 80 cm, a total height of 130 cm

(Fig. 3.6). Influent flow rate to the separator was 25 LPM. The 70 cm long cone section presented a 3.8 cm PVC tube and valve for manual draining. The 60° cone bottom was chosen based upon recommendations for tube settlers in order to provide the greatest degree of gravity driven self-cleaning of settled solids with minimal water discharge (Timmons et al., 2001; Metcalf and Eddy, 1991). Captured solids were flushed daily after sampling all trials.

3.2.1.1. Separator removal efficiency evaluation.

Tezontle (volcanic sand) was used to evaluate separator removal efficiency under the following parameters:(1) Three different bases to suck the solids from the bottom of the tank of 2.54, 3.8 and 5.08 cm; (2) Two different levels of head of 80 cm and 90 cm (Fig. 3.7b), and (3) different weight categories of tezontle particles (Table 3.1).

Table 3.1. Particle weight category

	Particle weight range, mg.	Particle diameter, mm
1	1.3-10.1	0.5-1
2	0.745-1.3	0.42-0.5
3	0.157-0.745	0.250-0.42
4	0.0333-0.157	0.149-0.250
5	0.0196-0.0333	0.125-0.149
6	0.0024-0.0196	0.062-0.125
7	< 0.0024	< 0.062

The Tezontle density was determined in the soils lab (UACH) to calculate the Tezontle particles weight, as other volcanic rockets particles were found with Tezontle particles; particles apparent density was of 2400 kg/m³.

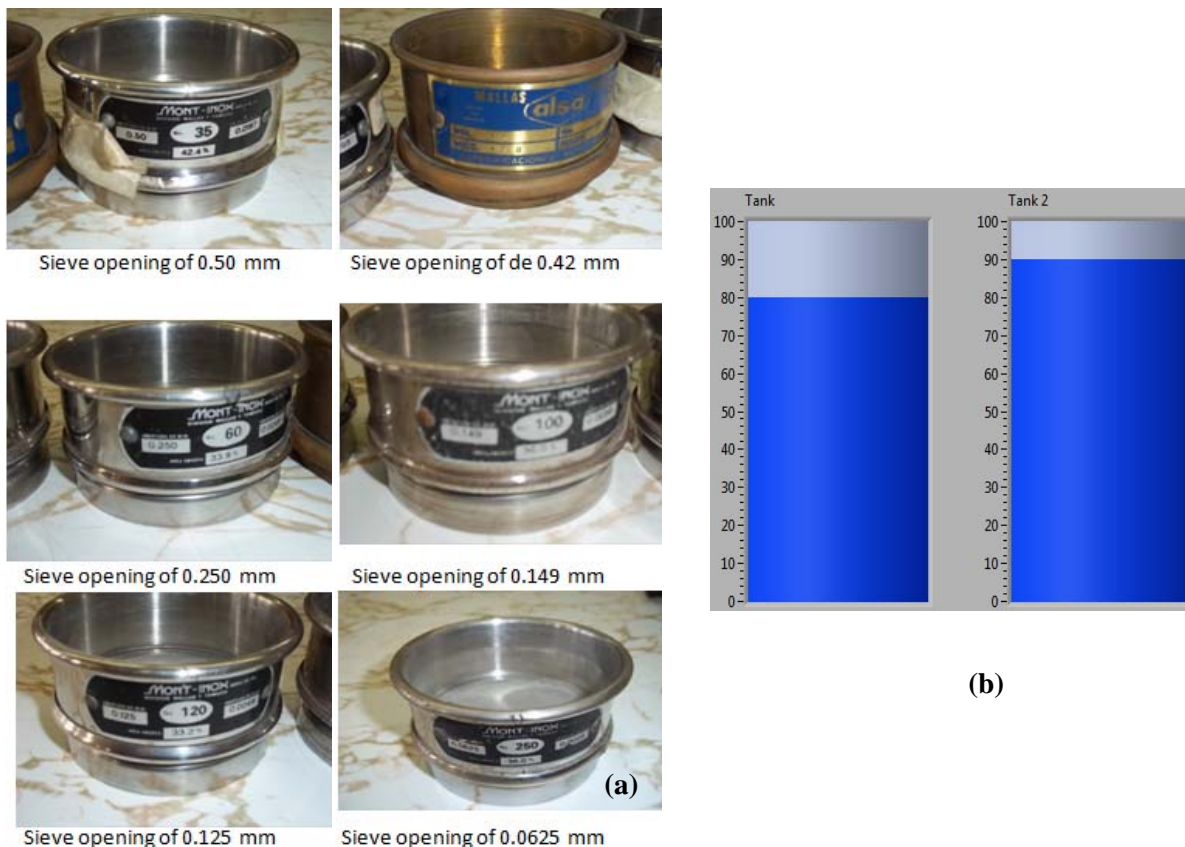


Fig. 3.7. (a) Sieves used to determine particle size (b) water tank level.

Tezontle apparent density Determination for particles appendix I (7.1). The mean particle size distribution for the tezontle that was used in the experiment was illustrated in Fig. 3.8.

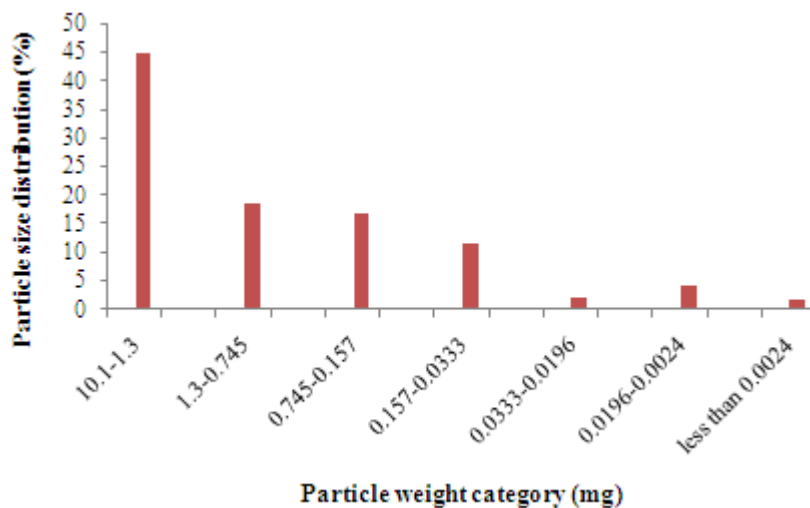


Fig. 3.8. Solids analysis for the Tezontle that was used for all the experiment

Experimental progress

The Tezontle particles were used to simulate fish feces generated in fish tank, different particles categories were used to study bottom cleanliness and separator removal efficiencies. Assuming 25% of food introduced to fishes produce wastes, at higher feeding rations 200 gram food was applied per meal, two meals daily. The tezontle applied to the tank in this experiment was 50 grams two times daily (100 gram per day), distributed on the water surface, the system let to run 20 hours as the time required for water recirculation in RAS system. It was observed that tezontle particles weight in water increases 35% of its dry weight.

After each experiment the water was sampled at the separator inlet, the top outlet, the channel and the bottom outlet. Samples were analyzed as TSS to calculate the separator removal efficiency for each category; sieves separated the samples in categories (Fig. 3.8, 3.9 and 3.10). Fig.3.9 show visually the effect of separator on solids removal. Fig.3.9IV show by naked eye the discharged concentrated waste water that captured by the sparator (bottom discharged) (A), the separator water inlet at the center from fish tank bottom (B), outlet water that treated by the separator (C) and Tap water (D).



Fig 3.9. Samples vision microscopy (I), bottom discharged (II) and Channel captured (III) separation and by naked eye (IV).



Fig. 3.10. The solids that captured in the channel of the separator and that discharged from the bottom.

The removal efficiency percent for each particle size category was computed as:

$$RE(\%) = \left[\frac{S_{in} - S_{out}}{S_{in}} \right] \times 100 \quad (3.4)$$

where RE , is the removal efficiency (%), S_{in} is the mean TSS concentration of the inlet sample for a specific screen mesh size (mg/L) and S_{out} is the mean TSS concentration of the outlet sample for the specific screen mesh size (mg/L).

3.2.1.2. Effect of tank base diameter and water level in the tank on bottom cleanliness

The effect of tank base diameter on particles drag forces was studied Fig. 3.11.



Fig. 3.11. Tank base of 2.54 cm diameter, under the effect of water level in the tank (A and B) at water level 90 cm and (C) water level 80 cm

Three different diameters of 2.54, 3.81 and 5.08 cm at the tank base had 6 lateral perforated tubes 1 m long with thickness of 1 cm, holes every lateral tube presented 14 holes.

3.2.2. Biofilters design

For dimensioning or sizing a trickling biofilter, only limited information is available (Ebling et al., 2006). In practice, TAN removal efficiency is often empirically determined for a fixed set of successful conditions such as fish species, feed load, filter height, filter media type, hydraulic surface load, suspended solids unit, and TAN influent concentration. TAN removal rates were determined from empirical relationships (Liao and May, 1974) and from the kinetics TAN removal (Bovendeur et al., 1987; Heinsbroek and Kamstra, 1990). The simplest case is when TAN removal efficiency for a certain trickling filter influent concentration is known, based on data for a fixed filter height, media type, hydraulic surface load, TAN removal rate, and temperature. The required total nitrification surface area (A_{media} , m^2) is calculated from the trickling filter TAN load (P_{TAN} , g/day) and the estimated nitrification rate (r_{TAN} , $\text{gTAN}/\text{m}^2/\text{day}$). The bioreactor volume (V_{media} , m^3) is a function of the total filter surface area and the specific surface area (SSA, m^2/m^3 biofilter media) of the filter media. The shape of the reactor depends on the hydraulic loading surface (HLR, $\text{m}^2/\text{m}^3/\text{day}$) (Losordo et al., 2000; Wheaton et al., 1995).

The design of a trickling tower follows a simple set of steps with the nitrification rate based on the active surface area of the media and since the trickling tower is self aerating, the oxygen requirement is limited to fish metabolism.

Step 1 : Calculate the dissolved oxygen requirement (R_{DO}).

Step 2: Calculate water flow requirement (Q_{tank}) required for fish dissolved oxygen demand.

Step 3: Calculate TAN production by fish (P_{TAN})

Step 4: Calculate the surface area of media (A_{media}) required to remove P_{TAN} from the areal TAN removal rate (ATR).

Step 5: Calculate the volume of media required based upon the required area (V_{media}) and the specific surface area (SSA) associated with the media being used.

Step 6: Calculate the biofilter cross-sectional area ($A_{\text{biofilter}}$).

Step 7: Calculate the biofilter depth from the biofilter cross-sectional area ($A_{\text{biofilter}}$) and volume

(V_{media}).

3.2.2.1 Design of the second re-circulating trickling biofilter

Calculate the feeding regime during the growth period

First month

$$0.09 \times 100 \text{ fish} \times 1 \text{ tank} \times 25 \frac{\text{g}}{\text{individual}} \times 30 \text{ day} = 6.75 \text{ kg food}$$

Second month

$$0.06 * 100 \text{ fish} \times 1 \text{ tank} \times 40 \frac{\text{g}}{\text{individual}} \times 30 \text{ day} = 7.2 \text{ kg food}$$

Third month

$$0.04 * 100 \text{ fish} \times 1 \text{ tank} \times 100 \frac{\text{g}}{\text{individual}} \times 30 \text{ day} = 12 \text{ kg food}$$

Fifth month

$$0.02 * 50 \text{ fish} \times 1 \text{ tank} \times 400 \frac{\text{g}}{\text{individual}} \times 30 \text{ day} = 12 \text{ kg food}$$

The peak feeding rate per kg carp is

$$\frac{12 \frac{\text{kg food}}{\text{month.tank}}}{30 \frac{\text{day.tank}}{\text{month.tank}}} \times \frac{\text{tank}}{10 \text{ kg fish}} = 0.04 \text{ kg food/kg fish. day}$$

Step 1: Calculate the dissolved oxygen requirement (calculated)

$$\begin{aligned} R_{\text{DO}} &= a_{\text{DO}} \times r_{\text{feed}} \times \rho \times V_{\text{tank}} \quad (3.5) \\ &= 0.376 \frac{\text{kg O}_2}{\text{kg feed}} \times 0.04 \frac{\text{kg feed}}{\text{kg fish. day}} \times 15 \frac{\text{kg fish}}{\text{m}^3} \times 1 \text{ m}^3 \\ R_{\text{DO}} &= 0.22 \frac{\text{kg O}_2}{\text{day}} \end{aligned}$$

Step 2: Calculate water flow requirement (Q_{tank}) required for fish dissolved oxygen demand.

Assume $DO_{\text{inlet}} = 6.3 \text{ mg/L}$

$$DO_{\text{tank}} = 3 \text{ mg/L}$$

$$Q_{\text{tank}} = \frac{R_{\text{DO}}}{DO_{\text{inlet}} - DO_{\text{tank}}} \quad (3.6)$$

$$Q_{\text{tank}} = \frac{0.22 \frac{\text{kgO}_2}{\text{day}}}{6.7 \frac{\text{mg}}{\text{L}} - 3 \frac{\text{mg}}{\text{L}}} \times \frac{1 \text{ day}}{1440 \text{ min}} \times \frac{10^6 \text{ mg}}{1 \text{ kg}} = 41.29 \text{ L/min}$$

$$\text{Tank exchange rate} = \frac{V_{\text{tank}}}{Q_{\text{tank}}} = \frac{1000 \text{ L}}{41.29 \text{ L/min}} = 24.2 \text{ min}$$

The 24.2 minutes tank exchange rate is adequate, and could be reduced if necessary (i.e. 2 water exchanges per hour) depending on tank hydraulics and solids removal efficiency.

Step 3: Calculate the TAN production using an approximation that the ammonia production by fish (P_{TAN}) is 3.2% of the feeding rate:

$$P_{\text{TAN}} = a_{\text{TAN}} * R_{\text{feed}} \quad (3.7)$$

$$P_{\text{TAN}} = 0.032 \frac{\text{kg}_{\text{TAN}}}{\text{kg}_{\text{feed}}} \times 0.4 \frac{\text{kg}_{\text{feed}}}{\text{day}} = 0.0128 \text{ kg} \frac{\text{TAN}}{\text{day}} = 12.8 \text{ g TAN/day}$$

Step 4: Calculate the media surface area (A_{media}) required to remove P_{TAN} . Assume that the superficial TAN removal rate (STR) is $0.45 \text{ g TAN/m}^2 \cdot \text{day}$

$$A_{\text{media}} = \frac{P_{\text{TAN}}}{\text{STR}} = \frac{12.8 \frac{\text{g}_{\text{TAN}}}{\text{day}}}{0.45 \frac{\text{g}_{\text{TAN}}}{\text{m}^2 \cdot \text{day}}} = 28.4 \text{ m}^2. \quad (3.8)$$

Step 5: Calculate the volume required of biostrata media based on its specific surface area (SSA) associated with the media being used Bio-Strata of $110 \text{ m}^2/\text{m}^3$ (Fig. 3.12).

$$V_{\text{media}} = \frac{A_{\text{media}}}{\text{SSA}} = \frac{28.4 \text{ m}^2}{110 \frac{\text{m}^2}{\text{m}^3}} = 0.2586 \text{ m}^3 \quad (3.9)$$

Step 6: Calculate the biofilter cross-sectional area ($A_{\text{biofilter}}$) from required flow for fish oxygen demand (Q_{tank}) and hydraulic load; HLR of $255 \text{ m}^3/\text{m}^2 \cdot \text{day}$ required to prevent clogging of the media bed (Timmons and Ebeling, 2007).

$$A_{\text{bed}} = \frac{Q_{\text{tank}}}{\text{HLR}} = \frac{34.72 \frac{\text{L}}{\text{min}} \times 1440 \frac{\text{min}}{\text{day}}}{255 \frac{\text{m}^3}{\text{m}^2} \times 1000 \frac{\text{m}^3}{\text{L}}} = 0.196 \text{ m}^2 \quad (3.10)$$

Step 7: Calculate the biofilter depth ($\text{Depth}_{\text{media}}$) from the biofilter cross-sectional area (A_{bed}) and the volume (V_{media})

$$\text{Depth}_{\text{media}} = \frac{V_{\text{media}}}{A_{\text{bed}}} = \frac{0.2586 \text{ m}^3}{0.196 \text{ m}^2} = 1.3 \text{ m} \quad (3.11)$$



Fig. 3.12. The Bio-strata used in the nitrification process.

The second biofilter had biostrata installed beneath water distributor (Fig. 3.13).



Fig. 3.13. The biofilter of Tank 2

3.2.2.2. Submerged packed biofilter design for the first re-circulating fish system

Tezontle volume required for the biofilter was calculated.

Step 1: Calculate water flow rate through the fluidized bed biofilter. Total ammonia nitrogen (TAN) production was calculated from (Brunty et al., 1997)

$$TAN = 0.604 \times FEEDN + 3.88 \quad (3.12)$$

where FEEDN is the nitrogen content expressed in grams per kilogram of feed. The feed protein content is composed of 35% crude protein, so nitrogen content 55 gram per kg of food.

The calculation was done for the fourth month, because this month has a high feeding rate of 0.4 kg feed /day in the system. The amount of feed nitrogen for one day,

$$= 55 \frac{gN}{kgfood} \times 0.4 \frac{kgfood}{day} = 22 gN/day$$

TAN production by the carp is:

$$TAN = 0.604 \times 22 + 3.88 = 17.17 g/day$$

Water flow rate through the biofilter was calculated using the formula developed by (Liao and Mayo, 1972):

$$TAN_{out} \cong \left\{ \frac{1}{f_{rem}} \right\} \left\{ \frac{r_{TAN}}{Q_{bio}} \right\} \quad (3.13)$$

where TAN_{out} is maintain constant concentration of total ammonia nitrogen desired in fish tanks f_{rem} is TAN removal efficiency for packed biofilter (assumed here 60%); r_{TAN} is the average daily rate that TAN is produced, (kg waste per day), and Q_{bio} is the water flow rate through the biofilter.

Toxic (un-ionized) ammonia fraction in aqueous solutions at different pH values and temperature was calculated from data in (Emerson, et al., 1975) Table 3.2. To determine the amount of un-ionized ammonia present, get the fraction of ammonia that is in the un-ionized form for a specific pH and temperature from the table. Multiply this fraction by the total ammonia nitrogen present in a sample to get the concentration in ppm (mg/L) of toxic (un-ionized) ammonia. It is necessary to maintain the concentration of un-Ionized ammonia (NH_3) in Tilapia tanks below 0.05 mg/l to obtain a good growth rate.

Table 3.2. Toxic (un-ionized) ammonia fraction in aqueous solutions at different pH values and temperature.

pH	Temperatures (°C)												
	6	8	10	12	14	16	18	20	22	24	26	28	30
7.0	.0013	.0016	.0018	.0022	.0025	.0029	.0034	.0039	.0046	.0052	.0060	.0069	.0080
7.2	.0021	.0025	.0029	.0034	.0040	.0046	.0054	.0062	.0072	.0083	.0096	.0110	.0126
7.4	.0034	.0040	.0046	.0054	.0063	.0073	.0085	.0098	.0114	.0131	.0150	.0173	.0198
7.6	.0053	.0063	.0073	.0086	.0100	.0116	.0134	.0155	.0179	.0206	.0236	.0271	.0310
7.8	.0084	.0099	.0116	.0135	.0157	.0182	.0211	.0244	.0281	.0322	.0370	.0423	.0482
8.0	.0133	.0156	.0182	.0212	.0247	.0286	.0330	.0381	.0438	.0502	.0574	.0654	.0743
8.2	.0210	.0245	.0286	.0332	.0385	.0445	.0514	.0590	.0676	.0772	.0880	.0998	.1129
8.4	.0328	.0383	.0445	.0517	.0597	.0688	.0790	.0904	.1031	.1171	.1326	.1495	.1678
8.6	.0510	.0593	.0688	.0795	.0914	.1048	.1197	.1361	.1541	.1737	.1950	.2178	.2422
8.8	.0785	.0909	.1048	.1204	.1376	.1566	.1773	.1998	.2241	.2500	.2774	.3062	.3362
9.0	.1190	.1368	.1565	.1782	.2018	.2273	.2546	.2836	.3140	.3456	.3783	.4116	.4453
9.2	.1763	.2008	.2273	.2558	.2861	.3180	.3512	.3855	.4204	.4557	.4909	.5258	.5599
9.4	.2533	.2847	.3180	.3526	.3884	.4249	.4618	.4985	.5348	.5702	.6045	.6373	.6685
9.6	.3496	.3868	.4249	.4633	.5016	.5394	.5762	.6117	.6456	.6777	.7078	.7358	.7617
9.8	.4600	.5000	.5394	.5778	.6147	.6499	.6831	.7140	.7428	.7692	.7933	.8153	.8351
10.0	.5745	.6131	.6498	.6844	.7166	.7463	.7735	.7983	.8207	.8408	.8588	.8749	.8892
10.2	.6815	.7152	.7463	.7746	.8003	.8234	.8441	.8625	.8788	.8933	.9060	.9173	.9271

Source: Emerson, K., R.C. Russo, R.E. Lund, and R.V. Thurston. 1975. *Aqueous ammonia equilibrium calculations: effect of pH and temperature.* Journal of the Fisheries Research Board of Canada. 32:2379-2383.

Table 3.2 converts un-ionized ammonia (NH₃) to total ammonia nitrogen under pH ranging between 7 and 7.5 and temperatures varied from (22-28°C). The total ammonia nitrogen value was 2 mg/l equivalent to 0.05 mg/l un-ionized ammonia. Equation 3.13 calculates the water flow rate through the biofilter

$$2 \cong \left\{ \frac{1}{0.6} \right\} \left\{ \frac{17.17 \times 10^3}{Q_{bio} \times 1440} \right\}$$

$$Q_{bio} = 10 \text{ L/min}$$

The superficial TAN removal rate, is 0.06 g/d/m², and the tezontle specific surface area 1400 m²/m³, the area required for the biofilter is 17.17/0.06 = 286.17 m², Tezontle volume required is 286.17/1400 = 0.2 m³. The biofilter with Tezontle installed for the first tank with its water distributor for the first tank was shown at Fig. 3.14.



Fig. 3.14. First submerged biofilter and its water distributor mounted above the biofilter media, Tezontle used as a media for the submerged biofilter with mean diameter 1 cm.

The third biofilter is a submerged biofilter having a different water distributor (Fig. 3.15).



Fig. 3.15. The biofilter of Tank 3.

3.2.3. Biofilter initialization

The characteristics for bringing a new biological filter system up to full capacity are shown below. Water quality sampling three times daily in the fish tank and the inlet and outlet of the biofilters, also dissolved oxygen samples were taken from the same positions to investigate the oxygen consumptions by carps. Ten milliliters of STRESS ZYME (Fig. 3.16) was added in 38 liter of water to the three biofilters every 1st, 7th, 14th day. Thereafter, (5 ml/38 liter) was added weekly. The bacteria in Stress-Zyme keep proper conditions in the aquarium for the development

MATERIALS AND METHODS

of the biological filter. Harmful organic pollutants are consumed promoting the heterotrophic bacteria growth. This speeds up the development of the biological filter in newly set up aquariums. Water quality and living conditions are improved when Stress Zyme is used on a regular basis. Each 5 ml of Stress Zyme contains 300 million bacteria. These bacteria are in a dormant state and become active when added to the aquarium. Stress Zyme has a five year shelf life and does not require refrigeration. Nitrifying bacteria swim through the system until they find the biofilter suitable media. The biofilm development on Tezontle surface area during the initialization was shown in Fig. 3.17.



Fig. 3.16. Stress Zyme

Trade marks of Mars

Fish care North America,

Inc.

(www.marsfishcare.com)

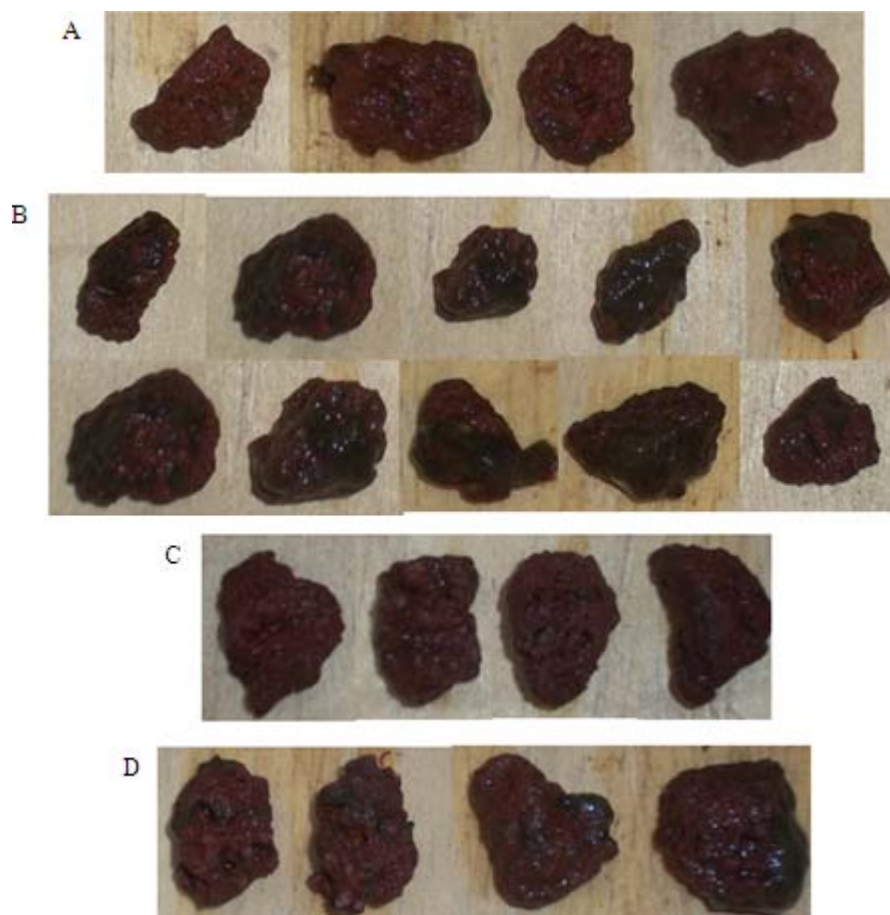


Fig. 3.17. Tezontle (Volcanic sand) biofilm development (A) first biofilter after 25 days and (B) after 45 days and the third biofilter after 25 days and 45 days.

3.2.4. Biofilter measurements.

Total ammonia nitrogen (TAN) and nitrate nitrogen were measured by a digital ammonia and nitrate photometer (low Range) 0 to 3 TAN and 0 to 100 NO₃-N mg/L (HANNA INSTRUMENTS, HI93700 and HI93828 Romania). The equipment operation is shown at appendix I (7.2). TAN and NO₃-N were measured daily at inlet (sample point 2) and outlet of the biofilters tanks (sample point 1) and for fish tanks (sample point 3) white circles Fig. 3.18.

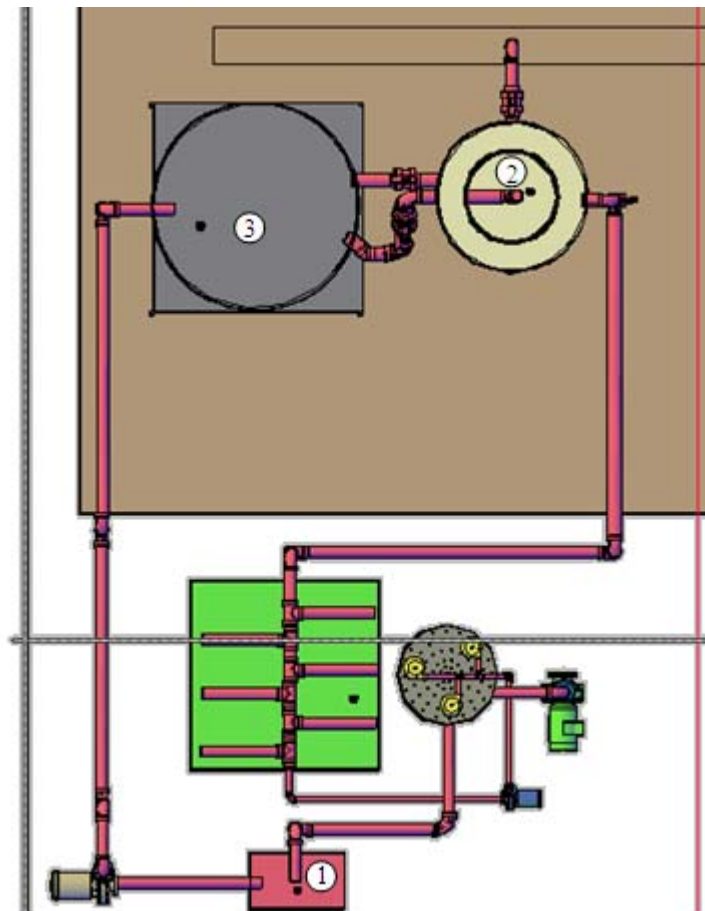


Fig. 3.18. TAN sampling points on RAS system.

The sampling points 1 and 2 were used to calculate total ammonia nitrogen produced by fish tank and converted by the biofilter. The point 3 was used to show the diurnal changes in TAN in the tank. It was observed that there is no differences in measurements for TAN at different tank levels for its rapidly diffusion in water body.

3.2.5. Biofilter performance indicators

The reporting standards for biofilter performance as follow (Colt et al., 2006):

1	Percent TAN removal (PTR %)	$(TAN_{in} - TAN_{out})/TAN_{in}$
2	Filter system ratio (FSR %)	$1440 Q_{filter}(TAN_{in} - TAN_{out})/(total\ TAN\ removed\ d)$
3	Volumetric TAN conversion rate (VTR mg TAN/(m ³ d))	$1440Q_{filter}(TAN_{in} - TAN_{out})/V_{media}$
4	Surface TAN conversion rate (STA mg TAN/(m ² d))	$1440Q_{filter}(TAN_{in} - TAN_{out})/A_{media}$
5	Volumetric oxygen consumption rate (VOCR _{tot} mg oxygen/(m ³ d))	$1440 Q_{filter}(DO_{in} - DO_{out})/V_{media}$
6	Volumetric oxygen consumption rate for nitrifying bacteria (VOCR _{nit} mg oxygen/(m ³ d))	$(3.47VTR + 1.09VNR)(0.92)$
7	Volumetric oxygen consumption rate for heterotrophic bacteria (VOCR mg oxygen/(m ³ d))	$VOCR_{tot} - VOCR_{nit}$
8	Pumping power (average daily) (P _{tot} kW)	Computed using actual filter head losses, bed height, and 70% efficiency
9	Ammonia removal efficiency (ARE mg TAN/kWh)	$1440Q_{filter}(TAN_{in} - TAN_{out})/24 P_{tot}$
10	Oxygen utilization efficiency (OUE mg O ₂ /kWh)	$(1440 Q_{filter} \Delta DO)/ 24 P_{tot}$

3.2.6. Aerators used in the RAS system:

3.2.6.1. Air lift pump.

Air lift pump aerator is the simplest aerator constructed and consists of a 113 cm long (Z) riser tube having a diameter of 10 cm (D) and 90 degree elbow. The air injected at the bottom of the riser tube by the compressor (Central Pneumatic 1 HP, 10 Gallon, 115 PSI). The tank was filled every 20 seconds and evacuate in 12 seconds through the cruciform base that has holes of 3 mm in diameter (Fig.3.19). In air lift pump aerators, the length to diameter ratio (Z:D) of the riser

tube has a significant effect on air lift pump performance. The length to diameter ratio is defined as the length of the riser tube divided by its diameter. When the Z:D ratio is below 50 the two phase flow patterns will not have develop fully. It results in increasing (slip) of the water, decreasing pumping volume and efficiency. In this study Z:D ratio was set to be 12.5.

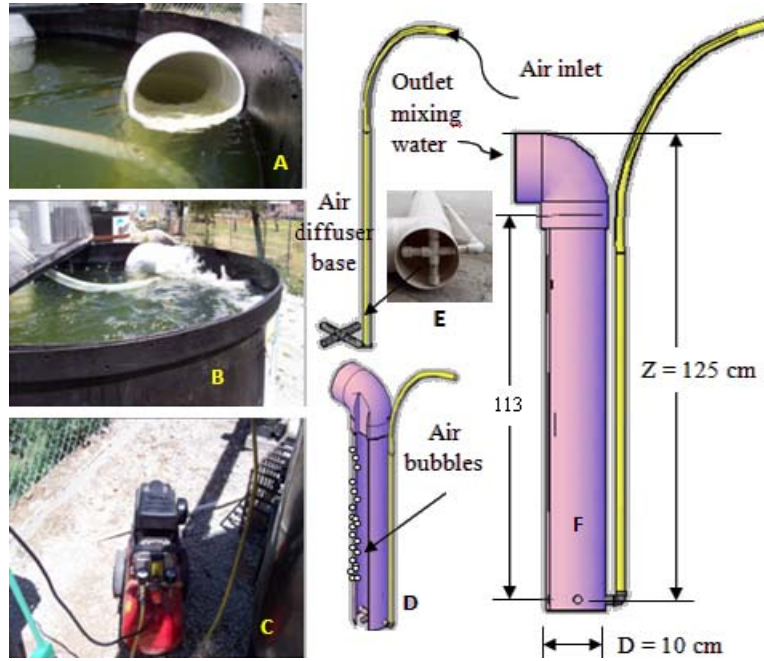


Fig. 3.19. Air lift pump aerator A air lift pump at the moment of compressor tank filling (A), and evacuating (B), air compressor (C), air bubbles raising inside raiser tube (D), cruciform base (E), and lateral view of airlift pump (F).

Three different air inlet pressures were studied to evaluate air lift pump aerator: 80 - 110, 50 - 80 and 25 - 50 PSI, air pressure inlet was measures by compressor manometer.

3.2.6.2. Diffused aerator.

This aerator has a diffused perforated circular tube (Fig.3.20B) positioned at the bottom of the tank (Fig.3.20A). The air was injected through this circular tube by the compressor. The bubbles diameter was differed nearly each 3 seconds due to the effect of air pressure that

MATERIALS AND METHODS

decreasing during compressor evacuating time, at first three seconds the bubbles diameter ranged between 5 to 7 cm at air pressures of 110 to 80 PSI with raising velocity 50-52 cm/s. In next three seconds, the bubbles diameter ranged between 2 to 4 cm at air pressures of 50 to 80 PSI with raising velocity 39-42 cm/s. In the last three seconds at air pressures of 25 to 50 PSI the bubbles diameter ranged between 0.7 to 2 cm with raising velocity of 3-30 cm/s. In the last three seconds air pressure ranged between 14 to 25 PSI, and the bubbles diameter from 0.3 to 0.5 cm with a raising velocity of 0.5-1.5 cm/s. Three different raising velocities of 0.5-1.5 cm /s, 39-42 cm/s and 50-52 cm/s were considered to evaluate the aeration efficiency for this type of aerator. Kodak Easy Share camara of M530 (12 Megapixels) was set to take videos, after that the taken videos were divided to photos every 0.5 second by the program of Real Player, the photos start to cut at the first air bubble realized, the divided photos were analyzed by the program of *ImageJ* (*ij124-jdk6*) to calculate air bubble diameter and bubble raising velocity for each category.

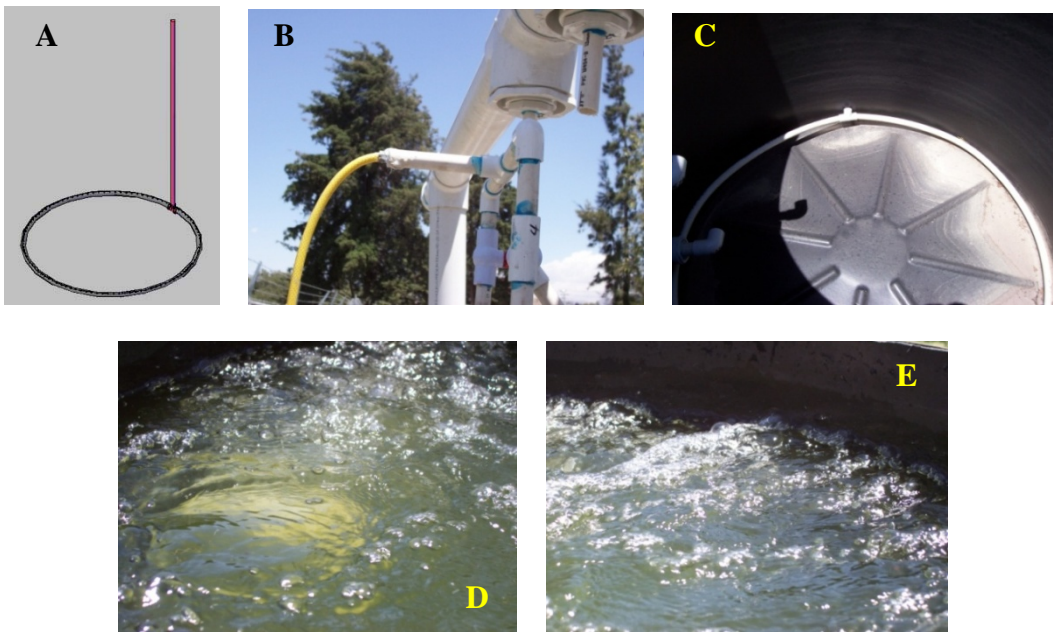


Fig. 3.20. Diffused aerator, diffuser tube (A), compressor hose connection with two PVC valves controlling air inlet pressure (B) tank bottom photo (C), air bubbles in movement in the water (D) and (E).

3.2.6.3. Venturi aerator.

As illustrated in (Fig.3.21.A) a 1.9 cm venturi (Mazzei) injected air into the water flow, inside a tank of 220 liters (Fig. 3.19.B). A PVC valve of 2.54 cm was placed in a by-pass tube to control the differential pressure between the water inlet and the venturi outlet (Fig.3.21.C). The differential pressure evaluates aerator performance at 14.7 kPa, 9.8 kPa and 4.9 kPa. The graduated transparent hose was used to measure the differential pressure. Water flowed at 18 L/min and air was injected at 25L/min. Turbulence is created in the mixing zone by shearing forces and transfer of kinetic energy, (Fig.3.21.E).

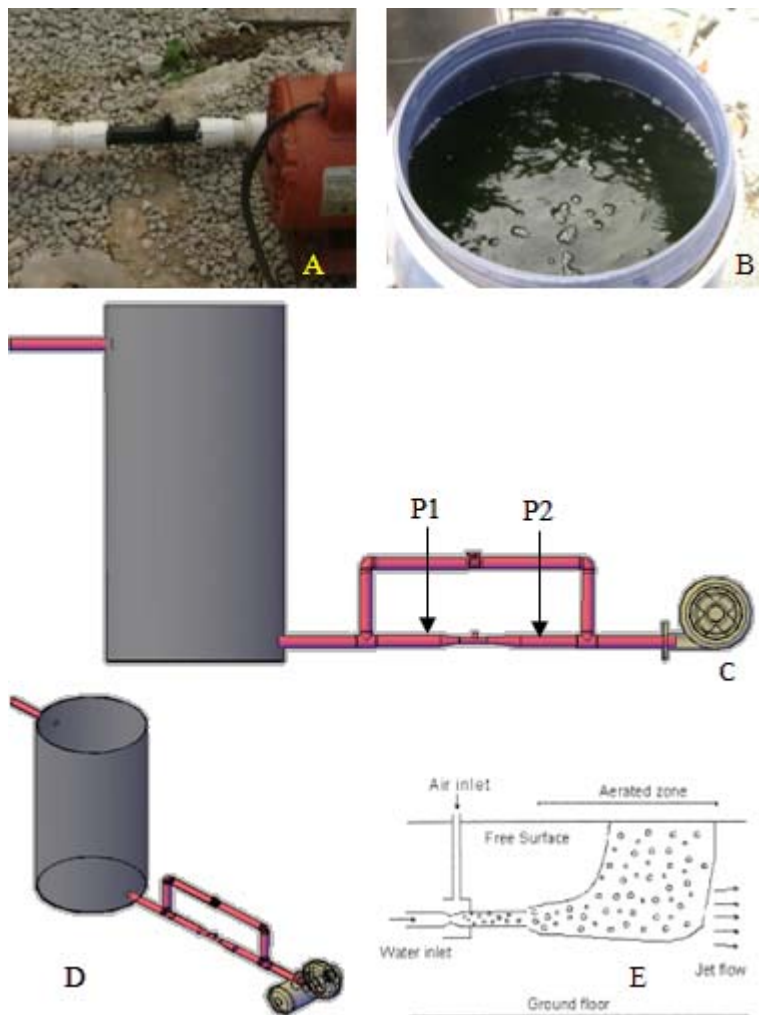


Fig 3.21. Venturi aerator, showing (A) venturi; (B) 200 liter tank; (C) lateral view; (D) isometric view; (E) aeration by venturi.

3.2.6.4. Spray column aerator.

Spray columns have been used extensively in the chemical process industry for gas-liquid absorption and desorption operations. Water is pumped to the top of the tower and through a liquid distributor allowed to flow by gravity. At the same time a blower introduced fresh air into the bottom of the tower; the air flows counter-current to water, sometimes pure oxygen is used in intensive aquaculture ponds. If water contains any volatile contaminant, the air can extract it from the water due to a large air-water interface area. [Colt and Orwicz, \(1991\)](#) indicated that the technique rely on moving water droplets through the air, as is done with surface aerators and packed column aerators. It is more effective than aeration technologies that move air bubbles through water. The column aerator consists of two mass transfer units each 0.9 m long, separated by a water distributor ([Fig.3.22](#)). The water was pumped at the top of the column by a 0.5 Hp pump. Water was divided into three cones using sprays (SURTEK 130027). These cones increase the solubility of oxygen in the water by increasing the contact surface between air and water. To introduce the air at the bottom a blower of 0.5 Hp motor was used. Water and air are introduced through the water distributor making a great turbulence between air and water as it passes through the plate, increasing oxygen solubility in water.

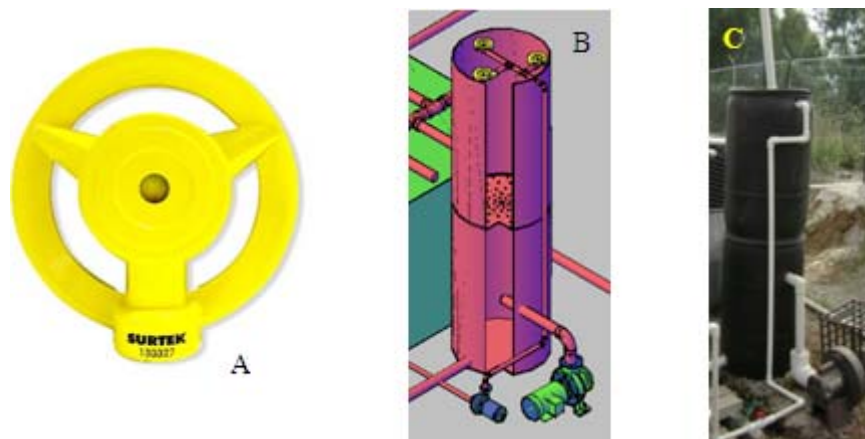


Fig. 3.22 Spray column aerator, (A) Water sprayer SURTEK 130027; (B) Isometric view; (C) Spray column aerator photo.

3.2.7. Aerators evaluation calculations:

These experiments were designed and carried out during May, June and July of year 2010 to acquire the most appropriate aerator designed for local RAS. Two important terms were used to compare the aerator performance as follow:

Oxygen transfer rate (OTR) which is the amount of oxygen that the aerator adds to the water per hour under standard conditions and is reported as kgO₂/hr.

Aeration efficiency index (AAE) which is the oxygen transfer rate divided by the amount of power required and is expressed as kg O₂/hr per kW.

Dissolved oxygen corrections

To correct the solubility at another atmospheric pressure, use the following equation (Boyd, 1998);

$$DO_c = DO_t \left(\frac{P_A}{760} \right) \quad (3.14)$$

The atmospheric pressure at Chapingo was 550 mmHg by solving the equation above:

$$DO_c = DO_t \left(\frac{550}{760} \right) = DO_t \times (0.72368)$$

Table 7.3 and Fig.7.1 (Appendix I) show the effect of the altitude on dissolved oxygen saturation and the effect of dissolved oxygen partial pressure on oxygen solubility. The pressure or tension of DO in water can be estimated by equation (2.32).

There are two basic types of aerator performance tests, the steady-state test and the unsteady-state test. The steady-state tests is conducted by mounting an aerator in a stream of water and measuring flow volume and DO concentration before and after aeration. The difference in the mass of DO between the inflow and the outflow represents the mass of oxygen transferred to the

water by the aerator (Watten and Boyd, 1989; Colt and Orwicz, 1991; Vinci et al., 1997 and Morchain et al., 2000). The un-steady method of testing aerators in basins of water (American Society of Civil Engineers, 1992) is used by several investigators (Boyd and Ahmad, 1987; Rutanggorigit et al., 1991; Boyd, 1998; Loyless and Malone, 1998; and Fast et al., 1999). In the present study the steady-state test was used to determine the aerator performance and this experiment was conducted at dissolved oxygen concentrations ranged between 10% and 70% saturation.

To enhance the reliability of experiment, the liquid was sampled at three different points along the path of water. The average mass transfer coefficient $k_L a$ in column can be calculated by (Linek et al., 1984);

$$k_L a = \frac{1}{n-1} \sum_0^{n-2} \frac{u_L}{h_i} \left[\ln \left(\frac{DO_s - DO_i}{DO_s - DO_{i+1}} \right) \right] \quad (3.15)$$

The oxygen transfer coefficient is adjusted to 20°C with the following equation:

$$K_L a_{20} = K_L a_T \div 1.024^{T-20} \quad (3.16)$$

where $K_L a_{20}$ is the oxygen transfer coefficient at 20°C (h^{-1}) and T is the water temperature (°C). If the test cannot be run in clean water, the α values must be determined for the water in which the aerator test was conducted (Boyd & Ahmad, 1987).

$$\alpha = \frac{K_L a_{20} \text{ test water}}{K_L a_{20} \text{ tap water}} \quad (3.17)$$

The α test can be conducted by using a laboratory-scale aerator to determine $K_L a_{20}$ values for small samples of test water tap water (Shelton & Boyd, 1983).

$$K_L a'_{20} = K_L a_{20} \div \alpha \quad (3.18)$$

where $K_L a'_{20}$ is the adjusted $K_L a_{20}$.

The rate of oxygen absorption can be calculated by (Lewis and Whiteman, 1924) equation:

$$\frac{dDO}{dt} = k_L a (DO^* - DO_m) \quad (3.19)$$

where, DO_m is measured dissolved oxygen at first point in (mg/l). The rate of oxygen absorption accelerates after increasing the oxygen deficit ($DO^* - DO_m$)

Outlet dissolved oxygen saturation percent can be determined by this formula (Boyd, 1998):

$$(\%DO) = \frac{DO_o}{DO^*} \chi 100 \quad (3.20)$$

The oxygen-transfer coefficient is used to estimate the standard oxygen-transfer rate for aerator:

$$SOTR = K_L a'_{20} (DO_{s20})(V)(10^{-3}) \quad (3.21)$$

where, V is tank volume (m^3) and 10^{-3} factor for converting grams to kilograms. The actual oxygen transfer rate for an aerator operating in a fish pond can be estimated with the following equation:

$$OTR = SOTRX \frac{DO_s - DO_f}{9.09} \chi 1.024^{T-20} \chi \alpha \quad (3.22)$$

Oxygen transferred per hour can also be computed by the following equation (Wheaton, 1993),

$$OTR = K_L a (DO_s - DO_m)(V)(10^{-3}) \quad (3.23)$$

Aeration efficiency index:

$$AAE = \frac{OTR}{BP} \quad (3.24)$$

where AAE is aeration efficiency index, OTR is oxygen transfer rate in gO_2/h and BP is the power used in kW.

3.3. Recirculating aquaculture system operation performance.

During the experimental running of RAS system some factors were identified such as the relationship between aeration level and water temperature, dissolved oxygen level on fish growth rate, algae presence and its effect on aeration process and water distributor as an additional aerator.

a. The effect of dissolved oxygen concentrations on carp growth rate.

Three different levels of dissolved oxygen concentration were studied; carp growth rate and energy consumption per each 10 gram of growth at three of dissolved oxygen concentrations levels. Dissolved oxygen concentration for the first, second and third tank was between, 2.0 - 4 and 3.5 - 5 ppm respectively. To maintain the dissolved oxygen levels in the tanks, three different aeration mechanisms were used: (1) Full capacity of countercurrent spray column aerator for the first tank, (2) Gravity aeration by biofilter distribution sprays, and (3) aeration by spray column aerator with water pump only as shown in Fig. 3.23.



Fig. 3.23. The three different aeration techniques that were used (1) spray column aerator (i.e. water pump with air fan), (2) Gravity aerator, and (3) spray column aerator with water pump only.

b. The effect of oxygen transfer rate on tank water temperature and its influential on carp oxygen consumption.

At cooler months such as January, February and March the aeration process can effect drastically on water tank temperature, at low air temperatures the spray column aerator operated as a chiller, for air-water surfaces contacting affecting heat enthalpy gained or lost for the aerated water. Carp oxygen consumption was used as an indicator for carp biological activities such as digestion, building and maintenance at different water temperatures.

c. The effect of algae presence on spray column aerator operation hours.

Algae influence the water quality of the pond mainly by affecting the balance among dissolved oxygen, pH, carbon dioxide, and nutrients. During photosynthesis, algae produce oxygen, remove nutrients, and take up respired carbon dioxide from both the fish and the algae itself. According to the amount of ammonia nitrogen and nitrate nitrogen released in the system the algae can grow rapidly for example in carp tank 3 the carp grow to be more intensively in three weeks as shown in Fig. 3.24. In heavily stocked ponds, the water becomes supersaturated with carbon dioxide. High levels of carbon dioxide can quickly depress the pH of the water to levels below seven if the operator is not careful to maintain proper alkalinity levels and adequate aeration for stripping. During active periods of photosynthesis (during daylight hours), algae can quickly strip the carbon dioxide out of the water, and pH levels can rise above nine in a matter of hours. Fish not acclimated to such sharp shifts may initially show signs of stress.

At night, both algae and fish consume oxygen from and exhale carbon dioxide into the system. Algae compete with the fish for available oxygen in the water. A potentially serious impact of an algae bloom is the risk of an “algae crash” triggered by temperature or barometric pressure. When an algae bloom collapses, dead algae cells settle to the bottom of the pond,

MATERIALS AND METHODS

adding to the decomposing sediment's oxygen demand. If the crash is severe, the pond's oxygen supply can be quickly depleted, causing spray column aerator to operate more continuously. Additionally, as the dead algae cells rupture, they can release organic nitrogen and phosphorous back into the water, adding to the system's nutrient load. The biological cycle starts again with bacteria converting the organic nutrients to inorganic elements. Which are then available to be recycled, and the algae bloom continues.



Fig. 3.24. Algae growth developing in the Tank 3 was 45, 56, 95, 150 and 420 NTU respectively.

d. The effect of three different water distributors on spray column aerator operation hours.

Water distributors mounted above the biofilters present as a gravity aerators which utilize the energy released when water loses altitude to transfer oxygen. A sprayer SURTEK 130027 was used to diffuse the water above the biofilter media, which worked as splashboards in tank 2 (Fig. 3.25 B); or by water distribution tube (Fig. 3.25A). The efficiency of a gravity aerator was calculated by equation 2.14.

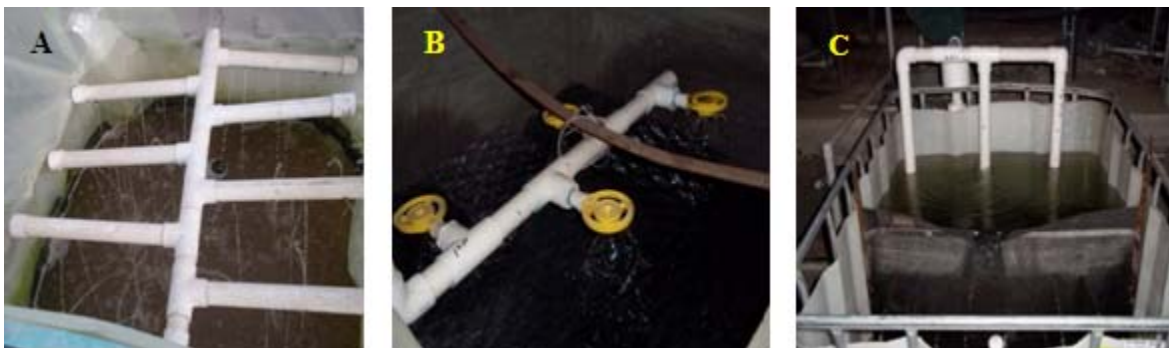


Fig. 3.25 Three different forms of gravity aeration through the biofilters.

3.4. Dissolved oxygen budget monitoring and sampling system.

3.4.1. Dissolved oxygen mass balance in RAS.

A basic task of fish tank management is the maintenance of dissolved oxygen for fish survival and growth. The managers can monitor the dissolved oxygen level at a given point in time, predicting potential critical periods of low concentration. Dissolved oxygen concentrations, are given by chemical, physical and biological reactions. In order to gain a better understanding of events which can contribute to low dissolved oxygen concentration, such as heavy phytoplankton blooms and high temperature. The parameters under-studies participating to the oxygen budget in the recirculating aquaculture system are Phytoplankton, Cultivating Fish, Nitrifying bacteria, and Sediments as shown in Fig. 3.26, Eq. 3.25 and Table 3.3 and 3.4.

$$\begin{aligned}
 DOD = & \text{Algae oxygen respiration or production} \\
 & + \text{Fish oxygen consumption} + \text{Nitrifying bacteria oxygen consumption} \quad (3.25) \\
 & + \text{Sediments oxygen consumption}
 \end{aligned}$$

Equation 3.25 can be used to calculate the amount of aeration required to RAS system.

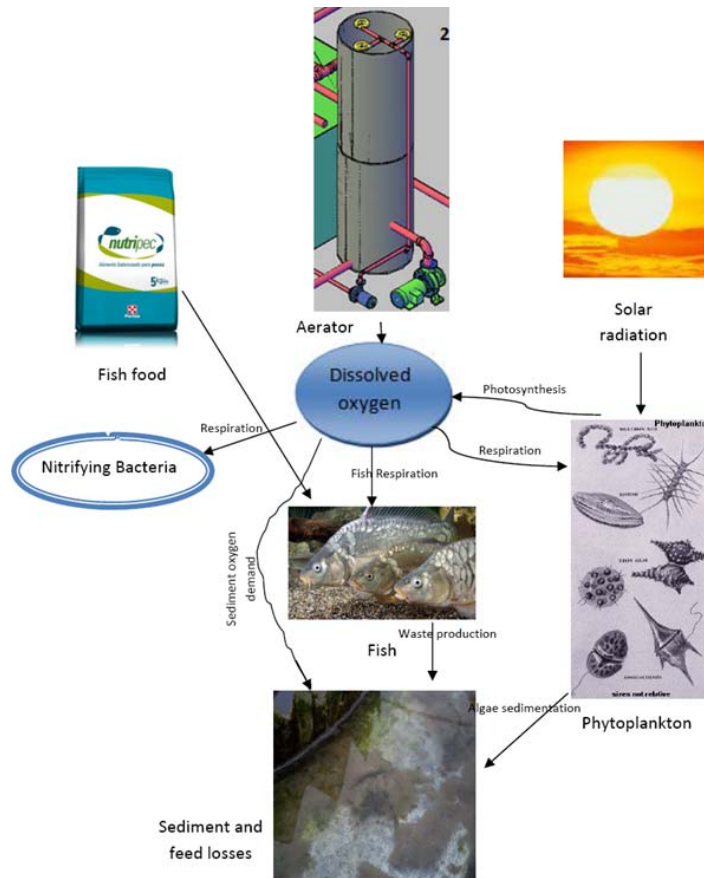


Fig. 3.26. Dissolved oxygen budget in RAS.

Table 3.3. Oxygen mass balance equations in RAS.

Inlet variables	Equation	R ²
Algae oxygen production	$AOP = 4.5795\ln(NTU) + 3.0793$	0.894
Algae oxygen consumption	$AOC = 0.0286(NTU) + 17.306$	0.9782
Fish oxygen consumption	$FOC = AW^2 + BW + C$	Table 3.4
Nitrobacter	$NBOC = (0.1936(W) - 2.0174) \times (V_m)$	0.8851
Sediments	$SOC = 1279.62(V_{sed})$	0.812

where AOP is accumulated oxygen production per day, AOC is accumulated oxygen consumption per day, NTU is water turbidity in NTU units, W is carp mean weight in grams, V_m is the biofilter media bulk volume in m³, FOC is carp oxygen consumption, NBOC is nitrobacter oxygen consumption, SOC is sediments oxygen consumption.

Table 3.4. Parameter definitions for carp oxygen consumption calculation.

Water temperature (°C)	A	B	C	R ²
18	-0.00001	0.0447	0.4306	0.994
20	-0.0001	0.0506	0.5103	0.99
22	-0.0001	0.058	0.523	0.97
24	-0.0001	0.0635	0.6812	0.96

3.4.2. Dissolved oxygen sampling system.

Galvanic dissolved oxygen sensor HI 76410/4 (Fig. 3.27C) was connected to the DO analyzer HI 8410 (Fig. 3.27D). It was equipped with Novus data logger to save dissolved oxygen concentration data every 10 minutes. The output current of the HI8410 was converted to dissolved oxygen values (ppm) using the programmed scale equation on the data logger (two analogue industrial sensors LOGBOX-AAIP65 electronic data logger, (Fig.3.27E)). The registered data was transferred to the computer by a wireless interface with USB cable.

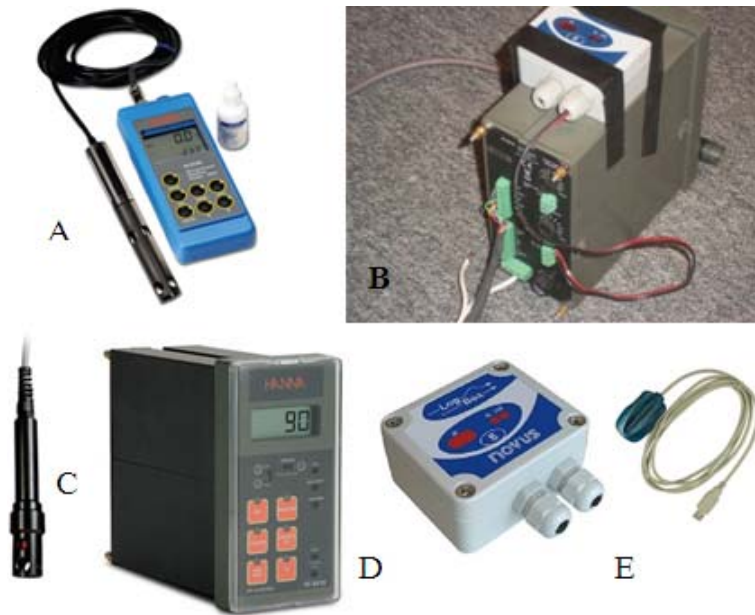


Fig. 3.27. Dissolved oxygen meters (A) hand meter (HI 9146), (B) controller and data logger, (C) DO sensor HI 76410/4, (D) DO analyzer HI 8410 and (E) electronic data logger LOGBOX-AAIP65 and its wireless interface with USB cable.

HI 76410/4 is a galvanic probe provided with a membrane covering the galvanic sensor and a built-in thermistor for temperature measurement and compensation; recommended for connection with HI 8410. DO hand meter has a polarographic probe (HI 76407/4F), (Fig. 3.27). Hand meter (HI 9146) and dissolved oxygen controller (HI 8410) characteristics illustrated at Tables 3.5, 3.6.

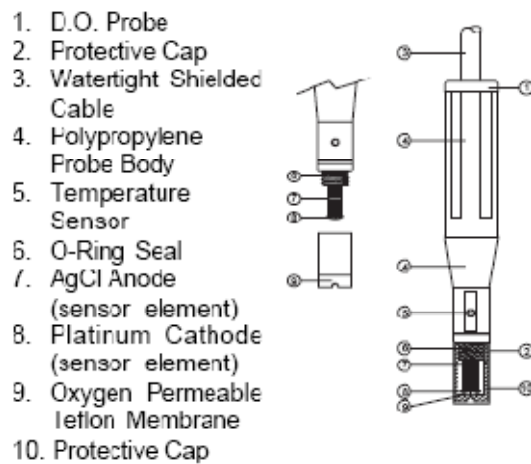


Fig. 3.28. Polarographic probe HI 76407/4F.

MATERIALS AND METHODS

Table 3.5. Hand meter (HI 9146)

specifications.

Range	0.00 to 45.00 mg/l O ₂ 0.0 to 300 % O ₂ 0.0 to 50.0 °C
Resolution	0.01 mg/l O ₂ 0.1 % O ₂ 0.1 °C
Accuracy (@25°C/77°F)	±1.5% Full Scale mg/l O ₂ ±1.5% Full Scale % O ₂ ±0.5 °C
Typical EMC Deviation	±0.3 mg/l O ₂ / ±3.5 % O ₂ ±0.5 °C
Calibration	Automatic in saturated air
Temperature Compensation	Automatic from 0 to 50°C (32 to 122°F)
Altitude Compensation	0 to 4000 m 100 m resolution
Salinity Compensation	0 to 80 g/l 1 g/l resolution
Environment	0 to 50°C (32 to 122°F) RH 100%
Power supply	• 4x1.5V AA batteries; 200 hours of continuous use; auto-off after 4 hours. • 12 VDC adapter
Dimensions	196 x 80 x 60 mm (7.7 x 3.1 x 2.4")
Weight	meter: 425 g (15 oz) kit: 1.4 kg (3.1 lb)

Table 3.6. Dissolved oxygen analyzer (HI 8410)

specifications.

Range	0.0 to 50.0 mg/L (ppm) O ₂ 0 to 600 % O ₂ -5.0 to 50.0 °C
Resolution	0.1 mg/L or 1% (O ₂) / 0.1 °C
Accuracy	±1% of reading (O ₂) / ±0.2 °C
Calibration	Manual, one point, in saturated air
Temp. Compensation	Automatic, from -5 to 50°C (23 to 122 °F)
Salinity Compensation	0 to 51 g/L (resolution 1 g/L)
Probe (not included)	HI 76410/4 with 4 m cable or HI 76410/10 with 10 m cable
Recorder Output	0 to 20 mA or 4 to 20 mA (isolated)
Setpoint Relay and Alarm Relay	1, Isolated, 2A, Max. 240V, resistive load, 1,000,000 strokes
Alarm Range	1.0 to 5.0 mg/L (ppm) O ₂
Setpoint Range	1 to 600 % O ₂ 0.1 to 50.0 mg/L (ppm) O ₂
Hysteresis Range	0.5 to 2.4 mg/L (ppm) O ₂
Dosing Control	OFF/AUTO/ON with selection switch
Over Dosing Control	Adjustable, from 5 min to 60 min with knob or Disable by wire strap - on rear panel
Backlight	Continuous ON
Power Supply	115 or 230 Vac ±10% (user selectable); 60/50 Hz
Enclosure	Black anodized aluminum body; front and back with ABS; transparent splash-proof front cover
Environment	-10 to 50°C (14 to 122°F); RH 95%
Panel Cutout	141 x 69 mm (5.6 x 2.7")
Weight	1 kg (2.2 lb.)

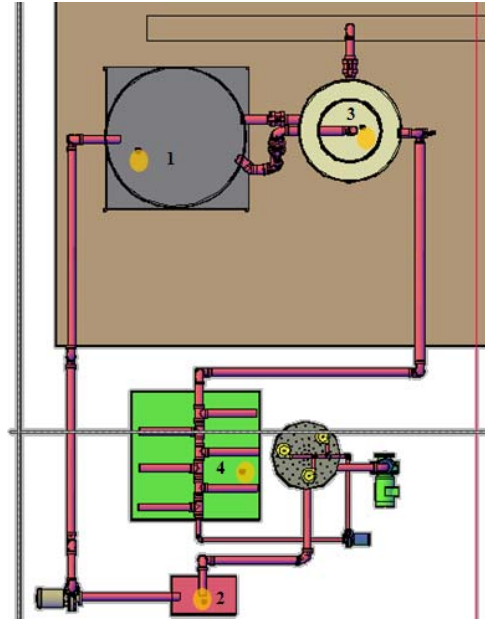


Fig. 3.29. DO sampling points on RAS system (Orange circles show sampling location points).

The first sampling point was in the Carp tank to monitor dissolved oxygen concentrations during 24 hours. Second and third points were positioned at the fish tank inlet (aerator outlet) and centre cylinder of the separator where the tank bottom outlet was discharged; these measurement points were used (second and third points) to calculate the fish oxygen consumption by the following equation;

$$SOC = (DO_{tin} - DO_{tout}) \frac{mgO_2}{liter} \times Q \frac{liter}{min} \times \frac{1}{60 \times 1000} \frac{gO_2}{hour} \times \frac{1}{FBM(kg)} \frac{gO_2}{kg.h} \quad (3.26)$$

where, SOC is the carp specific oxygen consumption ($\frac{gO_2}{kg.h}$), DO_{tin} is the dissolved oxygen concentration at tank inlet, DO_{tout} is the tank outlet and Q is the water flow rate of the system.

Dissolved oxygen concentration at the biofilter was measured and sampled at point 4 of the biofilter. Oxygen concentrations at the biofilter were higher than at the inlet, as water falling from the water distributor mounted over the biofilter increased air-water contact. For this reason the oxygen consumed by nitrifying bacteria was measured at the system turning off status. The reduction rate in dissolved oxygen calculated oxygen consumption by:

$$NBOC = \frac{(DO_{t1} - DO_{t2})}{T_{inv}} \times V_{water} \quad (3.27)$$

where, *NBOC* is the nitrifying bacteria oxygen consumption, DO_{t1} is the dissolved oxygen concentration at time 1, DO_{t2} is dissolved oxygen concentration at time 2, T_{inv} is the time interval between time 1 and time 2 and V_{water} is water volume in the biofilter. The sample point (4 and 2) (Fig. 3.24) used as aerator inlet and outlet sampling point to measure the amount of oxygen transferred to water stream in the system by following equation.

$$OTR = (DO_{out} - DO_{in}) \times Q_{water} \quad (3.28)$$

3.5. Oxygenation system automation.

Effective *DO* management is a key factor in the operation of commercial RAS. For this experiment of automation three tanks were stocked with different sizes of 50 organisms per m³ the first tank has an average of 198 grams, the second 130 grams and the third of 210 grams to optimize each tank control independently. Aeration system automation yielded real time control of oxygen levels in the production tank eliminating high oxygen levels during the night and low oxygen levels following feeding and temperature raises.

Dissolved oxygen concentrations from the three tanks measured and stored using only one sensor and one controller. A hydraulic head (Fig. 3.30) constructed with an inclination of 5° received the water sample from each tank through a hose. Each hose came from a 25W peristaltic pump (mod. 41k25GN-AUL-ES, Oriental Motor Co. LTD, Japan) providing a flow rate 0.356 liter/min. The water passed through the DO probe and returned back to the tank (Fig. 3.30). For accurate dissolved oxygen measurements a water flow of at least 5-7 cm/s is required. In this way a constant replenishment of the oxygen-depleted membrane surface is ensured.



Fig. 3.30. Overview of the peristaltic pumps mounted over the tanks and the hydraulic head system.

3.5.1. Data acquisition system installation.

A galvanic probe (HI 76410/4, Hanna Instruments, USA) was connected to the rear panel mounted controller (mod. HI 8410, Hanna Instruments, USA). Dissolved oxygen readings are automatically compensated for temperature changes of oxygen solubility and membrane permeability.

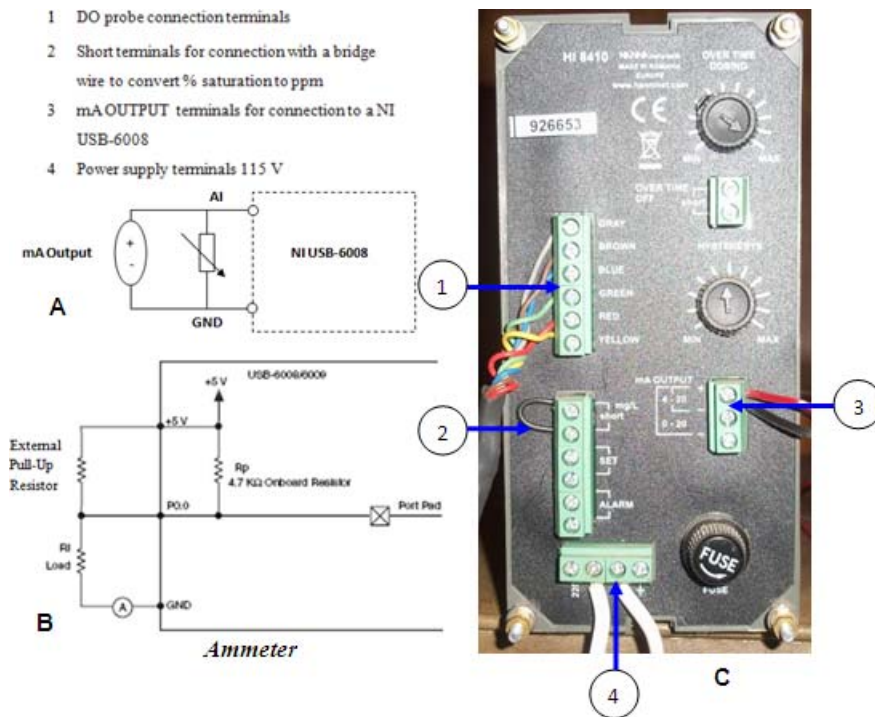


Fig. 3.31. Acquisition system connection.

MATERIALS AND METHODS

The dissolved oxygen analyzer (HI 8410) output was considered as a referenced single ended analog signal. The positive terminal of the 4-20 mA current signal was connected to the desired analog input of NI-USB 6008 (AI) and the negative terminal was connected to ground terminal (Figs. 3.31A and C). A variable resistor of 10 k Ω was connected in parallel with the sensor and the analog input terminals; the variable resistance was used for manual calibration in the field. The default configurations of the NI USB-6008DIO ports are open collector, allowing 5 V operations, with an onboard 4.7 k Ω pull-up resistor. An external pull-up resistor can be added to increase the source current drive up to a 8.5 mA limit per line. To determine the external pull-up resistor an ammeter was connected in series with the load (Fig. 3.31B). A variable resistor was placed between the digital output line and the +5 V supply and adjusted until the ammeter read the desired current. The current should be less than 8.5 mA, and the resistance of the variable resistor was measured. The measured resistance was 340 Ω so six static resistors of 390 Ω were chosen, three outputs were used by the relays to turn on the peristaltic pumps and the other three to start the aerators (Fig. 3.32).



Fig. 3.32. A central controller PC for dissolved oxygen controller with dissolved oxygen analyzer (HI 8410).

Table 3.7 NI-USB 6008 port configuration

Port configuration								
Digital Signal	P0.0	P0.1	P0.2	P0.3	P0.4	P0.5	P0.6	P0.7
Terminal	17	18	19	20	21	22	23	24
Define	1 st peristaltic pump	2 nd peristaltic pump	3 rd peristaltic pump	4 th peristaltic pump	1 st aerator	2 nd aerator	3 rd aerator	4 th aerator
Signal	GND	AI 0	P1.0	P1.1	P1.2	P1.3	GND	AI1
Terminal	1	2	25	26	27	28	4	5
	Single-Ended Mode DO sensor		digital				Single-Ended mode Thermopare	
Define	Analog current input -ve	Analog current input +ve	Water spray Pump	Vibrator Motor	Electrical voltage state	Alter. power source	Analog voltage	Analog voltage

3.5.2. LabView coding

LabVIEW (short for Laboratory Virtual Instrumentation Engineering Workbench) is a platform and development environment for a visual programming language from National Instruments. The purpose of such programming is automating the usage of processing and measuring equipment in any laboratory setup.

The graphical language is named "G" (not to be confused with G-code). Originally released for the Apple Macintosh in 1986, LabVIEW is commonly used for data acquisition, instrument control, and industrial automation on a variety of platforms including Microsoft Windows, various versions of UNIX, Linux and Mac OS X (<http://en.wikipedia.org/wiki/LabVIEW>). The version that used in this experiment is LabView 2009 (32-bit). LabView is a widely used graphical programming environment which allows designing systems in an intuitive block-based manner in shorter times as compared to the commonly used text-based programming languages. A closed loop ON/OFF control compared functions between the desired dissolved oxygen (DO)

concentrations for the three tanks and the DO concentration actually measured, sending on/off signal to each aerator independently (Fig. 3.33).

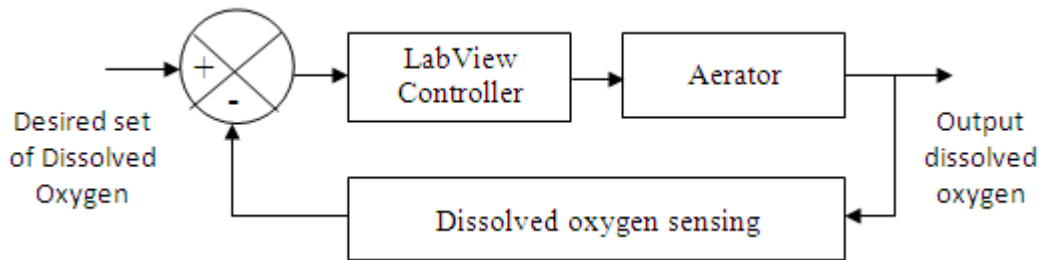


Fig. 3.33. Close loop control.

Basically, LabView consists of Front Panel – User Interface and Block Diagram – Compiled Code.

3.5.2.1. The user interface (front panel)

The user interface of the dissolved oxygen controller has three components: 1. Program definition, 2. Operation states and 3. Sensor operation.

The program presents four definitions

a. Digital output ports definition.

The digital output ports of the NI-USB DAQ 6008 are used to control the three peristaltic pumps and the three aerators.

b. Data logging timer.

Data logging timer and measurements interval timer can be timed by the user to take measurements from each of the three tanks every 10 min. Peristaltic pump turning on timer was programmed to be for the first two tanks at 3.3 m, taking 23.5 seconds to acquire the first water sample provided from the pump hose at depth of 80 cm. The third tank located 6.1 m away from the hydraulic head required 43.6 seconds in order that the water sample arrived to the DO sensor.

c. Data logger path.

Specific folder path at the PC should be defined, dissolved oxygen readings logged by LabView in a Microsoft Excel file with CVS extension. The program automatically generates three Excel files, one for each tank to be located in the predefined folder at PC; new acquired data was appended to it. LabView acknowledged the acquired data (e.g. if the data received from the first, second or third fish tank) according to the assigned peristaltic pump state. The acquired data was graphed daily by the user to monitor changes in dissolved oxygen and identify sensor problems.

d. Desired values.

Identify the maximum and minimum desired values of dissolved oxygen that the controller should maintain. Dissolved oxygen concentrations difference between minimum and maximum DO should be above 1 ppm.

The operation status module has some Boolean leds giving the user account about the status of the controller components of three peristaltic pumps and the three aerators ([Fig.3.34](#)).

The sensor operation monitoring module has a visual interface for measuring errors. It presents a suitable scale equation actually used by the program, a waveform chart for graphing the historical measurement. Manual calibration processes interface that require user presence replace sensor membrane and electrolyte. It is recommended to change the membrane every 2 months and once a month change the electrolyte. At the moment of electrolyte or membrane exchange if the user did not take a care for air bubbles inside the electrolyte the measurements reach higher peaks, LabView program can detect this error immediately the user should gently tap the membrane over a surface to ensure that no air bubbles remain trapped.

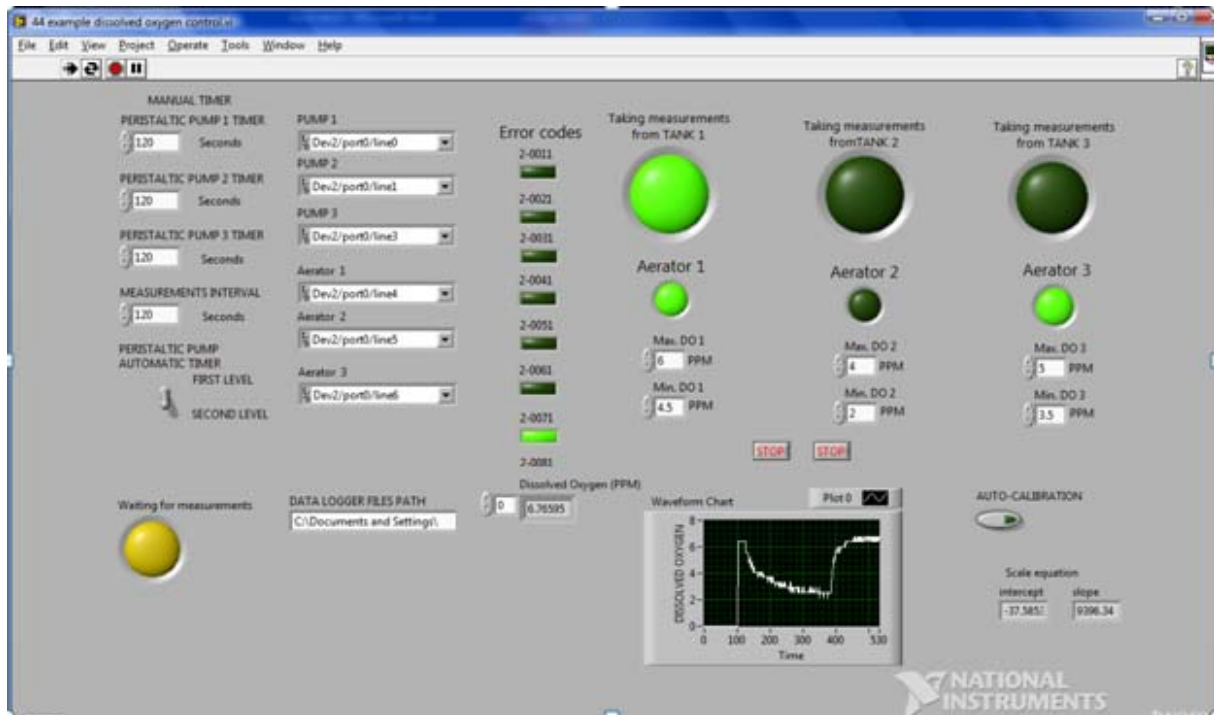


Fig. 3.34. Front panel-User Interface with dissolved oxygen control.

3.5.2.2. Compiled code algorithm.

At the moment of program starting, is sending true state (on) to the first peristaltic pump and its corresponding led at user interface. The elapsed time taken by the peristaltic pump until one sample reach to DO probe from each tank is varied and programmed built-in. The program makes dissolved oxygen sensor in idle status until 20 seconds before water sample reach, doing auto calibration with air, the controller acquires thirteen values of dissolved oxygen after 45 seconds (sensor stabilization elapsed time) of water sample reaching. The stored data are averaged and compared against a given set point. If the dissolved oxygen measurement is beneath the set point the first aerator will turn on simultaneously with its corresponding led at user interface. Once the peristaltic pump is turned-off water inside the hydraulic head returns to the tank and air fills the sensor head doing sensor auto diagnostic with one point (at saturation status air-membrane contact), for membrane antifouling processes see appendix II. The program will start to do the

same operation steps with the second tank and the third tank (Fig. 3.35). The RAS aeration requirements during the growing season under dissolved oxygen controller were reduced having minimum energy consumption; Table 3.8 shows hour's operations requirements for each life stage.

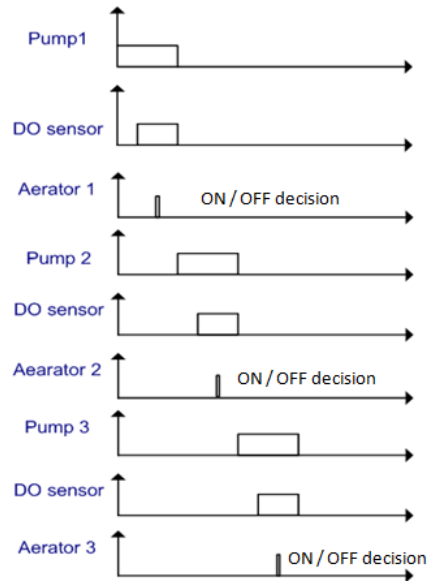


Fig. 3.35. Timing signals during system operation.

MATERIALS AND METHODS

Table 3.8. RAS system aeration requirement in hours during the day and the night at different water temperatures for 50 organisms per m³.

Individual fish weight	Water temperatures, °C							
	17	18	19	20	21	22	23	24
20	0.91	0.97	1.06	1.13	1.19	1.26	1.32	1.38
30	1.33	1.41	1.54	1.64	1.74	1.83	1.92	2.02
40	1.74	1.84	2.01	2.13	2.26	2.39	2.50	2.64
50	2.13	2.25	2.45	2.60	2.77	2.93	3.06	3.23
60	2.50	2.65	2.88	3.06	3.26	3.45	3.60	3.80
70	2.86	3.03	3.29	3.49	3.72	3.95	4.12	4.35
80	3.20	3.40	3.69	3.90	4.17	4.42	4.61	4.88
90	3.53	3.74	4.06	4.29	4.59	4.88	5.08	5.38
100	3.84	4.08	4.42	4.67	5.00	5.32	5.53	5.86
110	4.14	4.40	4.76	5.02	5.39	5.74	5.96	6.32
120	4.42	4.70	5.09	5.35	5.75	6.14	6.36	6.76
130	4.68	4.99	5.39	5.67	6.10	6.52	6.75	7.18
140	4.93	5.26	5.68	5.96	6.42	6.87	7.11	7.57
150	5.17	5.52	5.95	6.23	6.73	7.21	7.45	7.94
160	5.39	5.76	6.20	6.48	7.02	7.53	7.76	8.29
170	5.59	5.98	6.43	6.72	7.28	7.83	8.06	8.62
180	5.78	6.19	6.65	6.93	7.53	8.11	8.33	8.93
190	5.95	6.39	6.85	7.12	7.76	8.37	8.58	9.21
200	6.11	6.56	7.03	7.30	7.96	8.61	8.80	9.47
210	6.25	6.73	7.19	7.45	8.15	8.82	9.01	9.71
220	6.37	6.88	7.34	7.58	8.32	9.02	9.19	9.92
230	6.48	7.01	7.47	7.70	8.46	9.20	9.35	10.12
240	6.58	7.12	7.58	7.79	8.59	9.36	9.49	10.29
250	6.66	7.23	7.67	7.86	8.69	9.50	9.61	10.44
260	7.56	8.15	8.70	9.00	9.86	10.70	10.91	11.77
270	7.81	8.42	8.99	9.29	10.19	11.06	11.27	12.16
280	8.06	8.70	9.28	9.58	10.52	11.42	11.63	12.56
290	8.31	8.97	9.57	9.88	10.84	11.77	11.99	12.95
300	8.56	9.24	9.85	10.17	11.17	12.13	12.35	13.35
310	8.81	9.51	10.14	10.46	11.49	12.49	12.71	13.74
320	9.06	9.78	10.43	10.76	11.82	12.85	13.07	14.13
330	9.31	10.05	10.72	11.05	12.15	13.21	13.43	14.53
340	9.56	10.33	11.00	11.34	12.47	13.57	13.79	14.92
350	9.81	10.60	11.29	11.63	12.80	13.92	14.15	15.31
360	10.06	10.87	11.58	11.93	13.12	14.28	14.51	15.71
370	10.31	11.14	11.87	12.22	13.45	14.64	14.87	16.10
380	10.56	11.41	12.15	12.51	13.78	15.00	15.23	16.50
390	10.81	11.69	12.44	12.81	14.10	15.36	15.59	16.89
400	11.06	11.96	12.73	13.10	14.43	15.72	15.95	17.28

Open loop control as an alternative method for close loop control in emergency situations.

Due to the the presence of user to change the sensor electrolyte or membrane, LabView was programed to operate the control system as open loop during emergency situations (Fig. 3.36). Sensor failures resulted in higher frequency values and variation of the saturation point. For a given temperature and biomass density calculated according to the age, the program calculates aeration time per tank (Equations 3.16 and 3.17). This values were encountered to reach a dissolved oxygen set point between 4 and 5 ppm.

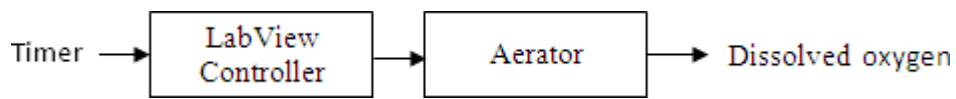


Fig. 3.36. Open-loop control system.

The following equations were used in programming obtained from the model of dissolved oxygen balance in RAS,

$$A_{req} = af^2 + bf + c \quad (3.29)$$

$$f = 0.0009T^2 + 0.0165T + 1.7713 \quad (3.30)$$

where A_{req} is the aeration requirement time, f is the carp biomass (kg per m³) and T is fish age (day). The equation constants were defined by table 3.9.

Table. 3.9. Aeration requirements equation constants

Temperature, °C	a	b	c
24	-0.0222	1.3879	0.0731
22	-0.02	1.2564	0.0781
20	-0.02	1.125	0.0791
18	-0.0155	0.9636	0.0768

3.5.2.3. Environment and dissolved oxygen sensor.

An important consideration in aquacultural control systems is the environment in which they are used. The corrosiveness of the water in which DO probe is placed can rapidly degrade its effectiveness. DO probe can also be fouled by microbial growth. A regular schedule of maintenance (electrolyte and membrane exchanging every month) and calibration should be used to insure that the probe is functioning properly. Program fault detection for DO probe determining its status and fouling problems see appendix II (Galvanic dissolved oxygen sensor auto-diagnostic monitoring and control during carp cultivation).

3.5.2.4. Signal filtering using LabView for temperature and dissolved oxygen measurements.

Thermocouple readings were recorded by LabView in an Excel file. In order to monitor changes in water temperature and identify problems for fish tanks. Water temperatures were taken manually twice daily with mercury thermometers to validate thermocouple records. Thermocouples were calibrated against the same mercury thermometer. Thermocouples were subject to electrical noise and occasionally recorded outlying temperature readings that we assumed were false (e.g., -90°C). Four different types of signal filtering were used for dissolved oxygen probe and thermocouple signals, Table 3.10. Treated signal by the different filters was illustrated graphically at the front panel (Fig. 3.38). Smoothing filter with higher time constant of exponential average (40.105) was used to remove the noises of the thermocouples, and 1 for dissolved oxygen probe as shown in Fig. 3.37 the voltage signals obtained by thermocouples was filtered and converted linearly to centigrade; dissolved oxygen probe signals already had linearity that done by dissolved oxygen analyzer (HI 8410).

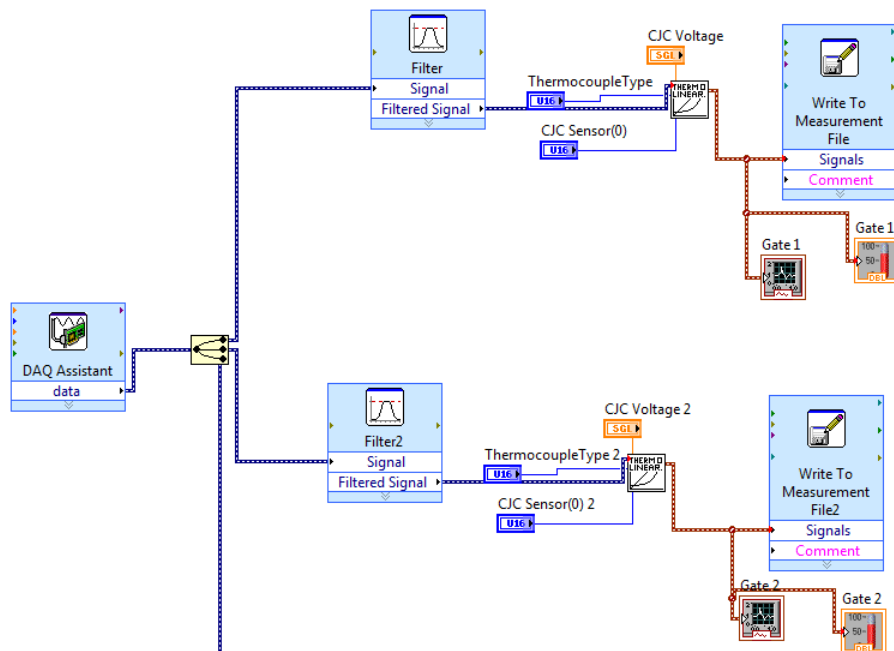


Fig. 3.37. Block diagram for thermocouples.

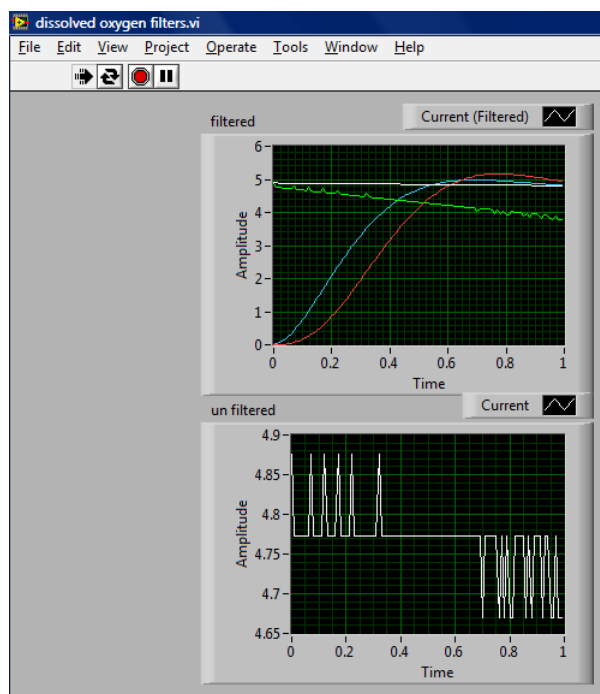


Fig. 3.38. Filtered and unfiltered DO signal using a) low pass filter (red line), band stop (blue line), high pass filter (green line) and smooth filter (exponential based method) (white line).

Table 3.10. Filters characteristics.

Filtering method	Filter specifications		Filter type	Design function	Order
	High cut off frequency	Low cut frequency			
Smoothing filter	---	---	Exponential	---	---
Low pass	---	1 Hz	Infinite impulse response	Butterworth	3
High pass	396 Hz	---	Infinite impulse response	Inverse Chebyshev	2
Band stop	500 Hz	1 Hz	Infinite impulse response	Butterworth	2

3.6. Water mass balance in RAS.

The amount of water lost across the system by evaporation, aeration, and discharged water by the separator and water exchanged during the growing season can be observed by the amount of water required to compensate it. The overall water loss (Q_T) can be determined by eq.3.31.

$$Q_T = Q_{aer} + Q_{evap} + Q_{dis} + Q_{exch} \quad (3.31)$$

where Q_{aer} is water loss by aeration effect, Q_{evap} is water loss by evaporation effect, Q_{dis} is water loss by system effluents, Q_{exch} is water loss by exchanging.

Water loss by aeration effect was determined by covering aerator top (foggy outlet) with plastic of polyethylene and measuring the amount of collected water per hour. Water loss by evaporation was determined by evaporation pan positioned inside the greenhouse, the amount of discharged and exchanged water was measured by a bucket of 20 liter.

3.7. Dosing system automation

Three food sessions 10:00, 14:00 and 18:00 h were applied per tank with one automated gate mounted above the second tank and with another two gates without automation; the three gates allowed better food dispersion. The food feeder was installed above the first tank and distributed to each tank's gate according to Table 3.11. The first motor (Fig. 3.39a) was connected to the outer tube by gear connection to stir the food at the cone bottom (Fig. 3.39f) above the three holes of the bottom of the cone (Fig. 3.39d) as shown in (Fig. 3.39c) that lead to the tanks or above the holes of weighting mechanism (Fig. 3.39g).

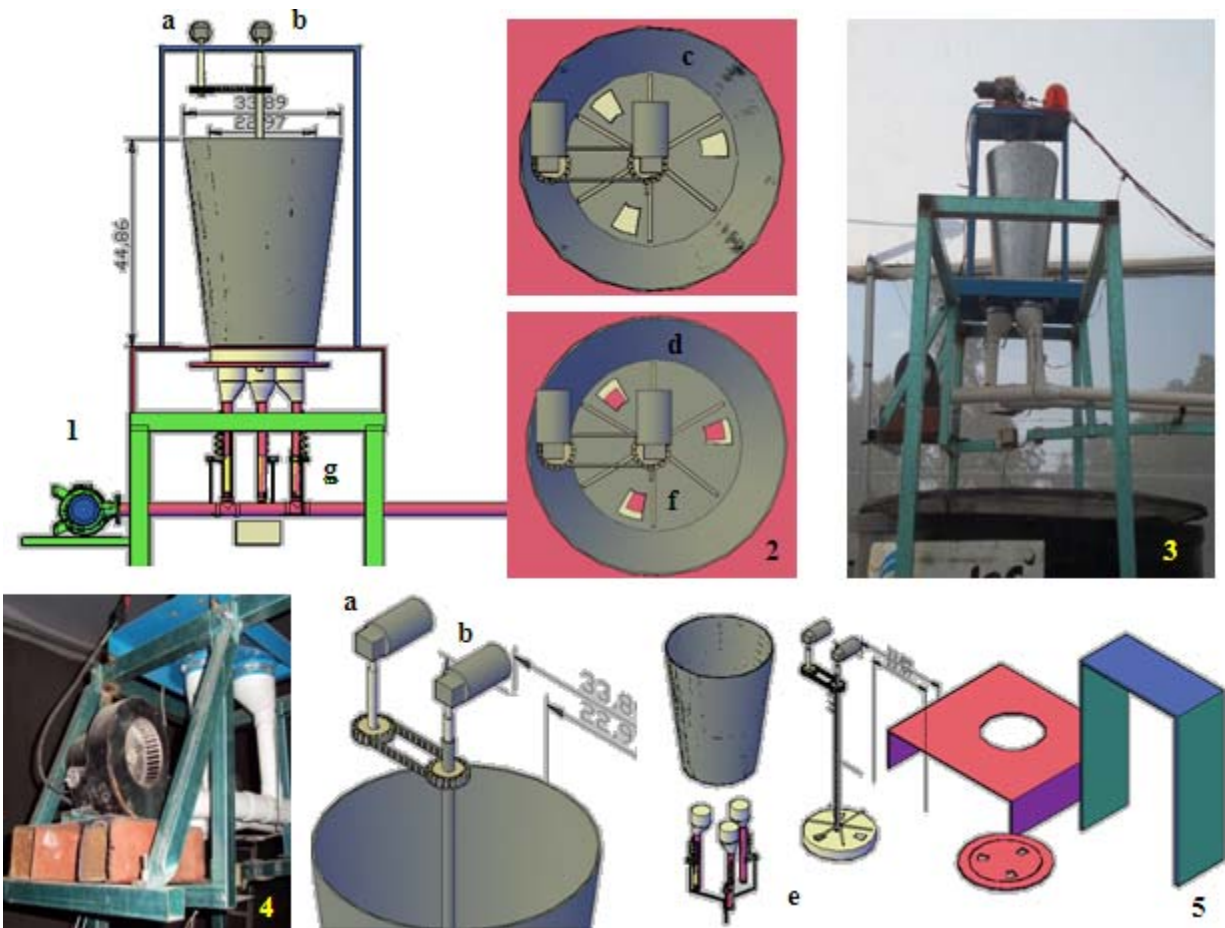


Fig. 3.39. Dosing system (1) lateral view, (2) top view, (3) feeder photo, (4) fan, and (5) feeder parts.

Table 3.11. Monthly feeding for each tank containing 100 organisms' three meals daily.

Time	Daily feeding weight (g) per tank	Meal weight (g)	Feeding (g) per every doses per tank		
			1st tank	2nd tank	3rd tank
1st month	150	50	50	50	50
2nd month	150	50	50	50	50
3rd month	300	100	100	100	100
4th month	300	100	100	100	100
5th month	450	150	150	150	150

2.1 Feeder operation

Four sections are encountered at the automatic feeder (Fig. 3.39): food hopper (1), feeding management control (2), weighting mechanism (3) and food delivery to tanks (4). The 25 liter food hopper was designed for feeding the fishes during two weeks; a capacitive proximity sensor detected food absence setting an alarm. The daily food delivered was of 150 gram during the first month (Table 3.11), and increased to a maximum of 450 gram on the last month.

The feeder controls the food delivered to the tanks by moving one motorized plate; when the holes (Fig. 3.39) of the two plates coincide the food passes to the weighting mechanism. The bottom plate turns around while the fixed top plate avoids excessive load to the motorized plate. The bottom plate is turned by a 17.8 W direct current motor supplied by 24 V DC (mod. AST-G002DC, Geared Motor, USA). The motor rated torque was of 34 Nm and rotated at 5 RPM.

Table 3.12. Port configuration

Port 1	P1.0	P1.1	P1.2	P1.4
Name	TF	M1	WMS	Gate motor
Defin	0- fan cont 1-coil turn off	Motors Feeder	Weight Micro Switch	0-for tank 2 1-for tank 3
Port 2	P2.0	P2.1	P2.2	
Name	T1	T2	T2	
Defin	0-1st month 1-2nd month	0-3rd month 1-4nd month	0-5th month 1-aut	

The automated feeder was controlled by an embedded system based on the ATM89C51 (ATMEL Inc, San Jose, California) microcontroller. The microcontroller port configuration is depicted in Table 3.12, and a LUT (look up table) stores the information for food dosing per gate during the different months for both rearing and nursing tanks (Table 3.12). Port 1 considers fan control, motors control and gate control (P1.4). Manual instructions of the operational status of the tanks are provided by external switches in Port 2.

If all the fishes have the same growth the system can run with an automatic routine by setting P2.2 to one. configuring monthly microcontroller Port 2 the appropriate feeding signals are sent to the feeder using Port 1.

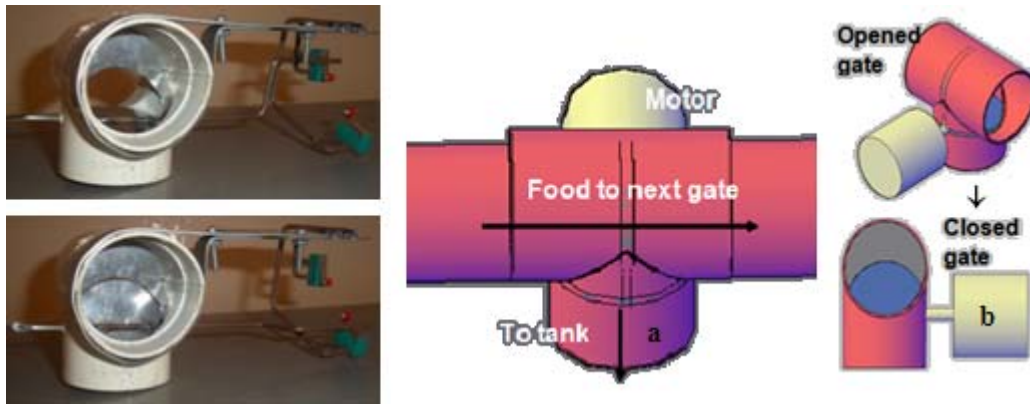


Fig.3.40. Gate (a) general view and (b) opening or closure ().

The weighting mechanism operations (see Appendix III).

Three output gates deliver the food to each tank by one PVC tube standing over the tanks (Fig. 3.40); one automated gate controlled the opening and closing of outlets 1 and 2. A thin circular plate rotated inside the gate was derived by a 4.22 W@12 V DC gear motor (model EMG30, Technobots Ltd. UK). Gates stayed normally opened allowing food application to gate 3. The gate motor drivers (Fig. 3.40a and b). Motor drivers activated by P1.4 signal close the valves; the gate closes for 12 seconds.

Feeder performance evaluation and pipe air flow analysis (see Appendix I and III).

3.8. Growth rate indicators

As fish feed is expensive, the feed conversion ratio (FCR) or feed efficiency (FE) is important for the grower, determining if feed is being used efficiently. FCR is calculated as the weight of the feed fed to the fish divided by fish growth weight. FCRs of 1.5-2.0 are considered good for most species.

$$FCR = \text{weight feed} / \text{fishweight gained} \quad (3.32)$$

FE is simply the reciprocal of FCRs (1/FCR); FEs greater than 50% are considered good. Fish are not completely efficient (FEs 100%), because they must use some of the energy in feed for metabolic heat, digestive processing, respiration, nerve impulses, salt balance, swimming, and other living activities. Feed conversion ratio will vary among species, sizes and fish activity levels, environmental parameters and the culture system used.

Other parameters were used to determine fish growth response were; Mean Weight Gain (MWG), Relative Growth Rate (RGR), Specific Growth Rate (SGR), Protein Efficiency Ratio (PER), and Mortality and Survival Rate.

$$MWG = Wt_2 - Wt_1 \quad (3.33)$$

$$RGR(\%) = [(W_f - W_i)/W_i] * 100 \quad (3.34)$$

$$PER = \text{Fish weight gain (g)}/\text{Protein intake (g)} \quad (3.35)$$

$$SGR = [(\ln W_f - \ln W_i)/\text{Time(days)}] * 100 \quad (3.36)$$

Survival Rate (%) = (Number of fish that survived / Total Number of Fish stocked) * 100.

where W_{t_1} is fish mean weight at time 1, W_{t_2} is mean fish weight at time 2, W_f is final fish weight and W_i is initial fish weight.

3.8.1. Fish weight determination and sampling process.

The three RAS units were stocked with carp 100 organism/m³. Carp uniformity is fallen into four categories (Fig. 3.41). The majorities of carps presented a weight between 15 - 20 and 20 - 25 grams, corresponding to 38% and 45% of the total stocked fish respectively. Ten percent of weighting samples are selected randomly from each tank every week. The overall standard deviation for fish weighting was of 3 to 31.5 gram. Initial and final weights were measured to determine the final growth rate (Fig.3.41). Webster and Regenstein, (2007) reported that the sample size collected determines the accuracy. For example, in the case of 10,000 fish ranging in size between 100 and 1000 gram requires a larger sampling than as the same population if fish size ranged between 100 and 150 gram. As a rule of thumb for collecting weight data, at least 100 fish should be sampled being 1% of the entire population.

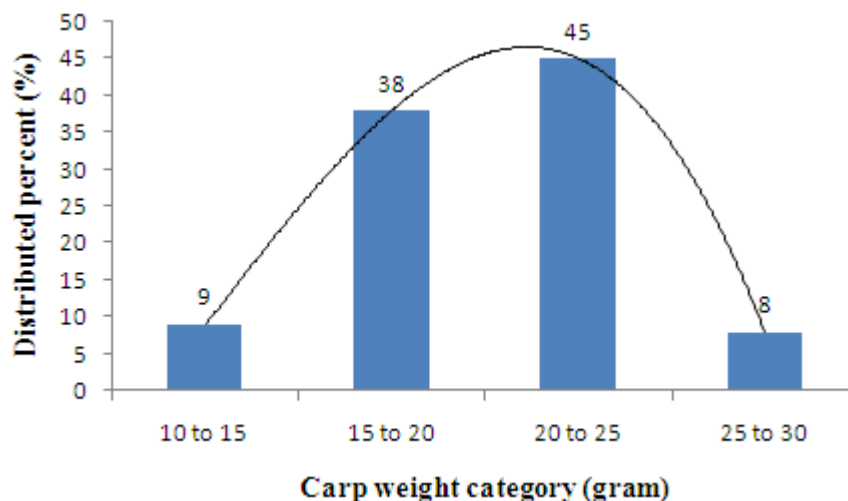


Fig. 3.41. Weight carp sorting at the moment of initial tanks stocking.

Fish sample procedure

Sufficient water was added from the sample tank to the bucket; the bucket was placed on the scale; the scale was tared, the random sample of (9 fishes) was divided into three categories (Fig. 3.42), repeating the process three times, the first category was added to the bucket; the scale gives the total weight and the average fish weight was calculated as *Total weight/Number of fish* and the sample repeated three times to get an average.

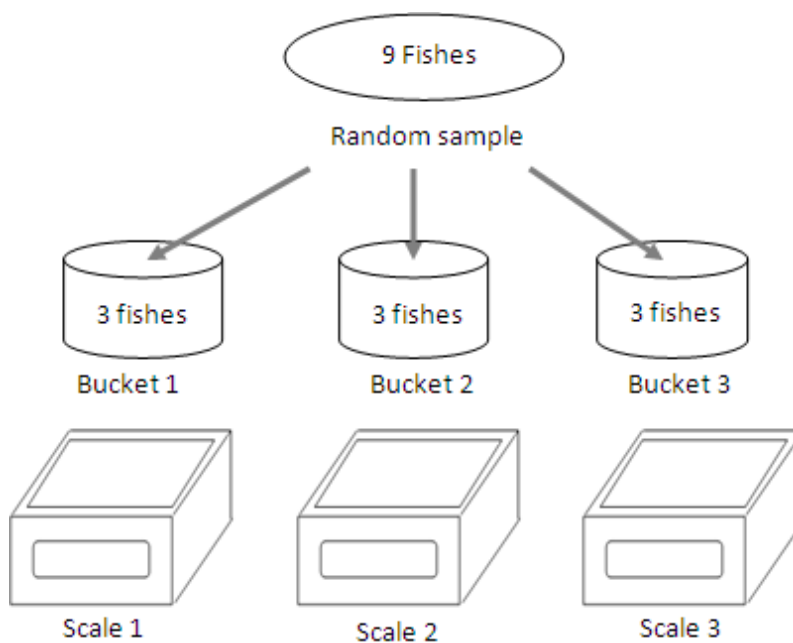


Fig. 3.42. Sampling process.

4. RESULTS AND DISCUSSIONS

4.1 Building automatic aeration and alimentation control system.

Fig. 4.1 is overall system diagram of automatic aeration control system. It is composed of a sensor unit, a managing for extracting samples from the three tanks, monitoring and controlling unit. The sensor node installed inside a measurement tube allows dissolved sensor to collect data from three different sampling points by peristaltic pumps. The automatic aeration control can be applied as an open loop control based on the data collected by evaluating each component in RAS system as explained at the section of dissolved oxygen balance in RAS system.

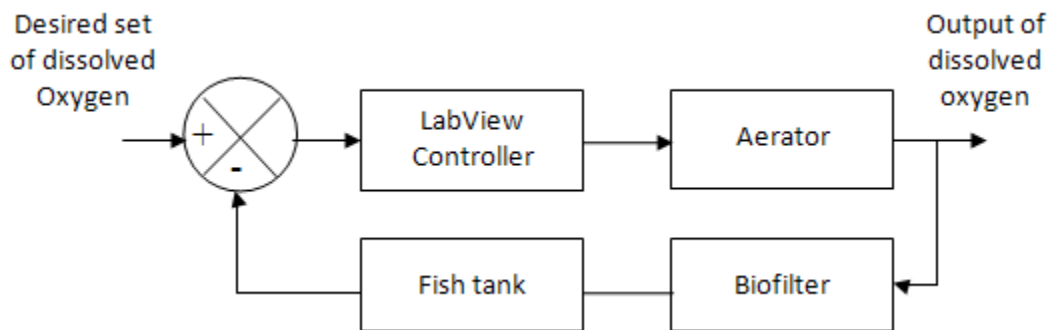


Fig. 4.1. Closed loop control diagram.

The automatic feeder constructed in this experiment was evaluated to introduce a predetermined amount of fish food three or two times daily according to fish sizes.

Results ordering

The results in this chapter were ordered to illustrate each component evaluation, and the most suitable operators for each unit; dissolved oxygen balance in the system to clarify oxygen fluxes processes in the system obtaining results to open loop control; system performance indicators of water and energy consumption and carp biomass gained per m³ water in section (4.6); automatic aeration control behavior in the system.

4.1. Separator evaluation

Tank bottom cleanliness and separator removal efficiency were analyzed under the following parameters:

1. Tank water level of 80 and 90 cm;
2. Tank base diameter of 2.54, 3.81 and 5.08 cm.

4.1.1. The effect of water level in fish tank on separator removal efficiency and tank bottom cleanliness efficiency.

The water flow rate through the separator was 25 Lpm providing a hydraulic retention time of approximately 15 min for particle settling resulting in a considerable portion of the large particles to be removed. The average TSS of the separator in flow was 8.15 ± 4.3 mg/L and the average TSS of the separator out flow was 2.165 ± 0.84 mg/L. The overall average removal efficiency for suspended solids removal through the separator was 78.38 and 73 % for 80 cm and 90 cm of water tank level respectively, (Pfeiffer et al., 2008) showed an average TSS water in flow of the bead filter (after the sump) of 6.63 ± 0.44 mg/L and the average bead filter outflow TSS was 1.78 ± 0.08 mg/L for an average removal efficiency of 73.1%. The removal efficiency for each category is presented in Fig. 4.2. The influent water into the separator from the tanks had a majority of particles in the 0.157–0.745 at 80 cm head and 1.3–10 mg at 90 cm head respectively.

The separator removal for the particles larger than 0.033 mg has higher average separator removal efficiency of 95.93% due to its higher gravity forces to precipitate in the separator, solid removal performance in separators is mainly due to gravity rather than centrifugal forces and separation is mainly by sedimentation, (Veerapen et al., 2005). A lower tank bottom removal efficiency of 36%, due to their higher weight the suction forces of the base cannot overcome to

RESULTS AND DISCUSSION

drag all the particles at the tank bottom, the particles smaller than 0.033 mg has higher tank bottom removal efficiency of 90.67% and average separator removal efficiency of 44.33%, the lower separator removal efficiency was 15 % for the particles lower than 0.0024 mg at 90 cm head due to the ability of these particles to dissolve or suspend in the water.

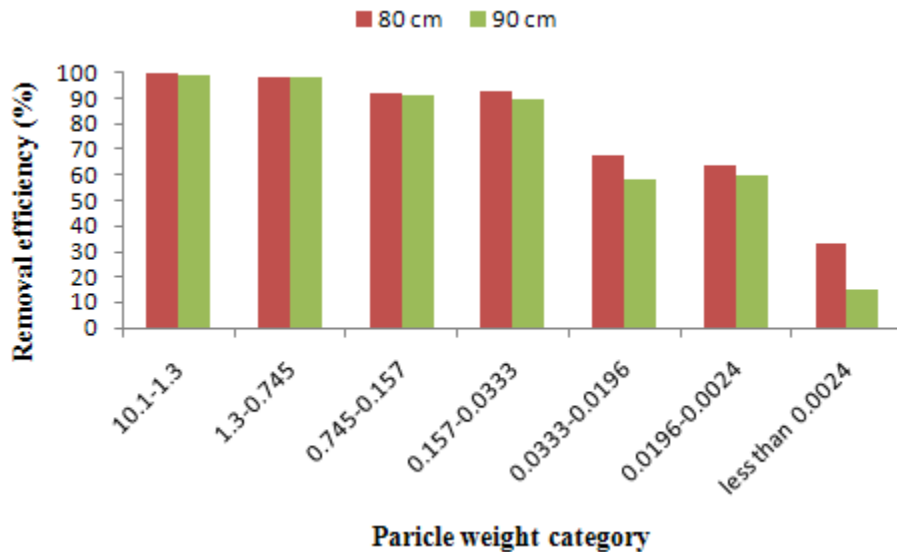


Fig. 4.2. Separator Removal Efficiency.

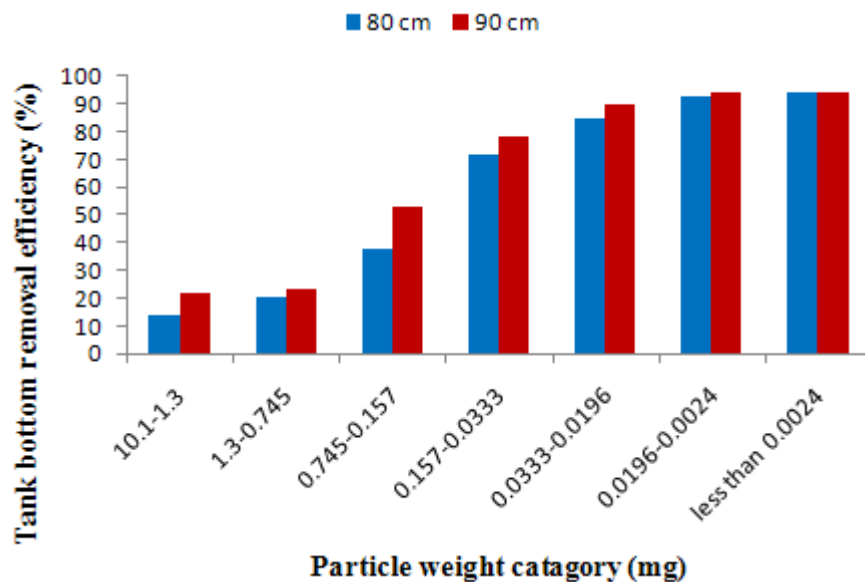


Fig. 4.3. Tank bottom cleanliness efficiency.

RESULTS AND DISCUSSION

Tank bottom cleanliness efficiency per categories of 1.3-10.1, 0.745-1.3, 0.157-0.745 and 0.0333-0.157 mg has inverse relationship with the base diameter, that increased from 11 to 22, 19 to 23, 45 to 53 and 74 to 78 % respectively for a 90 cm head. For categories lower than 0.0333 mg the removal efficiency was similar, so the base diameter had higher suction force that can drag a higher amount of solids bigger than 0.0333 mg Fig.4.3.

Generally at 80 cm head the tank bottom cleanliness is less efficient than the cleanliness efficiency at 90 cm head due to lower drag forces generated at tank bottom by higher water level, but on the other hand creates higher central damping forces of the separator central that affect separator removal efficiency Fig. 4.2.

Table 4.1. Tank bottom removal efficiency.

	1 inch		1.5 inch		2 inch	
	80 cm	90 cm	80 cm	90 cm	80 cm	90 cm
1.3-10.1	14.12	22.32	10.87	13.45	5.47	11
0.745-1.3	20.43	23.35	17.33	20	15	19
0.157-0.745	38.56	53.55	35.09	47	33	45
0.0333-0.157	72.67	78	71.89	76	72	74
0.0196-0.0333	85.3	90.2	85.1	90.63	84.7	90.87
0.0024-0.0196	93.1	94.32	92.67	94.04	93.92	94
< 0.0024	94.45	95.5	94.2	94.99	94.15	95.1

4.1.2. The effect of tank base diameter on tank bottom cleanliness and separator removal efficiency.

When the tank base having 5 cm of diameter and water level in fish tank was 90 cm, the separator effluent flow had less than 10% of the particles lower than 0.0024 mg and the particle distribution increased in the other size range categories. Distribution of particles in the 1.3–10.1 mg group increased to 40, 45 and 50% for tank base diameters of 5.08, 3.81 and 2.54 cm,

RESULTS AND DISCUSSION

respectively. Particles within 0.157–0.745 mg increased to 46.03% with a tank base of 5cm, and decreased to 36.55% with a tank base of 3.81 cm. The majority of the precipitated particles of the separator channel was of 48.78% for particles lower than 0.0024 mg when the water level was of 80 cm. With a water level of 90 cm particles of 0.0333-0.157 mg increased to 24.6% , 23.6 and 22.5% for 5.08, 3.81 and 2.54 cm, respectively. For all tank bases the particles within 1.3-10.1 and 0.157-0.745 mg had the majority separator effluent for water levels of 90 and 80 cm, respectively (Fig. 4.4, 4.5 and 4.6). The water level also effect clearly on the majority group that precipitate in the separator channel it was found that particles lower than 0.0024 mg and between 0.0333-0.157 mg had the majority precipitation at water columns of 80 and 90 cm, respectively. It is due to the damping forces at the separator center were higher with a water column 90 cm than for a column of 80 cm.

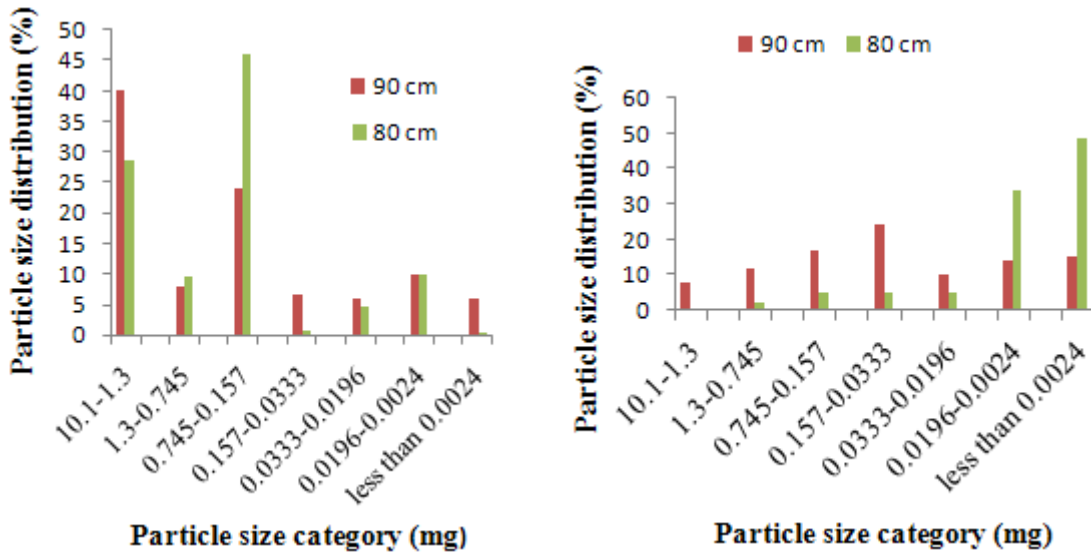


Fig. 4.4. Solids distribution in the (a) discharged water and (b) separator channel using a tank base of 5 cm.

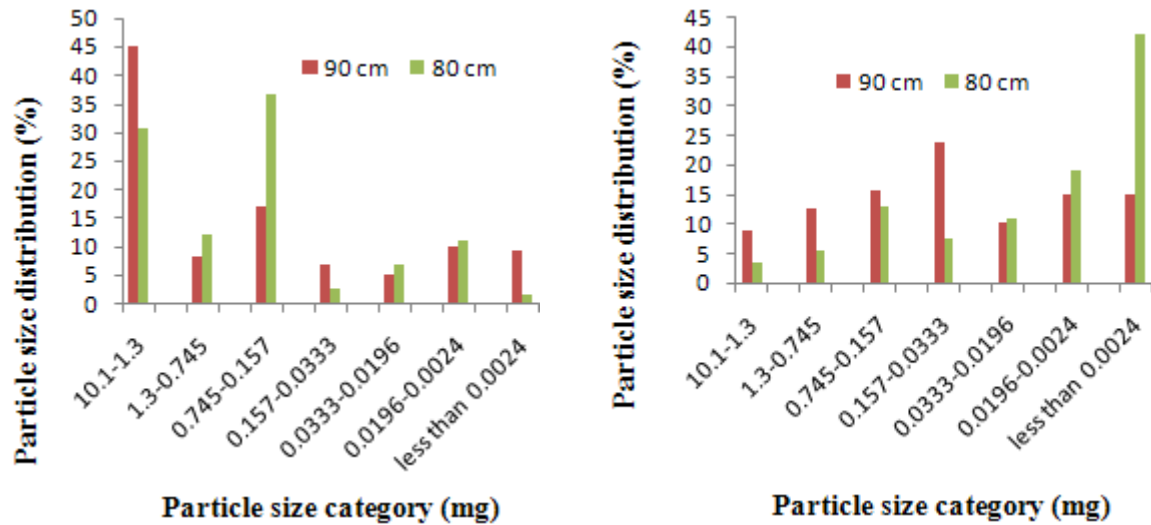


Fig. 4.5. Solids distribution in the (a) discharged water and (b) separator channel using tank base of 3.81 cm.

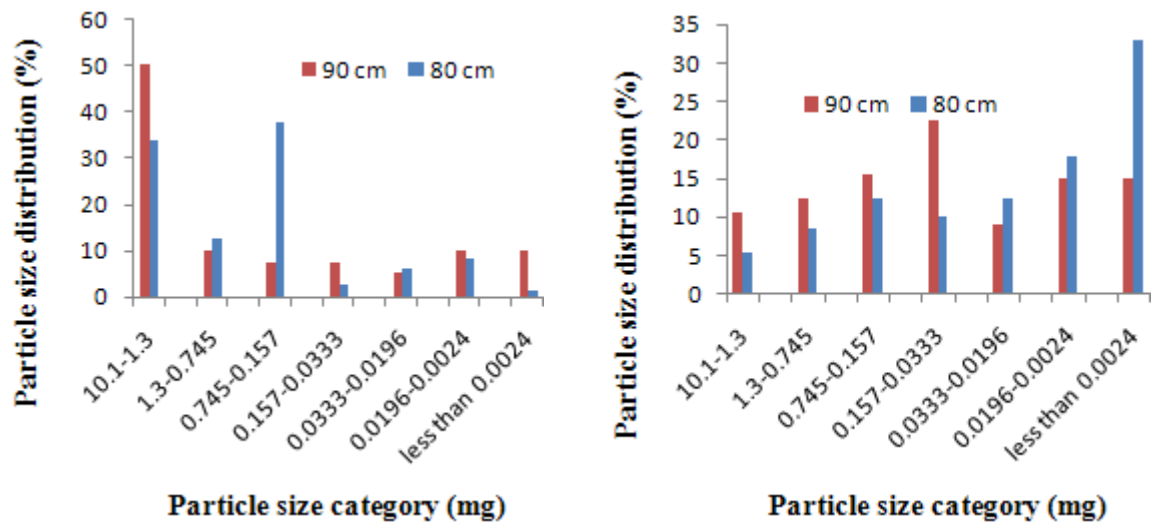


Fig. 4.6. Solids distribution in the (a) discharged water and (b) separator channel using tank base of 2.54 cm.

The optimum operators for separator removal efficiency and tank bottom cleanliness were set to be 90 cm for tank water level and 2.54 cm for tank base diameter.

4.2. Biofilters performance

4.2.1. Biofilter Initialization.

Total ammonia concentration peaks were found from the 23th to 29th, for biofilter 1 (Fig.4.7). In biofilter 2, total ammonia concentration peaks were found between the days 19-28. And for biofilter 3 maximum ammonia peak were encountered between days 24 to 29. Nitrate accumulation starts 15 days after for biofilters (Fig. 4.7d).

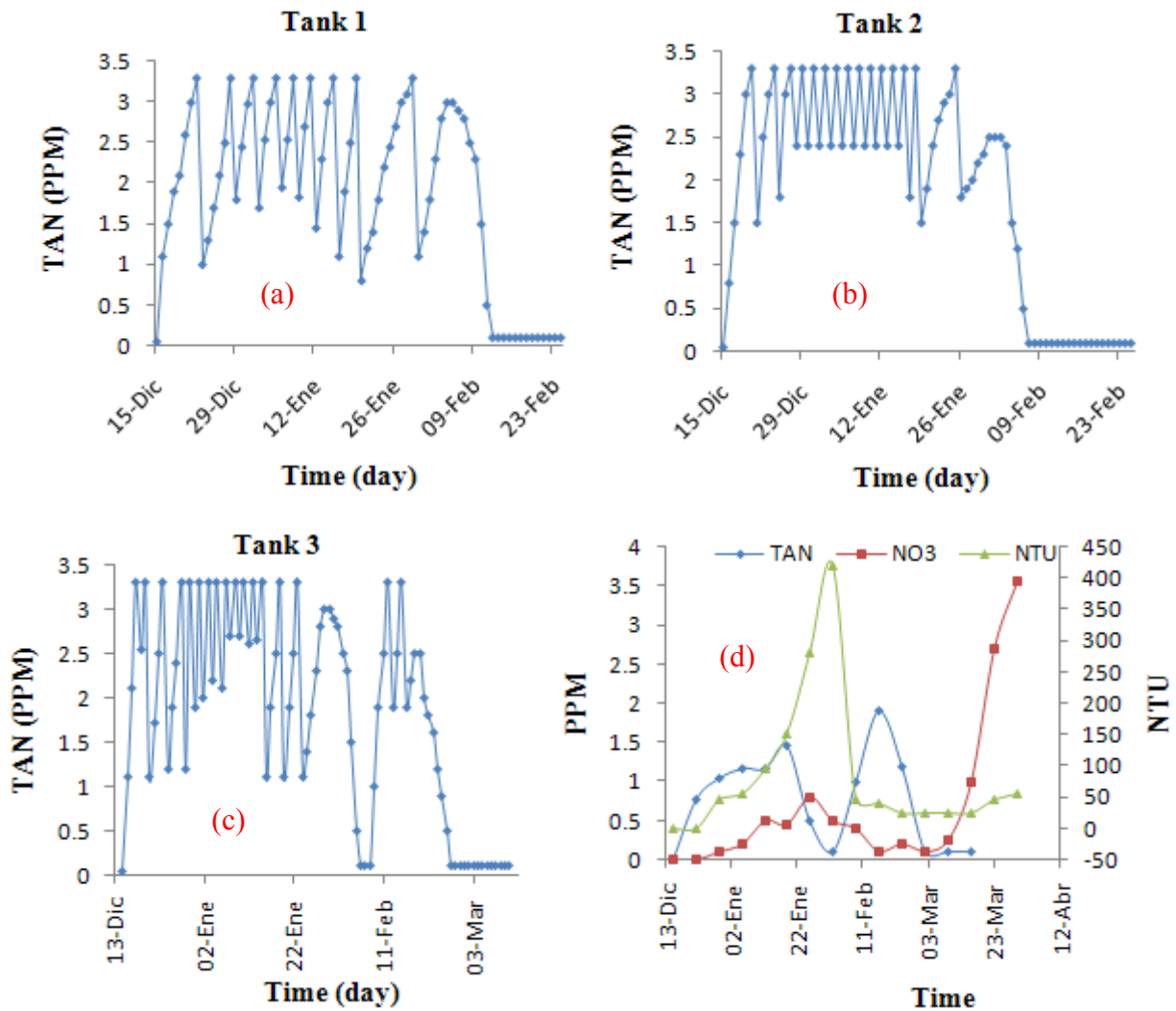


Fig. 4.7. Biofilter initialization for the first (a), second (b) and third (c) biofilter and the nitrate accumulation in biofilter 3 (d).

Total ammonia nitrogen was monitored during the start up days up to 3.3 ppm, and at this concentration 10% of water was exchanged with new fresh water. This process was followed until the biofilter reached the full capacity operation in the system 60, 53 and 53 days for biofilter 1, 2 and 3, respectively. In the biofilter 3 the biofilter was stabilized at the day 53th with the presence of microalgae, after that the microalgae was positioned in a competition case with the nitrifying bacteria causing all microalgae to die suddenly in the system that affect biofilter stabilization and the ammonia start to accumulate due to the ammonia generated by algae cells decompositions and still about 10 days to stabilize again. Fig. 4.7d shows microalgae behavior that is growing to 420 NTU causes ammonia declining to be minimum that operated synchronically with nitrifying bacteria and its disappearing in the system for food competition.

4.2.2. Comparative study among the biofilters

Three different designed biofilters were used in RAS system. The second biofilter has biostrata to cultivate the nitrifying bacteria, the biostrata purchase cost (US\$ 50 / panel (9 panels/biofilter)) is higher than Tezontle (volcanic sand widely available in Mexico), the comparative study was done to obtain knowledge about the performance of the three designed biofilters in RAS system, if there is no significantly differences between the three biofilters, then the Tezontle biofilter is more useful and profitable to use due to its low construction costs. As for the other Tezontle biofilters the difference between them only is water distributors that affect biofilter gravity aeration. The evaluative performance parameters are used in this study.

1. Total ammonia nitrogen conversion rate;
2. Total ammonia nitrogen removal efficiency and index;
3. Nitrifying bacteria growth rate.

4.2.2.1. Total ammonia nitrogen conversion rate.

Total ammonia nitrogen removal or conversion rate of biofilters was positively affected by TAN and temperature linearly, for the nitrifying bacteria and carp activity related to water temperature, the amount of the TAN generated by carp increases as water temperature raises. Throughout the day, the amount of exerted ammonia was differing due to water temperature fluctuation during the day (Fig. 4.9). As the TAN concentration increased, a proportional improvement in the conversion ability of biofilters occurred (Fig. 4.8a). Statistical analysis (ANOVA) that done with SAS program showed that temperature, ammonia concentration, and the interaction between them significantly affected nitrification performance ($P < 0.05$); Similar results have been reported for other types of biofilter (De Los Reyes and Lawson, 1996; Malone *et al.*, 1999; Sanduet *al.*,2002). Other researchers have shown that the specific growth rate of nitrifying bacteria and the ammonia removal rate of the biofilm increase as the ammonia level increases (Paller, 1992; Zhu and Chen, 1999). The relationship between temperature and TAN removal is shown in Fig. 4.8b during the first week of March.

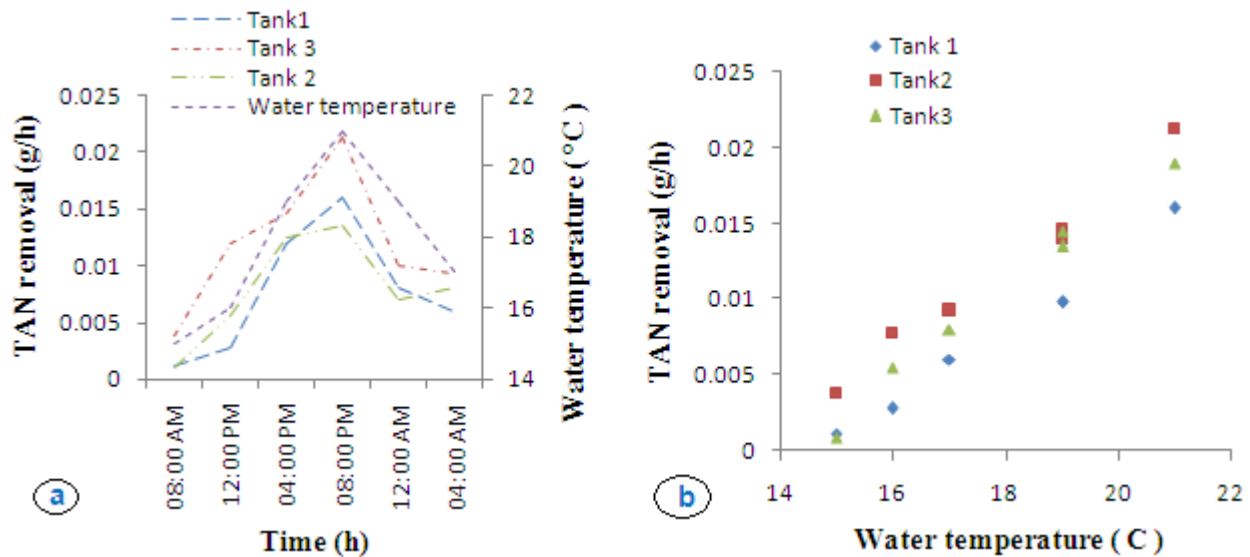


Fig. 4.8. (a) Diurnal changes in TAN removal rates (b) the relationship between water temperature and TAN removal rates.

RESULTS AND DISCUSSION

Water temperatures variations during one day give a chance studying the effect of water temperature for three tanks on TAN removal rate (g/h) (Fig. 4.9). The impact of temperature on nitrification performance due to dissolved oxygen limitation is different from that due to TAN limitation. When oxygen is limited, the decrease in saturation of dissolved oxygen as temperature increases results in a negative temperature impact on the nitrification rate (Tseng and Wu, 2004).

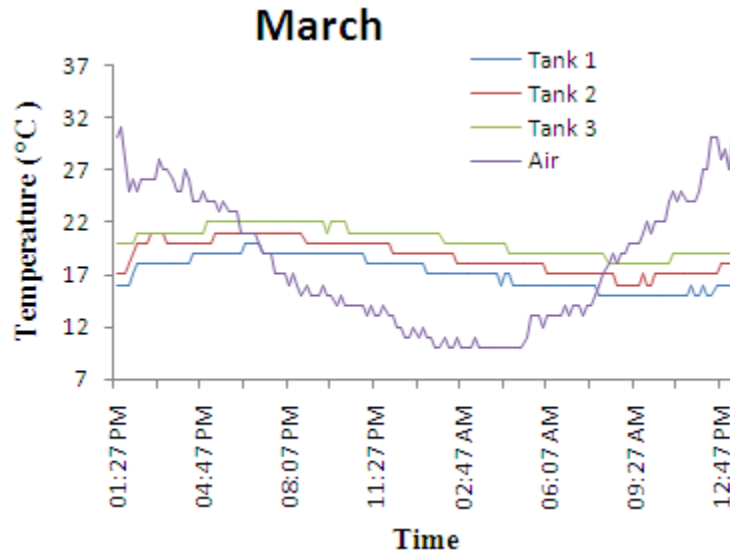


Fig. 4.9. Air and water temperatures for the three tanks at March.

Because nitrification rates are known to vary over the course of a day, due to fish feedings and associated ammonia production, diurnal fluctuations in TAN mass removal rate and percent removal values were investigated. Carps normally were fed in the morning around 9 to 10 AM and again in the evening around 5 or 6 PM at March. TAN mass removal rates were not significantly different among biofilter types at time 0 of feeding ($p = 0.01$). TAN removal mass rates increased gradually as fish activity increased by the effect of water temperature and feeding times due the digestive processes (Fig.4.8). However, removal rates increased in all filter types between the periods of 4:00 pm and 12:00 am (Fig. 4.8). Tezontle biofilter systems exhibited lower TAN mass removal rates which different significantly from these in trickling filters ($p = 0.05$); Removal rates among the two tezontle filters were not statistically different ($p = 0.95$).

RESULTS AND DISCUSSION

After peaking at 8 p.m., filter mass removal rates declined in all filter types. [Twarowska et al., \(1997\)](#) and [Westerman et al., \(1996\)](#) observed similar results in their filtration studies, where 24 h analyses of various biofilters showed TAN removal to increase with increasing TAN concentrations before peaking and declining.

The relationship between the volumetric total ammonia nitrogen removal rate (VTR) (mg TAN/m³·day) and TAN concentration produced daily by fish was studied. In the current study, TAN concentration significantly affected the VTR ($P < 0.05$). Figs. 4.10 and 4.11 show that daily VTR and surface TAN removal was increased as carp size increasing. The amount of TAN converted per surface unit (Surface TAN conversion rate) it was observed that the Tezontle biofilters had lower surface TAN conversion rate. It is concluded that the biostrata had surface conversion rate about 10 times higher than the tezontle (Fig. 4.11). Due to the laminar form of the biostrata that give a higher opportunity for nitrifying bacteria to be in contact with atmospheric air, but in the case of tezontle particles, the biofilm accumulated or grown on the porous space limiting gases exchanges from the bulk to the surface.

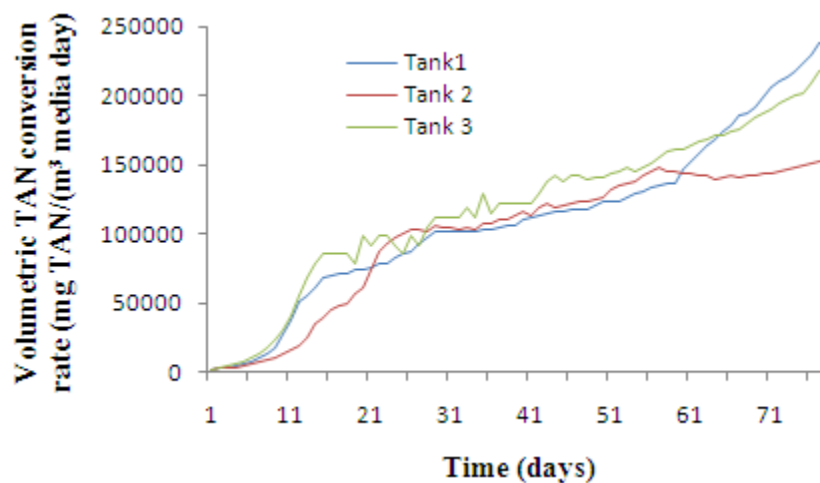


Fig. 4.10. Volumetric TAN conversion rate (mg TAN/m³·day) for three biofilters.

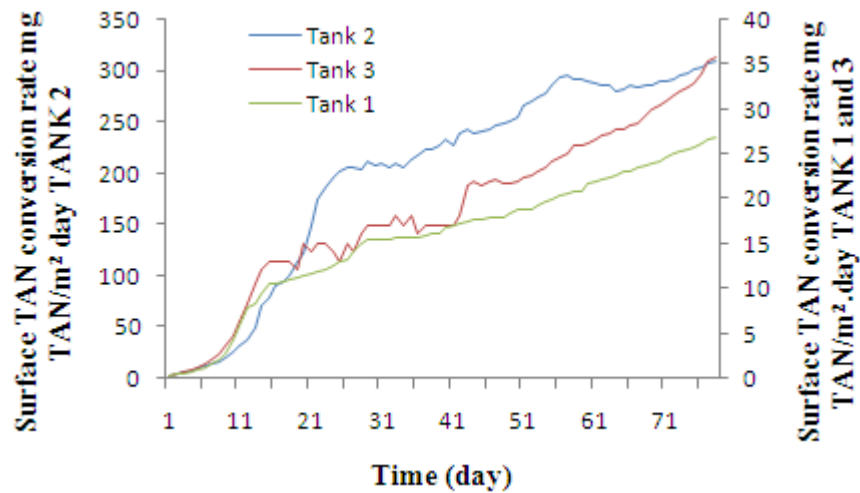


Fig. 4.11. Surface TAN conversion rate (mg TAN/m² day) for the biofilters.

4.2.2.2. Total ammonia nitrogen removal efficiency percentage and index.

The second biofilter can respond quicker to TAN fluctuations in the system (Fig. 4.12). The media helped to distribute homogenously the nitrifying bacteria in the entire areal surface. This result was similar to the ones obtained by Hall, (1999) in its comparative study between the trickling biofilter, the rotating biological contactor and the up flow pulsed bed bead filter. TAN removal efficiency for first, second and third tank was stabilized between the 51 and 55th day to 52.08, 73.7 and 64.7%, respectively.

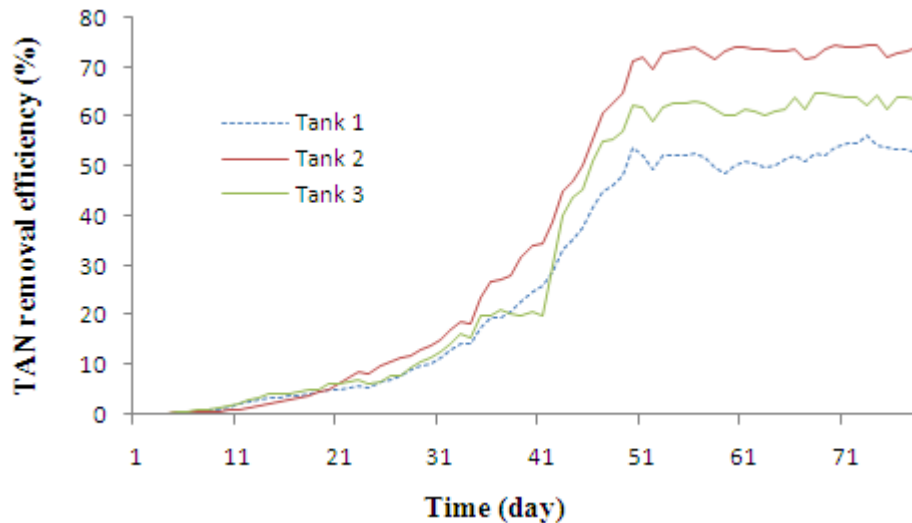


Fig. 4.12. Total ammonia nitrogen removal efficiency (%) for the biofilters.

Ammonia removal efficiency index increased for the biofilters to be 105.6 mgTAN/kW.h at the 71th day (Fig. 4.13). There were not significantly difference between the biofilters ($p = 0.99$) due to the higher energy requirement for the second biofilter to lift the water at the media surface. The energy consumption for water rising to be distributed above the biofilter media was calculated as energy lost by water fallen by gravity, as TAN conversion rate increases ammonia removal efficiency index improves (Fig. 4.13).

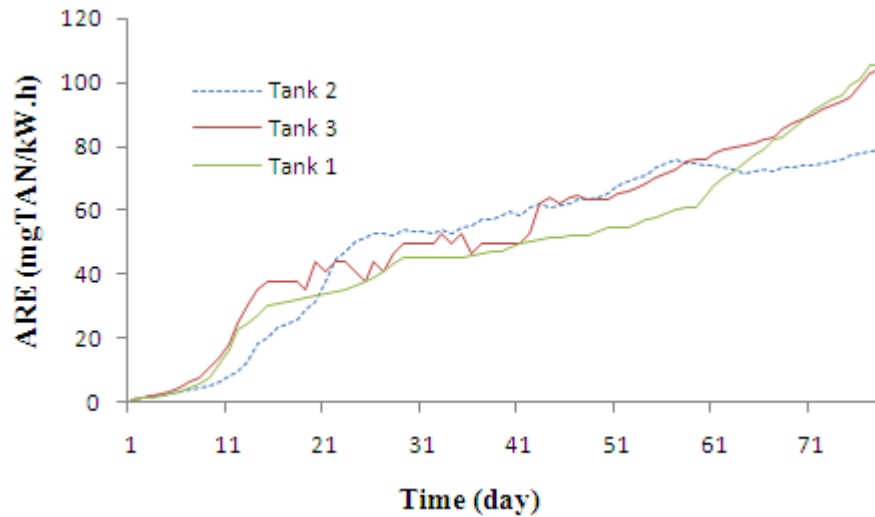


Fig. 4.13. Total ammonia nitrogen removal efficiency (mg TAN/kW.h) for the biofilters.

4.2.2.3. Total ammonia nitrogen conversion rate and volumetric oxygen consumption rate as indicators for nitrifying bacteria growth rate.

The growth behavior of the nitrifying bacteria for the three biofilters was exponential in the first 15, 23, 14 days as shown in the Fig. 4.14b, 4.16a and 4.17a. Nitrifying bacteria growth was determined by system TAN consumption. TAN was consumed by both types of nitrifying bacteria autotrophic and heterotrophic that can be determined by volumetric oxygen consumption rate for water column and biofilter media. Total volumetric oxygen consumption rate (VOCR_{tot}) is the sum of volumetric oxygen consumption rate for fixed (nitrifying) (VOCR_{nit}) and suspended

RESULTS AND DISCUSSION

(heterotrophic) ($\text{VOCR}_{\text{heter}}$) bacteria. In the biofilters 1 and 3 the algae accidentally created, but the algae in the biofilter 3 (Fig. 4.17a) was more intensive than biofilter 1 (Fig. 4.14a); the algae in the biofilter 1 not exceed 45 NTU during biofilter initialization. There are some competitions between the microalgae suspended in water column and the heterotrophic bacteria on food at the starting up time of biofilters. It is difficult to distinguish the volumetric oxygen consumption by microalgae or by heterotrophic bacteria in biofilters 1 and 3.

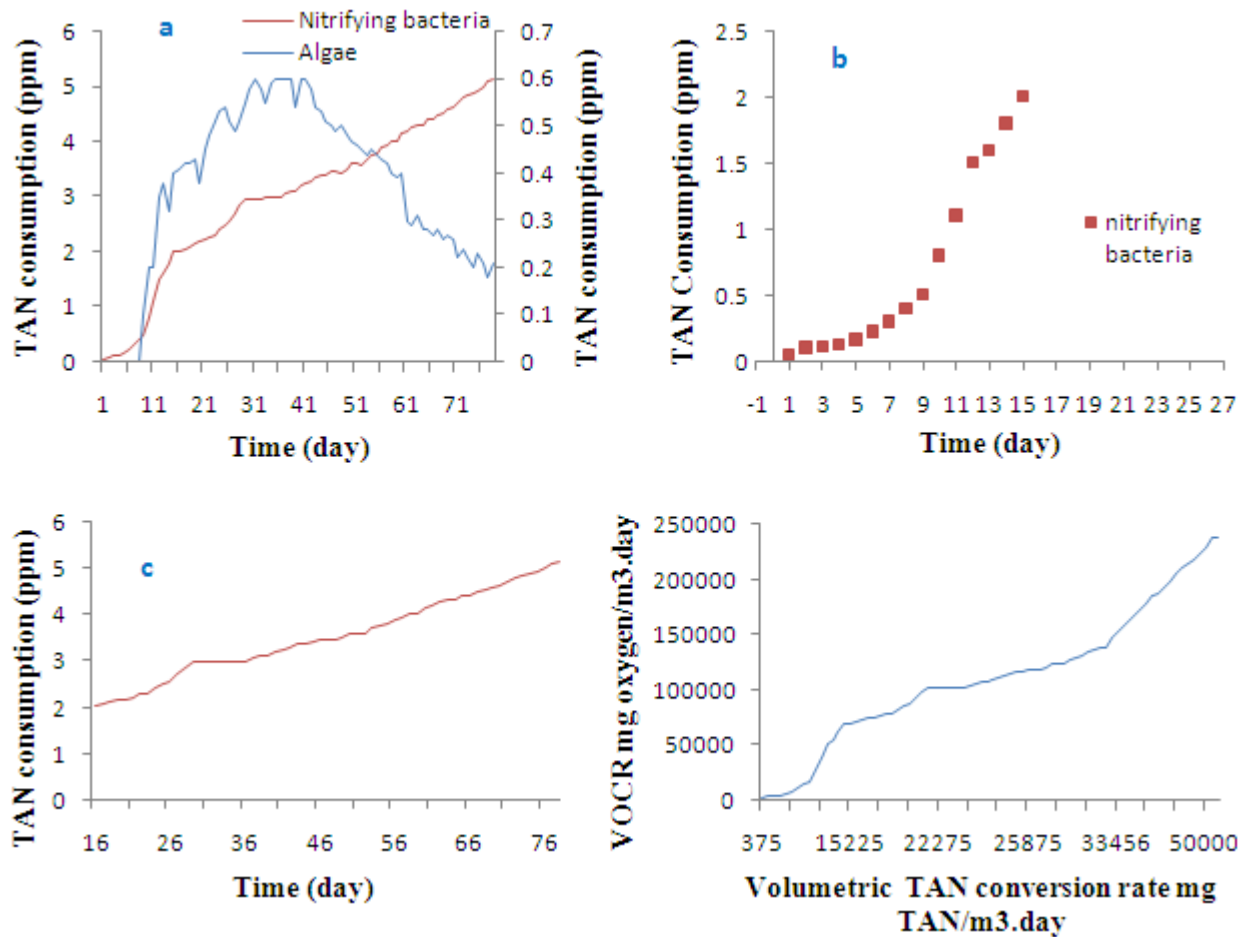


Fig. 4.14. Total ammonia nitrogen consumed by nitrifying bacteria and algae in the 1st biofilter (a) the overall growth of nitrifying bacteria during biofilter initialization (b) the nitrifying bacteria growth behavior in the first 15 days and (c). The nitrifying bacteria growth behavior after math (d). The relationship between the TAN conversion rate and volumetric oxygen consumption rate $\text{mg O}_2 / \text{m}^3 \cdot \text{day}$ for biofilter 1.

RESULTS AND DISCUSSION

Due to the participation of microalgae that is producing oxygen during the day that affect the oxygen consumption measurements. The microalgae which appeared accidentally accompanied the tezontle biofilters represent an effect of effluent treatment. The algae that found in the third biofilter consumes at maximum state 1.42 ppm per day (Fig. 4.17), where the first biofilter the maximum TAN consumed was 0.6 (Fig. 4.14). [Andrade et al., \(2009\)](#) showed that the microalgae removal efficiencies of 94.44% (23.80 mg/L) for ammonia nitrogen that can be used instead of biofilters in algal based systems.

The major disadvantage of algae based systems are the wide diurnal variations in dissolved oxygen, pH and ammonia-nitrogen and the long term changes in algal density and frequent (die-offs) ([Burford, et al., 2003](#)); that was observed in the two tezontle biofilters the frequent die off for the competition between the bacteria and the algae for the food and dissolved oxygen demand. The algae found in the biofilter 3 had higher impact on the nitrifying bacteria performance than the algae in biofilter 1.

Fig. 4.14c shows that TAN consumed by nitrifying bacteria that indicates biofilm grow this linearly with time, the amount of algae found in the biofilter1 does not affect significantly on nitrifying bacteria growth or biological activity, so that the nitrifying bacteria grow linearly with one slope. In biofilter 3 (Fig. 4.17a), the nitrifying bacteria growth behave linearly with two slopes, the first slope was followed in the presence of algae (pink square) from the day 27th to the day 53rd the TAN consumed by bacteria only increased from 3.79 to 4.32 ppm. After algae die off the nitrifying bacteria grow incrementally to compensate the TAN difference, this growth was done as a buffering respond to the amount of TAN increased in the RAS system due to algae absence (blue square) from the days 53rd to 77th with increasing in TAN consumed by bacteria from 4.32 to 6.72.

RESULTS AND DISCUSSION

The biofilm growth was measured during biofilter initialization weekly for the three biofilters (Figs. 4.15, 4.16d and 4.17c). Fixed or attached biofilm was increased as TAN conversion rate developed; the nitrifying bacterial biomass increases for all the biofilters in the range of 170 to 190 μg per each mg of TAN converted that falls in the range of 170-210 μg , (Wheaton et al., 1991; Wheaton et al., 1994).

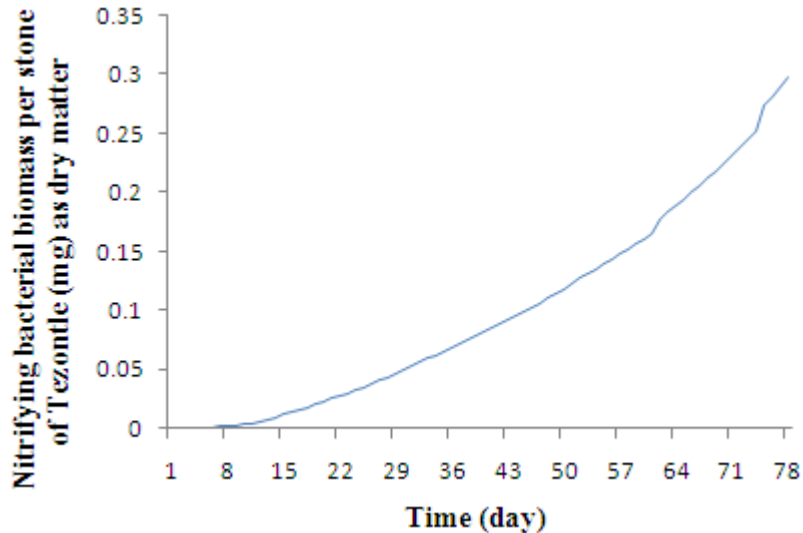


Fig. 4.15. Nitrifying bacterial biomass per stone of Tezontle (mg) for the first biofilter.

It was observed that volumetric oxygen consumption rate was increased by increasing volumetric TAN conversion rate due to the nitrification process as shown in Fig. 4.16c for biofilter 2. The oxygen consumption rate was used as a measure of microbial metabolic activity (Persson et al., 2006) but the oxygen consumption was increased in 15 of February this due to the effect of water temperature increasing with difference of 2 to 4°C, in the first 15 days the nitrifying bacteria was increased exponentially for the exponential growth of nitrifying bacteria until biofilm stabilization, so the (VOCR_{tot}) was increased from 1713 $\text{mg O}_2/\text{m}^3\cdot\text{day}$ to 68550 $\text{mg O}_2/\text{m}^3\cdot\text{day}$, after that the (VOCR_{tot}) was increased linearly up to 146240 $\text{mg O}_2/\text{m}^3\cdot\text{day}$ in the day 60, and the 18 days later the (VOCR_{tot}) was also increased linearly with higher slope until

RESULTS AND DISCUSSION

237868.5 mg O₂/m³day. Data collected on bead biofilter systems (Wimberly, 1990; Chitta, 1993; Sastry, 1995) indicate that bacterial oxygen consumption is roughly 165 g O₂ kg⁻¹ feed.

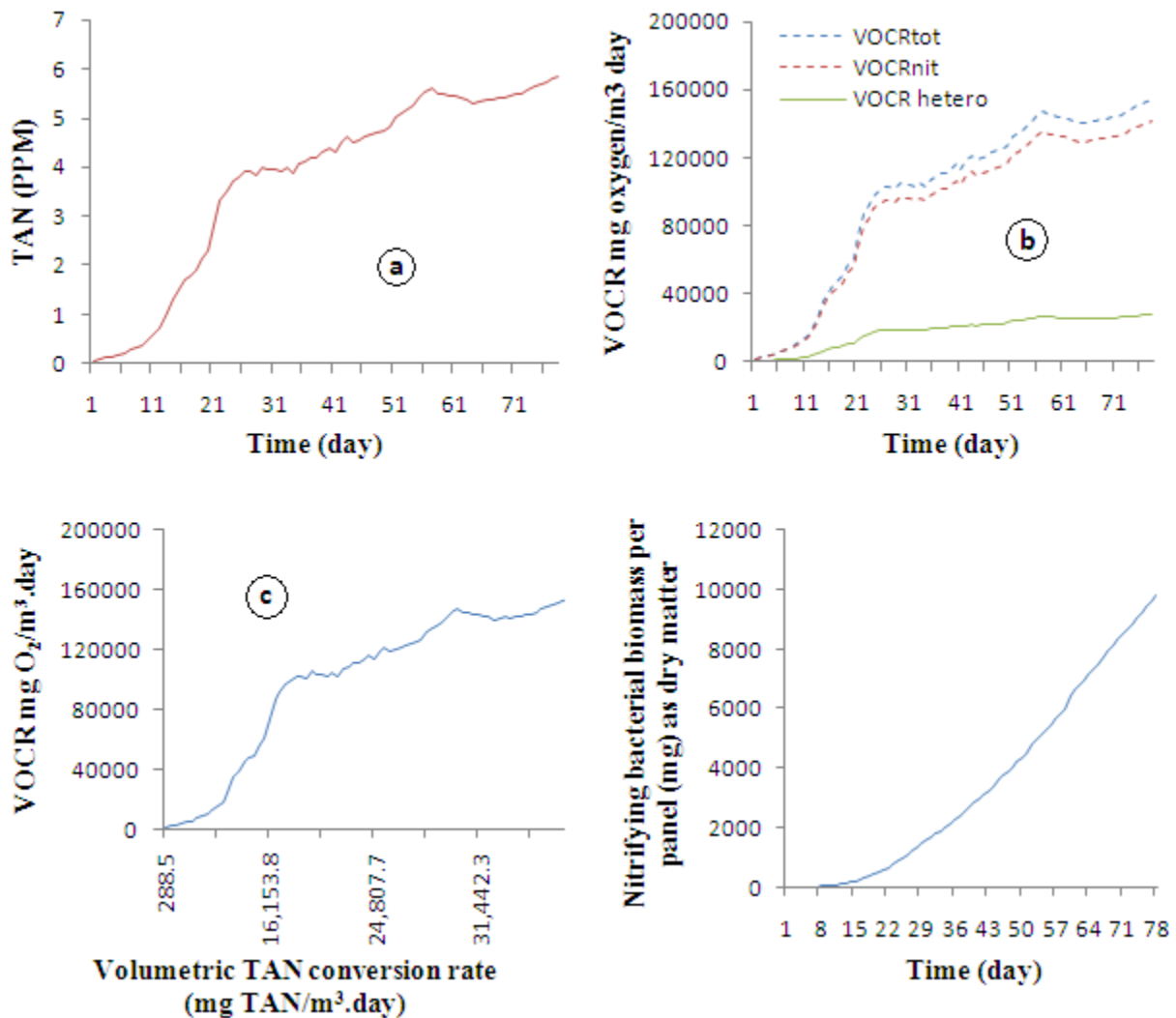


Fig. 4.16. (a) Overall growth rate for the nitrifying as TAN consumption in the tank 2. (b) Overall growths of heterotrophic and autotrophic bacteria during biofilter initialization expressed as volumetric oxygen consumption rate. (c) The relationship between the TAN conversion rate and volumetric oxygen consumption rate for biofilter 2. (d) Nitrifying bacterial biomass growth per panel (mg).

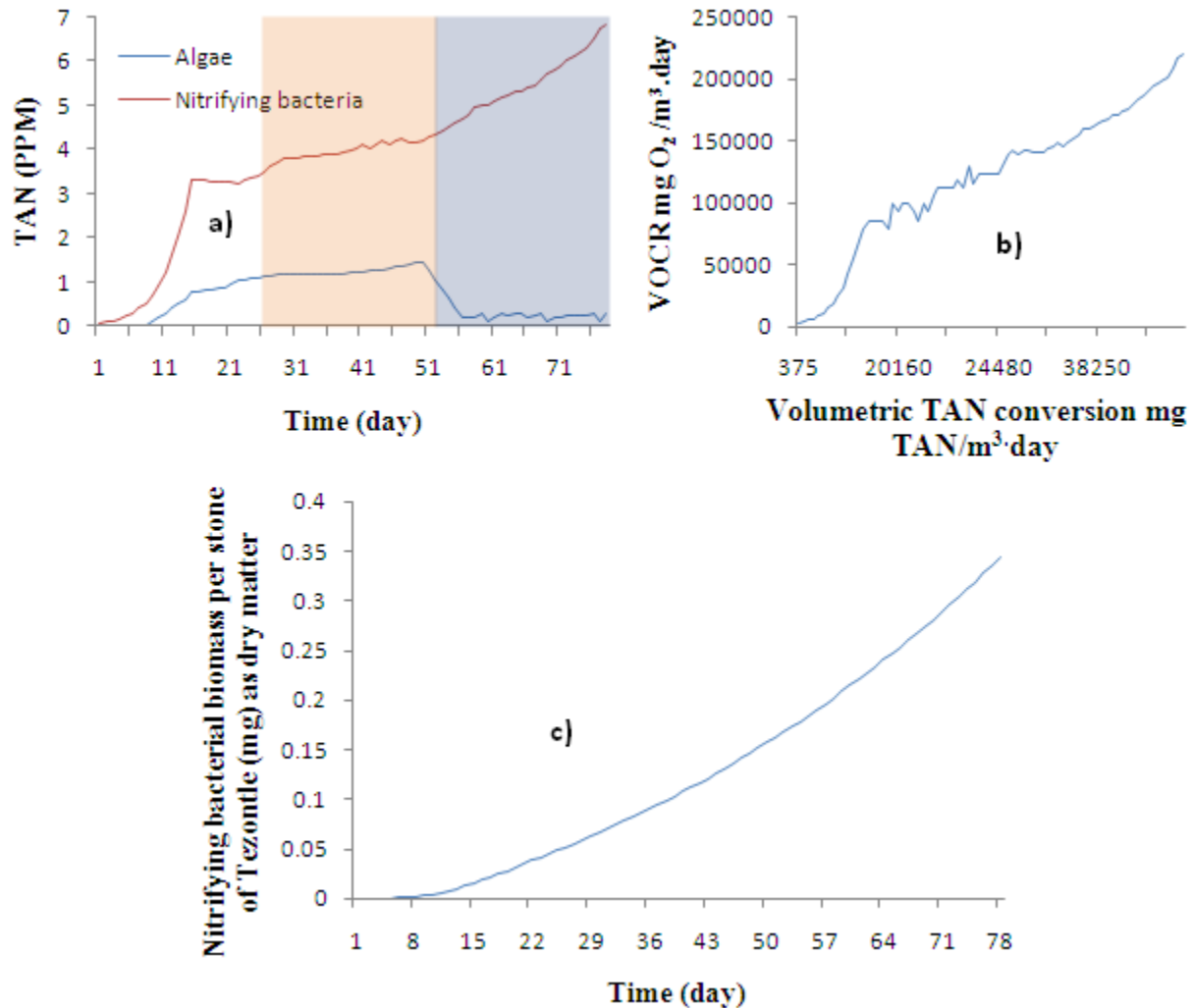


Fig 4.17 (a) Overall TAN consumption for biofilter 3. (b) The relationship between Volumetric TAN conversion rate (mg TAN/m³.day) and Volumetric oxygen consumption rate mg O₂/m³.day for the third biofilter. (c) Nitrifying bacterial biomass per stone of Tezontle (mg) for the third biofilter.

4.3. Aeration experiments

The experiments were carried out to choose and evaluate an aerator designed locally to meet dissolved oxygen requirements in local intensive re-circulating aquaculture systems; the aerators performance indicators are: 1) Change rate in dissolved oxygen (mg/l.min), 2) Outlet dissolved oxygen saturation percent (%), 3) Oxygen transfer rate (gO₂/h), 4) Actual aeration efficiency index (gO₂/kW.h).

It was necessary to determine the amount of dissolved oxygen required for every fish growth stage. Normally the water movement through the biofilters adds some part of aeration named gravity aeration. Three different levels of dissolved oxygen and water temperature were analyzed to study the effect of dissolved oxygen and water temperature on carp growth rate, and which has the priority effect on growth rate. The altitude above sea level of the experimental site is 2400m and has an inverse effect on dissolved oxygen saturation and thereby on oxygen tension (Table 7.3 Appendix 1).

4.3.1. The effect of air inlet pressure on airlift pump aerator performance.

The relationship between air inlet pressure and oxygen transfer rate, dissolved oxygen change rate, outlet dissolved oxygen percentage, and aeration efficiency index are shown in Fig. 4.18. It's observed that, the oxygen transfer rate increased with air injected between 69.53 and 758.42 kPa; energy usage increased, yielding a reduction in the actual aeration efficiency index (AAE) from 451.7 to 246.12gO₂/kW.h. Similar results were obtained by [Loyless and Malone, \(1998\)](#), where the outlet dissolved oxygen percentage and the change rate in dissolved oxygen raised with the increase of air injection from 53.73 to 62.69 % and from 0.04 to 0.08 mg/l.min.

4.3.2. Effect of air bubbles velocity on diffused aerator performance.

The relationships between air inlet pressure as air bubbles raising velocity and oxygen transfer rate, change rate in dissolved oxygen and aeration efficiency index were shown in Fig.4.19. It's observed that, the oxygen transfer rate increased from 1.6 to 3.3 gO₂/h as air bubbles raising velocities increased from 0.5 to 52cm/s. Energy consumption increased to meet the higher air raising velocities requirements needing a higher amount of air injection. It reduces the actual aeration efficiency index (AAE) from 271.02 to 174.045 gO₂/kW.h.

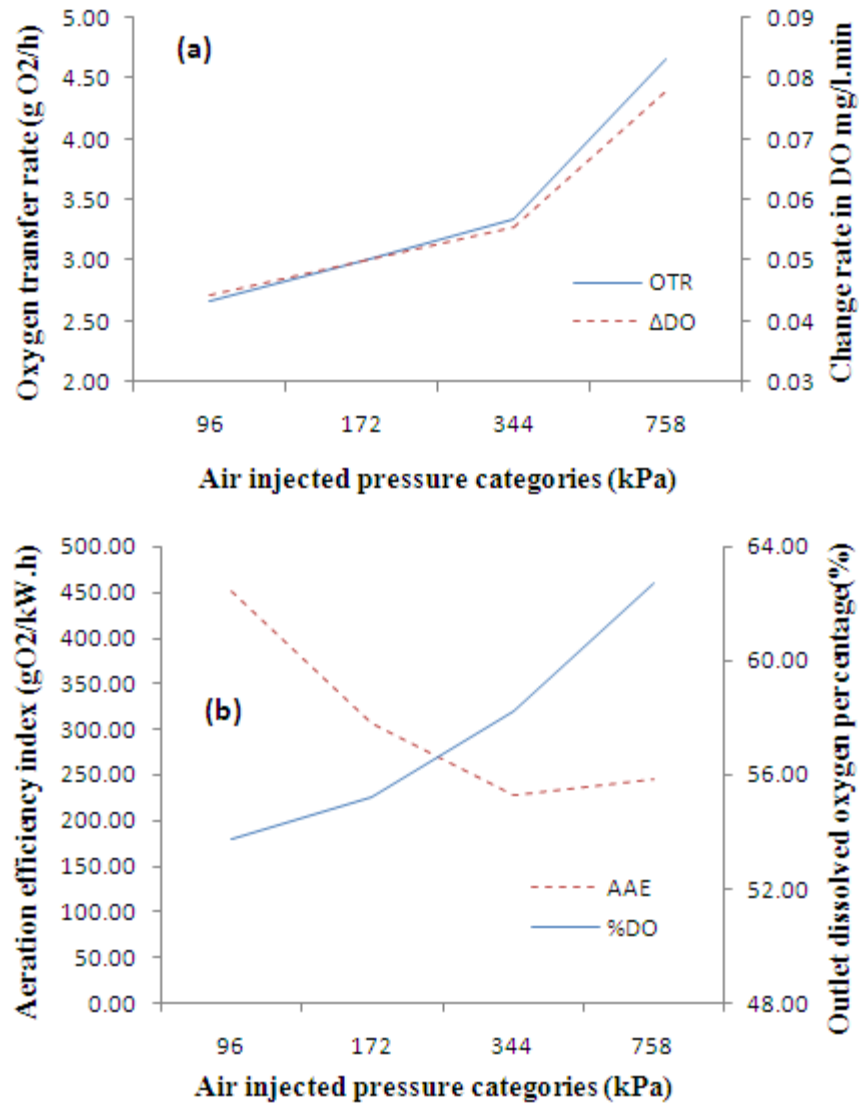


Fig. 4.18. Effect of air injection pressure on (a) oxygen transfer rate and change rate in DO and (b) Aeration efficiency index and outlet dissolved oxygen percentage (%) for the air lift pump aerator.

The standard aeration efficiency index and the standard oxygen transfer rate indicated by [Boyd, \(1998\)](#) for a diffused aerator ranged from 0.7 to 1.2 kgO₂/kW.h and from 0.6 to 3.9 kgO₂/h, respectively. The lower values of AAE and OTR compared with the data obtained by continuously air feed aerator of [Boyd, \(1998\)](#) was due to the elapsed time by the compressor to refill the compressor tank, the change rate in dissolved oxygen normally followed the amount of

RESULTS AND DISCUSSION

oxygen transferred to increase from 0.027 to 0.056 mg/l.min. Moreover [Boyd and Ahmad, \(1987\)](#) stated that simple diffused aeration is not efficient in shallow ponds commonly used for fish production (depth = 1.0-1.5 m) because the contact time of the air bubbles with the water is not great enough for sufficient oxygen transfer.

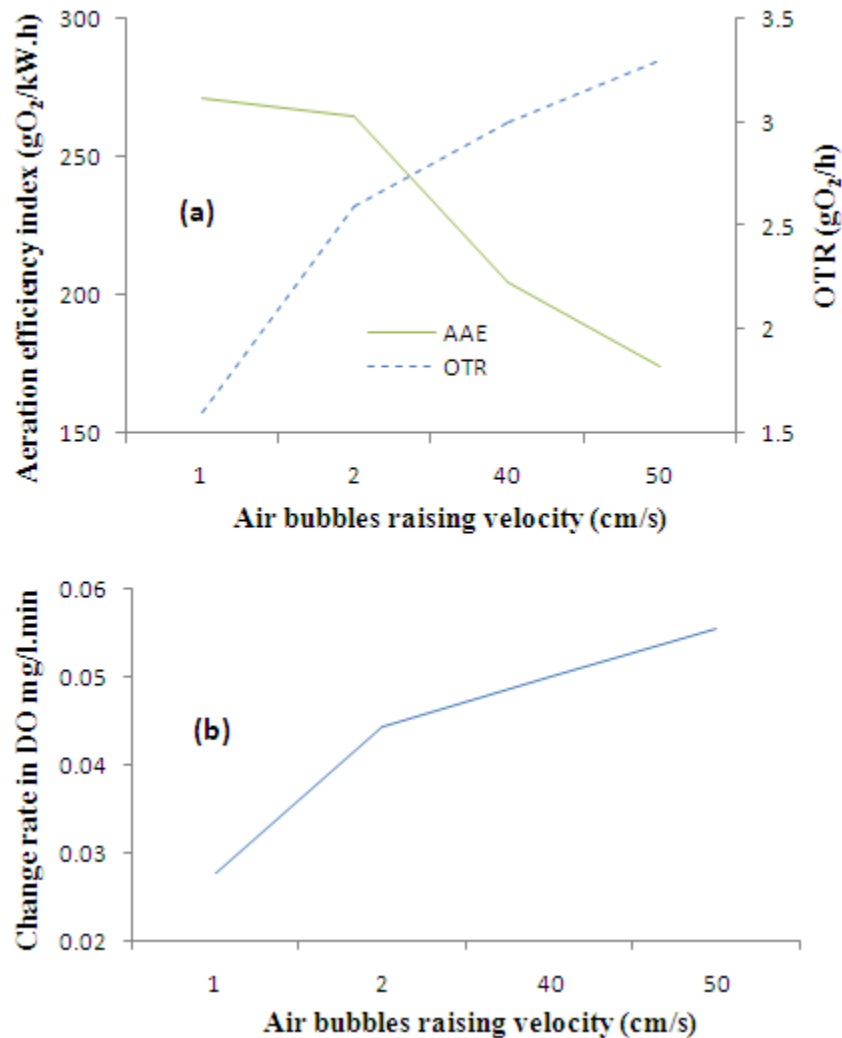


Fig. 4.19. Effect of air bubbles raising velocity on (a) oxygen transfer rate and change rate in DO and (b) aeration efficiency index for the diffused aerator.

4.3.3. Effect of differential pressure on venturi aerator performance.

The relationships between the differential pressure and oxygen transfer rate, change rate in dissolved oxygen, outlet dissolved oxygen percentage, and aeration efficiency index were shown in Fig. 4.20. It's observed that, the oxygen transfer rate increased from 1.75 to 3.25 gO₂/h as air differential pressure increased from 3 to 14.7 kPa. Energy consumption was the same for all differential pressures at the by-pass tube, increasing the actual aeration efficiency index (AAE) from 356.91 to 622.83 gO₂/kW.h, DO change rate and outlet dissolved oxygen percentage increased from 0.039 to 0.072 mg/l.min and 52.24 to 61.19 %, respectively.

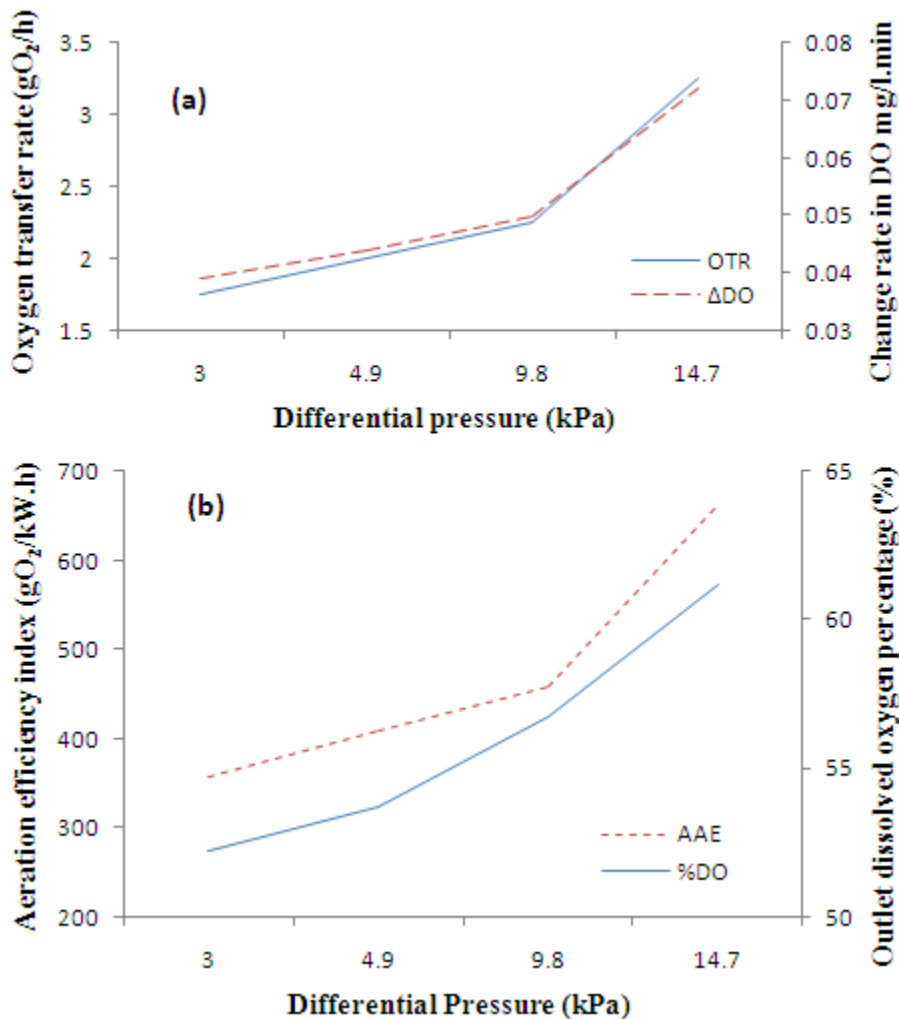


Fig. 4.20. Effect of differential pressure (kPa) on DO change rate, oxygen transfer rate, outlet dissolved oxygen percentage (%) and aeration efficiency index.

4.3.4. Spray column aerator performance

The effect of superficial air velocity, hydraulic loading rate and spray numbers on spray column aerator performance was studied. Relationships between oxygen transfer rate, change rate, outlet dissolved oxygen saturation percentage and aeration efficiency index, for different superficial air-water velocities are shown in Figs. 4.20, and 4.21. With an increase in superficial air velocity, and superficial water velocity, both SOTR and AOTR increased.

The effect of superficial air velocity on aerator performance with two sprayers, and hydraulic loading rate of $0.0013 \text{ m}^3/\text{m}^2.\text{s}$ was analyzed. As superficial air velocity increased from 0.04 to 0.66 m/s, OTR, ΔDO , %DO and AAE increased from 3.6 to 10.8 gO_2/h , 0.03 to 0.1 $\text{mg}/\text{l}.\text{min}$, 61.19 to 74.63 % and 167.99 to 503.97 $\text{gO}_2/\text{kW}.\text{h}$, respectively.

The effect of hydraulic loading rate on aerator performance with two sprayers and superficial air velocity of 0.04 m/s is illustrated in Table 4.2. As the hydraulic loading rate increased from 0.0013 to 0.0021. OTR, ΔDO , %DO and AAE increased from 3.6 to 8.64 gO_2/h , 0.0033 to 0.08 $\text{mg}/\text{l}.\text{min}$, 61.19 to 71.64%, 167.99 to 403.17, respectively.

The effect of number of water jets on aerator performance at hydraulic loading rate of $0.0013 \text{ m}^3/\text{m}^2.\text{s}$ and superficial air velocity of 0.04 m/s was studied. As the column aerator increased from two to three sprays, the OTR, ΔDO , %DO and AAE increased from 3.6 to 6.48 gO_2/h , 0.033 to 0.06 $\text{mg}/\text{l}.\text{min}$, 61.19 to 70.14 % and 167.99 to 302.38 $\text{gO}_2/\text{kW}.\text{h}$.

The air/water ratio was used as an indicator parameter to obtain a better performance for the aerator. The superficial air/water ratio was generated by two hydraulic loading rates (0.0013 and 0.0021) and four superficial air velocities (0.04, 0.08, 0.37 and 0.66). For each category of superficial air velocity marked by a different color (Table 4.2) as air/water ratio decreases AAE increases. Therefore, the spray column aerator will need a higher hydraulic rate to give a higher aeration efficiency index for each superficial air water velocity.

RESULTS AND DISCUSSION

Air/water ratio is proportional outlet dissolved oxygen saturation percent (%DO), as obtained by [Watten, \(1990\)](#).

Table 4.2. Effect of hydraulic loading rate and sprayers' number on spray column aerator performance.

Hydraulic loading rate	SV air	Air/Water ratio	2 SPRAYS				3 SPRAYS			
			OTR	Δ DO	%DO	AAE	OTR	Δ DO	%DO	AAE
0.0013	0.04	30.76	3.6	0.033	61.19	167.99	6.48	0.06	70.14925	302.38
0.0021	0.04	19.05	8.64	0.08	71.64	403.17	11.52	0.1067	80.597	537.56
0.0013	0.08	61.54	6.48	0.06	67.16	302.38	8.64	0.08	73.13433	403.17
0.0021	0.08	38.095	9.36	0.087	73.13	436.77	13.68	0.127	83.58209	638.36
0.0013	0.37	284.62	7.92	0.073	70.15	369.58	10.08	0.093	77.61194	470.37
0.0021	0.37	176.19	11.52	0.1067	77.61	537.56	18	0.167	94.02985	839.94
0.0013	0.66	507.69	10.8	0.1	74.63	503.97	13.68	0.127	82.08955	638.36
0.0021	0.66	314.29	14.4	0.133	82.09	671.96	23.04	0.213	101.4925	1075.13

Generally, oxygen mass transfer rate (OTR) becomes greater as the hydraulic loading rate increases for all air flow rates, superficial air velocity and sprayers number due to the aerator's column. Oxygen transferred to the water is proportional to the shearing forces applied of the liquid surface as the contact area causes a significant increase in mass transfer. These results were also obtained by [Morchain et al., \(2000\)](#) and [Yuan et al., \(2004\)](#).

From the results obtained the spray column aerator has the highest OTR and AEE at water flow rate of 30 LPM and air flow rate of 0.157 m³/s gaining 23.04 gO₂/h and 1.075 kgO₂/kW.h with three sprayers. Spray column aerator was used in RAS now has OTR of 13.68 gO₂/h, achieved with 0.5 Hp water pump, if the user want higher OTR the pump of 0.5 Hp can be changed with water pump of 0.75 Hp obtaining OTR of 23.04 gO₂/h.

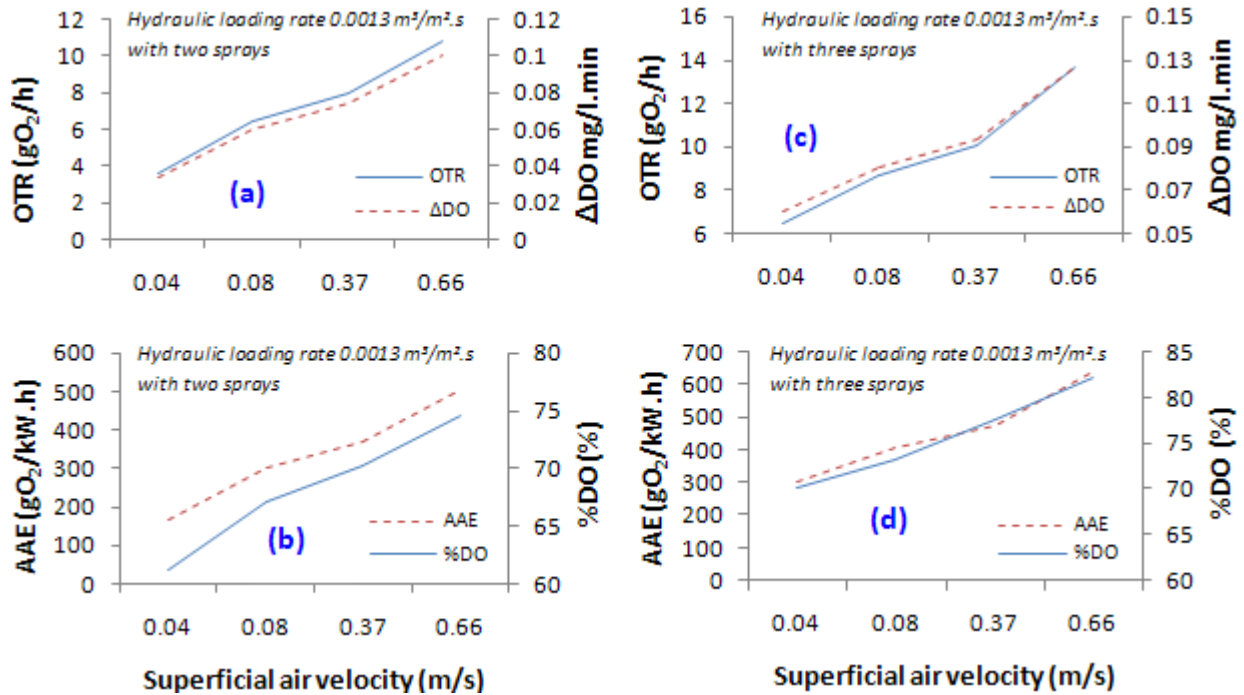


Fig. 4.21. Effect of superficial air velocity on DO change rate and OTR with two sprayers (a) and three sprayers (c) and on %DO and AAE for two sprayers (b) and three sprayers (d) at hydraulic loading rate of 0.0013 m³/m².s.

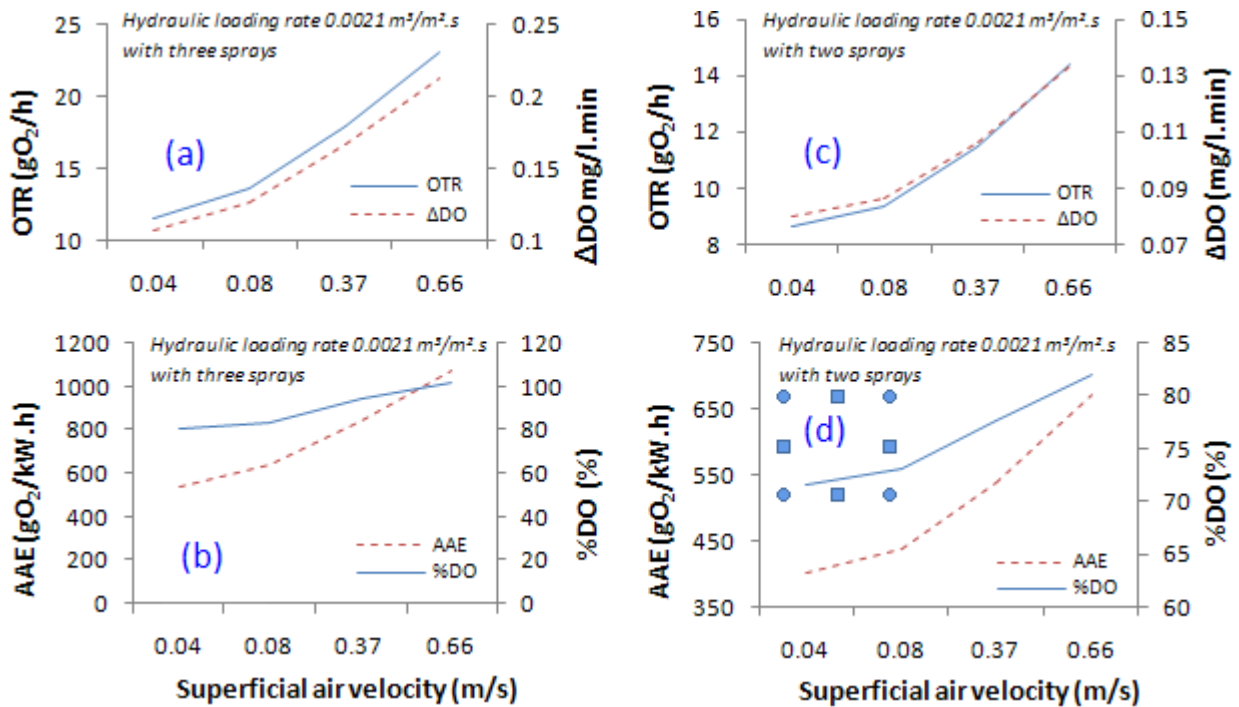


Fig. 4.22. Effect of superficial air velocity on DO change rate and OTR with two sprayers (a) and three sprayers (c) and on %DO and AAE for two sprayers (b) and three sprayers (d) at hydraulic loading rate of 0.0021 m³/m².s.

4.4. Dissolved oxygen transfer analysis

4.4.1. Effect of temperature and oxygen deficit on oxygen transfer rate (OTR).

Fig. 4.23 shows that the temperature affects inversely oxygen transfer rate. As the temperature decreased from 24°C to 14°C, the oxygen transfer rate increased from 8.8 to 9.4 gO₂/h with a rate of 0.0547 gO₂/h/°C, and its regression equation is:

$$OTR = -0.0547 \times T + 10.224 R^2 = 0.9635 \quad (4.1)$$

where *T* is water temperature in °C.

Oxygen deficit (OD) is proportional to OTR having an average value of (1.852 gO₂/h)/PPM and obtained from the following equation,

$$OTR = 1.852 \times OD + 0.06 \quad R^2 = 0.9982 \quad (4.2)$$

Oxygen moves from the atmosphere to the water and vice-versa by diffusion, and the rate of oxygen diffusion depends upon the oxygen deficit. The oxygen deficit is the driving force causing oxygen to enter or exit the water surface (Fig.4.23 and 4.24). Oxygen deficit per unit has higher effect on oxygen transfer than the temperature effect [Boyd, \(1998\)](#).

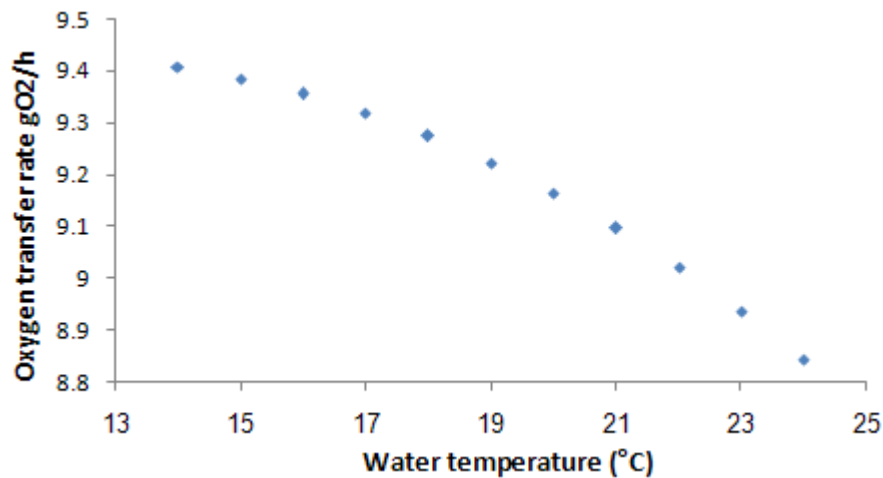


Fig. 4.23. Effect of temperature on oxygen transfer rate at dissolved oxygen of 2 PPM.

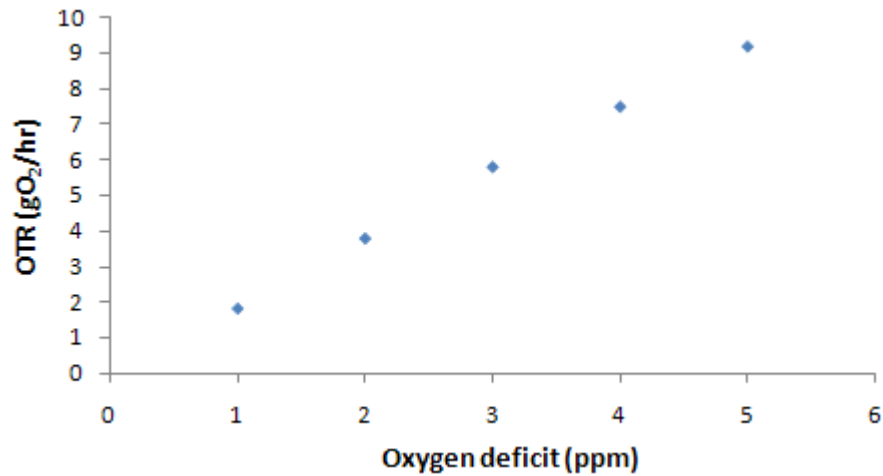


Fig. 4.24. Effect of oxygen deficit on oxygen transfer rate at 20°C.

4.4.2. Effect of oxygen transfer and air temperature on tank water temperature.

As OTR increases water becomes hotter at higher air temperatures, as a greater superficial contact area exists between air and water allowing a better heat transfer given by:

$$\Delta H = 0.0003OTR - 0.0048R^2 = 0.9374 \quad (4.3)$$

where ΔH is the enthalpy gained or lost (°C/min). Fig. 4.25 shows that tank 3 has the lowest OTR, being its temperature shows the highest.

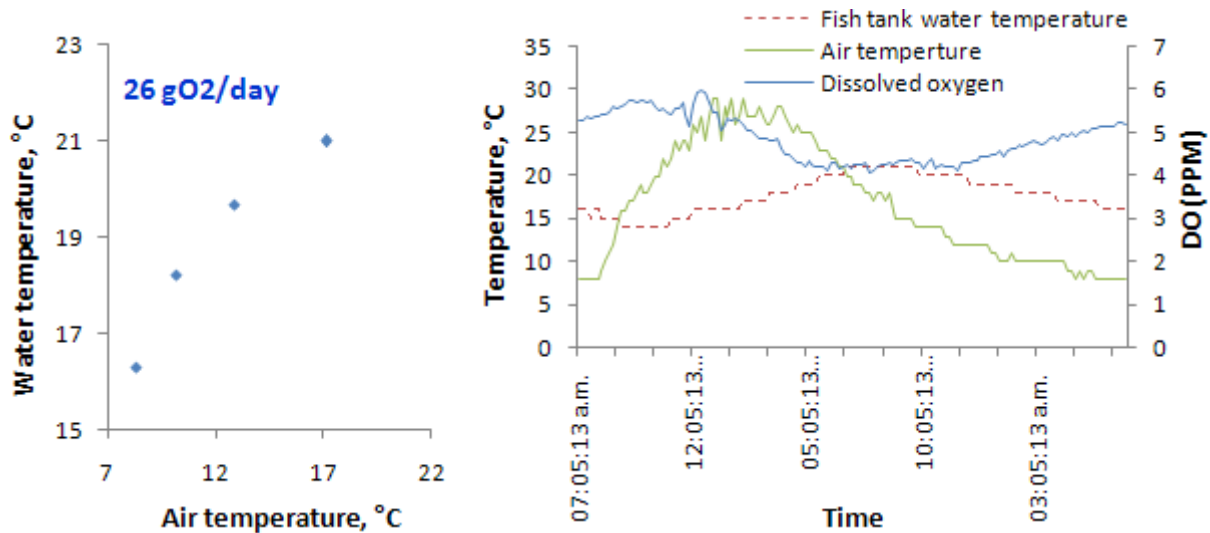


Fig. 4.25. The effect of air temperature on water temperature and dissolved oxygen concentrations at OTR of 26 gO₂/day.

RESULTS AND DISCUSSION

Figs. 4.26 and 4.27 show the effect of air temperatures on the tanks water temperature at different months applied three oxygen transfer rate (OTR) for each tank affecting dissolved oxygen concentrations.

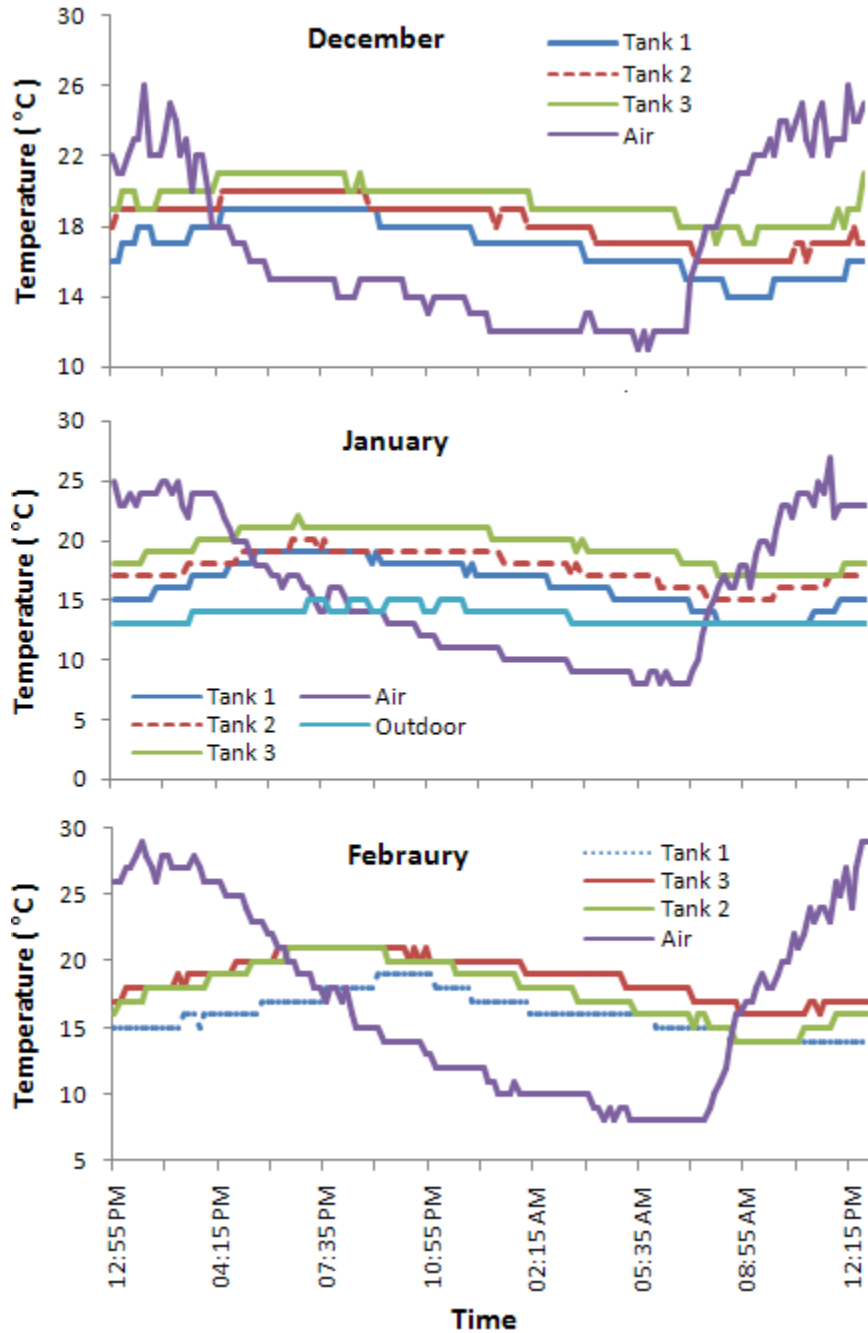


Fig. 4.26. The effect of air temperature on water tanks temperature at December, January and February.

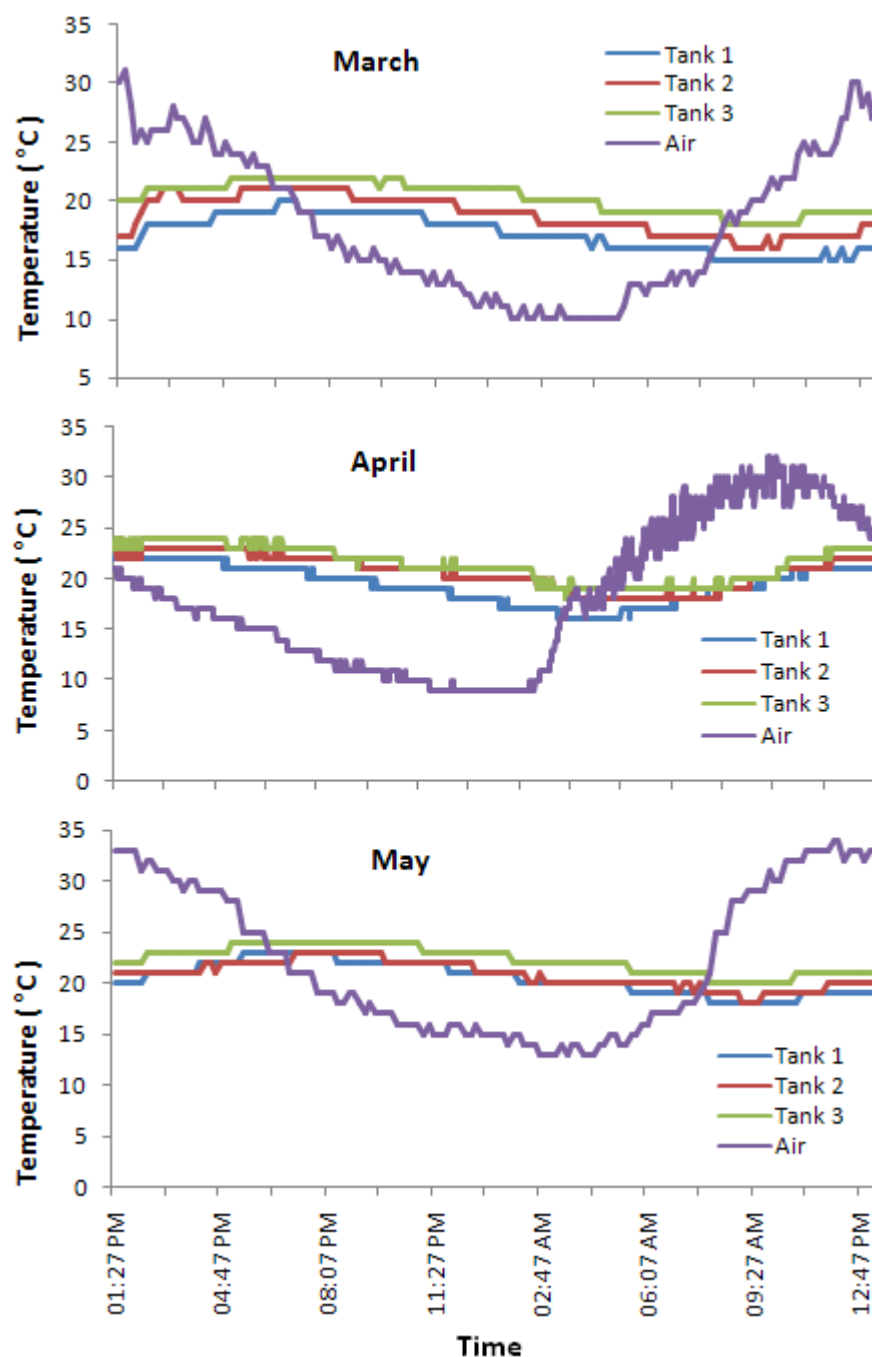


Fig. 4.27. The effect of air temperature on water tanks temperature at March, April and May.

It was observed that air temperatures were different inside the green house covered with shade net Table 4.3 shows the diversity in air temperatures between the indoor and outdoor temperatures, affected water temperature; the differences between water temperatures at indoor and outdoor illustrated at Fig. 4.26, in January water temperatures for the three tanks recorded

RESULTS AND DISCUSSION

water temperatures higher than water temperatures at outdoors, also the effect of three distinct aeration processes for three tanks on water temperatures variations.

Table 4.3. Temperature measurements for three tanks at December.

Month	Outdoor air temperatures		Indoor air temperatures	
	Maximum	Minimum	Maximum	Minimum
December	21	7	26	11
January	21	6	25	8
February	22	7	28	8
March	25	9	30	10
April	26	10	32	10
May	27	12	34	13

4.4.3. Dissolved oxygen mass balance in RAS:

4.4.3.1. The effect of algae on dissolved oxygen demand.

Planktonic algae (algae bloom) usually occurs as a result of increased levels of nutrients and carbon dioxide in water, combined with the energy of sunlight. The nitrifying bacteria compete with algae for the nutrient available. As alga blooms grow more intensively in RAS show the die off phenomena and nearly disappeared except for some cells that attached to the walls. Fig. 4.28 shows the effect of algae turbidity in the system on oxygen level. Algae participate during the day as an oxygen generator producing at 12:00 pm the higher amount oxygen as gO_2 per hour of 7.02, 5.76, 5.58, 5.4 and 3.6 for 420, 280, 150, 95, 56 and 45 NTU, respectively.

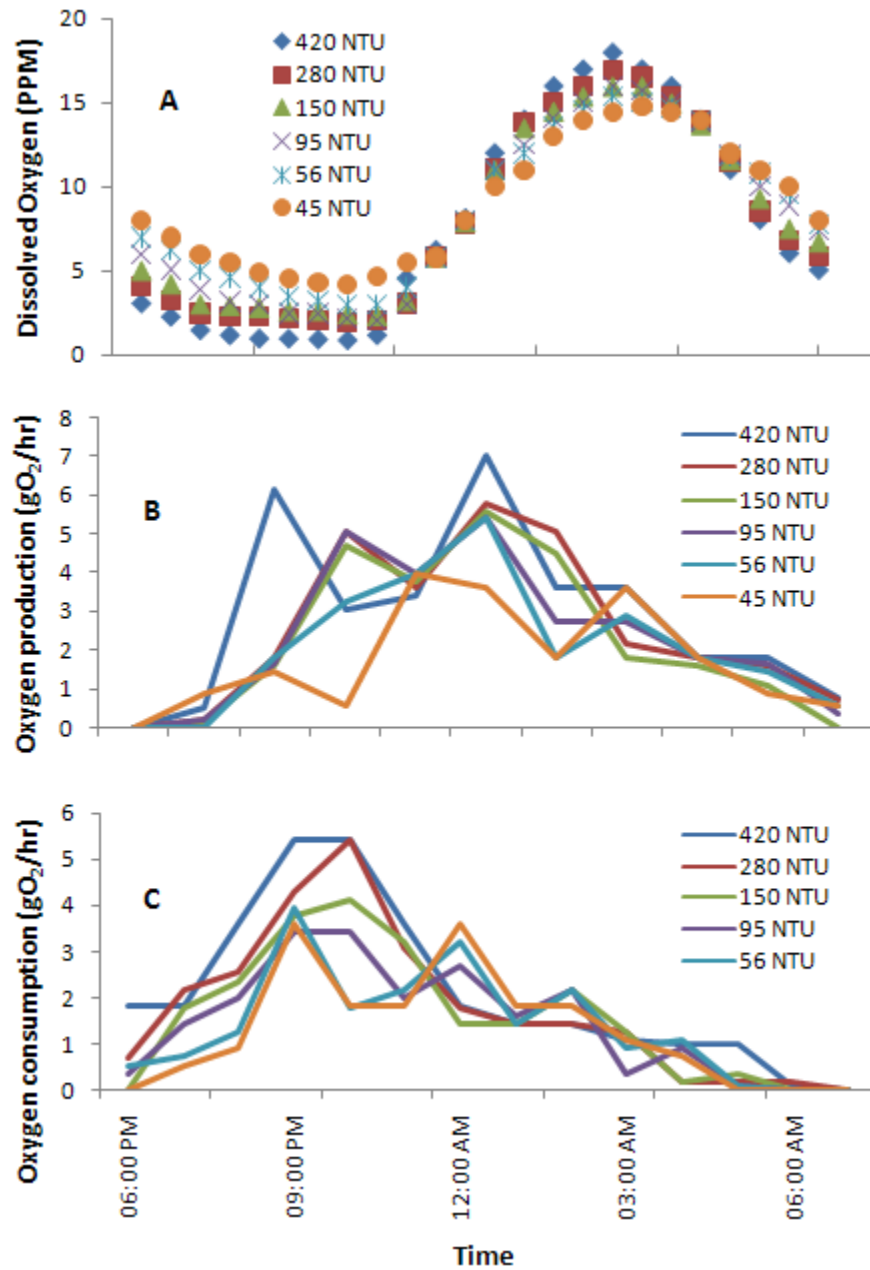


Fig. 4.28. The effect of algae density on dissolved oxygen concentration (A) and its effect on the amount of oxygen that produced (B) or consumed (C) per hour.

The accumulated oxygen production per day is illustrated at Fig. 4.29. It consumes the highest amount of oxygen at 9:00 p.m. and 10:00 p.m. with values of 5.4 and 5.4, 4.266 and 5.4, 3.78 and 4.14, 3.42 and 3.42, 3.96 and 1.8 and 3.6 and 1.8 for 420, 280, 150, 95, 56 and 45 NTU, respectively. The accumulated oxygen consumption per day is illustrated at Fig. 4.29. The

RESULTS AND DISCUSSION

amount of oxygen produced or consumed per hour in the RAS can be calculated by the following equations:

$$AOP = 4.5795 \ln(NTU) + 3.0793R^2 = 0.8943 \quad (4.4)$$

where AOP is the accumulated oxygen produced during the day.

$$AOC = 0.0286 (NTU) + 17.306R^2 = 0.9782 \quad (4.5)$$

where AOC is the accumulated oxygen consumed per day.

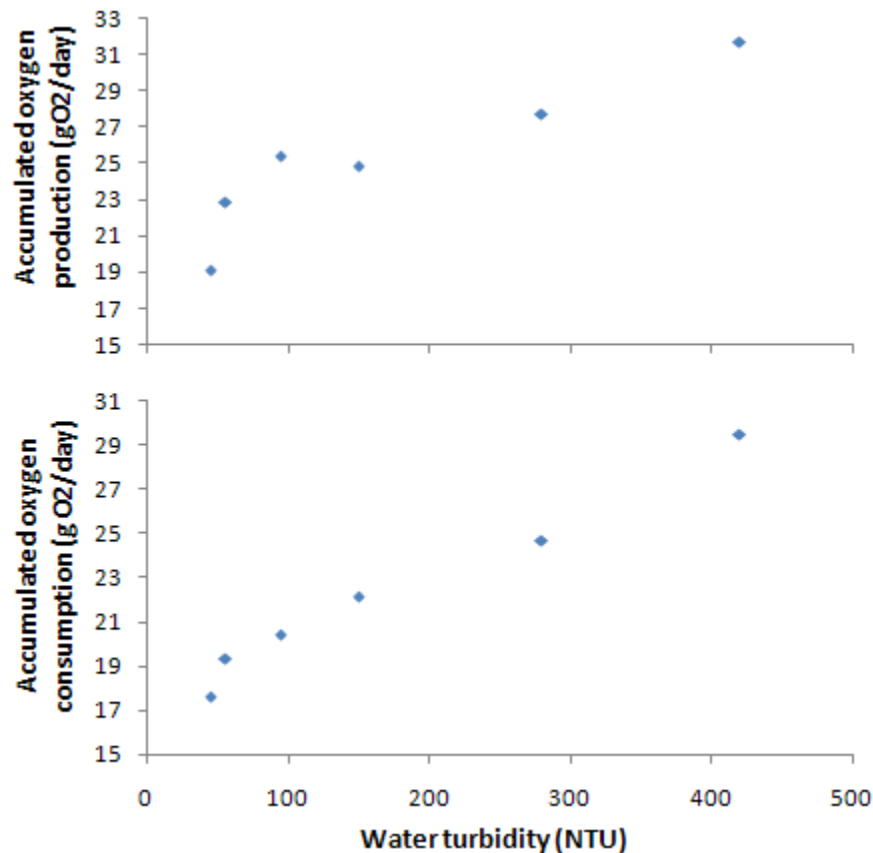


Fig. 4.29. The effect of algae density on the accumulated oxygen production (A) or consumption (B) per day.

It was observed that as water turbidity increases in the water the accumulated oxygen consumption raises linearly, but the accumulated oxygen production has a logarithmic behavior as the water column has higher algal blooms that affect light penetration. Therefore, water levels have not sufficient light and consume oxygen.

4.4.3.2. Carp dissolved oxygen demand.

Oxygen consumption by the carps was studied under water temperatures ranging between 17 and 24°C for different carp sizes.

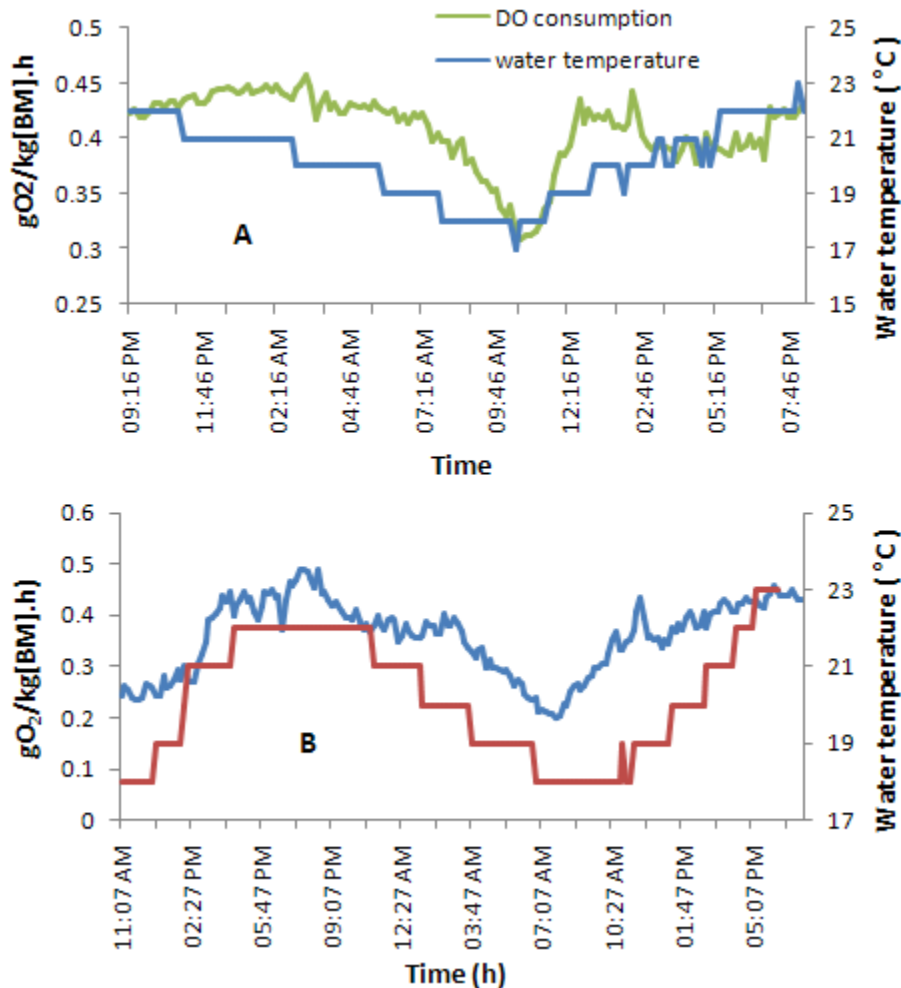


Fig. 4.30. Diurnal fish oxygen consumption (mgO₂/hr) for carp mean weight (A) 200 grams and (B) 150 grams.

Carp feeding is often strongly affected by reduced oxygen (Doudoroff & Shumway, 1970; Carlson et al. 1980, Kramer, 1987). Search, digestion and assimilation are major components of the energy budget of many fishes (Brett & Groves 1979). Two daily meals were applied starting from carp weight 100 grams at 11:16 and 18:30 hr. with a feed ratio of 5% of fish bio-mass. Digestive respiration increases oxygen demand by 0.03 gO₂/kg[BM].h during three hours.

RESULTS AND DISCUSSION

Growth respiration was recorded for each week of monitoring to be between 9:16 pm and 3:26 am, the growth respiration detection was as an increment in oxygen consumption for times longer than 3 hours if there is no stresses. Maintenance respiration obtained at 17 °C was of 0.32 gO₂/kg[BM].h. Fish respiration varied during the day limited by water temperature decreasing from 0.422 to 0.32 gO₂/kg[BM].h, Fig. 4.30. As water temperature decreased from 20 to 17 °C from 4:26 to 11:16 AM, fish activity decreased as well as oxygen consumption.

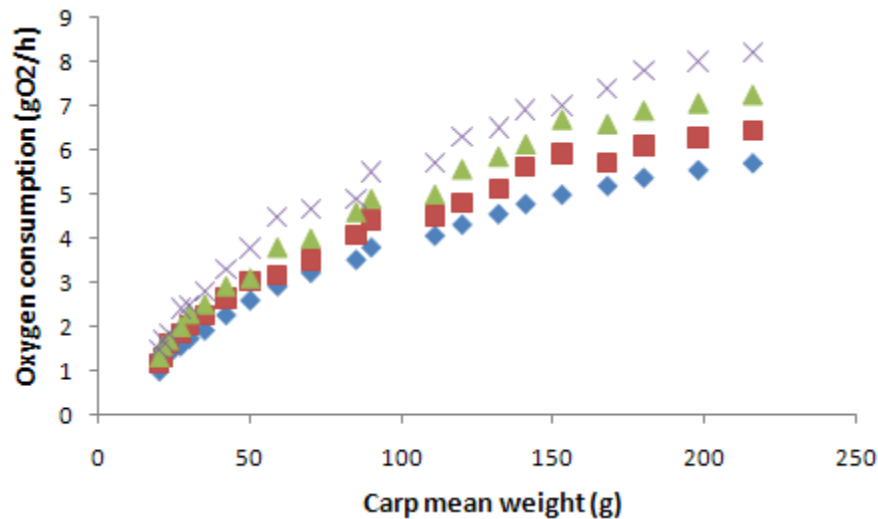


Fig 4.31. Effect of water temperature on carp oxygen consumption at different carp mean weight.

It was observed that as food supply numbers increases carp oxygen consumption after feeding will be lower in its raising as obtained by [Zakes et al. \(2006\)](#), as shown in Fig. 4.30a. As food introduced one time per day, the carps has higher appetite than the food introduced two times daily, the mean oxygen consumption for one two times food applications increases from 0.39 to 0.42 gO₂/kg[BM].h (Fig. 4.30B). Due to carp has higher starvation during feeding for their activities for searching, eating, and digesting. Therefore, it's recommended to apply the food at the highest water temperatures during the day to obtain maximum feed conversion factor (g food/ g fish), nevertheless if the food introduced at cooling temperatures, lower number of fish will eat and the majority will not, increasing food losses.

RESULTS AND DISCUSSION

Temperature has been long recognized as one of the fundamental extrinsic factors affecting biologic processes of poikilothermic organisms, such as feeding, respiration, growth, and reproduction (Newell and Branch, 1980; Shumway, 1982; Bayne and Newell, 1983). It was observed that the rapid shift in water temperatures (according to weather conditions in the State Mexico) affects drastically carp oxygen consumption, (Fig. 4.31); similar results were similar to (Saucedo et al., 2004). Carp oxygen consumption decreased during the night as water temperature cools to 17°C. At places that has lower changes in temperature between day and night and in open ponds oxygen requirements increased during night as plants and algae consume oxygen (Madenjian et al., 1987). The following regression relationship calculates the oxygen demand by the carp at different temperatures and fish size.

$$FOC = AW^2 + BW + C$$

Table 4.3. Fish oxygen consumption equation's parameters.

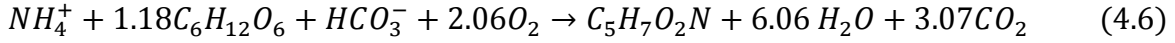
Water temperature, °C	A	B	C	R ²
18	-0.00001	0.0447	0.4306	0.994
20	-0.0001	0.0506	0.5103	0.99
22	-0.0001	0.058	0.523	0.97
24	-0.0001	0.0635	0.6812	0.98

Fig.4.31 shows the effect of water temperature on the carp oxygen consumption. Minimum carp oxygen consumption was observed at 7:07 a.m. and started to increase as water heats up reaching maximum oxygen consumption at 7:37 p.m. Specific oxygen consumption rise 146.67% two hours after feeding at 9:00 a.m. and 137.5% two hours after feeding at 12:00 a.m.

4.4.3.3. Biofilter dissolved oxygen demand.

The removal of ammonia by heterotrophic bacteria can be described in general by the following relationship (Ebling, et al., 2006a) for ammonia as the nitrogen source:

RESULTS AND DISCUSSION



This equation indicates that for every gram of ammonia-nitrogen converted to microbial biomass consumes 4.71 g of dissolved oxygen, 3.57 g of alkalinity (0.86 g inorganic carbon) and 15.17 carbohydrates (6.07 g organic carbon). A total of 8.07 g of microbial biomass having 2.63 g of inorganic carbon will be produced. Fig.4.32 shows the effect of carp mean weight on the amount of oxygen consumed by the nitrifying bacteria, due to the direct relationship between the amount of ammonia produced by the carp and the nitrifying bacteria growth. It will demand oxygen to convert the ammonia to nitrate in the biofilter.

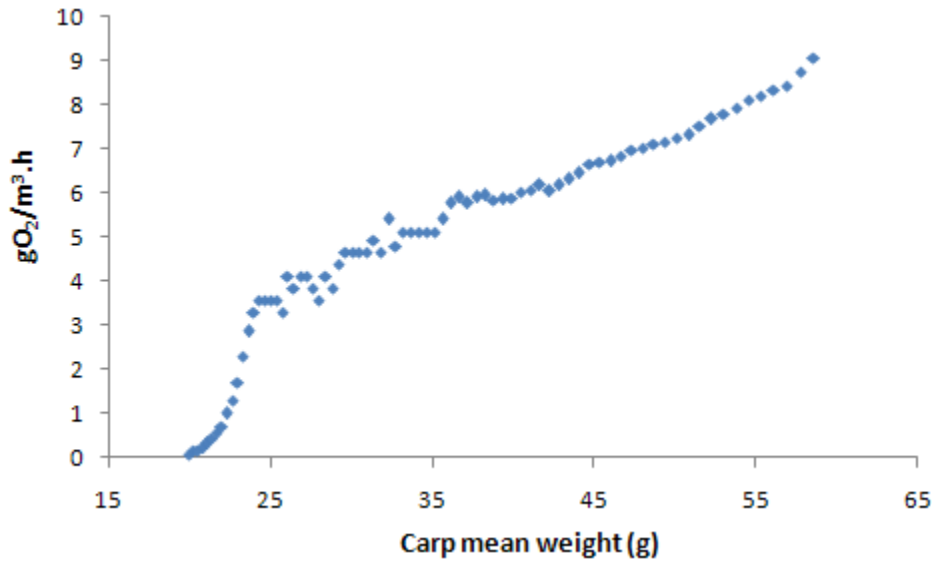


Fig. 4.32. Effect of the carp mean weight on nitrifying bacteria oxygen consumption.

The following equation can be used to calculate the amount of dissolved oxygen consumption in the biofilter.

$$NBOC = (0.1936W - 2.0174) \times (V_m)R^2 = 0.8851 \quad (4.7)$$

where W is the carp mean weight in grams and V_m is the biofilter media volume in m^3 and NBOC is the biofilter oxygen consumption gO_2 /hour.

4.4.3.4. Sediments dissolved oxygen demand.

The accumulation of sediments in RAS affects significantly the amount of overall oxygen demand by the system to be decomposed by the aerobic bacteria. It is necessary to remove these sediments daily by the separator of solids and perform a complete cleaning every week to remove all the solids in the separator. Fig.4.33 shows the effect of sediments on overall oxygen consumption during the day and the night that ranged from 3.5 to 28.9 gO₂/m³ sediments per hour, respectively. Sediment oxygen demand (SOC) in commercial channel catfish ponds was determined as oxygen demand per each surface unit. Estimated SOC ranged from 62 to 962 mg. m⁻² h⁻¹, with a mean of 478 mg. m⁻² h⁻¹ (Steeby et al., 2004).

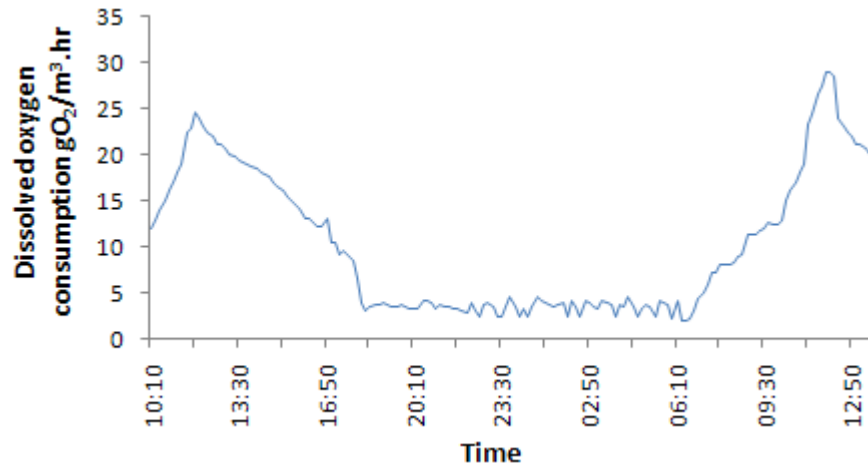


Fig. 4.33. Diurnal oxygen consumption by the sediments.

The accumulative oxygen demand by the sediments per day can be calculated by the following equation.

$$SOC = 1279.62(V_{Sed}) \quad (4.8)$$

where *SOC* is the accumulative oxygen consumption by the sediments per day and *V_{Sed}* is the sediments wetted volume.

4.4.3.5. Overall dissolved oxygen demand

The overall dissolved oxygen demand is the main parameter for the RAS designer when designing a suitable aerator to meet the dissolved oxygen requirements of the system. It is necessary to take into account all parameters that can affect dissolved oxygen requirements as:

1. Fish weight at harvest,
2. Maximum algae turbidity in the water,
3. Effluents management,
4. Biofilter volume and their parameters,
5. Water temperature range.

4.4.3.6. Model Expectations

Depending on the data collected in the experiment we can calculate the overall oxygen demand for the system by the following relationship.

$$\begin{aligned} DOD &= \text{Algae oxygen respiration or production} \\ &+ \text{Fish oxygen consumption} + \text{Nitrifying bacteria oxygen consumption} \\ &+ \text{Sediment oxygen consumption} \\ DOD &= (0.0286 NTU + 17.306) - (4.5795 \ln(NTU) + 3.0793) \\ &+ 24 \left(\frac{-9}{10^5} W^2 + 0.0609 \times W - \frac{3}{10^5} \right) + 24(0.1936W - 2.0174)V_m + 1279.62 * V_{sed} \end{aligned} \quad (4.9)$$

Fig. 4.34 shows the effect of algae turbidity on overall oxygen demand, and can be noted for carps weighting 250 grams without algae blooms consume 170.155 gO₂/day, and with algae blooms consume 167.049, 167.2294, 167.4094, 167.5894 and 167.7694 gO₂/day for 100, 200, 300, 400, 500 NTU, respectively.

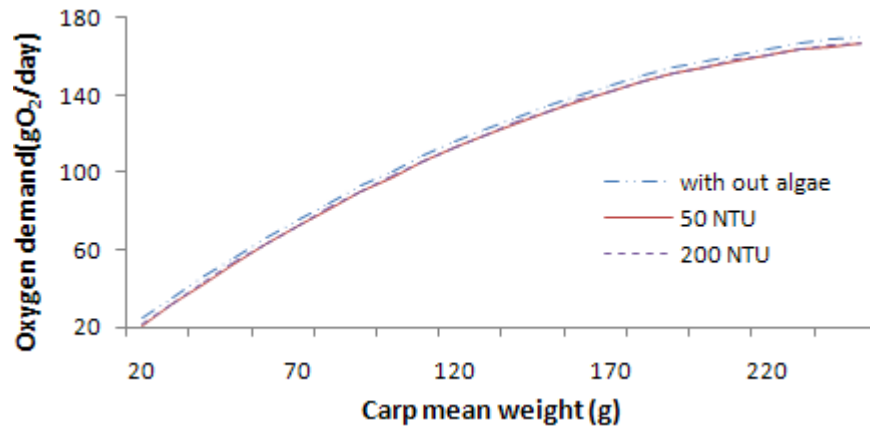


Fig. 4.34. Effect of algae turbidity on overall dissolved oxygen demand at 20°C and 0.001 m³ sediments using tezontle of 0.2 m³ as biofilter media.

Fig.4.35 shows the effect of algae of 50 NTU on overall oxygen demand during the day and the night. It was observed that the RAS with algae of 50NTU and without algae consume 48.06 and 61.27 gO₂ during the day, respectively.

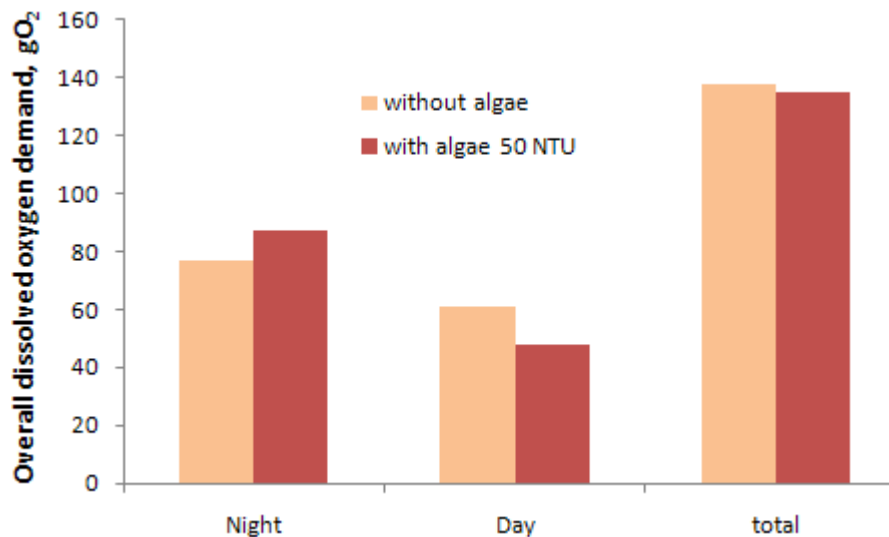


Fig. 4.35. The effect of algae on overall oxygen demand during day and night.

The model can predict the effect of water temperatures on hourly carp oxygen consumption (Fig. 4.36A), as water temperature increases from 18 to 24 °C, carp oxygen consumption consequently increases from 5.68 to 8.248 gO₂/h.

RESULTS AND DISCUSSION

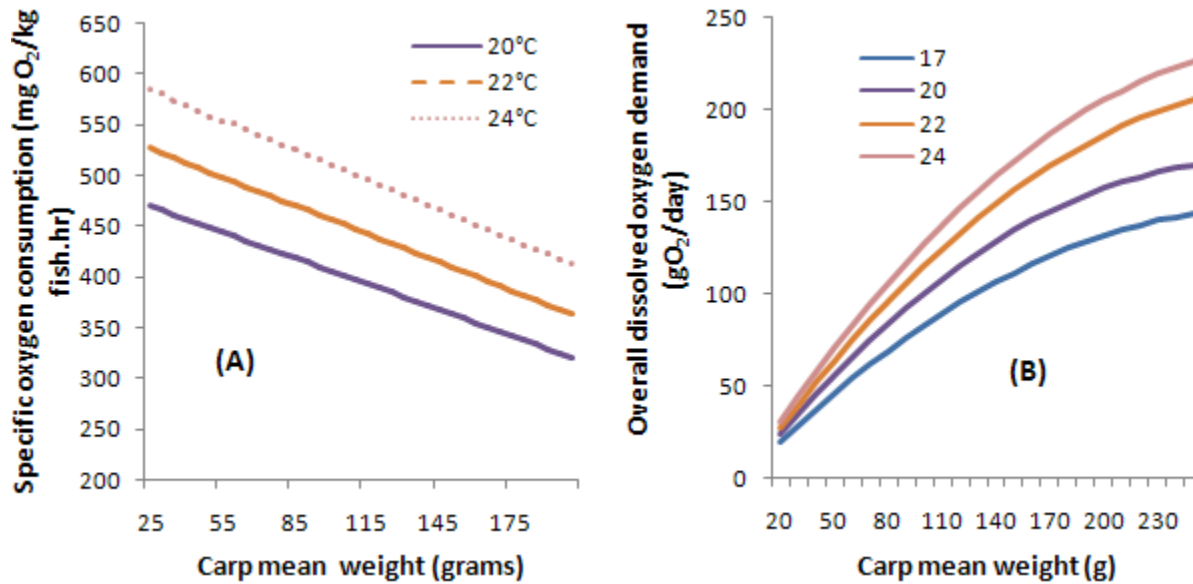


Fig. 4.36. The effect of water temperatures on (A) specific oxygen consumption(mgO₂/kg fish.h) and (B) Overall dissolved oxygen demand at without algae and 0.001 sediments (gO₂/h).

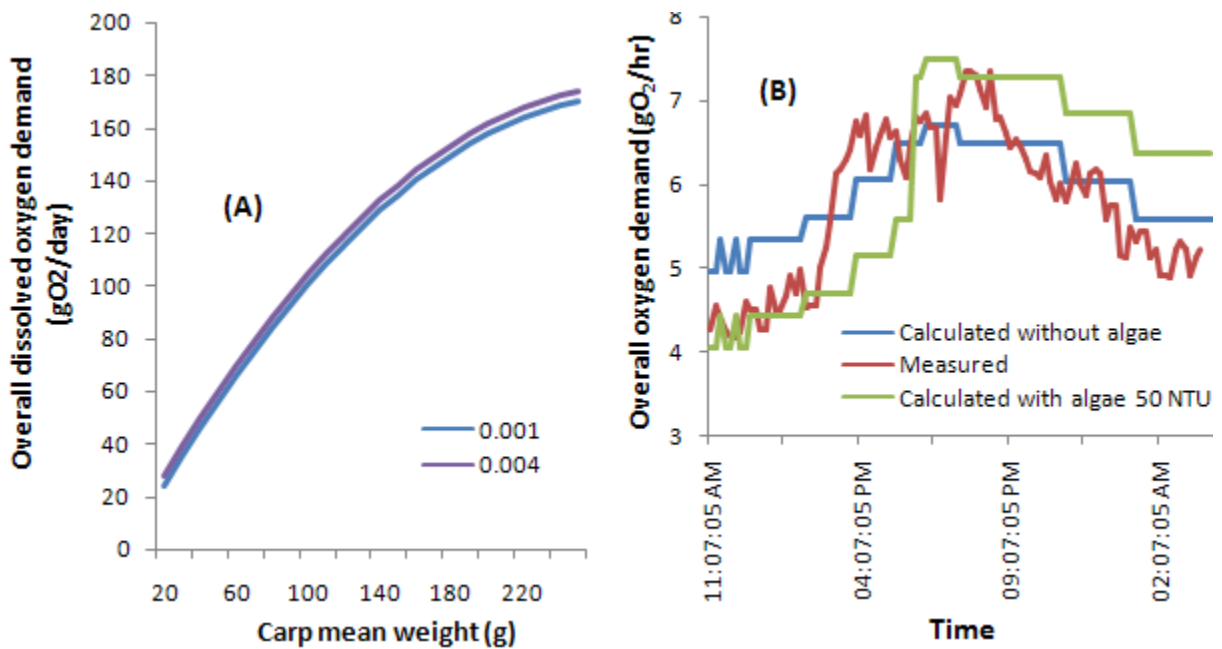


Fig. 4.37. (A) The effect of sediments volume on overall dissolved oxygen demand at without algae and 20°C. (B) The overall dissolved oxygen demand expected and measured according to the diurnal change in temperature at carp mean weight of 70 grams.

RESULTS AND DISCUSSION

Fig. 4.37 shows the effect of water temperatures on expected overall dissolved oxygen demand it was observed that at carp mean weight of 20 grams the overall dissolved oxygen demand was increased from 21.04 to 24.4 to 27.2 and finally to 29.91 gO₂/day for 18, 20, 22 and 24°C, respectively. As carp mean weight increased to 250 gram the overall oxygen demand increased to 156.35, 170.16, 205.55 and 225.94 gO₂/day, respectively.

The model can predict hourly overall oxygen consumption according to temperature variation in cases of algae presence or not (Fig. 4.37) in compared with oxygen consumption measured at fish carp weight 70 grams.

Aeration Energy Consumption

Daily growth rate as specific growth rate (SGR) was varied between 0.7 to 5.5% of carp biomass according to water temperature ranging between 14 and 25°C during the growing season from January to June. SGR was highest at 25°C. As obtained by [Ruyet et al., \(2004\)](#) for the eel.

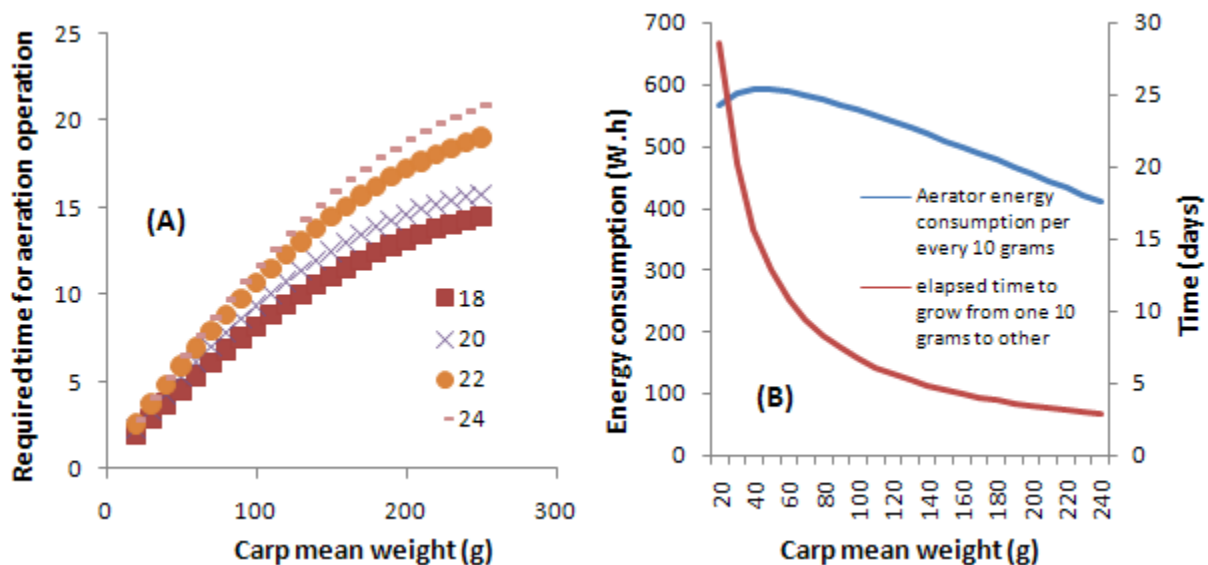


Fig. 4.38. (A) Aeration requirements at different temperatures for different carp sizes; (B) Aeration energy consumption per each 10 grams of carp growth.

RESULTS AND DISCUSSION

At certain temperatures the SGR did not varied and the daily growth rate (gram Biomass/day) between 40 to 60 grams was lower than when the carp was between 200 to 300 grams. With a 2% of carp growth rate at 20 grams gives a daily increase of 0.4 gram; at 200 grams gives 4 grams daily (Fig. 4.38B). Aerator energy consumption required to carp grow from 20 to 30 grams was higher than the aeration required to carp grow from 220 to 230 gram due to daily carp growth rate (Biomass/day) was 0.3 gram/day.fish and at 220 grams was 2 gram/day.fish.

4.4.4. Effect of three different aeration levels on carp growth rate.

The effect of three aeration techniques was analyzed in the 4.5-6, 2.0-4 and 3.5-5 ppm, ranges. No significant difference was found in daily growth rate between the aeration treatments of 4.5 to 6 and 3.5 to 5 ppm. The aeration level of 2.0-4.0 ppm registers lower daily growth rate; the aeration range of 3.5-5 ppm supports higher growth rate with lower energy consumption (Fig. 4.39). All the aerators used in RAS had a lower aeration efficiency index at higher altitude above sea level due to lower dissolved oxygen saturation ([Table 7.3 Appendix 1](#)).

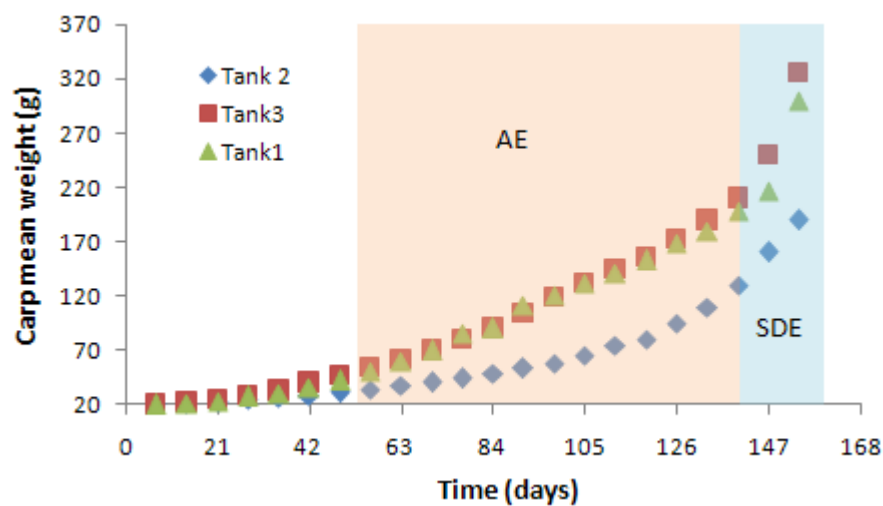


Fig. 4.39. Weekly carp growth rate for three different aeration techniques (AE) and carp growth rate under a reduced stocking density of 50 organisms per m^3 (SDE).

RESULTS AND DISCUSSION

It was observed that the oxygen level in the tank affect on carp appetite due to the stress which carps faced to compensate lower aeration (Table 4.4). The mean feed conversion factor (FCR) obtained for Tank 1, 2, 3 was 1.78 ± 0.5 , 2.14 ± 0.73 , 1.6 ± 0.24 g food/g biomass.

Table 4.4. Food supply for different carp sizes under three different aeration levels.

Time	4.5-6 ppm		2-4 ppm		3.5-5 ppm	
	Weight (g)	Food g/100fish	Weight (g)	Food g/100fish	Weight (g)	Food g/100fish
7	20	50	20	50	20	50
14	21	50	21	50	22	50
21	23	50	22	50	25	50
28	27	50	24	50	28	100
35	30	100	26	100	33	150
42	35	150	28	100	40	150
49	42	150	31	100	47	150
56	50	200	34	100	54	200
63	59	200	37	100	62	200
70	70	250	40	100	70	250
77	85	250	44	100	80	300
84	90	300	48	150	91	300
91	111	300	53	150	104	300
98	120	300	58	150	119	300
105	132	300	65	200	132	350
112	141	350	75	200	144	350
119	153	350	80	300	156	400
126	168	400	95	300	172	400
133	180	400	110	350	190	400
140	198	400	130	350	210	450

4.4.5. Carp sorting based on their size as a percent.

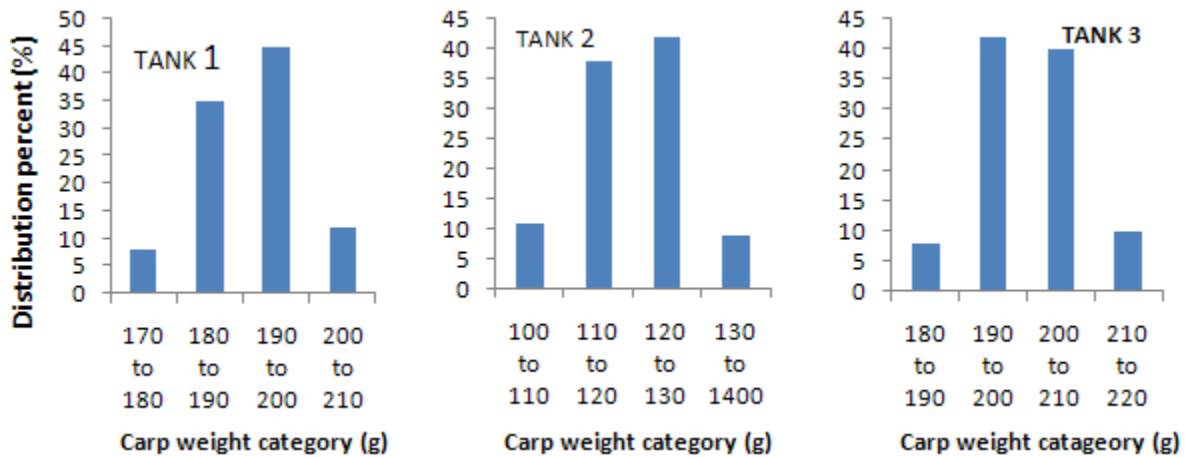


Fig. 4.40. Carp sorting for first, second and third tank at the 140th day, for 100 organisms per m³ water.

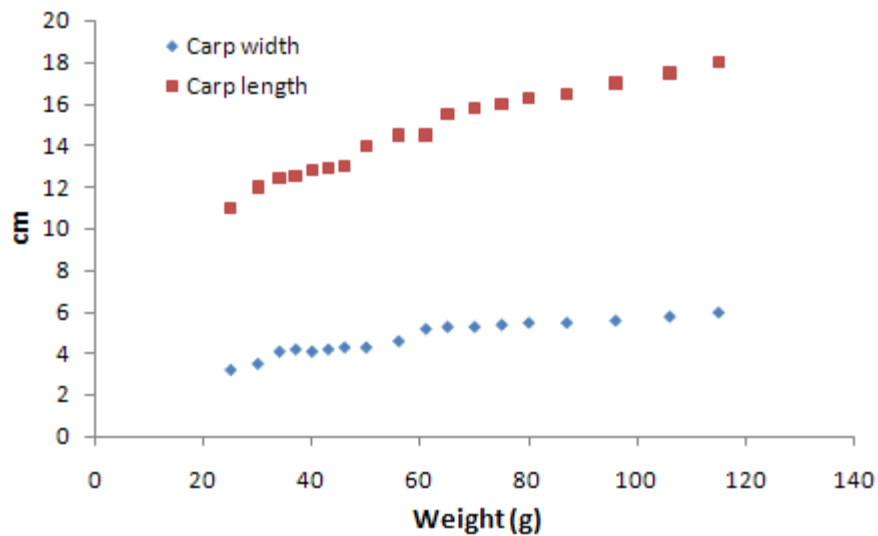


Fig. 4.41. Carp physiological changes during the growing season.

4.5. Dissolved oxygen automation.

The three tanks were redistributed having 50 organism per m³. The first tank had an average of 198 g, the second 130 g and the third of 210 g the daily growth rate was increased rapidly in three weeks from 198 to 300 g, from 130 to 190 g and 210 to 325 g for the first, second and third tank, respectively. The weight increase was attributed to a lower stocking density per m³

RESULTS AND DISCUSSION

(Fig.4.39). Feed conversion efficiency was lower in high densities (Siddiqui and Al-Harbi, 1999; Al-Harbi and Siddiqui, 2000). Lower stocking densities provide more space and less competition. The carrying capacity of the system was 18 kg/m^3 . Comparatively with open production systems, Loyacano (1974) reported that channel catfish production was 5500 kg/ha (0.55 kg/m^3) in aerated ponds with continuous diffused aeration and 15000 kg/ha (1.5 kg/m^3) without air (Parker, 1979).

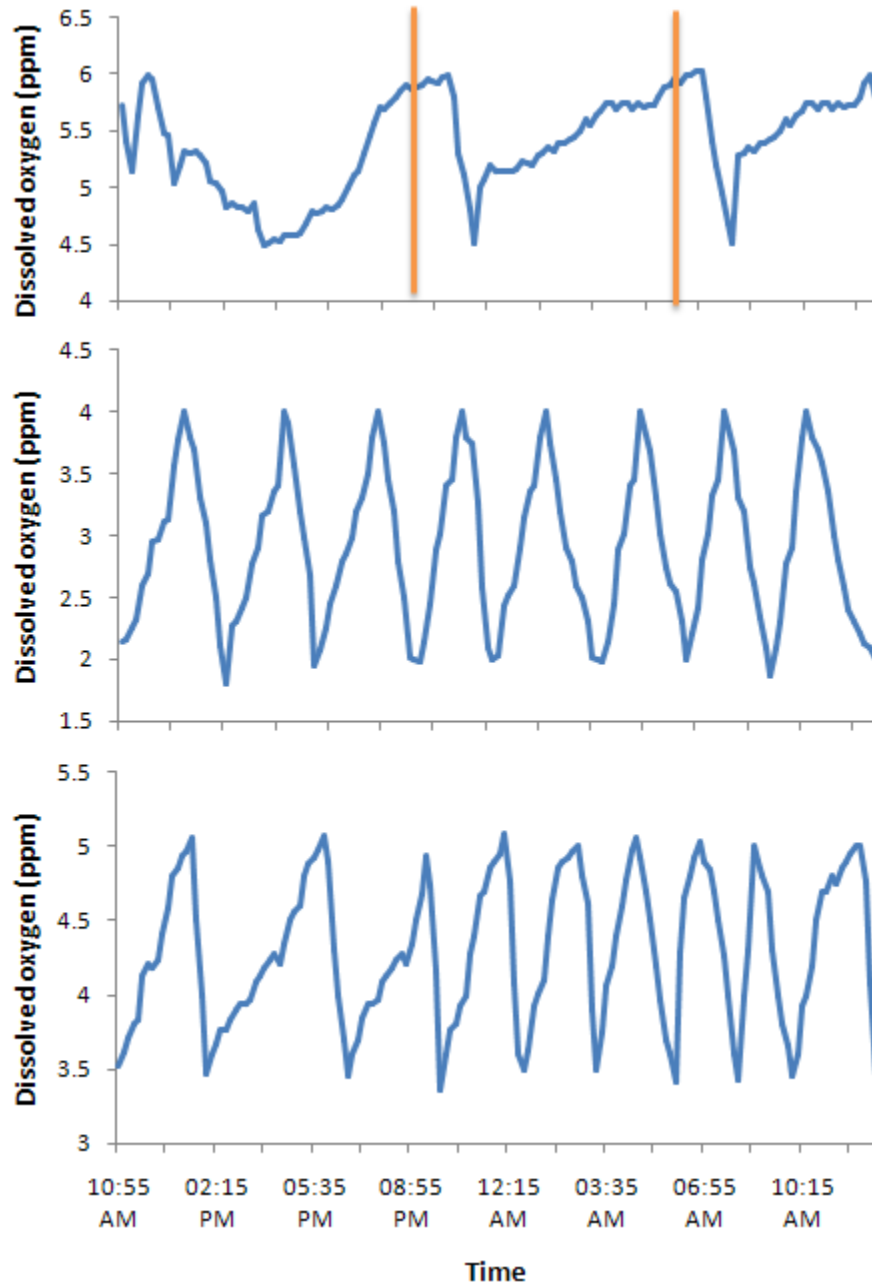


Fig. 4.42. Dissolved oxygen concentrations for the three tanks under three DO levels.

RESULTS AND DISCUSSION

Diana et al., (1994) and Diana et al., (1995) reported tilapia yields of 11,000-15,000 kg/ha (1.1 to 1.5 kg/m³) in 5-8 months; these ponds located in Thailand were aerated, fertilized and fed with a stock population of 3 fish/m³. Yi and Lin (2001) produced caged tilapia in aerated ponds which yielded an average of 6.92 ± 0.60 t/ha/crop. The aeration processes for the three tanks in this experiment were modified to be monitored and controlled by LabView program. Three level ranges were setting in the front panel to be 4.5-6, 2-4 and 3.5-5 ppm for the first, second and third tank respectively (Fig. 4.42). Before controller installation processes starting in the camp, DO and thermocouple measurements were checked to be resistant for any electrical noises, the difference between filtered and unfiltered measurements are shown in Fig. 4.43.

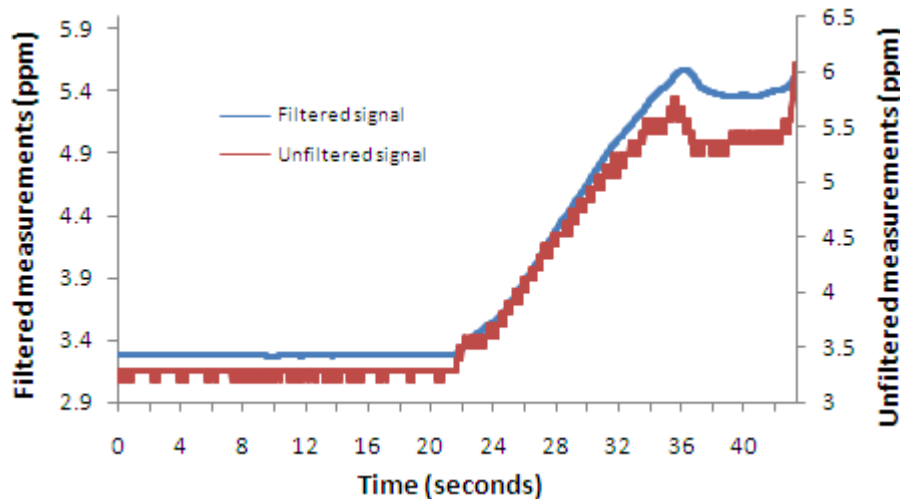


Fig. 4.43. Filtered and unfiltered dissolved oxygen measurements.

The open loop control for RAS system

To calculate the system operation time two conditions were considered if the RAS system has and has not algae. The colors most opacity is the most urgent. As shown in Fig. 4.44 the most opacity color indicates highest oxygen requirements during the period (from 7:00 p.m. to 1 a.m.), due to two reasons, maximum carp oxygen consumption for highest water temperatures and the oxygen demand for algae respiration. As water temperatures decreases carp oxygen consumption declines, but algae not yet can produce oxygen until 7:00 a.m. As algae realizes oxygen in water body, the total oxygen requirements reduces to be minimum until 1 p.m. as water temperatures raises after 1 p.m. Carp oxygen consumption increases until 1 a.m. and coinciding with algae respiration after 7 p.m. to 1 a.m. to be very urgent. The aeration requirements for four periods at the case of RAS system having algae were illustrated at tables 4.5 and 4.6.



Fig. 4.44. Aeration requirements levels during the day in the case with algae and without algae.

Water movements through the biofilters are participating aeration. The OTR for biofilter 1, 2 and 3 are 2.87, 2.46 and 2.2 gO₂/h respectively. The recirculating pump only can add oxygen to water without needing to spray column aerator at first rearing days was shown in the Tables 4.5, 4.6 and 4.8 until the colored cells, aeration requirements in these was based dissolved oxygen set points 3.5 to 5 ppm, 4 to 6 and 2 to 4 ppm.

RESULTS AND DISCUSSION

Table 4.5. Aeration requirements (h) when RAS system has algae at period 1:00 am to 1:00 pm.

Date	W	TOD	Aeration at 1:00 am to 7 am						Aeration at 7:00 a.m. to 1:00 pm						
			Aeration by water movements through the biofilter (h)			Spray column aerator (h)			TOD	Aeration by water movements through the biofilter (h)			Spray column aerator (h)		
			1	2	3	1	2	3		1	2	3	1	2	3
23-Dec.	20	1.80	3.77	4.40	4.92	0.00	0.00	0.00	0.54	1.13	1.32	1.47	0.00	0.00	0.00
30-Dec.	22	1.93	4.02	4.70	5.00	0.00	0.00	0.04	0.66	1.39	1.62	1.81	0.00	0.00	0.00
6-Jan.	25	2.11	4.41	5.00	5.00	0.00	0.03	0.12	0.85	1.77	2.06	2.31	0.00	0.00	0.00
13-Jan.	28	2.29	4.80	5.00	5.00	0.00	0.10	0.20	1.03	2.15	2.50	2.80	0.00	0.00	0.00
20-Jan.	33	2.59	5.00	5.00	5.00	0.09	0.24	0.33	1.32	2.77	3.23	3.61	0.00	0.00	0.00
27-Jan.	40	3.00	5.00	5.00	5.00	0.26	0.41	0.51	1.73	3.62	4.23	4.73	0.00	0.00	0.00
03-Feb.	47	2.98	5.00	5.00	5.00	0.26	0.41	0.50	1.72	3.59	4.19	4.68	0.00	0.00	0.00
10-Feb.	54	3.32	5.00	5.00	5.00	0.41	0.56	0.65	2.06	4.30	5.00	5.00	0.00	0.00	0.10
17-Feb.	62	3.71	5.00	5.00	5.00	0.58	0.73	0.82	2.44	5.00	5.00	5.00	0.02	0.17	0.27
24-Feb.	70	4.08	5.00	5.00	5.00	0.74	0.89	0.99	2.82	5.00	5.00	5.00	0.19	0.34	0.43
03-Mar.	80	5.56	5.00	5.00	5.00	1.39	1.54	1.63	4.29	5.00	5.00	5.00	0.83	0.98	1.08
10-Mar.	91	6.17	5.00	5.00	5.00	1.70	1.81	1.90	4.90	5.00	5.00	5.00	1.10	1.25	1.35
17-Mar.	104	6.86	5.00	5.00	5.00	1.96	2.11	2.21	5.60	5.00	5.00	5.00	1.41	1.56	1.65
24-Mar.	119	7.63	5.00	5.00	5.00	2.30	2.45	2.54	6.37	5.00	5.00	5.00	1.74	1.89	1.99
31-Mar.	132	8.27	5.00	5.00	5.00	2.50	2.73	2.82	7.01	5.00	5.00	5.00	2.02	2.17	2.27
07-Apr.	144	9.09	5.00	5.00	5.00	2.90	3.09	3.18	7.83	5.00	5.00	5.00	2.38	2.53	2.63
14-Apr.	156	9.63	5.00	5.00	5.00	3.18	3.33	3.42	8.37	5.00	5.00	5.00	2.62	2.77	2.87
21-Apr.	172	10.32	5.00	5.00	5.00	3.48	3.63	3.72	9.05	5.00	5.00	5.00	2.92	3.07	3.17
28-Apr.	190	11.03	5.00	5.00	5.00	3.79	3.94	4.03	9.77	5.00	5.00	5.00	3.24	3.39	3.48
05-May.	210	12.39	5.00	5.00	5.00	4.38	4.53	4.63	11.13	5.00	5.00	5.00	3.83	3.98	4.08

RESULTS AND DISCUSSION

Table 4.6. Aeration requirements (h) when RAS system has algae at period 1:00 pm to 1:00 am.

Date	W	TOD	Aeration at 1:00 pm. to 7 pm						Aeration at 7:00 pm. to 1:00 am						
			Aeration by water movements through the biofilter (h)			Spray column aerator (h)			TOD	Aeration by water movements through the biofilter (h)			Spray column aerator (h)		
			1	2	3	1	2	3		1	2	3	1	2	3
23-Dec.	20	0.76	1.59	1.86	2.07	0.00	0.00	0.00	2.02	4.23	4.94	5.00	0.00	0.00	0.08
30-Dec.	22	0.91	1.91	2.23	2.49	0.00	0.00	0.00	2.18	4.55	5.00	5.00	0.00	0.06	0.15
6-Jan.	25	1.14	2.38	2.78	3.11	0.00	0.00	0.00	2.40	5.02	5.00	5.00	0.00	0.16	0.25
13-Jan.	28	1.37	2.86	3.33	3.73	0.00	0.00	0.00	2.63	5.00	5.00	5.00	0.10	0.25	0.35
20-Jan.	33	1.74	3.64	4.24	4.74	0.00	0.00	0.00	3.00	5.00	5.00	5.00	0.27	0.42	0.51
27-Jan.	40	2.25	4.71	5.00	5.00	0.00	0.09	0.18	3.52	5.00	5.00	5.00	0.49	0.64	0.74
03-Feb.	47	2.63	5.00	5.00	5.00	0.11	0.26	0.35	3.89	5.00	5.00	5.00	0.66	0.81	0.90
10-Feb.	54	3.11	5.00	5.00	5.00	0.32	0.47	0.56	4.38	5.00	5.00	5.00	0.87	1.02	1.12
17-Feb.	62	3.65	5.00	5.00	5.00	0.55	0.70	0.80	4.92	5.00	5.00	5.00	1.11	1.26	1.35
24-Feb.	70	4.18	5.00	5.00	5.00	0.79	0.94	1.03	5.45	5.00	5.00	5.00	1.34	1.49	1.59
03-Mar.	80	5.27	5.00	5.00	5.00	1.26	1.41	1.51	6.53	5.00	5.00	5.00	1.81	1.96	2.06
10-Mar.	91	6.01	5.00	5.00	5.00	1.59	1.74	1.83	7.27	5.00	5.00	5.00	2.14	2.29	2.39
17-Mar.	104	6.86	5.00	5.00	5.00	1.96	2.11	2.21	8.12	5.00	5.00	5.00	2.51	2.66	2.76
24-Mar.	119	7.81	5.00	5.00	5.00	2.37	2.52	2.62	9.07	5.00	5.00	5.00	2.93	3.08	3.17
31-Mar.	132	8.59	5.00	5.00	5.00	2.72	2.87	2.96	9.86	5.00	5.00	5.00	3.27	3.42	3.52
07-Apr.	144	9.71	5.00	5.00	5.00	3.21	3.36	3.45	10.97	5.00	5.00	5.00	3.76	3.91	4.01
14-Apr.	156	10.42	5.00	5.00	5.00	3.52	3.67	3.76	11.68	5.00	5.00	5.00	4.07	4.22	4.32
21-Apr.	172	11.32	5.00	5.00	5.00	3.92	4.07	4.16	12.58	5.00	5.00	5.00	4.47	4.62	4.71
28-Apr.	190	12.28	5.00	5.00	5.00	4.34	4.49	4.58	13.54	5.00	6.00	6.00	4.89	4.86	4.98
05-May.	210	14.08	6.00	6.00	6.00	4.92	5.10	5.21	15.34	6.00	6.00	6.00	5.47	5.65	5.76

RESULTS AND DISCUSSION

Table 4.7. Oxygen requirements when RAS system has not algae.

Date	Weight (g)	Biofilter oxygen demand (gO ₂ /h)		Tank oxygen demand (gO ₂ /h)		TOD (gO ₂ /h)	
		1:00 pm - 1:00 am	1:00 am - 1:00 pm	1:00 pm - 1:00 am	1:00 am - 1:00 pm	1:00 pm - 1:00 am	1:00 am - 1:00 pm
23-Dec.	20	0.30	0.24	0.95	0.80	1.24	1.04
30-Dec.	22	0.36	0.29	1.04	0.88	1.40	1.17
6-Jan.	25	0.45	0.37	1.17	0.99	1.62	1.36
13-Jan.	28	0.54	0.44	1.30	1.10	1.85	1.54
20-Jan.	33	0.70	0.57	1.52	1.28	2.22	1.85
27-Jan.	40	0.92	0.74	1.82	1.53	2.74	2.27
03-Feb.	47	1.13	0.92	1.98	1.35	3.11	2.27
10-Feb.	54	1.35	1.10	2.25	1.53	3.60	2.63
17-Feb.	62	1.60	1.30	2.54	1.73	4.14	3.03
24-Feb.	70	1.85	1.50	2.82	1.92	4.67	3.42
03-Mar.	80	2.16	1.75	3.59	3.16	5.75	4.91
10-Mar.	91	2.50	2.03	4.00	3.51	6.49	5.54
17-Mar.	104	2.90	2.36	4.44	3.91	7.34	6.26
24-Mar.	119	3.26	2.73	4.93	4.33	8.19	7.06
31-Mar.	132	3.47	2.76	5.31	4.66	8.78	7.42
07-Apr.	144	3.74	2.96	6.05	5.20	9.79	8.17
14-Apr.	156	4.01	3.16	6.39	5.47	10.40	8.63
21-Apr.	172	4.41	3.47	6.80	5.78	11.20	9.25
28-Apr.	190	4.86	3.82	7.20	6.08	12.06	9.90
05-May.	210	5.38	4.22	8.38	6.97	13.76	11.19

RESULTS AND DISCUSSION

Table 4.8. Aeration requirements (h) when RAS system has not algae based on DO set point 3.5-5 ppm.

Date	Aeration at 1:00 pm to 1:00 am						Aeration at 1:00 am to 1 pm					
	Aeration by water movements through the biofilter (h)			Spray column aerator (h)			Aeration by water movements through the biofilter (h)			Spray column aerator (h)		
	1	2	3	1	2	3	1	2	3	1	2	3
23-Dec.	5.20	6.06	6.78	0.00	0.00	0.00	4.35	5.08	5.68	0.00	0.00	0.00
30-Dec.	5.83	6.81	7.61	0.00	0.00	0.00	4.88	5.69	6.37	0.00	0.00	0.00
6-Jan.	6.79	7.92	8.85	0.00	0.00	0.00	5.67	6.61	7.39	0.00	0.00	0.00
13-Jan.	7.73	9.02	10.08	0.00	0.00	0.00	6.45	7.52	8.41	0.00	0.00	0.00
20-Jan.	9.29	10.84	10.00	0.00	0.00	0.00	7.73	9.02	10.09	0.00	0.00	0.00
27-Jan.	11.44	10.00	10.00	0.00	0.60	0.79	9.50	11.08	10.00	0.00	0.20	0.39
03-Feb.	10.00	10.00	10.00	0.63	0.93	1.12	9.49	11.07	10.00	0.00	0.19	0.38
10-Feb.	10.00	10.00	10.00	1.06	1.36	1.55	10.98	10.00	10.00	0.00	0.51	0.70
17-Feb.	10.00	10.00	10.00	1.53	1.83	2.02	10.00	10.00	10.00	0.56	0.86	1.05
24-Feb.	10.00	10.00	10.00	2.00	2.30	2.49	10.00	10.00	10.00	0.90	1.20	1.39
03-Mar.	10.00	10.00	10.00	2.94	3.24	3.43	10.00	10.00	10.00	2.21	2.51	2.70
10-Mar.	10.00	10.00	10.00	3.60	3.90	4.09	10.00	10.00	10.00	2.76	3.06	3.25
17-Mar.	10.00	10.00	10.00	4.34	4.64	4.83	10.00	10.00	10.00	3.40	3.70	3.89
24-Mar.	10.00	10.00	10.00	5.09	5.38	5.57	10.00	10.00	10.00	4.10	4.40	4.59
31-Mar.	10.00	10.00	10.00	5.60	5.90	6.09	10.00	10.00	10.00	4.42	4.71	4.90
07-Apr.	10.00	10.00	10.00	6.49	6.79	6.98	10.00	10.00	10.00	5.07	5.36	5.56
14-Apr.	10.00	10.00	10.00	7.02	7.32	7.51	10.00	10.00	10.00	5.48	5.77	5.96
21-Apr.	10.00	10.00	10.00	7.73	8.03	8.22	10.00	10.00	10.00	6.02	6.32	6.51
28-Apr.	10.00	10.00	10.00	8.48	8.78	8.97	10.00	10.00	10.00	6.59	6.89	7.08
05-May.	10.00	10.00	10.00	9.97	10.27	10.46	10.00	10.00	10.00	7.72	8.02	8.21

RESULTS AND DISCUSSION

Table 4.9. Aeration requirements (h) when RAS system has not algae based on DO set point 4-6 ppm.

Date	Aeration at 1:00 pm to 1:00 am						Aeration at 1:00 am to 1 pm					
	Aeration by water movements through the biofilter (h)			Spray column aerator (h)			Aeration by water movements through the biofilter (h)			Spray column aerator (h)		
	1	2	3	1	2	3	1	2	3	1	2	3
23-Dec.	6.24	7.27	8.14	0.00	0.00	0.00	5.22	6.10	6.82	0.00	0.00	0.00
30-Dec.	7.00	8.17	9.13	0.00	0.00	0.00	5.86	6.83	7.64	0.00	0.00	0.00
6-Jan.	8.15	9.50	10.00	0.00	0.00	0.95	6.80	7.93	8.87	0.00	0.00	0.00
13-Jan.	9.28	10.00	10.00	0.00	0.72	1.34	7.74	9.02	10.00	0.00	0.00	0.47
20-Jan.	10.00	10.00	10.00	0.76	1.12	1.86	9.28	10.00	10.00	0.00	0.24	0.46
27-Jan.	10.00	10.00	10.00	1.27	1.63	2.42	10.00	10.00	10.00	0.67	0.23	0.84
03-Feb.	10.00	10.00	10.00	1.84	2.20	2.99	10.00	10.00	10.00	1.08	0.61	1.26
10-Feb.	10.00	10.00	10.00	2.40	2.76	4.12	10.00	10.00	10.00	2.65	1.03	1.67
17-Feb.	10.00	10.00	10.00	3.53	3.89	4.91	10.00	10.00	10.00	3.31	1.44	3.24
24-Feb.	10.00	10.00	10.00	4.32	4.68	5.80	10.00	10.00	10.00	4.08	3.01	3.90
03-Mar.	10.00	10.00	10.00	5.21	5.57	6.68	10.00	10.00	10.00	4.92	3.67	4.67
10-Mar.	10.00	10.00	10.00	6.11	6.46	7.31	10.00	10.00	10.00	5.30	4.44	5.51
17-Mar.	10.00	10.00	10.00	6.72	7.08	8.38	10.00	10.00	10.00	6.08	5.28	5.88
24-Mar.	10.00	10.00	10.00	7.79	8.15	9.01	10.00	10.00	10.00	6.58	5.65	6.67
31-Mar.	10.00	10.00	11.00	8.42	8.78	9.86	10.00	10.00	10.00	7.22	6.43	7.15
07-Apr.	10.00	11.00	11.00	9.28	9.64	10.76	10.00	10.00	10.00	7.91	6.92	7.81
14-Apr.	11.00	11.00	12.00	10.18	10.54	12.00	10.00	10.00	10.00	9.26	7.58	8.50
21-Apr.	12.00	12.00	12.00	11.96	12.00	12.00	10.00	10.00	10.00	9.60	8.27	9.85
28-Apr.	12.00	12.00	12.00	12.00	12.00	12.00	10.00	10.00	11.00	9.80	9.62	10.10
05-May.	12.00	12.00	12.00	12.00	12.00	12.00	11.00	11.00	11.00	10.30	11.00	10.20

RESULTS AND DISCUSSION

Table 4.10. Aeration requirements (h) when RAS system has not algae based on DO set point 2-4 ppm.

Date	Aeration at 1:00 pm to 1:00 am						Aeration at 1:00 am to 1 pm					
	Aeration by water movements through the biofilter (h)			Spray column aerator (h)			Aeration by water movements through the biofilter (h)			Spray column aerator (h)		
	1	2	3	1	2	3	1	2	3	1	2	3
23-Dec.	4.32	5.03	5.63	0.00	0.00	0.00	3.61	4.22	4.71	0.00	0.00	0.00
30-Dec.	4.84	5.65	6.32	0.00	0.00	0.00	4.05	4.72	5.29	0.00	0.00	0.00
6-Jan.	5.64	6.57	7.35	0.00	0.00	0.00	4.71	5.49	6.13	0.00	0.00	0.00
13-Jan.	6.42	7.49	8.37	0.00	0.00	0.00	5.35	6.24	6.98	0.00	0.00	0.00
20-Jan.	7.71	9.00	10.00	0.00	0.00	0.00	6.42	7.49	8.37	0.00	0.00	0.00
27-Jan.	9.50	10.00	10.00	0.00	0.50	0.66	7.89	9.20	9.00	0.00	0.00	0.00
03-Feb.	10.00	10.00	10.00	0.52	0.77	0.93	7.88	9.19	10.00	0.00	0.00	0.32
10-Feb.	10.00	10.00	10.00	0.88	1.13	1.29	9.11	10.00	10.00	0.00	0.42	0.58
17-Feb.	10.00	10.00	10.00	1.27	1.52	1.68	10.00	10.00	10.00	0.46	0.71	0.87
24-Feb.	10.00	10.00	10.00	1.66	1.91	2.07	10.00	10.00	10.00	0.75	1.00	1.15
03-Mar.	10.00	10.00	10.00	2.44	2.69	2.85	10.00	10.00	10.00	1.83	2.08	2.24
10-Mar.	10.00	10.00	10.00	2.99	3.24	3.39	10.00	10.00	10.00	2.29	2.54	2.70
17-Mar.	10.00	10.00	10.00	3.60	3.85	4.01	10.00	10.00	10.00	2.82	3.07	3.23
24-Mar.	10.00	10.00	10.00	4.22	4.47	4.62	10.00	10.00	10.00	3.40	3.65	3.81
31-Mar.	10.00	10.00	10.00	4.65	4.90	5.05	10.00	10.00	10.00	3.67	3.91	4.07
07-Apr.	10.00	10.00	10.00	5.39	5.64	5.79	10.00	10.00	10.00	4.21	4.45	4.61
14-Apr.	10.00	10.00	10.00	5.83	6.08	6.23	10.00	10.00	10.00	4.55	4.79	4.95
21-Apr.	10.00	10.00	10.00	6.42	6.66	6.82	10.00	10.00	10.00	5.00	5.25	5.40
28-Apr.	10.00	10.00	10.00	7.04	7.29	7.45	10.00	10.00	10.00	5.47	5.72	5.88
05-May.	10.00	10.00	10.00	8.28	8.52	8.68	10.00	10.00	10.00	6.41	6.66	6.81

4.6. Water mass study

Water losses due to the evaporation:

The water lost by evaporation was determined by calculating the amount of water evaporating from an open pan, which ranged between 0.5 to 1.5 liter per day according to weather conditions. The water was exchanged with newer fresh water in the system for two reasons:

1. Biofilters initialization from the 23rd of December to the 20th of January. Ten percent of total water in the system was exchanged to control the unionized ammonia in the system until the biofilters have their capacity to remove all the total ammonia nitrogen produced by the system.
2. Separator cleaning to remove the solids accumulated in the separator channel and inside the cone wall each two weeks.

Water exchange strategy followed to control TAN and sediments accumulated in RAS system illustrated in Table 4.11, the X symbol indicates that ten percent of water was exchanged for tank 1, 2 or 3.

The mean solids concentrated water (system effluents) from the separator was 2.5 liters per day. And the water loss by spray column aerator due to the effect of aeration was 0.479 liter per hour. Monthly, water losses for carp production is illustrated in Table 4.12.

RESULTS AND DISCUSSION

Table 4.11. Water exchange strategy that applied during the growing season.

Date	Tank 1	Tank 2	Tank 3	Date	Tank 1	Tank 2	Tank 3
21-dec.			X	13- Jan.		X	
22-dec.	X			14- Jan.			X
24-dec.		X		15- Jan.		X	
25-dec.			X	16- Jan.	X		X
28-dec.		X		17- Jan.		X	
29-dec.	X		X	19- Jan.		X	
30-dec.		X		20- Jan.	X		X
31-dec.			X	24- Jan.			X
01-Jan.		X		26- Jan.		X	
02-Jan.	X		X	30- Jan.	X	X	X
03- Jan.		X		14-feb	X	X	X
05- Jan.		X		28-feb	X	X	X
06- Jan.	X		X	14-mar	X	X	X
07- Jan.		X		28-mar	X	X	X
08- Jan.			X	14-abr	X	X	X
09- Jan.	X	X		01-may	X	X	X
10- Jan.			X	15-may	X	X	X
11- Jan.		X		22-may	X	X	X
12- Jan.	X		X	01-Jun	X	X	X

Table 4.12. Monthly water loss in the system.

Date	Water exchange	Water loss by aerator	Water loss by separator effluent	Water loss by evaporation	Total water losses
1 st month	1400	50	30	21	1501
2 nd month	400	109.6	45	30	585
3 rd month	400	155.63	60	30	645.6
4 th month	400	188.22	60	36	684.22
5 th month	400	154.7	60	36	650.7
Total	3000	685.15	255	153	4066.55

RESULTS AND DISCUSSION

The total water used during the growing season to produce 18 kg/tank was 4666.55 liter of water, or about 260 liter of water per kg carp. That can produce 441,000 kg/ha.year compared with other systems reported by [Timmons and Ebeling \(2007\)](#) (Table 4.13).

Table 4.13. Water and land use per kg of production of aquaculture products and a relative comparison to an intensive RAS Tilapia farm (RAS assumed to discharge 5% of system volume per day).

System	Species	Production Intensity (kg/ha/y)	Water required (Liter/kg)	Ratio	
				Land	Water
RAS Produced	<i>O. niloticus</i> (Nile tilapia)	1,340,000 ^a	500	1	1
Ponds	<i>O. niloticus</i> (Nile tilapia)	17,400	21,000	154	420
Ponds	<i>I. punctatus</i> (Channel catfish)	3,000	3,000-5,000	896	800
Raceways	<i>S. gairdneri</i> (Rainbow trout)	150,000	210,000	18	4,200
Pond	Panaeid Shrimp (Taiwan)	4,200-11,000	11,000-21,340	354	320

^a does not account for land used external to building space.

It was observed that our system has lower (about half) use of water consumption, but at higher water exchanges has higher production, as daily water exchanges rate increases to 17%, the carrying capacity arrives to 137 kg/m³ ([Boyd, 1998](#)).

5. CONCLUSIONS

The main objectives of the present study was to design a recirculating aquaculture system under local Mexican conditions by select the aerator (locally designed) that has the highest performance between four different aerators that can use in RAS, study the performance of Tezontle as an alternative media for the bio-strata for its higher cost in biofilters, design a suitable separator and study its ideal operating factors, model to calculate aeration requirements and oxygen budget in RAS, studying water consumption per 1kg carp biomass, study three different oxygen ranges on carp growth rate to choose the lower level that do not affect carp growth rate, consequently lower energy consumption, design and evaluate the performance of automatic feeder and introduce an intelligent dissolved oxygen control system with auto-calibration. The obtained results was summerized as follows:

5.1. Separator evaluation

The effect of water level and tank base diameter in fish tank on separator removal efficiency and tank bottom cleanliness efficiency was studied; the overall average removal efficiency for suspended solids removal through the separator was 78.38 and 73% for 80 and 90 cm of water tank level, respectively.

Tank bottom cleanliness at 80 cm is less efficient than the cleanliness efficiency at 90 cm head due to lower drag forces generated at tank bottom by higher water level.

The optimum operators for separator removal efficiency and tank bottom cleanliness were set to be 90 cm for tank water level and 2.54 cm for tank base diameter.

CONCLUSIONS

5.2. Biofilters performance

Tezontle (volcanic sand) biofilters had lower surface TAN conversion rate than biostrata biofilter that has surface conversion rate about 10 times higher than the tezontle and TAN removal efficiency for biostrata biofilter was the highest 73.7%, but there is no significant difference between biofilters in TAN removal. So the Tezontle can substitute the biostrata as an alternative media for the biofilter for its lower cost.

5.3. Aeration experiments

The oxygen transfer rate of air lift pump aerator was increased from 2.67 to 4.67 gO₂/h with air injected between 69.53 and 758.42 kPa; energy usage increased, yielding a reduction in the actual aeration efficiency index (AAE) from 451.7 to 246.12 gO₂/kW.h, and the maximum actual aeration efficiency index and OTR obtained by diffused aerator was 271.02 gO₂/kW.h and 3.3 gO₂/h. The oxygen transfer rate obtained by venturi aerator was 3.25 gO₂/h. with actual aeration efficiency index of 622.83 gO₂/kW.h. Spray column aerator has the highest OTR and AEE among all the aerators at water flow rate of 30 LPM and air flow rate of 0.157 m³/s gaining 23.04 gO₂/h and 1.075 kgO₂/kW.h with three sprayers. Spray column aerator was used in RAS now has OTR of 13.68 gO₂/h, achieved with 0.5 Hp water pump, if the user want higher OTR the pump of 0.5 hp can be changed with water pump of 0.75 Hp obtaining OTR of 23.04 gO₂/h.

CONCLUSIONS

5.4. Dissolved oxygen transfer analysis.

Water temperatures affects inversely on oxygen transfer rate that can be calculated by the following equation:

$$OTR = -0.0547 \times T + 10.224$$

Oxygen deficit has direct effect on oxygen transfer rate that can be obtained by the following equation:

$$OTR = 1.852 \times OD + 0.06$$

Due to air temperature fluctuations during the day the amount of oxygen transferred by the aerator per hour affect water temperature.

$$\Delta H = 0.0003OTR - 0.0048$$

where ΔH is the enthalpy gained or lost ($^{\circ}\text{C}/\text{min}$).

5.5. Dissolved oxygen mass balance in RAS and dissolved oxygen model.

In RAS the factors affect oxygen level in the system were algae, cultivated fish, nitrifying bacteria and sediments. These factors were studied to introduce one model can calculate aerator size need to the system and predict oxygen level at each fish life stage.

The effect of algae blooms on oxygen level in the system, Algae participate during the day as an oxygen generator producing at 12:00 pm the higher amount oxygen as gO_2 per hour of 7.02, 5.76, 5.58, 5.4 and 3.6 for 420, 280, 150, 95, 56 and 45 NTU, respectively.

The amount of oxygen produced or consumed per hour in the RAS can be calculated by the following equations:

$$AOP = 4.5795\ln(NTU) + 3.0793$$

where AOP is the accumulated oxygen produced during the day,

CONCLUSIONS

$$AOC = 0.0286 (NTU) + 17.306$$

where *AOC* is the accumulated oxygen consumed per day.

The oxygen consumed by carp (*FOC*) can be calculated by the following equation:

$$FOC = AW^2 + BW + C$$

Water temperature, °C	A	B	C	R ²
18	-0.00001	0.0447	0.4306	0.994
20	-0.0001	0.0506	0.5103	0.99
22	-0.0001	0.058	0.523	0.97
24	-0.0001	0.0635	0.6812	0.98

The following equation can be used to calculate the amount of dissolved oxygen consumption in the biofilter.

$$NBOC = (0.1936W - 2.0174) \times (V_m)$$

where *W* is the carp mean weight in grams and *V_m* is the biofilter media volume in m³ and *NBOC* is the biofilter oxygen consumption gO₂/hour.

The accumulated sediments oxygen demand (*SOC*) can be calculated by the following equation:

$$SOC = 1279.62(V_{sed})$$

As every factor was studied, oxygen requirement for RAS system can be calculated by the following equation:

$$DOD = (0.0286 NTU + 17.306) - (4.5795 \ln(NTU) + 3.0793) + \left(\frac{-9}{10^5} W^2 + 0.0609 \times W - \frac{3}{10^5}\right) \times 24 + (0.1936W - 2.0174) \times (V_m) \times 24 + 1279.62 \times (V_{sed}).$$

CONCLUSIONS

5.6. Water consumption

The total water used during the growing season to produce 18 kg/tank was 4666.55 liter of water, or about 260 liter of water per kg carp. That can produce 441,000 kg/ha.

5.7. Effect of three different aeration levels on carp growth rate.

No significant difference was found in daily growth rate between the aeration treatments of 4.5 to 6 and 3.5 to 5 ppm achieving carp mean weight after 140 days, 198 and 210 grams, respectively. The aeration level of 2.0 - 4.0 ppm registers lower daily growth rate with carp mean weight 130 gram after 140 days; the aeration range of 3.5 - 5 ppm supports higher growth rate with lower energy consumption.

5.8. Automatic feeder

See Appendix 3

5.9. intelligent dissolved oxygen control system with auto-calibration

See Appendix 3

6. REFERENCES

- Ahmad, T. and C.E. Boyd. 1988.** Design and performance of paddle wheel aerators. *Aquacultural Engineering*, 7: 39-62.
- Alanärä, A. 1992.** The effect of time-restricted demand feeding on feeding activity, growth and feed conversion in rainbow trout (*Oncorhynchus mykiss*). *Aquaculture*, 108: 357– 368.
- Alanärä, A. 1996.** The use of self-feeder in rainbow trout (*Oncorhynchus mykiss*) production. *Aquaculture*, 145: 1– 20.
- Alexander, P., B. Victor and A. Samuel. 1993.** A universal inexpensive self-demand feeder for elvers. *Aquacultural Engineering*, 12(2): 125-127.
- Al-Harbi, A.H. and A.Q. Siddiqui. 2000.** Effects of tilapia stocking densities on fish growth and water quality in tanks. *Asian Fisheries Science* 13: 391-396.
- Ali, S.A. 1999.** Study of some engineering and environmental parameters on fish production in tanks. Ph.D. dissertations, Agric. Eng. Dept., Fac. of Agric., Zagazig University-Benha branch, Moshtohor.
- Alver, M. O.; T. Tennøy; J. A. Alfredsen and G. Øie. 2007.** Automatic measurement of rotifer *Brachionus plicatilis* densities in first feeding tanks. *Aquacultural Engineering*, 36: 115-121.
- American Society of Civil Engineers. 1992.** Measurement of oxygen transfer in clean water. ANSI: ASCE 2–91, American Society of Civil Engineers, New York.
- Andrade C. E. R.; A. L. B. Vera; C. H. L. Cárdenas and E. D. A. Morales. 2009.** Biomass production of microalga *Scenedesmus sp.* with wastewater from fishery. *Rev. Téc. Ing. Univ. Zulia*. Vol. 32, No. 2,

REFERENCES

- Andrews, J.W. and Y. Matsuda. 1975.** The influence of various culture conditions on the oxygen consumption of channel catfish. *Transactions of the American Fisheries Society*, 104: 322-327.
- APHA, American Public Health Association, Water Pollution Central Federation and American Water Works Association, 1998.** Standard methods for the examination of water and wastewater. 16 th ed. Boyd. Printing Company, Albana, New york. USA.
- Appelbaum, S. and V. Birkan. 1999.** A live food feeder. *Aquacultural Engineering*, 20: 37–41.
- Appelbaum, S.; A. Parilutsky and V. Birkan. 1999.** An emergency aeration system for use in aquaculture. *Aquacult. Eng.*, 20: 17-20.
- Avnimelech, Y. 1999.** Carbon/nitrogen ratio as a control element in aquaculture systems. *Aquaculture*, 167: 277-235.
- Baldwin, W. J., 1983.** The design and operation of an automatic feed dispenser. *Aquaculture*, 34: 151 -155.
- Barcelona, M.J. 1983.** Sediment oxygen demand fractionation, kinetics and reduced chemical substances. *Water Research*, 17: 1081 – 1093.
- Bayne, B.L. and R.C. Newell. 1983.** Physiological energetics of marine mollusks. In: Wilburg, K.M., Saleuddin, A.S.M. (Eds.), *The Mollusca*, vol. 4. Academic Press, London, pp. 407– 415.
- Bertholson, C. 1992.** In situ respirometry for determining sediment oxygen demand in channel catfish ponds of the Mississippi Delta region. M.Sc. thesis Mississippi State University.
- Bodansky, O. 1951.** Methemoglobinemia and methemoglobin-producing compounds. *Pharmacological Review* 3:144-196.
- Boller, M. and J. Gudjer. 1986.** Nitrification in tertiary trickling filters followed by deep bed filters. *Water Res.* 20, 1363–1373.
- Boller, M.; W. Gujer and M. Tschui. 1994.** Parameters affecting nitrifying biofilm reactors. *Water Science Technology* 29, 1-11.

REFERENCES

- Bovendeur, J.; G.H. Zding and A.M. Henken. 1987.** Design and performance of a water recirculation system for high-density culture of the African Catfish, *Clazias gariepinus* (Burchell, 1822). *Aquaculture* 63, 329–353.
- Boyd, C.E. 1973.** Summer algal communities and primary productivity in fish ponds. *Hydrobiologia*, 41: 357 – 390.
- Boyd, C.E. 1979.** Water quality in warm water fish ponds. Auburn, Al: Auburn University / Alabama Agricultural Experiment Station.
- Boyd, C.E. 1990.** Water quality in ponds for aquaculture. Auburn, Al: Auburn University/Alabama Agricultural Experiment station.
- Boyd, C.E. 1995.** Deep water installation of a diffused-air aeration system in a shallow pond. *Journal of Applied Aquaculture*, 5: 1–10.
- Boyd, C.E. 1998.** Pond water aeration systems. *Aquacultural Engineering*, 18: 9-40.
- Boyd, C.E. and B.J. Watten. 1989.** Aeration systems in aquaculture. *Reviews in Aquatic Science*, 1: 425 – 472.
- Boyd, C.E. and C.S. Tucker. 1998.** Pond aquaculture water quality management. Kluwer Academic Publishers.
- Boyd, C.E. and D.J. Martinson. 1984.** Evaluation of propeller aspirator pump aerators. *Aquaculture*, 36: 283 – 292.
- Boyd, C.E. and T. Ahmad. 1987.** Evaluation of aerators for channel catfish farming. Bulletin No.584. Auburn University / Alabama Agricultural Experiment Station.
- Boyd, C.E.; R.P. Romire and E. Johnston. 1978.** Predicting early morning dissolved oxygen concentrations in channel catfish ponds. *Transactions of the American Fisheries Society*, 107: 484 – 492.
- Boyd, C.E.; R.P. Romire and E. Johnston. 1978.** Predicting early morning dissolved oxygen concentrations in channel catfish ponds. *Transactions of the American Fisheries Society*, 107: 484 – 492.

REFERENCES

- Brazil, B. L. 2006.** Performance and operation of a rotating biological contactor in a tilapia recirculating aquaculture system. *Aquacultural Engineering*, 34: 261–274
- Brett, J.R. and T.D.D Groves. 1979.** Physiological energetics. In: Hoar, W.S.; Randall D.J.; Brett, J.R. (ed.) *Fish Physiology*, Vol. 8, Academic Press, New York, pp., 279-352.
- Brune, D.E.; G. Schwartz; A. G. Eversole; J.A. Collier and T.E. Schewedler. 2003.** Intensification of pond aquaculture and high rate photosynthetic systems. *Aquacultural Engineering*, 28: 65 – 86.
- Brunty, J.L.; R.A. Bucklin; J. Davis; C.D. Baird and R.A. Noedstedt. 1997.** The influence of feed protein intake on tilapia ammonia production. *Aquac. Eng.* 16: 161– 166.
- Bryan, A. and M. Cushman. 1991.** System for monitoring and reporting the operability and calibration status of a dissolved oxygen sensor. *Environment International*, vol. 17
- Burford, M.A.; P.J. Thompson; R.P. McIntosh; R.H. Bauman and D.C. Person. 2003.** Nutrient and microbial dynamics in high intensity, zero exchange shrimp ponds in Belize. *Aquaculture* 219:393-411.
- Cameron, J.N. 1971.** Methemoglobin in erythrocytes of rainbow trout. *Comparative Biochemistry and Physiology A, Comparative Physiology* 40:743-749.
- Carlson, A.R.; J. Blocher; and L.J. Herman. 1980.** Growth and survival of channel catfish and yellow perch exposed to lowered constant and diurnally fluctuating dissolved oxygen concentrations. *Prog. Fish-Cult.*, 42, 73-78.
- Castilho, L.R. and R.A. Medronho. 2000.** A simple procedure for design and performance prediction of bradley and rietema hydrocyclones. *Miner. Eng.* 13 (2): 183–191.

- Chang, C.M.; W. Fang; R.C. Jao; C.Z. Shyu and I.C. Liao. 2005.** Development of an intelligent feeding controller for indoor intensive culturing of eel. *Aquacult. Eng.* 32: 343-353.
- Charlton, N and P. Bergot. 1986.** An improved automatic dry food dispenser for fish larvae. *Prog. Fish Cult.*, 48: 156 -158.
- Chuang, H., Arnold, M.A., 1998.** Linear calibration function for optical sensors based on quenching of ruthenium fluorescence. *Analytica Chimica Acta* 368: 83-89.
- Chen, J.L.; C. Liu; Y. Lin and C. Lee. 1988.** Super intensive culture of red-tailed shrimp *Penaeus penicillatus*. *Journal of the World Aquaculture Society*, 16: 316-332.
- Chen, S.; M.B. Timmons; D.J. Aneshansley and J.J. Bisogni. 1993.** Suspended solids characteristics from recirculating aquacultural systems and design implications. *Aquaculture* 112: 143–155.
- Chen, W., Zydek, N., Parma, F., 2000.** Evaluation of Hydrocyclone Models for Practical Applications. *Chem. Eng.J.* 80: 295–303.
- Chesness, J.L. and J.L. Stephnes. 1971.** A model study of gravity flow aerators for catfish raceway systems. *Transactions of the American Society of Agricultural Engineers*, 14: 1167-1169.
- Chitta, B.S., 1993.** Effects of Backwash Frequency on Nitrification in Plastic Bead Media Biofilters Used in Recirculating Finfish Culture Systems. MS thesis, Louisiana State University, Baton Rouge, LA.
- Colt, J. 1984.** Computation of dissolved gas concentrations in water as a functions of temperature, salinity, and pressure. Special Publication No. 14. American Fisheries Society, Bethesda, Maryland.
- Colt, J. and C. Orwicz. 1991.** Aeration in intensive culture. In Brune, D.E. and J.R. Tomasso (eds.), *Aquaculture and Water Quality*. Baton Rouge, LA: The World Aquaculture Society.

- Colt, J.; J. Lamoureux; R. Patterson and G.Rogers. 2006.** Reporting standards for biofilter performance studies. *Aquacultural Engineering* 34:377-388.
- Costa-Pierce, B.A.; D.B. Craven, M.D. Karl and E.A. Laws. 1987.** Correlation of in situ respiration rates and microbial biomass in prawn (*Macrobrachium rosenbergii*) ponds. *Aquaculture*, 37: 157-168.
- DeLosReyes Jr., A.A. and T.B. Lawson. 1996.** Combination of a bead filter and rotating biological contactor in a recirculating fish culture system. *Aquacult. Eng.*, 15:27–39.
- Diana, J. S.; C. K. Lin and K. Jaiyen. 1994.** Pond dynamics under semi-intensive and intensive culture practices. In: H. S. Egna, J. Bowman, B. Goetze, and N. Weidner (eds.). Eleventh Annual Administrative Report Pond Dynamics/Aquaculture Collaborative Research Support Program 1993. Oregon State University, Corvallis, OR. PP. 94-99.
- Diana, J. S.; C. K. Lin and Y. Yi. 1995.** Timing of supplemental feeding for tilapia production. In: H. S. Egna, J. Bowman, B. Goetze, and N. Weidner, (eds.). Twelfth Annual Administrative Report Pond Dynamics/Aquaculture Collaborative Research Support Program 1994. Oregon State University, Corvallis, OR. PP. 147-152.
- Doudoroff, P. and D.L Shumway. 1970.** Dissolved oxygen requirements of freshwater fishes. Food and Agricultural Organization of the United Nations Technical Paper., 86-291 pp.
- Drapcho, C.M. and D.E. Brune. 2000.** The partitioned aquaculture system: impact of design and environmental parameters on algal productivity and photosynthetic oxygen production. *Aquacultural Engineering*, 21: 151-168.
- Dunn, Z. 2008.** Improved feed utilization in cage aquaculture by use of machine vision. M. Sc. Thesis. Stellenbosch University.

REFERENCES

- Ebling , J. M.; M. B. Timmons and J.J. Bisogni. 2006.** Engineering analysis of the stoichiometry of photoautotrophic, autotrophic, and heterotrophic control of ammonia-nitrogen in aquaculture production systems. *Aquaculture* 257:346-358.
- Eding, E. H.; A. Kamstra; J.A.J. Verreth; E. A. Huisman and A. Klapwijk. 2006.** Design and operation of nitrifying trickling filters in recirculating aquaculture: A review. *Aquacultural Engineering* 34:234-260.
- EEC. 1978.** Directive (78/659/EEC) on the quality of freshwater needing protection or improvement in order to support fish life. Oj L222. 14.8.78.
- Egna, H.S.; C.E. Boyd and D.A. Burke. 1997.** Introduction. Pond Dynamics / Aquaculture CRSP press LLC.
- Elliot, J.W. 1969.** The oxygen requirements of Chinook salmon. *Progressive Fish Culturist*, 31: 67-73.
- Eutech Instruments, 1997.** <http://www.eutechinst.com/techtips/techtips16.htm>
- Fang, W. and C.M Chang. 1999.** Development of an automatic feeder with the capability of knowing when to stop feeding. In: Proceedings of the Annual International Conference and Exposition of the World Aquaculture society, Australia, 26 April–2 May, 251.
- Fang, W. and C.M. Chang; C.Z. Shyu; I.C. Liao. 2002.** Development of an intelligent feeding system for indoor intensive culturing of eel. World Aquaculture Beijing, China, 23–April 27.
- FAO. 2006.** Fishery and aquaculture statistics. Food and Agriculture Organization, Rome.
- Farmer, G.L. and F.W.H. Beamish. 1969.** Oxygen consumption of tilapia nilotica in relation to swimming speed and salinity. *Journal of the Fisheries Research Board of Canada*, 26: 2807-2821.

REFERENCES

- Fast, A.W.; T. Qin and J.P. Szyper.** 1997. A new method for assessing fish feeding rhythms using demand feeders and automated data acquisition. *Aquacult. Eng.* 16, 213–220.
- Fast, W.A.; C.T. Edmundo; F.S. Desmond; J.C. Olson; J. Qin and D.K. Barclay.** 1999. Paddlewheel aerator oxygen transfer efficiencies at three salinities. *Aquacultural Engineering*, 19: 99-103.
- Foster, M. D.** 1993. An automated vision system for detection and counting of uneaten food pellets in a fish sea cage. M. Sc. Thesis. The University of British Columbia. Canada.
- Foster, M.; R. Petrell; M.R. Ito and R. Ward.** 1995. Detection and counting of uneaten food pellets in a sea cage using image analysis. *Aquacult. Eng.* 14, 251–269.
- Fowler P.; D. Baird; R. Bucklin; S. Yerlan; C. Watson and F. Chapman.** 1994. Microcontrollers in recirculating aquaculture systems. EES-326, Florida Cooperative Extension service, University of Florida.
- Gilbert, R.G.; F.S. Nakayama; D.A. Bucks; O.F. French and K.C. Adamson,** 1981. Trickle irrigation: Emitter clogging and other flow problems. *Agricultural Water Management.* 3(3), 159-178.
- Golz, W. J.** 1995. Biological Treatment in Recirculating Aquaculture Systems. In Recirculating aquaculture in the classroom: a training workshop for agricultural science teachers, a proceedings of a workshop sponsored by the Louisiana Sea Grant College Program, Louisiana State University, and the Louisiana Department of Education, 6-7 December 1995, Louisiana State University, Baton Rouge, Louisiana.
- Greeley, M.** 1994. Nitrite Toxicosis in freshwater fish (Brown blood disease)<http://www.addl.purdue.edu/newsletters/1998/spring/nitrate.shtml>

- Greiner, A.D. and M.B. Timmons.** 1998. Evaluation of the nitrification rates of microbead and trickling filters in an intensive recirculating tilapia production facility. *Aquacult. Eng.* 18, 189–200.
- Grottum, J.A. and T. Sigholt.** 1998. A model for oxygen consumption of Atlantic salmon (*Salmo salar*) based on measurements of individual fish in a tunnel respirometer. *Aquacultural Engineering*, 17: 241-251.
- Hagopian, D.S. and J.G. Riley.** 1998. A closer look at the bacteriology of nitrification. *Aquacultural Engineering* 18, 223 – 244.
- Hall, A.G.** 1999. A comparative analysis of three biofilter types treating wastewater produced in recirculating aquaculture systems. M.Sc. dissertations, Blacksburg, Virginia, USA.
- Hanson, HM.** 1992. A flexible temperature and environmental controller. *Progressive Fish culturist*, 54: 130-131.
- Haug, R. T. and P. L. McCarty.** 1972. Nitrification with submerged filters. *J. Water Pollut. Control Fed.* 44:2086.
- Heinsbroek, L.T.N. and A. Kamstra.** 1990. Design and performance of water recirculation systems for eel culture. *Aquacult. Eng.* 9, 87– 207.
- Henderson, J.P. and N.R. Bromage.** 1988. Optimizing the removal of suspended solids from aquaculture effluents in settlement lakes. *Aquacultural Engineering*, 7:167-188.
- Hobbs, A.; T. Losordo; D. DeLong; J. Regan; S. Bennett; R. Gron and B. Foster.** 1997. A commercial, public demonstration of recirculating aquaculture technology: The CP&L/EPRI Fish Barn at North Carolina State University. In: M.B.Timmons and T.M. Losordo (editors). *Advances in aquacultural engineering. Proceedings from the aquacultural engineering society technical sessions at the fourth international symposium on tilapia in aquaculture.* NRAES-

REFERENCES

105. Northeast Regional Agricultural Engineering Service, 152 Riley-Robb Hall, Ithaca, NY. pp. 151-158.
- Hochheimer, J.N. and F.W. Wheaton.** 1998. Biological filters: trickling and RBC design. In: Libey, G.S., Timmons, M.B. (Eds.), Proceedings of the Second International Conference on Recirculating Aquaculture, Roanoke, VA, 16–19 July, pp. 291–318.
- Jackson, C.B. and E.C. Craig.** 2004. Measurement of dissolved oxygen with a luminescence-based oxygen quenching sensor, HACH.
http://acwi.gov/monitoring/conference/2004/conference_agenda_links/power_points_etc/06_ConcurrentSessionD/93_Rm15_Jackson.pdf
- Jhingran, V.G. and V. Gopalakrishnam.** 1974. Catalog of cultivated aquatic organisms. FAO Fisheries Technical Paper Number 130, Food and Agriculture Organization of the United Nations, Rome, Italy.
- Jobling, M.** 1981. The feeding on the metabolic rate of fishes: a short review. *J. Fish Biol.*, 18: 385-400.
- Johnson, W. and S. Chen.** 2006. Performance evaluation of radial/vertical flow clarification applied to recirculating aquaculture systems. *Aquacultural Engineering*, 34: 47-55.
- Juell, J. E.; D. M. Furevik and A. Bjordal.** 1993. Demand feeding in salmon farming by Hydroacoustic food detection. *Aquacultural Engineering*, 12: 155-167.
- Juell, J.E. and H. Westerberg.** 1993. An ultrasonic telemetric system for automatic positioning of individual fish used to track Atlantic salmon (*Salmo salar* L.) in a sea cage. *Aquacult. Eng.* 12: 1–18.
- Kamstra, A.; J.W. van derHeul and M. Nijhof.** 1998. Performance and optimization of trickling filters on eel farms. *Aquacult. Eng.* 17: 175–192.

REFERENCES

- Keise, M. 1974.** Methemoglobinemia. A comprehensive treatise. CRC Press, Cleveland.
- Kevin, D.P. and J.P. Royann. 2003.** Accuracy of a machine-vision pellet detection system. *Aquacult. Eng.* 29: 109–123.
- Kimura R.; S. Kawaguch and S. Sugitani. 1993.** Automatic feeding control system for fish; Fish farming technology, pp. 217-225, Balema, Rotterdam.
- Kir, M. 2009.** Nitrification Performance of a Submerged Biofilter in a Laboratory Scale Size of the Recirculating Shrimp System. *Turkish Journal of fisheries and aquatic sciences* 9: 209-214.
- Koni`e`ek, Z.; K. Pryl and M. Sucha`nek. 1996.** Practical applications of vortex flow separators in the Czech Republic. *Water Sci. Technol.* 33 (9): 253–260.
- Kramer, DL. 1987.** Dissolved oxygen and fish behavior. *Environmental Biology of Fishes.* 18(2): 81-92.
- Lawson, T.B. 1995.** Fundamentals of aquacultural engineering. Chapman and Hall, An International Thomson Publishing Company.
- Lehman, J.T.; D.B. Botkin and G.E. Likens. 1975.** The assumptions and rationale of a computer model of phytoplankton population dynamics. *Limnol. Oceanogr.*, 20 (3): 343–364.
- Lewis, W.K. and W.C. Whitman. 1924.** Principles of gas adsorption. *Journal Industrial Engineering*, 16: 1215-1220.
- Liao, P. B., and R. D. Mayo. 1972.** Salmonid Hatchery Water Reuse Systems. *Aquaculture* 1: 317-335.
- Liao, P.B. 1971.** Water requirements of salmonids. *Progressive Fish Culturist*, 33: 67-73.
- Liao, P.B. and R.D. Mayo. 1974.** Intensified fish culture combining water reconditioning with pollution abatement. *Aquaculture* 3, 61–85.

López Muñoz B. E., J.M. Duran Blanco, J.L. Iturbe Garcia, and M.T.Olguin Gutierrez. 2009. Uranium Sorption on Tezontle (Volcanic Rock). *J. Mex. Chem. Soc.*, 53, 4,p. 239-242.

Losordo, T.M. 1997. Tilapia culture in intensive recirculating systems. In: Costa-Pierce, B. and Rakocy, J. (editors), *Tilapia Aquaculture in the Americas, Volume 1.* World Aquaculture Society, Baton Rouge, LA. pp. 185-208

Losordo, T. M.; A.O. Hobbs and D.P. DeLong. 2000. The design and operational characteristics of the CP&L/EPRI fish barn: a demonstration of recirculation aquaculture technology. *Aquacult. Eng.* 22, 3–16.

Losordo T. M.; M. P. Masser and J. E. Rakocy. 1998. Recirculating aquaculture tank production systems: An overview of critical consideration. Southern Regional Aquaculture, SRAC Publication No.451.

Losordo, T.M.; M.P. Masser and J.E. Rakocy. 1999. Recirculating aquaculture tank production systems: A review of Component options. Southern Regional Aquaculture Centre, SRAC Publication No. 453.

Losordo, T.M.; J.E. Rakocy and M.P. Masser. 1992. Recirculating aquaculture tank production systems. Publication No. 453, North Carolina Cooperative Extension Service, North Carolina State University, Raleigh.

Loyacana, H.A. 1974. Effects of aeration in earthen ponds on water quality and production and production of white catfish. *Aquaculture*, 3: 261-271.

Loyless, J.C. and R.F. Malone. 1998. Evaluation of air lift-pump capabilities for water delivery, aeration, and degasification for

REFERENCES

- application to recirculating aquaculture systems. *Aquacultural Engineering*, 18: 117-133.
- Lu, Z. and R.H. Piedrohita. 1997.** Aquaculture pond modeling for the analysis of environmental and integration with agriculture: Modeling of temperature, dissolved oxygen, and fish growth rate in stratified ponds using stochastic input variables. In: D. Burke, J. Baker, B. Goetze, D. Clair, and H. Egna (eds.). Fifteenth Annual Technical Report. Pond dynamics/Aquaculture CRSP, Office of International Research and Development, Oregon State University, Corvallis, Oregon, USA, pp.68-74.
- Madenjian, C. P.; G. L. Rogers and A. W. Fast. 1987.** Predicting night time dissolved oxygen loss in prawn ponds of Hawaii: Part II. A new method. *Aquacultural Engineering* 6: 209-225.
- Mallekh, R.; J.P. Lagarde`re; J.P. Eneau and C. Cloutour. 2003.** An acoustic detector of turbot feeding activity. *Aquaculture* 221, 481–489.
- Malone R.F and T.J. Pfeiffer. 2006.** Rating fixed film nitrifying biofilters used in recirculating aquaculture systems. *Aquaculture Engineering*, 34: 389-402.
- Malone, R.F. and L.E. Beecher. 2000.** Use of floating bead filters to recondition recirculating waters in warmwater aquaculture production systems. *Aquacult. Eng.* 22: 57–74.
- Malone, R.F.; L.E. Beecher and A. De Los Reyes Jr. 1999.** Sizing and management of floating bead bioclarifiers. In: *Aquaculture Engineering and Waste Management, Proceedings from the Aquaculture Exposition VIII and Aquaculture Mid-Atlantic Conference*, June 24–28 Washington, DC: 256–267.
- Malone, R.F.; B.S. Chitta and D.G. Drennan II. 1993.** Optimizing nitrification bead filters for warm water recirculating aquaculture. In:

REFERENCES

- Wang, J.K. (Ed.), Techniques for Modern Aquaculture. American Society of Agricultural Engineers, St. Joseph, MI, pp. 315–325.
- Manci W. E.; K. G. Richardson and J. F. Bauer. 1992.** Design and Performance of an Electronic Lighting-Control Circuit That Simulates Sunrise and Sunset. *Progressive Fish culturist*, 54: 127-129.
- Manthe, D.P.; R.F. Malone and S. Kumar, 1988.** Submerged rock filter evaluation using an oxygen consumption criterion for closed recirculating system. *Aquacult. Eng.* 7: 97–111.
- McIntosh, R.P. 2001.** High rate bacterial systems for culturing shrimp. In S. T. Summerfelt et al (eds). Proceedings from the Aquacultural Engineering Society's 2001 Issues Forum. Shepherdstown, West Virginia, USA. Aquaculture Engineering Society, Pp. 117-129.
- McMillan, J.D.; F.W. Wheaton; J.N. Hochheimer and J. Soares. 2003.** Pumping effect on particle sizes in a recirculating aquaculture system. *Aquacult. Eng.* 27: 53–59.
- Meriwether, F. H. 1986.** An inexpensive demand feeder for cage reared Tilapia. *Prog. Fish Cult.*, 48: 226-228.
- Metcalf and Eddy Inc. 1991.** Wastewater Engineering: Treatment, Disposal, Reuse. 3rd Ed., New York, McGraw Hill, 929 p.
- Mitchell, T. O. 2006.** Luminescence based measurement of dissolved oxygen in natural waters. www.hachenvironmental.com.
- Mohapatra, B. C.; B. Sarkar and S. K. Singh. 2003.** Use of plastics in aquaculture. In: Satapathy, K. K. and Ashwani Kumar (Ed.) *Plasticulture intervention for agriculture development in North Eastern Region*. ICAR Research Complex for NEH Region, Umiam, Meghalaya: pp 290-305.
- Mohapatra, B. C.; S. K. Singh, B. Sarkar and D. Majhi, 2004.** Portable carp hatchery for carp seed production. In: Technologies on

REFERENCES

- Livestock and Fisheries for Poverty Alleviation in SAARC Countries. SAARC Agricultural Information Centre, Dhaka: pp 132-135.
- Montgomery, J. M., Inc. 1985.** Water Treatment Principles and Design. New York: Wiley-Interscience.
- Moore, J.M. and G.N. Whitis. 1999.** Vertical water circulation capabilities of an electric paddlewheel aerator and dissolved oxygen loss due to day time aeration. *Journal of Applied Aquaculture*, 9(3): 25-36.
- Morchain, J.; C. Maranges and C. Fonade. 2000.** CFD modeling a two – phase jet aerator under influence of a cross flow. *Water Research*, 34(13): 3460-3472.
- Mudrak, V. A. 1981.** Guidelines for economical commercial fish hatchery wastewater treatment systems. In: L.J. Allen, Kinney, E.C. (Eds.). Proceedings of the Bio-engineering Symposium for Fish Culture. American Fisheries Society, Fish culture Section, Bethesda, MD, pp. 174-182.
- Muller-Fuga, A., A. Petit and J.J. Sabbaut. 1978.** The influence of temperature and wet weight on the oxygen demand of rainbow trout (*Salmo gairdneri* R.) in freshwater. *Aquaculture*, 14: 355-363.
- Navia R., B. Fuentes, M.C. Diez and KE. Lorber. 2005.** The use of volcanic soil as mineral landfill liner III. Heavy metal retention capacity. *Waste Manage Res.*, 23, p. 260-269.
- Newell, R.C., Branch, G.M., 1980.** The influence of temperature on the maintenance of metabolic energy balance in marine invertebrates. *Adv. Mar. Biol.* 17: 329– 396.
- Ortiz Polo A., R. M. Richards, E. M. Otazo, O. A. Acevedo, F. Prieto, J. Hernandez, A. Gordillo. 2007.** New organo-inorganic materials for water contaminants remediation. Materials Research Society Spring Meeting Proceedings.

- Ortiz Polo A., E. M. Otazo Sanchez, F. Prieto Garcia, A. J. Gordillo Martinez and O. A. Acevedo Sandoval. 2009.** Perspectivas Ambientales del uso del tezontle en la descontaminación de iones metálicos en agua. En: Estudios Ambientales 2004-2009. Editores. Otazo Sanchez E. M., C. Coronel Olivares, F. Prieto Garcia, C. A. Gonzalez Ramirez, A. J. Gordillo Martinez. Pachuca de Solo, Ed Universidad Autónoma del Estado de Hidalgo. 17-20 p.
- Paller, M.H. 1992.** An analytical model for predicting the carrying capacity of submerged biofilters used in aquaculture. *J. Appl. Aquacult.*, 1: 1–25.
- Papandroulakis, N., P. Dimitris and D. Pascal. 2002.** An automated feeding system for intensive hatcheries. *Aquacult. Eng.*, 26: 13-26.
- Parker, N. C. 1989.** Low cost automated feeder for fry & fingerlings. *Prog. Fish Cult.*, 51: 42- 46.
- Parker, N.C. 1979.** Channel catfish production in continuously aerated ponds. Research Workshop Summary of Papers, Catfish Farmers of America Annual Meeting, Jackson, Miss., 44 pp.
- Parker, N.C. 1983.** Air-lift pumps and other aeration techniques in water quality in channel catfish ponds. In: Tucker, C.S. Jr. (ed.), Southern Cooperative Bulletin, vol. 290. Agriculture and Forestry Experiment Station, Mississippi State University.
- Paspatis, M. and T. Boujard. 1996.** A comparative study of automatic feeding and self-feeding in juvenile Atlantic salmon fed diets of different energy levels. *Aquaculture*, 145:245
- Persson, W.Uhl,F., G.Heinicke, M. Hermansson and T. Hedberg. 2006.** Removal of geosmin and MIB in biofilters – On the role of biodegradation and adsorption. In: Rolf, G., G. Niegel, and C. Robin (Eds.) Recent progress in slow sand and alternative biofiltration processes. IWA, UK.

REFERENCES

- Peterson, M.S., Ardahl, B.E., 1992.** Automated maintenance of dissolved oxygen concentrations in flow-through aquaria. *Aquaculture*, 101: 379-384.
- Pfeiffer T. J.; A. Osborn and M. Davis. 2008.** Particle sieve analysis for determining solids removal efficiency of water treatment components in a recirculating aquaculture system. *Aquacultural Engineering*, 39: 24–29.
- Pillay, T.V.R. 1990.** Aquaculture: Principles and Practice, Fishing News Books, Inc., Surry, England.
- Plemmons, B. and J.W. Jr. Avault. 1980.** Six tons of catfish per acre with constant aeration. *Louisiana Agricult.* 23: 6–8.
- Rakocy, J.E. 1989.** Tank culture of tilapia. In: R.V.S. Pullin and R.H. Lowe-Mc-Conell (eds.). The biology and culture of tilapias. ICLARM Conference Proceedings 7. International Center for Living Aquatic Resources Management, Manila, The Philippines.
- Rockey, J.E. and A.S. McGinty. 1989.** Pond culture of tilapia. Southern Regional Aquaculture Center, SRAC. Publication No. 280.
- Rubio, V. C.; M. Vivas; A. Sánchez-Mut; F. J. Sánchez-Vázquez; D. Covès; G. Dutto and J. A. Madrid, 2004.** Self-feeding of European sea bass (*Dicentrarchus labrax*, L.) under laboratory and farming conditions using a string sensor. *Aquaculture*, 233(1-4): 393-403.
- Ruttanagosrigit, W.; Y. Musig; C.E. Boyd and L. Sukhareon. 1991.** Effect of salinity on oxygen transfer by propeller-aspirator-pump and paddlewheel aerators used in shrimp farming. *Aquacultural Engineering*, 10: 121-131.
- Ruyet, J. P.; K. Mahe; N. Le Bayon; H. Le Delliou. 2004.** Effects of temperature on growth and metabolism in a Mediterranean population of European sea bass, *Dicentrarchus labrax*. *Aquaculture*. 237: 269–280.

REFERENCES

- Sandifer, P.A.; J.S. Hopkins and A.D. Stokes. 1987.** Intensive culture potential of *Penaeus vannamei*. *Journal of the World Aquaculture Society*, 18: 94–100.
- Sandu, S.I.; G.D. Boardman; B.J. Watten and B.L. Brazil. 2002.** Factors influencing the nitrification efficiency of fluidized bed filter with a plastic medium. *Aquacult. Eng.*, 26: 41–60.
- Saravanan, M.R. and K.L. Santhanam. 2008.** International encyclopedia of fishery science and technology: fish nutrition and biochemistry, volume two. International Scientific Publishing Academy, India.
- Sastry, B.J. 1995.** A comparison of nitrification capacity in bead and tubular plastic media. MS thesis, Louisiana State University, Baton Rouge, LA.
- Saucedo, P. E.; L. Ocampo; M. Monteforte and H. Bervera. 2004.** Effect of temperature on oxygen consumption and ammonia excretion in the Calafia mother-of-pearl oyster, *Pinctada mazatlanica* (Hanley, 1856) *Aquaculture*, 229: 377–387
- Sawyer, C.N. and P.L. McCarty. 1967.** Chemistry for sanitary engineers. New York: McGraw-Hill.
- Schroeder, G.L. 1975.** Nighttime material balance for oxygen in fish ponds receiving organic wastes. *Bamigeh*, 27: 65 – 74.
- Shepherd, J. and N. Bromage. 1989.** Intensive Fish Farming. Blackwell, Oxford, pp. 78-83.
- Shnel, N.; Y. Barak; T. Ezer; Z. Dafni and J. van Rijn. 2002.** Design and performance of a zero-discharge tilapia recirculating system. *Aquacultural Engineering* 26 (3): 191–203.
- Shumway, S.E. 1982.** Oxygen consumption in oysters: an overview. *Mar. Biol. Lett.* 3; 1 – 23.

- Siddiqui, A.Q. and A.H. Al-Harbi. 1999.** Nutrient budget in tilapia tanks with four different stocking densities. *Aquaculture*, 170: 245-252.
- Soderberg, R.W. 1982.** Aeration of water supplies for fish culture in flowing water. *Progressive fish culturist*, 44(2): 89 – 93.
- Stachey, D.M. and Y. Trudell. 1990.** Aquaculture wastewater treatment: Wastewater characterization and development of appropriate treatment technologies for the new Brunswick smolt production industry. Prepared for New Brunswick Department of the Environment and Local Government, PO Box 6000, Fredericton, New Brunswick, Canada, E3B5H1. 101 p.
- Steeby, J. A., J. A. Hargreaves, C. S. Tucker, T. P. Cathcart. 2004.** Modeling industry-wide sediment oxygen demand and estimation of the contribution of sediment to total respiration in commercial channel catfish ponds. *Aquacultural Engineering*, 31: 247–262.
- Steele, J.H., 1962.** Environmental control of photosynthesis in the sea. *Limnol. Oceanogr.*, 7: 137– 150.
- Stickney, R.R. 1994.** Principles of aquaculture. John Wiley and Sons, Inc.
- Stone, N.; Daniels, M. 2006.** Algal Blooms, Scums and Mats in Ponds. Report No. FSA9094. *University of Arkansas*.
- Stumm, W. and J.J. Morgan. 1996.** Aquatic chemistry: Chemical Equilibria and rates in Natural waters. John Wiley & sons, Inc.. New York, 1022 P.
- Sullivan, R.H.; M.M.Cohn; J.E. Ure; F. Parkinson; G. Galiana; R.R. Boericke; C. Koch and P. Zielinski. 1978.** The swirl primary separator: development and pilot demonstration. EPA-600/2-78-122. U.S. E.P.A., Cincinnati, OH, USA.

- Sullivan, R.H.; J.E. Ure; F. Parkinson and P. Zielinski. 1982.** Design manual: swirl and helical bend pollution control devices. EPA-600/8-82-013. U.S. E.P.A., Athens, GA, USA.
- Summerfelt, S.T. 1999.** Waste-handling systems. In: CIGR (Series Ed.) and F. Wheaton (Volume Ed.), CIGR handbook of agricultural engineering: Volume II, Aquacultural Engineering St. Joseph, MI, *American Society of Agricultural Engineers*, PP. 309-350.
- Summerfelt, S.T.; J. Bebak-Williams and S. Tsukuda. 2001.** Controlled systems: water reuse and recirculation. In: Wedemeyer, G. (Ed.), Second Edition of Fish Hatchery Management. American Fisheries Society, Bethesda, MD, pp. 285–395.
- Summerfelt, S.T. and E.M. Wade. 1997.** Recent advances in water treatment processes to intensify fish production in large recirculating systems. In Advances in aquacultural Engineering Proceedings from Aquacultural Engineering Society Technical Sessions at the 4th International Symposium on Tilapia in Aquaculture, November 9 – 12 Orlando, FL, NRAES – 105, PP. 350-367.
- Svarovsky, L. 1984.** Hydrocyclones. Holt. Rinehart and Winston Ltd., London, UK.
- Tafangenyasha, C.; B. E. Marshall and L. T. Dube. 2010.** The diurnal variation of the physico-chemical parameters of a lowland river flow in a semi-arid landscape with human interferences in Zimbabwe. *International Journal of Water Resources and Environmental Engineering.*, Vol. 2(6), pp. 148-163.
- Tebbutt, T.H.Y. 1972.** Some studies on reaeration in cascades. *Water research*, 6: 297-304.

- Teichert-Coddington, D. and B. Green. 1993.** Comparison of two techniques for determining community respiration in tropical fish ponds. *Aquaculture*, 114: 41 – 50.
- The Task Committee on Design of Wastewaters Filtration Facilities. 1996.** Tertiary filtration of wastewaters, *Journal of Environmental Engineering*, 112(6): 1008-1025.
- Thorn, R. 1998.** Reengineering the cyclone separator. *Met. Finish.* 96 (8): 30–35.
- Timmons, M.B. 2000.** Aquacultural Engineering – experiences with recirculating aquaculture system technology, Part 1. *Aquaculture Magazine*, 26 (1): 52-56.
- Timmons, M.B. and J.M. Ebeling. 2007.** Recirculating aquaculture. NRAC Publication No. 01-007. USDA.
- Timmons, M.B.; J.M. Ebeling; F.W. Wheaton; S.T. Summerfelt and B.J. Vinci. 2001.** Recirculating Aquaculture Systems. Cayuga Aqua Ventures, Ithaca, NY, USA.
- Timmons, M.B., J.L. Holder, J.M. Ebeling. 2006.** Application of microbead filters. *Aquacult. Eng.* 34(3): 332-343.
- Timmons, M.B., Summerfelt, S.T. 1998.** Application of fluidized sand biofilters. In: Libey, G.S., Timmons, M.B. (Eds.), The 2nd International Conference on Recirculating Aquaculture, Virginia Polytechnic Institute and State University, July 16–19, Roanoke, VA, pp. 342–354.
- Timmons, M.B., S.T. Summerfelt and B.J. Vinci. 1998.** Review of circular tank technology and management. *Aquacult. Eng.* 18, 51–69.
- Traoré A.; S. Grieu; S. Puig; L. Corominas; F. Thiery; M. Polit and J. Colprim. 2005.** Fuzzy control of dissolved oxygen in a sequencing batch pilot plant. *Chemical Engineering Journal*, 111: 13-19.

REFERENCES

- True, B.; W. Johnson and S. Chen. 2004.** Reducing phosphorous discharge from flow-through aquaculture. I. Facility and effluent characterization. *Aquacult. Eng.* 32: 109–124.
- Tseng, K.F. and K.L. Wu. 2004.** The ammonia removal cycle for submerged biofilter used in a recirculating eel culture system. *Aquacult. Eng.*, 31: 17–30.
- Twarowska, J.G.; P. W. Westerman and T.M. Losordo. 1997.** Water treatment and waste characterization evaluation of an intensive recirculating fish production system. *Aquacultural Engineering*, 16: 133-147.
- U.S. E.P.A. 1993.** Nitrogen. EPA/625/R-93/010, U.S. Environmental Protection Agency., Washington, DC, USA.
- U.S. E.P.A. 1999.** Storm Water Technology Fact Sheet: Hydrodynamic Separators. EPA 832-F-99-017. U.S. Environmental Protection Agency, Washington, DC, USA.
- Vaca Mier M., C. L. Magdaleno, C. M. Sosa, M. M. Monroy and C. B. Jiménez. 2001.** Tratamiento terciario de Aguas Residuales por Filtración e Intercambio Iónico, UAM, UNAM, México.
- Valdivia Soto C. A., B. O. González and M. S. González. 2000.** Filtración combinada en lechos de piedras porosas para el tratamiento de aguas residuales. Coordinación de Ingeniería Ambiental, Instituto de Ingeniería Universidad Nacional Autónoma de México, Ciudad Universitaria, México D.F.
- Valverde, J.C. and B.G. García. 2004.** Influence of body weight and temperature on post – prandial oxygen consumption of common octopus (*Octopus vulgaris*). *Aquaculture*, 233: 599-613.
- van Gorder, S.D. 1994.** Operating and managing water reuse systems. In: Timmons, M., Losordo, T. (Eds.), *Aquaculture Water Reuse*

REFERENCES

- Systems: Engineering Design and Management. Elsevier Science, Amsterdam, 333 pp.
- van Gorder, S.D. and J. Jug-Dujakovic. 2005.** Performance characteristics of rotating biological within two commercial recirculating aquaculture systems. *Int'l J. of Rec. Aquacul.* 6:23-38.
- Vargas Tapia P., R. J.Z. Castellanos, R. J.J. Muñoz, G. P.Sánchez, C. L. Tijerina, R. R.M. López and S. C. Martínez and J.L. Ojo de agua Arredondo. 2008 .** Efecto del tamaño de partícula sobre algunas propiedades físicas del tezontle de Guanajuato, México. *Agricultura Técnica en México.* 34, 3, p. 323-331.
- <http://redalyc.uaemex.mx/redalyc/pdf/608/60811116007.Pdf>.
- Vasile, A. 2008.** The implications of water chemical properties from the breeding nursery pond on the fish pathological state. *Innovative Romanian Food Biotechnology.* 2, 25 – 29.
- Veerapen, J.P., Lowry, B.J., Couturier, M.F., 2005.** Design methodology for the swirl separator. *Aquacultural Engineering* 33, 21–45.
- Villeneuve, J.P. and E. Gaume. 1994.** Efficiency evaluation of an installed swirl separator. *Can. J. Civ. Eng.* 21 (6): 924–930.
- Vinci, B.J., B.J. Watten, and M.B. Timmons. 1997.** Modeling gas transfer in a spray tower oxygen absorber. *Aquacultural Engineering,* 16: 91-105.
- Wang, W. 1980.** Fractionation of sediment oxygen demand. *Water Research,* 14: 603 – 612.
- Watten, B.J. 1990.** Design of packed columns for commercial oxygen addition and dissolved nitrogen removal based on effluent criteria. *Aquacultural Engineering,* 9: 305-328.

REFERENCES

- Watten, B.J. and C.E. Boyd. 1989.** Gas phase axial dispersion in a packed column oxygen absorber. *Aquacultural Engineering* 8:199-205.
- Webster, D. and J.M. Regenstein. 2007.** System management and operations In: Timmons, M.B. and J.M. Ebeling, *Recirculating aquaculture*. NRAC Publication No. 01-007. USDA.
- Welch, E.B. 1980.** Ecological effects of waste water. Cambridge University Press, Cambridge, UK.
- Wells, M.J.; R.K. O'Dor; K. Mangold and J. Wells. 1983.** Feeding and metabolic rate of octopus. *Mar. Behav. Physiol.*, 9: 305-317.
- Westerman, P.W.; T.M. Losordo and M.L. Wildhaber. 1996.** Evaluation of various biofilters in an intensive recirculating fish production facility. *Transactions of the American Society of Agricultural Engineers* 39: 723-727.
- Wheaton, F. W.; J. N. Hochheimer; G. E. Kaiser and M. J. Krones. 1991.** Principles of biological filtration. In Northeast Regional Agricultural Engineering Service. *Engineering Aspects of Intensive Aquaculture*. Proceedings from the Aquaculture Symposium.
- Wheaton, F.W. 1993.** *Aquacultural engineering*. Krieger Publishing Company, Malabar, Florida.
- Wheaton, F. W.; J. N. Hochheimer; G. E. Kaiser; M. J. Krones; G. S. Libey and C. C. Easter. 1994.** Nitrification Principles. In: M.B. Timmons and T.M. Losordo, Eds. *Aquaculture Reuse Systems: Engineering Design and Management*. Development in Aquaculture and Fisheries Sciences, Vol. 27, Elsevier Science B.V., Amsterdam, the Netherlands, PP.101-126.
- Widmer A. M.; C. J. Carveth; J. W. Keffler and S. A. Bonar. 2006.** Design of a computerized, temperature-controlled, Re-circulating aquaria system, *Aquacultural Engineering*, 35: 152-160.

REFERENCES

- Willoughby, H. 1968.** A method for calculating carrying capacities of hatchery troughs and ponds. *Progressive Fish culturist*, 30: 173-174.
- Wimberly, D.M. 1990.** Development and Evaluation of a Low-Density Media Biofiltration Unit For Use in Recirculating Finfish Culture Systems. MS thesis, Louisiana State University, Baton Rouge, LA.
- Wong, K.B. and R.H. Piedrahita. 2000.** Settling velocity characterization of aquaculture solids. *Aquacultural Engineering* 21:233-246.
- Woodbury, L.A. 1941.** A sudden mortality of fishes accompanying a supersaturation of oxygen in lake Waubesa, Wisconsin. *Trans. Amer. Fish. Soc.*, , 71, 112-117.
- Wyban, J.A.; G.D. Pruder and K.M. Leber. 1989.** Paddlewheel effects on shrimp growth, production and crop value in commercial earthen ponds. *Journal of the World Aquaculture Society*, 20: 18-23.
- Yeoh, S.J.; F.S. Taip; J. Endan; R.A. Talib and M.K.S. Mazlina. 2010.** Development of automatic feeding machine for aquaculture industry. *Pertanika J. Sci. & Technol.* 18(1): 105-110.
- Yi, Y. and C.K. Lin. 2001.** Effects of biomass of caged Nile tilapia (*Oreochromis niloticus*) and aeration on the growth and yields in an integrated cage-cum-pond system. *Aquaculture*, 195: 253-267.
- Yoo, K.H. and Boyd, C.E. 1994.** Hydrology and water supply for pond aquaculture, Chapman and Hall, New York.
- YSI. 2008.** <http://www.ysi.com/media/pdfs/E32-6150-ROX-DO-Sensor.pdf>
- Yuan, Y.; M. Han; L. Wang; D. Wang and Y. Jin. 2004.** Mass transfer coefficient for two-phase countercurrent flow in a packed column with a novel internal: Short communication. *Chemical Engineering Journal*, 99: 273-277.

REFERENCES

- Zakes, Z.; K. Demska-Zakes; P. Jarocki and K. Stawecki. 2006.** The effect of feeding on oxygen consumption and ammonia excretion of juvenile tench *Tinca tinca* (L.) reared in a water recirculating system. *Aquacult. Int.* 14, 127–140.
- Zhu, S. and S. Chen. 1999.** An experimental study on nitrification biofilm performances using a series reactor system. *Aquacult. Eng.*, 20: 245–259.

7. APPENDIX I

7.1. Apparent density Determination for Tezontle (paraffin) Method : As-06-1998

Three grains of tezontle was selected from the sample as shown in Figure 3.8A, the paraffin was dissolved above the flame till its temperature eaching to (56-60 °C) Figure 3.8B, one of three grains selected and holded by a treat to the arm of balance Figure 3.8C and its weight was resigested as grain air weighting (Pt)a, the grain was dipped in the melted paraffin at 60°C to cover it totally and in uniformly suface and its weight figure 3.8D was registred as the parafin grain air weighting (Ptp)a, after that the grain was weighted immesed in the water (Ptp)w figure 3.8E, finally the calculations.

- a) $(Ptp)a - (Ptp)w = (Vt + Vp)$
- b) $(Ptp)a - (Pt)a = (Pp)(the\ paraffin\ weight)$
- c) $\frac{Pp}{\rho_p} = V(paraffin\ volume)$
- d) $(V_t + V_p) - V_p = (Vt)the\ grain\ volume$
- e) $\frac{(Pt)a}{Vt} = \rho (aparent\ density)$

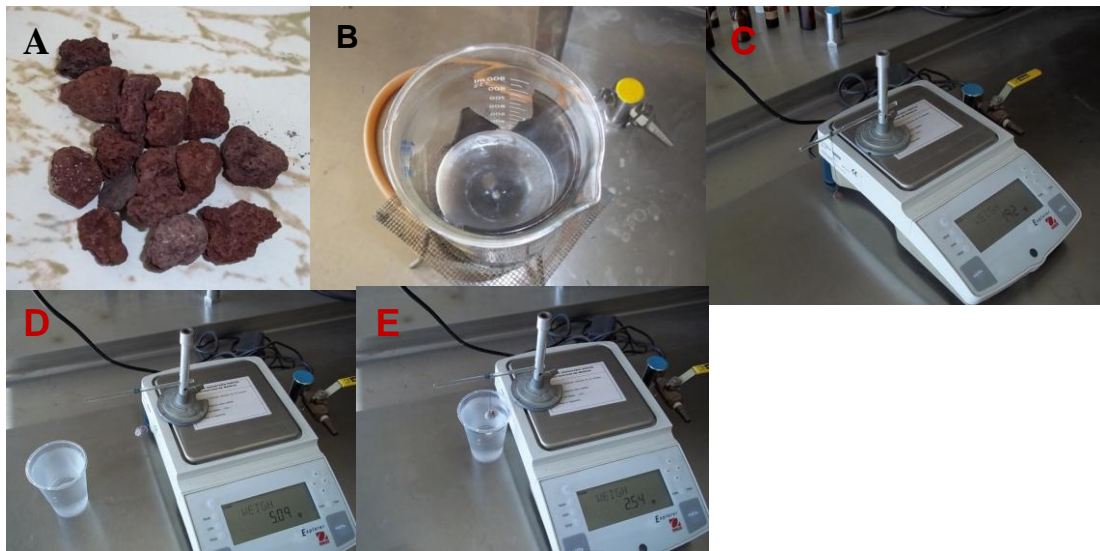


Fig. 7.1 (A)Tezontle grains that were used to determine the apparent density according to the mexican leys to determine the prosity and density for the soils, (B) the paraffin used to cover the grains of tezontle, (C) The grains was weighted in hanging position without covering with paraffin(D) The grains was weighted in hanging position covering with paraffin, (E) The grains was weighted in floating and hanging position to determine the amount of water that displaced according to the lay of Archimedes.

APPENDIX I

Table 7.1: Water vapor pressure and dissolved oxygen solubility parameters as a function of water temperature (Colt, 1984)

T	γ	P_w	β	β k 1000	F
5	9.806	6.54	0.04302	26.259	28.937
7	9.806	7.51	0.04095	58.519	12.989
9	9.805	8.61	0.03905	55.804	13.621
11	9.803	9.85	0.03730	53.303	14.257
13	9.801	11.23	0.03570	51.016	14.895
15	9.798	12.79	0.03423	48.916	15.535
17	9.795	14.53	0.03288	46.987	16.175
19	9.791	16.48	0.03163	45.200	16.812
21	9.787	18.66	0.03048	43.557	17.446
23	9.783	21.08	0.02942	42.042	18.076
25	9.778	23.77	0.02844	40.642	18.699
27	9.772	26.75	0.02754	39.355	19.314
30	9.764	31.84	0.02630	37.583	20.218

Symbols

β k 1000	=	Gas solubility, mg/l-at a partial pressure of 760 mmHg
γ	=	Specific mass of water, kN/m ³
T	=	Water temperature, °C
F	=	Gas tension per mg/l-1, mmHg

APPENDIX I

Table 7.2: The solubility of oxygen (mg l^{-1}) in water at different temperatures and salinities from moist air with pressure of 760 mm Hg.

Temperature (°C)	Salinity (PPT)								
	0	5	10	15	20	25	30	35	40
0	14.60	14.11	13.64	13.18	12.74	12.31	11.90	11.50	11.11
1	14.20	13.72	13.27	12.82	12.40	11.98	11.58	11.20	10.82
2	13.81	13.36	12.91	12.49	12.07	11.67	11.29	10.91	10.55
3	13.44	13.00	12.58	12.16	11.76	11.38	11.00	10.64	10.29
4	13.09	12.67	12.25	11.85	11.47	11.09	10.73	10.38	10.04
5	12.76	12.34	11.94	11.56	11.18	10.82	10.47	10.13	9.80
6	12.44	12.04	11.65	11.27	10.91	10.56	10.22	9.89	9.57
7	12.13	11.74	11.36	11.00	10.65	10.31	9.98	9.66	9.35
8	11.83	11.46	11.09	10.74	10.40	10.07	9.75	9.44	9.14
9	11.55	11.18	10.83	10.49	10.16	9.84	9.53	9.23	8.94
10	11.28	10.92	10.58	10.25	9.93	9.62	9.32	9.03	8.75
11	11.02	10.67	10.34	10.02	9.71	9.41	9.12	8.83	8.56
12	10.77	10.43	10.11	9.80	9.50	9.21	8.92	8.65	8.38
13	10.52	10.20	9.89	9.59	9.29	9.01	8.73	8.47	8.21
14	10.29	9.98	9.68	9.38	9.10	8.82	8.55	8.29	8.04
15	10.07	9.77	9.47	9.19	8.91	8.64	8.38	8.13	7.88
16	9.86	9.56	9.28	9.00	8.73	8.47	8.21	7.97	7.73
17	9.65	9.36	9.09	8.82	8.55	8.30	8.05	7.81	7.58
18	9.45	9.17	8.90	8.64	8.38	8.14	7.90	7.66	7.44
19	9.26	8.99	8.73	8.47	8.22	7.98	7.75	7.52	7.30
20	9.08	8.81	8.56	8.31	8.06	7.83	7.60	7.38	7.17
21	8.90	8.64	8.39	8.15	7.91	7.68	7.46	7.25	7.04
22	8.73	8.48	8.23	8.00	7.77	7.54	7.33	7.12	6.91
23	8.56	8.32	8.08	7.85	7.63	7.41	7.20	6.99	6.79
24	8.40	8.16	7.93	7.71	7.49	7.28	7.07	6.87	6.68
25	8.24	8.01	7.79	7.57	7.36	7.15	6.95	6.75	6.56
26	8.09	7.87	7.65	7.44	7.23	7.03	6.83	6.64	6.46
27	7.95	7.73	7.51	7.31	7.10	6.91	6.72	6.53	6.35
28	7.81	7.59	7.38	7.18	7.98	7.79	6.61	6.42	6.25
29	7.67	7.46	7.26	7.06	6.87	6.68	6.50	6.32	6.15
30	7.54	7.33	7.14	6.94	6.75	6.57	6.39	6.22	6.05

Source (Boyd,1990) notice that the solubility of oxygen in water decreases as water temperature and salinity increases

APPENDIX I

Table7.3: The solubility of oxygen (mg l^{-1}) in water at different temperatures and altitudes above sea level.

°C	Altitude above sea level (in meters)												
	0	300	600	900	1200	1500	1800	2100	2400	2700	3000	3300	3600
0	14.6	14.1	13.6	13.2	12.7	12.3	11.8	10.9	10.2	9.4	8.7	8.1	7.6
2	13.8	13.3	12.9	12.4	12.0	11.6	11.2	10.3	9.6	8.9	8.2	7.7	7.1
4	13.1	12.7	12.2	11.9	11.4	11.0	10.6	9.8	9.1	8.5	7.8	7.3	6.7
6	12.4	12.0	11.6	11.2	10.8	10.4	10.1	9.3	8.6	8.0	7.4	6.9	6.4
8	11.8	11.4	11.0	10.6	10.3	9.9	9.6	8.9	8.2	7.6	7.1	6.5	6.1
10	11.3	10.9	10.5	10.2	9.8	9.5	9.2	8.5	7.8	7.3	6.8	6.3	5.8
12	10.8	10.4	10.1	9.7	9.4	9.1	8.8	8.1	7.5	7.0	6.4	6.0	5.6
14	10.3	9.9	9.6	9.3	9.0	8.7	8.3	7.8	7.2	6.6	6.2	5.7	5.3
16	9.9	9.7	9.2	8.9	8.6	8.3	8.0	7.5	6.9	6.4	5.9	5.5	5.1
18	9.5	9.2	8.7	8.6	8.3	8.0	7.7	7.2	6.6	6.1	5.7	5.3	4.9
20	9.1	8.8	8.5	8.2	7.9	7.7	7.4	6.9	6.3	5.9	5.5	5.1	4.7
22	8.7	8.4	8.1	7.8	7.7	7.3	7.1	6.6	6.0	5.6	5.3	4.9	4.5
24	8.4	8.1	7.8	7.5	7.3	7.1	6.8	6.3	5.8	5.5	5.1	4.7	4.4
26	8.1	7.8	7.5	7.3	7.0	6.8	6.6	6.1	5.7	5.2	4.8	4.5	4.2
28	7.8	7.5	7.3	7.0	6.8	6.6	6.3	5.9	5.4	5.0	4.7	4.3	4.0
30	7.5	7.2	7.0	6.8	6.5	6.3	6.1	5.7	5.2	4.9	4.6	4.2	3.9
32	7.3	7.1	6.8	6.6	6.4	6.1	5.9	5.5	5.1	4.7	4.4	4.1	3.8
34	7.1	6.9	6.6	6.4	6.2	6.0	5.8	5.4	4.9	4.6	4.2	3.9	3.7
36	6.8	6.6	6.4	6.1	5.9	5.7	5.5	5.2	4.8	4.5	4.1	3.8	3.5
38	6.6	6.4	6.1	5.9	5.7	5.6	5.4	5.0	4.6	4.3	4.0	3.7	3.5
40	6.4	6.2	5.9	5.8	5.6	5.4	5.2	4.8	4.5	4.2	3.9	3.6	3.3
42	6.3	6.0	5.8	5.6	5.4	5.2	5.0	4.7	4.3	4.0	3.7	3.5	3.2
44	6.1	5.9	5.7	5.5	5.3	5.1	4.9	4.6	4.3	4.0	3.7	3.4	3.1
46	5.9	5.7	5.5	5.3	5.1	4.9	4.8	4.4	4.1	3.8	3.5	3.3	3.1

Instruction manual HI 9146 Portable Waterproof Microprocessor Dissolved Oxygen Meter, Man9146 - 10/2005, www.hannacan.com.

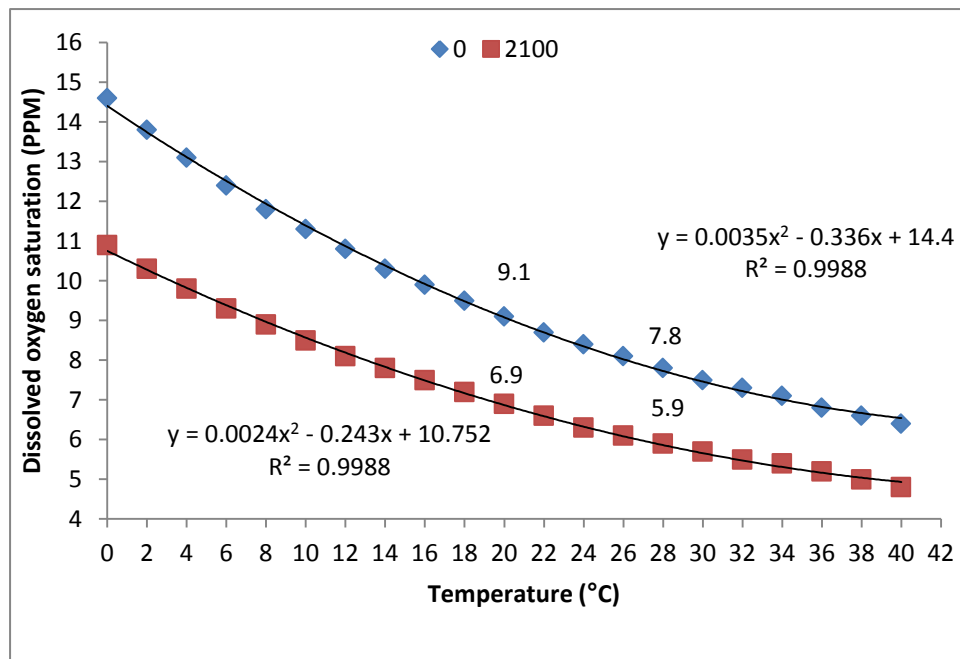


Fig. 7.2 The solubility of oxygen (mg^l-1) in water at sea level and 2100 m above sea level.

7.2. Ammonia photometer (low range) 0 to 3 mg/l.

The instrument was used firstly by filling the cuvet up to 1.5 cm ($\frac{3}{4}$ ") below the rim with 10 mL of sample, and replacing the cap. Placing the cuvet into the holder and ensure that the notch on the cap is positioned securely into the groove. Pressing (ZERO) button and "SIP" appears in the display. Waiting a few seconds and the display will show "-0.0-." The meter is now ready to measure. Remove the cuvet and add 4 drops of first reagent. Replacing the cap and swirl the solution. adding 4 drops of the second reagent. Replacing the cap and swirl the solution. Reinserting the cuvet into the instrument and pressing READ TIMED and the display shows the account prior to measurement or wait 3 minutes and 30 seconds and pressing READ DIRECT. In both cases the "SIP" during the measurement. The instrument directly on the display shows the concentration of ammonia nitrogen (NH₃-N). To convert the reading to mg / l of ammonia (NH₃), multiply the value in the display by a factor of 1.214.



Fig. 7.3. Ammonia Photometer (Low Range) 0 to 3 mg/L **HI93700**
www.hannainst.com

SPECIFICATIONS

Range	0.00 to 3.00 mg/L
Resolution	0.01 mg/L
Accuracy	±0.04 mg/L ±4% of reading
Typical EMC Deviation	±0.01 mg/L

Light Source Light Emitting Diode @ 470 nm

Method Adaptation of the ASTM Manual of Water and Environmental Technology, D1426-92, Nessler method.

The reaction between ammonia and reagents causes a yellow tint in the sample.

Environment 0 to 50°C (32 to 122°F); max 95% RH non-condensing

Battery Type/Life 1 x 9 volt/40 hours

Auto-Shut off After 10' of non-use

Dimensions 180 x 83 x 46 mm (7.1 x 3.3 x 1.8")

Weight 290 g (10 oz.).

The REAGENTS

Code Description	Quantity
HI 93700A-0	Second Reagent 4 drops (10 drops in seawater)
HI 93700B-0	First Reagent 4 drops (6 drops in seawater)

7.3. Nitrate Photometer range 0 to 100 mg/L

Nitrate nitrogen (NO₃-N) was measured by a digital Nitrate photometer (low Range) 0 to 3 mg/L (HANNA INSTRUMENTS made in Romania, Europe) as shown at Fig. 5.4. NO₃-N was measured daily at inlet and outlet of the biofilters tanks and for fish tanks. The instrument was used firstly by filling the cuvet up 6 mL of sample, up to about half of its height, and replaces. Placing the cuvet into the holder and ensure that the notch on the cap is positioned securely into the groove. Placing the bucket in the cuvet holder and ensures top notch securely into the groove. Pressing (ZERO) button and "SIP" appears in the display. Waiting a few seconds and the display will show "-0.0-." The meter is now ready to measure. Removing the cuvet and add the contents of a packet of HI 93728. Place the lid and shaken vigorously immediately the solution for exactly 10 seconds. Moving the bucket up and down. Further mixed by inverting the cuvet gently and slowly for 50 seconds, while being careful not to cause air bubbles. Reinserting the cuvet into the instrument and press READ and the TIME display counts prior to measurement or wait 4 minutes and 30 seconds and press READ DIRECT. In both cases the "SIP" during the measurement. The instrument

directly displays the liquid crystal display the concentration of nitrate-nitrogen in mg / L. To convert the reading to mg / L of nitrate (NO₃-N), multiply by a factor of 4.43.



Fig. 7.4. Nitrate Photometer (Low Range) 0 to 100 mg/L **HI93828**
www.hannainst.com

SPECIFICATIONS

Range	0.0 to 30.0 mg/L
Resolution	0.1 mg/L
Accuracy	±0.5 mg/L ±10% of reading
Typical EMC Deviation	±0.1 mg/L
Light Source	Light Emitting Diode @ 555 nm
Method	Adaptation of the cadmium reduction method. The reaction between nitrate nitrogen and the reagent causes an amber tint in the sample
Light Detector	Silicon Photocell
Environment	0 to 50°C (32 to 122°F); max 95% RH non-condensing
Battery Type/Life	1 x 9 volt/40 hours
Auto-Shut off	after 10' of non-use
Dimensions	180 x 83 x 46 mm (7.1 x 3.3 x 1.8")
Weight	290 g (10 oz.).

REQUIRED REAGENTS

Code	Description	Quantity
HI 93728-0	Powder reagent	1 packet

7.4. Dosing automation system

1. Microcontroller peripherals

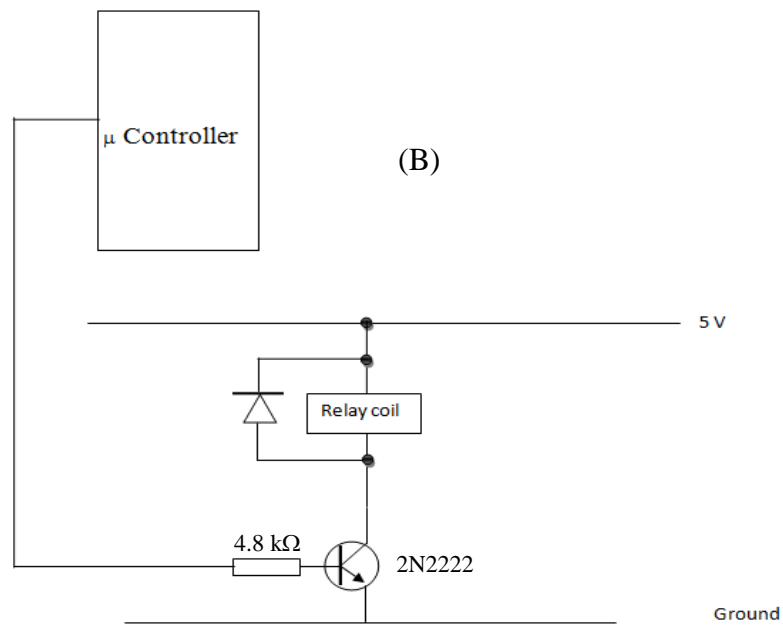
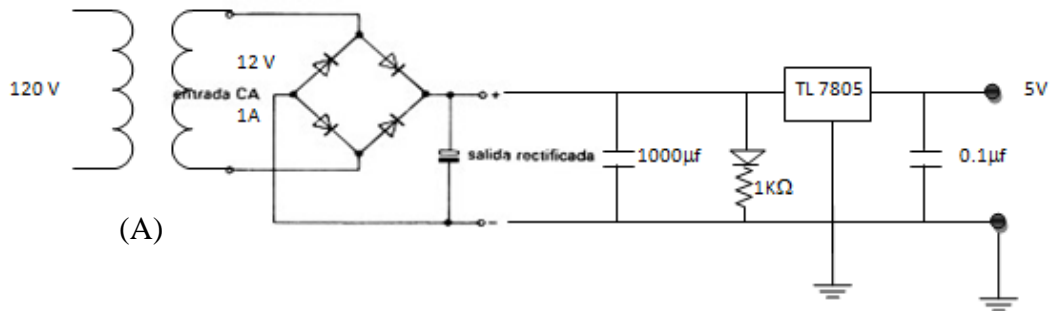


Fig. 7.5. (A) Convert 120 V AC to 5 V CD, (B) microcontroller signal outlet connection to relays

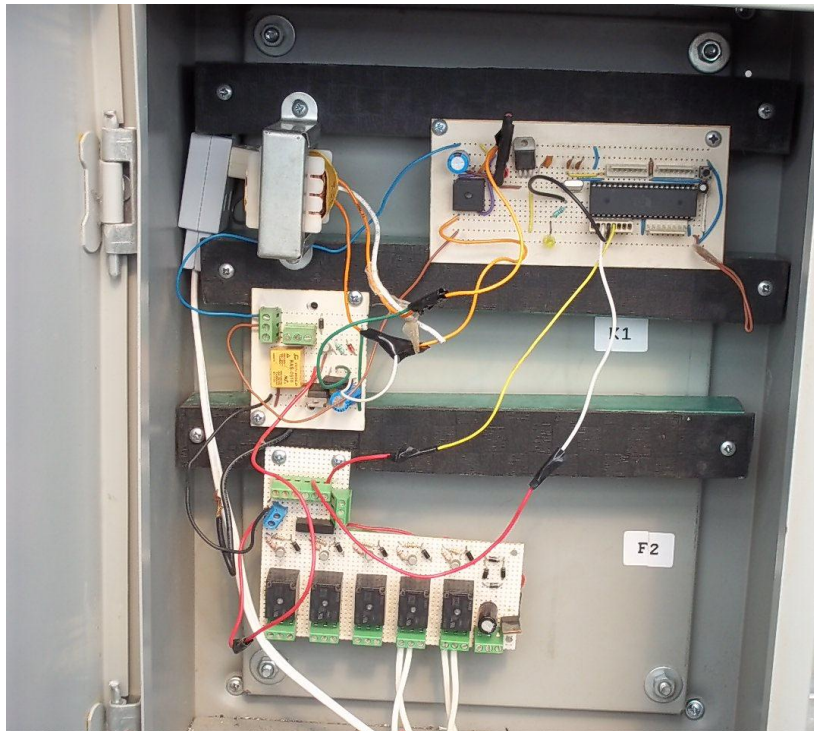


Fig. 7.6. The microcontroller that was used for automatic feeder.

Microcontroller codes simulation by Proteuos program.

The Proteuos program is using to show a simulation of the micro codes where D1 is feeder motors, D2 is electromagnetic coil and the extractor and D3 is the gate motor (Fig. 7.7).

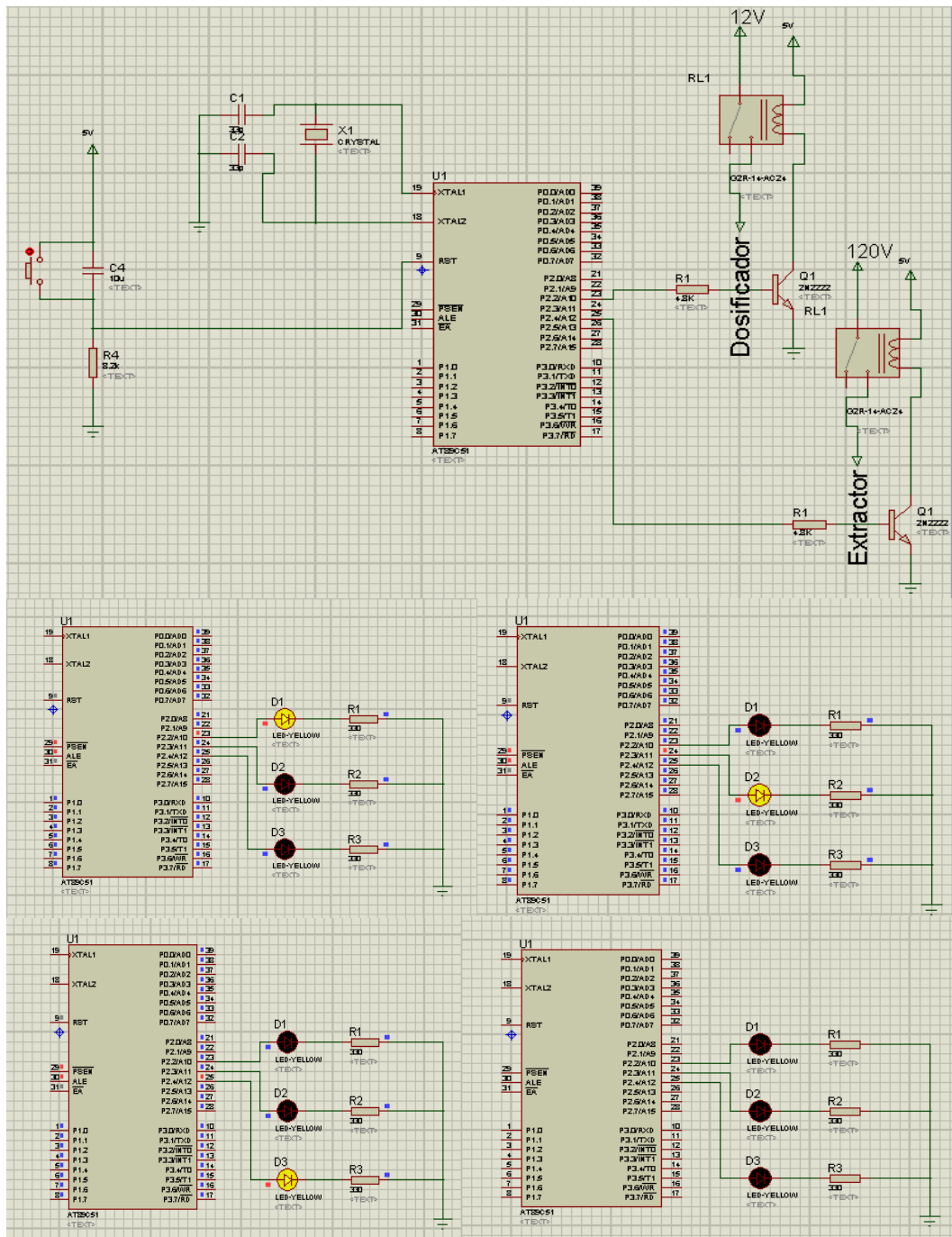


Fig.7.7. micro codes simulation by the proteuos.

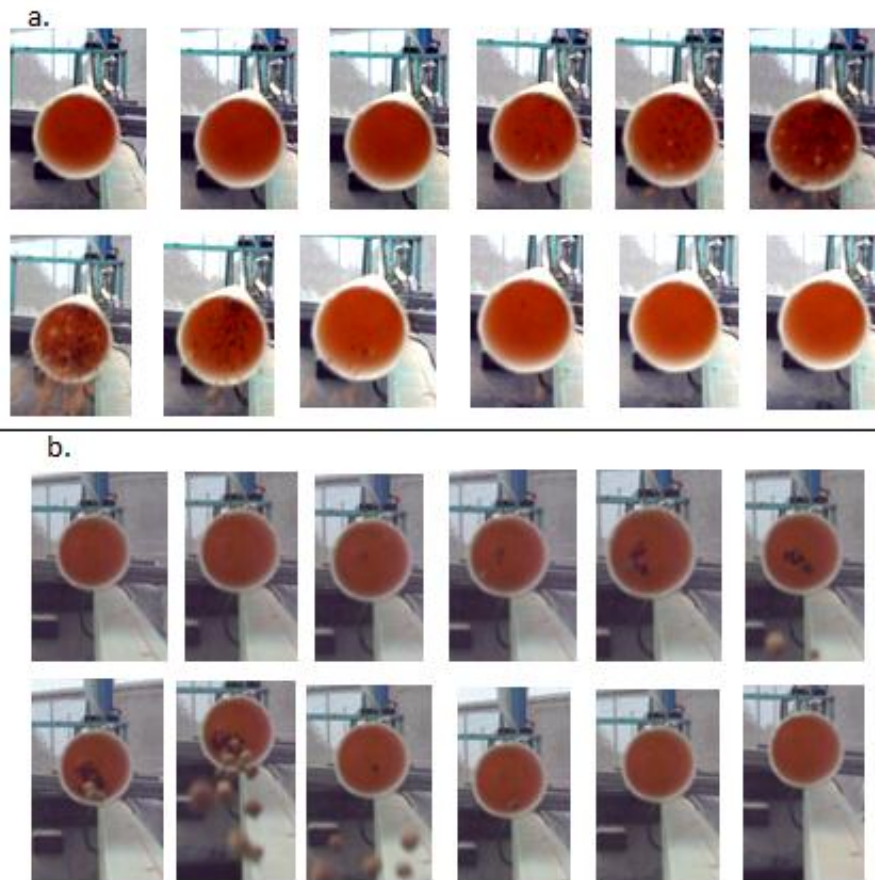


Fig. 7.8. Food movement analysis by photos.

Air velocity was measured by anemometer EXTECH



Fig. 7.9. EXTECH anemometer.



Fig. 7.10. Food falling in the carp tank using one and two fans

APPENDIX I



1st gate with one fan for Nutripec 4418C



2nd gate with one fan for Nutripec 4418C



3rd gate with one fan for Nutripec 4418C



1st gate with one fan for Nutripec 3508



2nd gate with one fan for Nutripec 3508



3rd gate with one fan for Nutripec 3508



1st gate with two fans for Nutripec 3508



2nd gate with two fans Nutipec 3508



3rd gate with two fans Nutipec 3508



1st gate with two fans Nutipec 4418C



2nd gate with two fans Nutipec 4418C



3rd gate with two fans Nutipec 4418C

Fig. 7.11. Food particles movement analysis

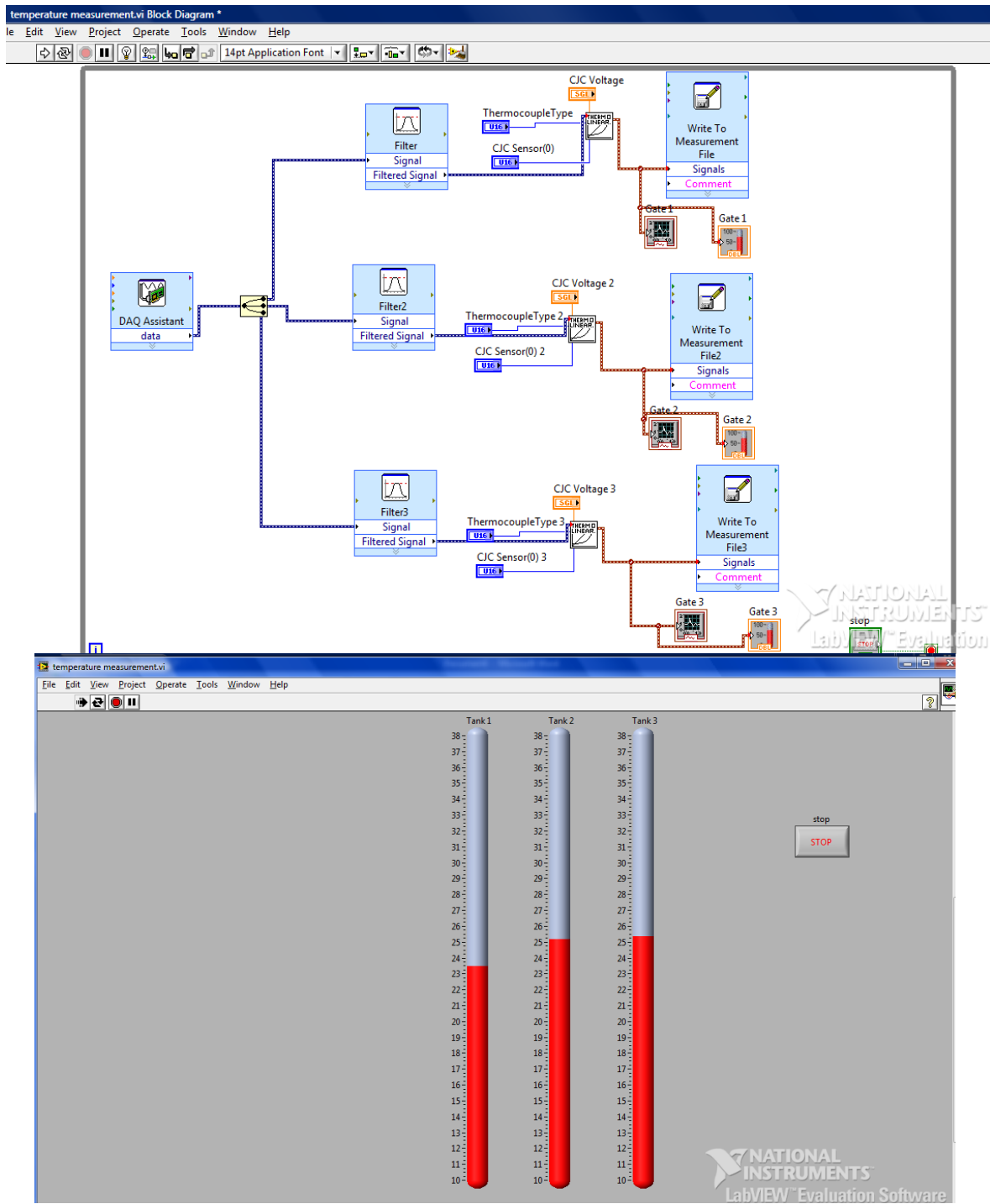


Fig. 8.1 Thermocouple implement by LabView.

8.1. Dissolved oxygen control description

The program consists of two parallel subprogram are dissolved oxygen logging and control Block diagram (compiled code) of dissolved oxygen controller was programmed as shown in Fig 8.5. One Excel files with extension .CSV for each tank having its name Tank 1, Tank 2 and Tank 3 saved on specific folder on PC. As shown in Fig. 8.2 the user should detail folder location on his PC; for example the folder (Nueva Carpeta) was selected to be the container of the three excel files. Naming the excel file was divided to two parts. The first part of the excel file was identified by the user (e.g. Tank) Fig. 4.000, but the second part of its name will be determined by the program according to which one of the three peristaltic pumps is turning on and attached the number 1, 2 or 3 to the first part of its name, as the three excel files generated to be one for each tank, the program will append the new acquired data to its file.

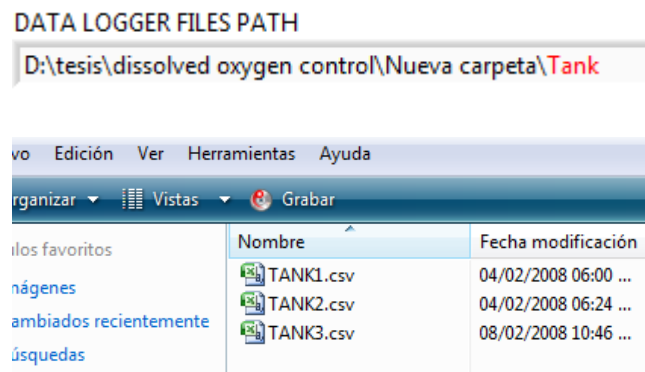


Fig. 8.2 Data logger files path definition in the program front panel and its location in the PC.

APPENDIX II

The program has the ability to run the three RAS units simultaneously or independently under closed loop or opened loop control, the control type can be selected automatically or manually according to the unit condition and fish biomass Fig.8.3.

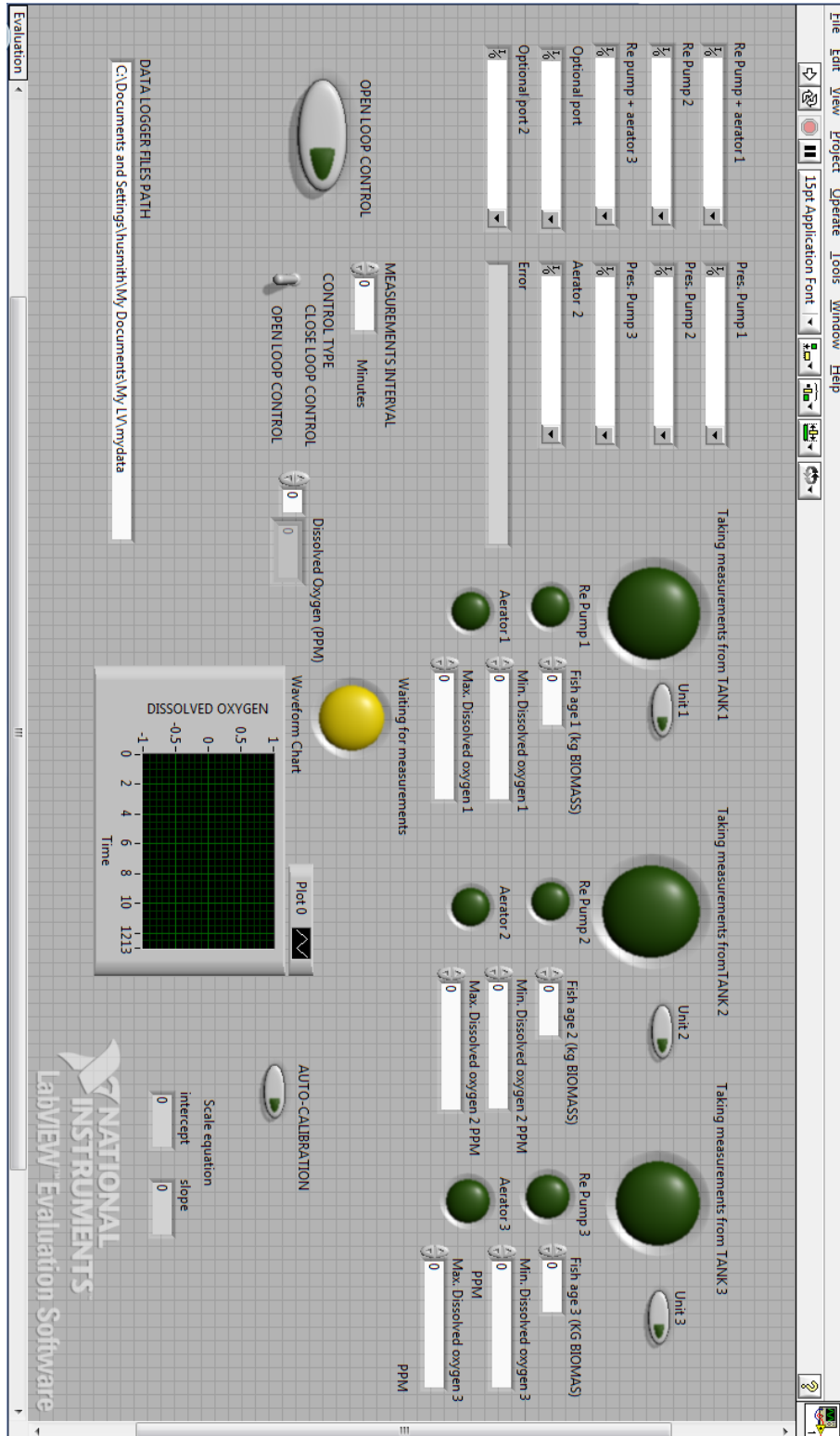


Fig. 8.3 system front panel for the opened and closed loop control

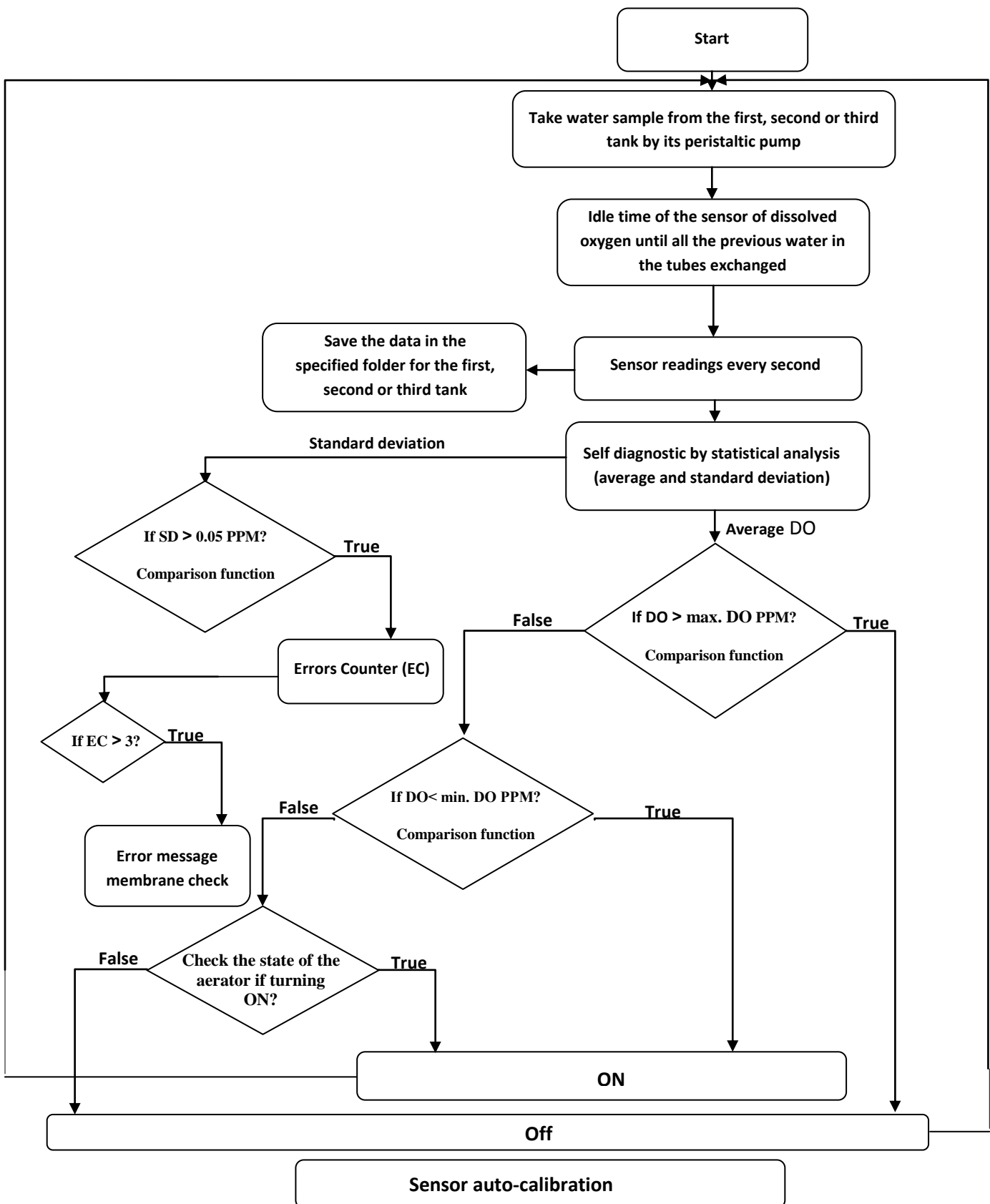


Fig. 8.5 LabView programming flow chart for the controller.

8.1.1.2. Excel files numbering program.

Three case structures were used sending (1 or 0) to formula node through three input ports of X, Y and Z depending on peristaltic pumps status acknowledged by three property nodes and one output port of A sending 1, 2 or 3 to be the second part of excel file naming Fig. 8.6. These numbers should be converting to string by number to decimal string.vi. As the number and file extension desired (.CSV) are attached to (D:\tesis\dissolved oxygen control\Nueva carpeta\Tank) by concatenate strings.vi and converted to path by string to path.vi can be connected to write to spreadsheet file.vi

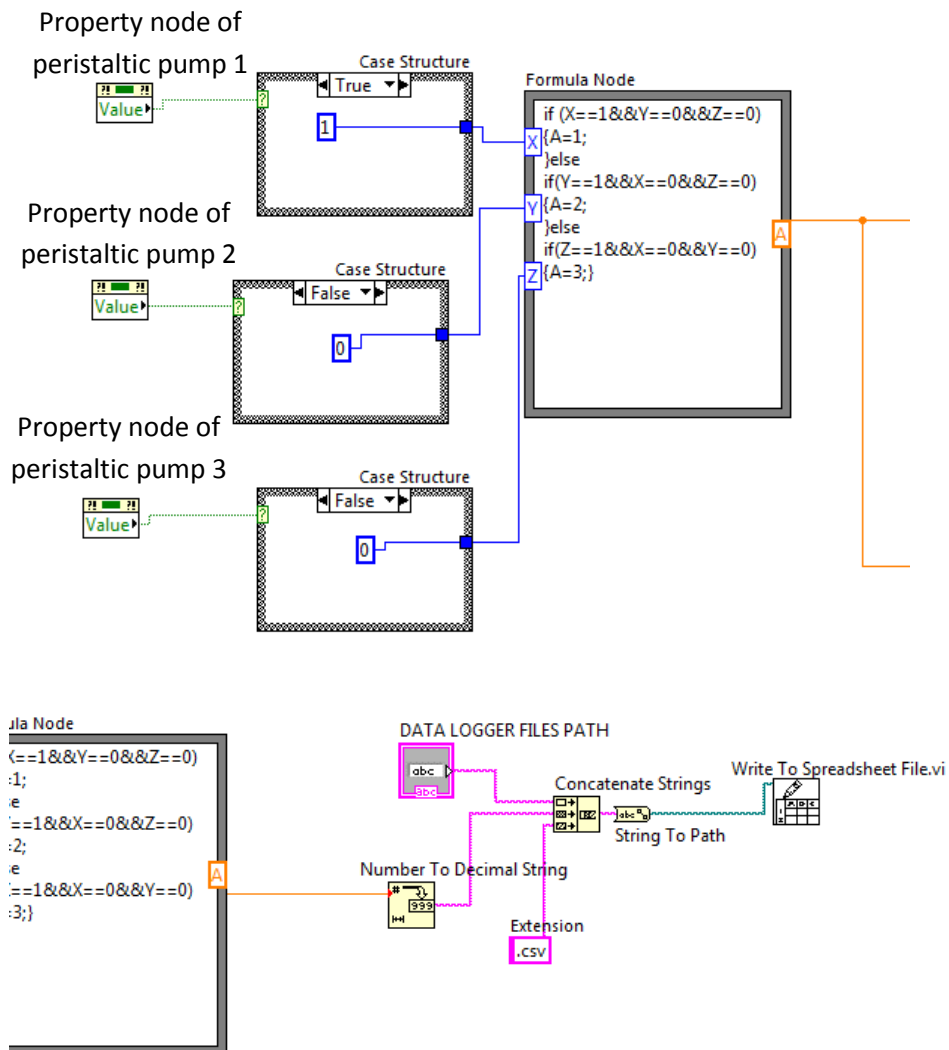


Fig. 8.6. Attaching the output number of formula node to the first part of the tank

8.1.1.3. Logging the acquired data and auto-calibration

As the user press at the front panel auto-calibration the case structure will execute the true case generating newer values of the slope and intercept of scale equation. Linear fit.vi requires two points (X1, X2) and (Y1, Y2) by Build array X.vi and Build array Y.vi. For example the two points used (0.004, signal output at saturation) and (0, 6) (Fig.8.7).

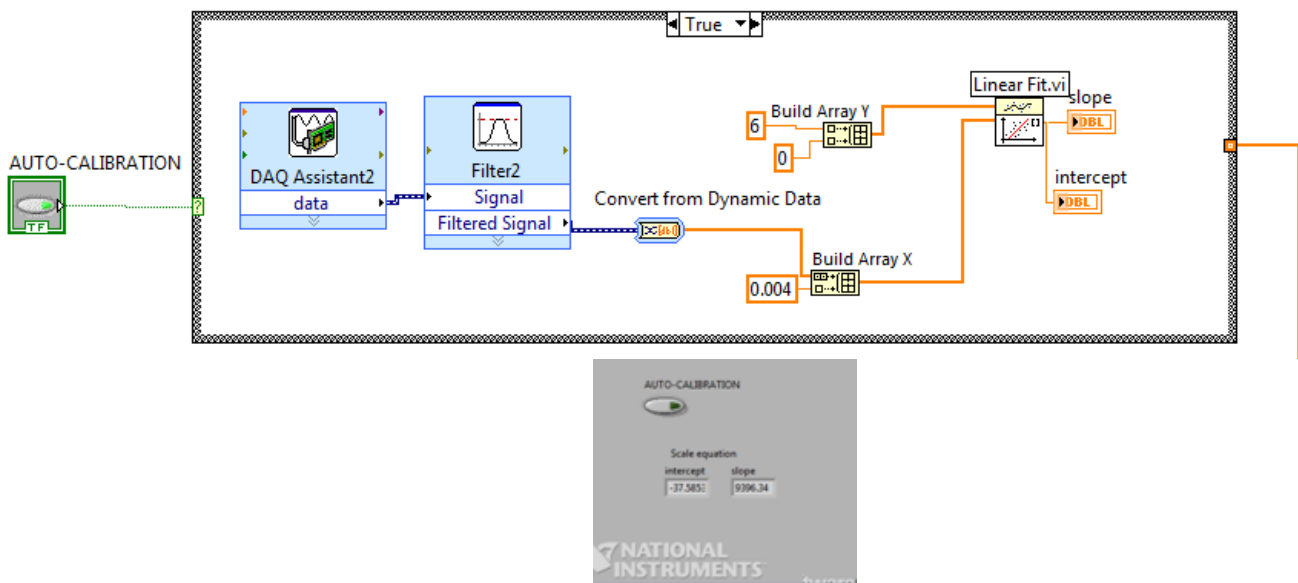


Fig. 8.7. Auto-calibration with one point coding

As the sensor was calibrated automatically (Calibration with one point in contact with air) (Fig.8.8) by depressing auto-calibration button in front panel, the intercept and slop of the scale equation created directly used to convert the output signal of (4-20 mA) to dissolved oxygen measurements in ppm by the newer scale equation.

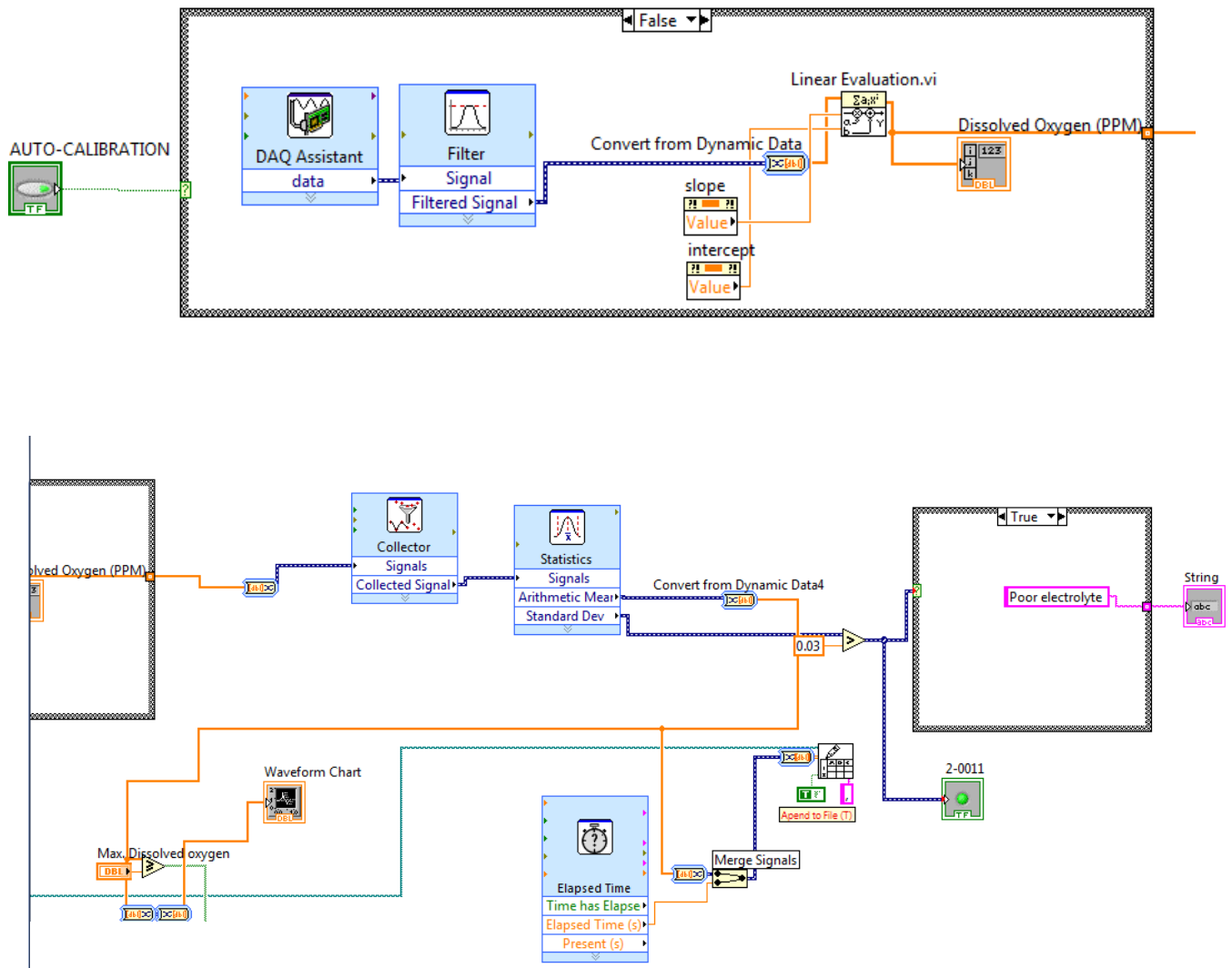


Fig.8.8. (a) The acquired data by DAQ assistant was filtered by smoothing filter.

(b) auto-diagnostic coding.

Dissolved oxygen measurements were processed statistically by collecting thirteen data, calculating arithmetic mean and standard deviation. The standard deviation was compared against 0.03 ppm, sending to the front panel the message of (poor electrolyte or membrane fail) if the condition case is true. On the other hand the average of thirteen data will be recorded to the spread sheet for each tank every 10 min.

The processed data as mean values will compare against the preset points (Max. Dissolved oxygen) and (Min. Dissolved oxygen); the formula node

send binary values of 0 or 1 to case structure to convert it to Boolean number (True or False) turning on or off the aerator (Fig.8.9).

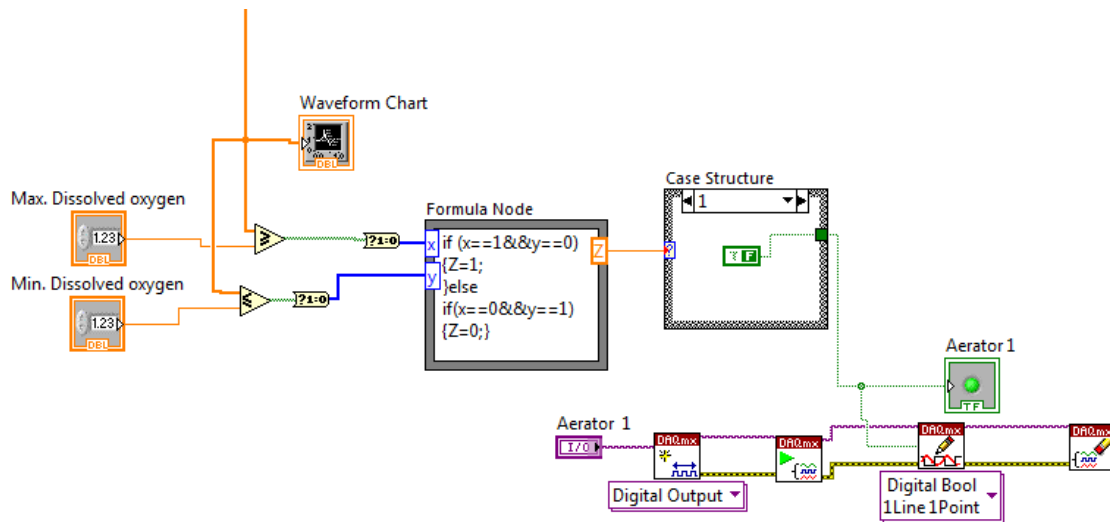


Fig. 8.9. Aerator control

8.1.2. Open loop control coding

For the first and second unit LabView was programmed to make a control on whole pumps in the system (ON/OFF), As Fish biomass in the tank was set the program through the case structure will recognize directly the timing of system operation. The case structure was used as time table for each specific carp biomass in the tank that has the time required to turn ON/OFF the specified RAS unit (Fig. 8.10).

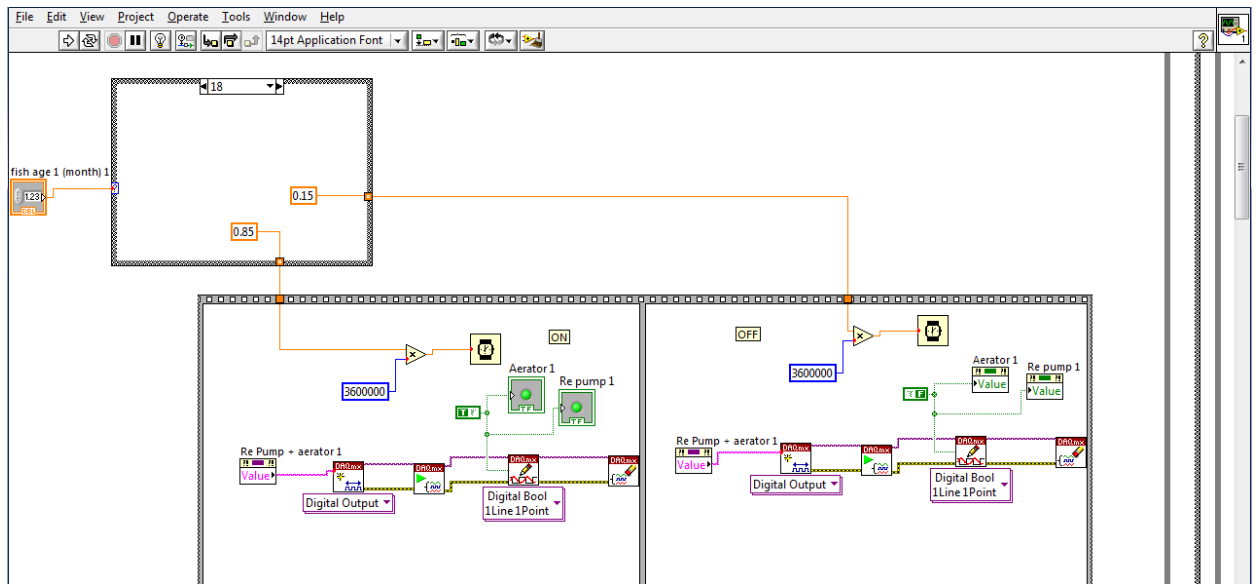


Fig. 8.10. Lab view coding for the first and the third system

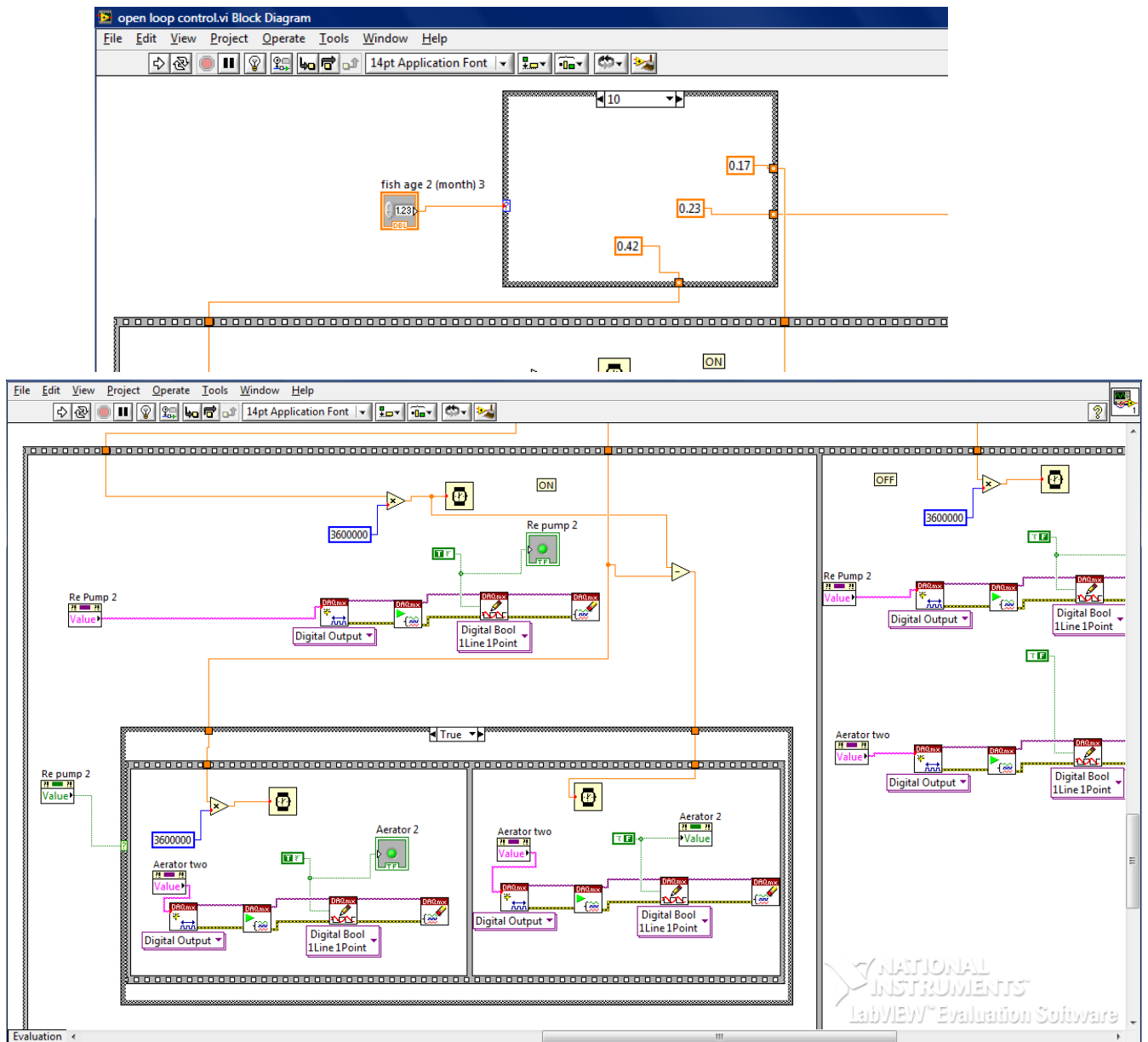


Fig. 8.11. Lab view coding for the second system

LabView coding for the second system was different due to recirculating pump was controlled independently, the coding was done timing the aerator and recirculating pump according to the fish biomass in the tanks, the control of aerator takes in account the state of running of the recirculating pump (e.g. the aerator will not operate if the recirculating pump is not) (Fig. 8.11).

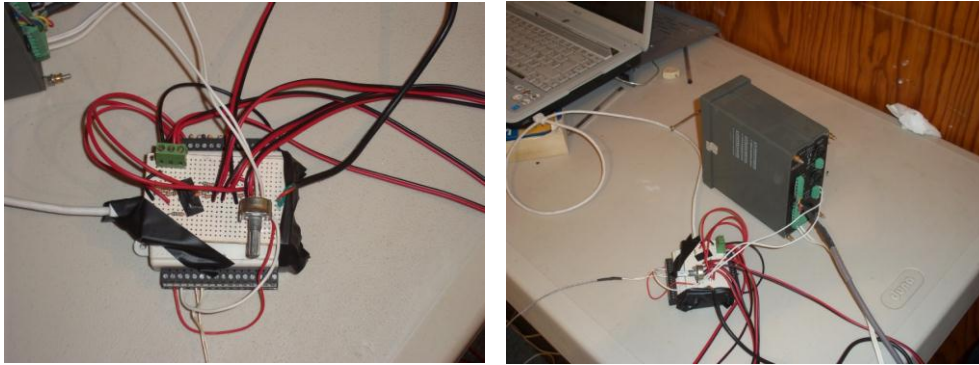


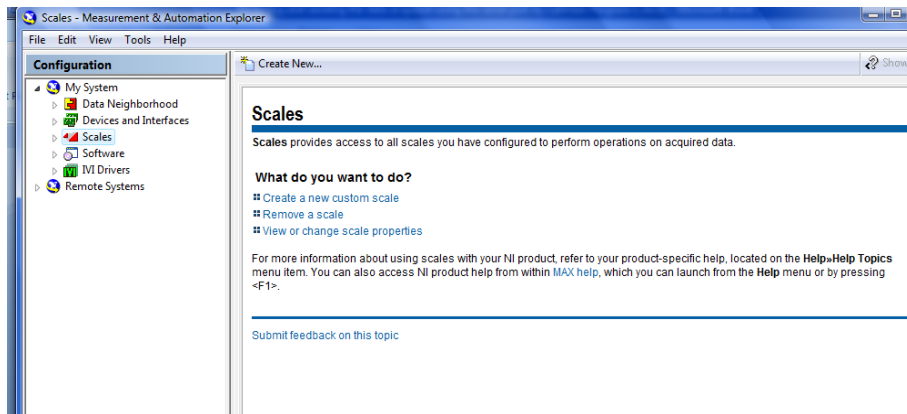
Fig. 8.12. Provided circuit acquisition system of the NI USB 6008



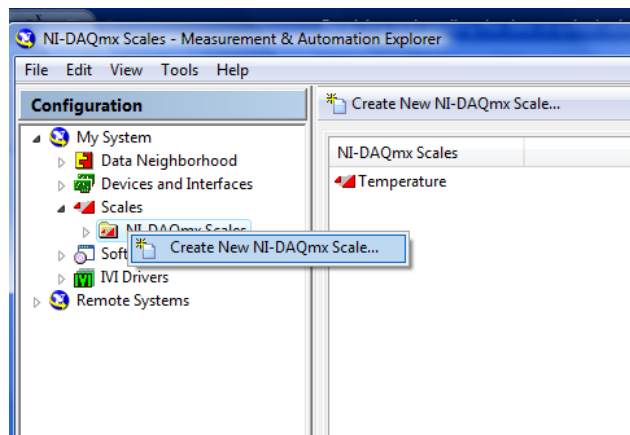
Fig. 8.13. Three inputs of the samples of three tank that was extracted by the peristaltic pumps.

8.1.3. Scales Building for Sensors.

1. Firstly generate a relationship between the 4-20 mA obtained by the sensor and the physical quantity that require to measure, this relationship is polynomial.
2. Secondly Open **Measurement & Automation Explorer** to build the scale, as shown in the following figure.

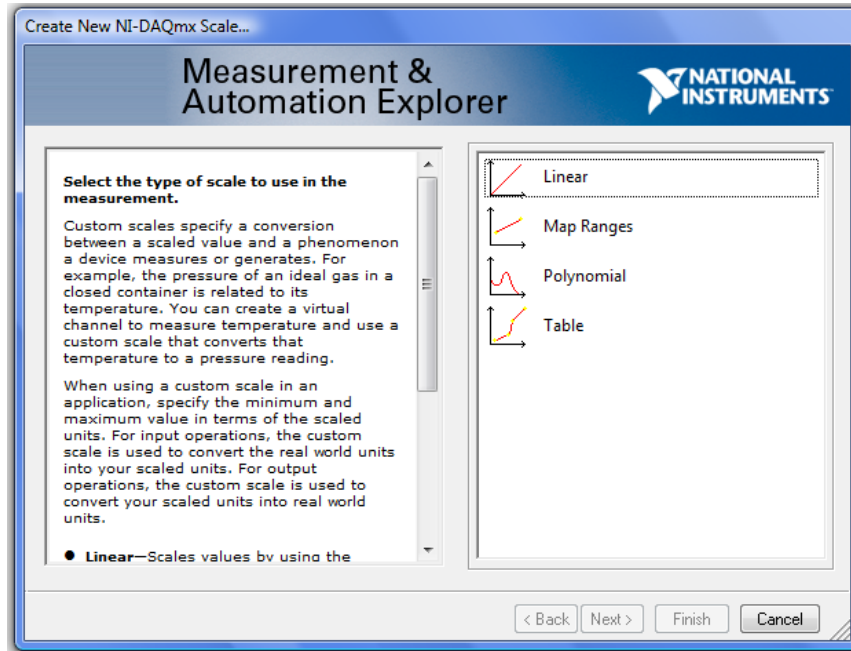


This scale that was made before for the sensor of temperature.

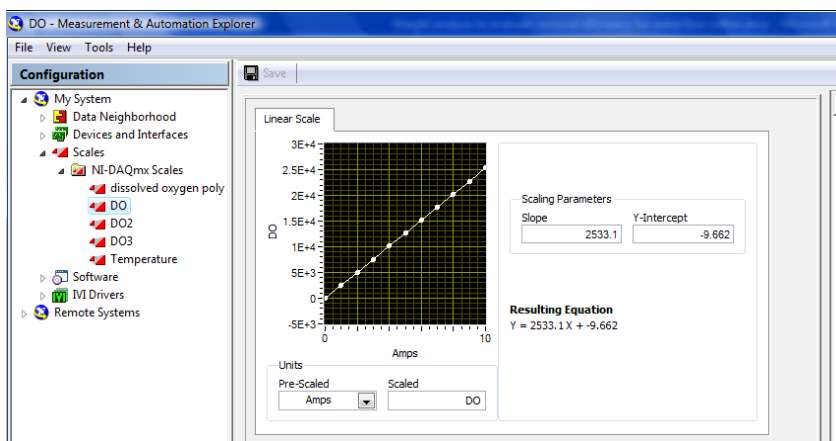


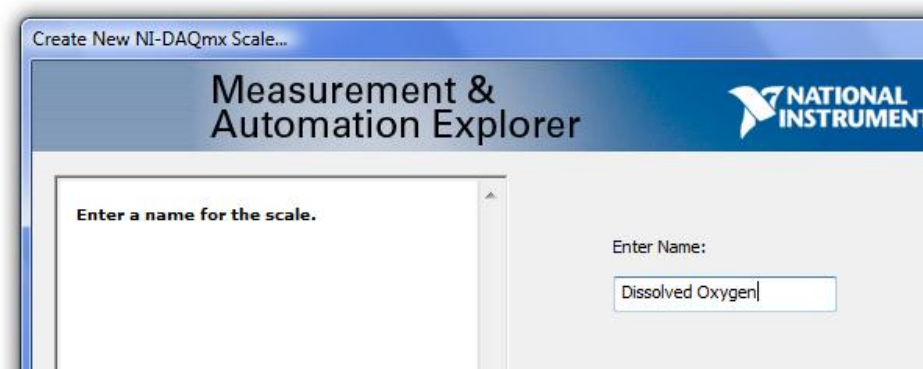
APPENDIX II

Right click on the NI-DAQmx Scale to Create New NI-DAQmx scale and the scale of temperature was made before.

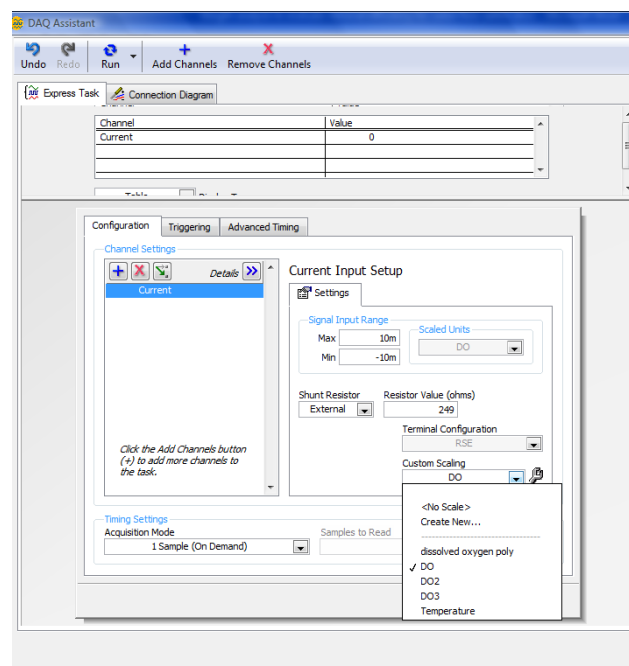


As shown in the figure, there are four types of scales (Linear, Map Ranges, Polynomial and Table) the linear equation was selected to set the equation of DO $Y = 2533.1X - 9.662$ Where X is the ampere, Y is the Dissolved Oxygen.





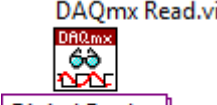
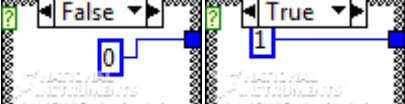
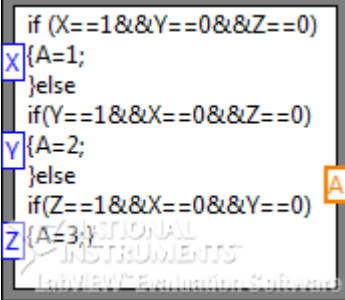
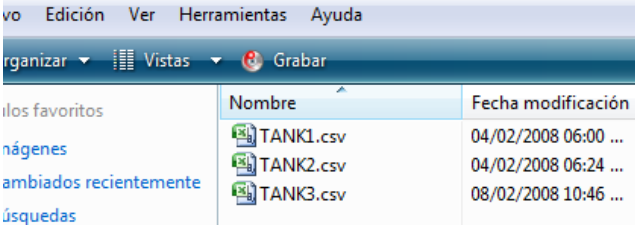
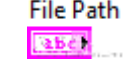
The name of the scale was typed to use later



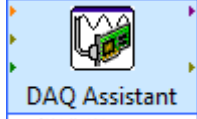
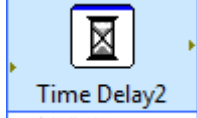
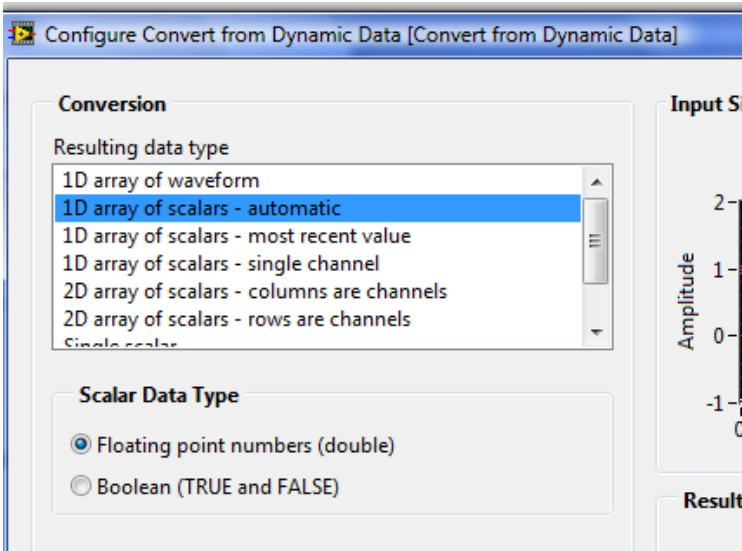
Then we can use this scale for DAQ assistant as shown in the figure from custom scaling.

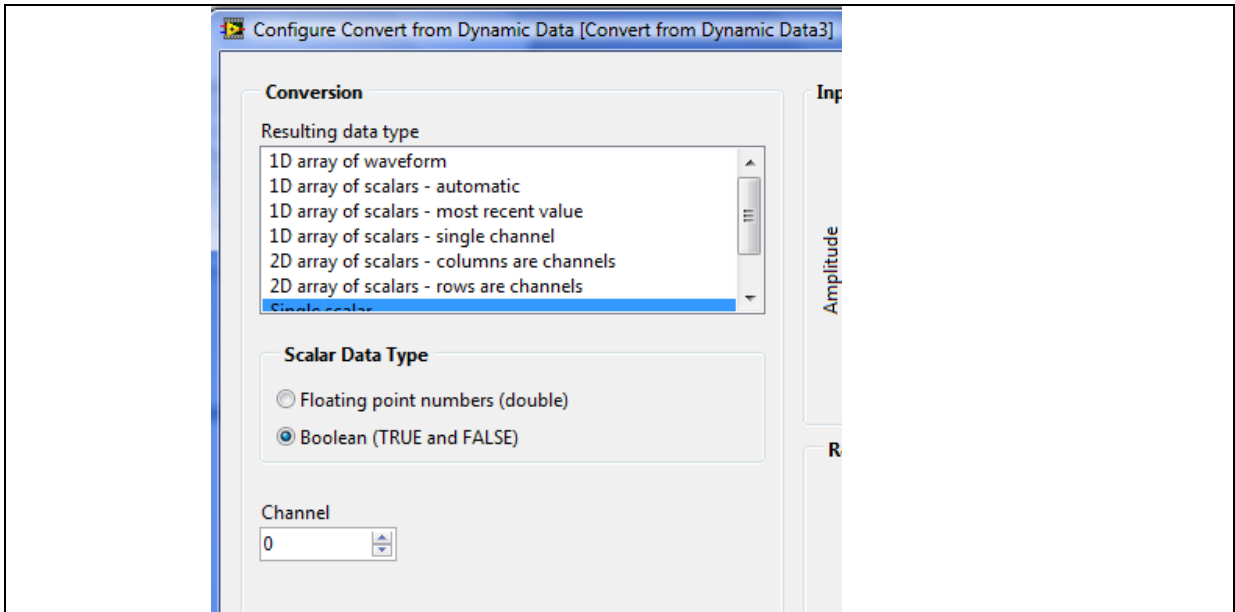
APPENDIX II

Table 8.1. Graphical definitions used in programming

 <p>Digital Input 1</p> 	<p>Create physical channels that specify the name of the physical channel (device name, port number, line number) to use to create virtual channels. The DAQmx physical channel constant lists all physical channels on devices and modules installed in the system.</p>
	<p>Three of DAQmx Create Virtual Channel.vi was placed in the block diagram to create three virtual channel of digital input for the photo optical sensors to use.</p>
	<p>Three of DAQmx Start Task.vi was Placed to running state to begin the analog measurement.</p>
	<p>DAQmx Read.vi was Place and established to read a single Boolean from a task that contains a digital input channel composed of a single line.</p>
	<p>Three case structures were placed to convert three Boolean(True, False) that received from the DAQmx Read.vi to number (0,1) to send 0 or 1 to the formula node.</p>
 <pre> if (X==1&&Y==0&&Z==0) {A=1; } else if (Y==1&&X==0&&Z==0) {A=2; } else if (Z==1&&X==0&&Y==0) {A=3;} </pre>	<p>Formula Node</p> <p>The formula node receive through three ports of variables (X,Y,Z) to send numbers of (1,2,3) to create the names of Tank1, Tank2 or Tank3.</p> 
	<p>While Loop was placed to repeat the subdiagram inside it</p>
	<p>The numbers of (1,2,3)that sent by formula node the Number To Decimal String.vi convert it to string and send it to the Concatenate Strings.vi</p>
 <p>File Path</p> <p>D:\tesis\dissolved oxygen control\Tank</p>	<p>Also the file path send the predetermined location (D:\tesis\dissolved oxygen control\)and the name of required archive Tank to the Concatenate Strings.vi</p>
	<p>Send the extension type (.csv) to the Concatenate Strings.vi</p>
	<p>The Concatenate Strings.vi collect all the strings of the File path, the number (1,2 or 3), and the extension type</p>

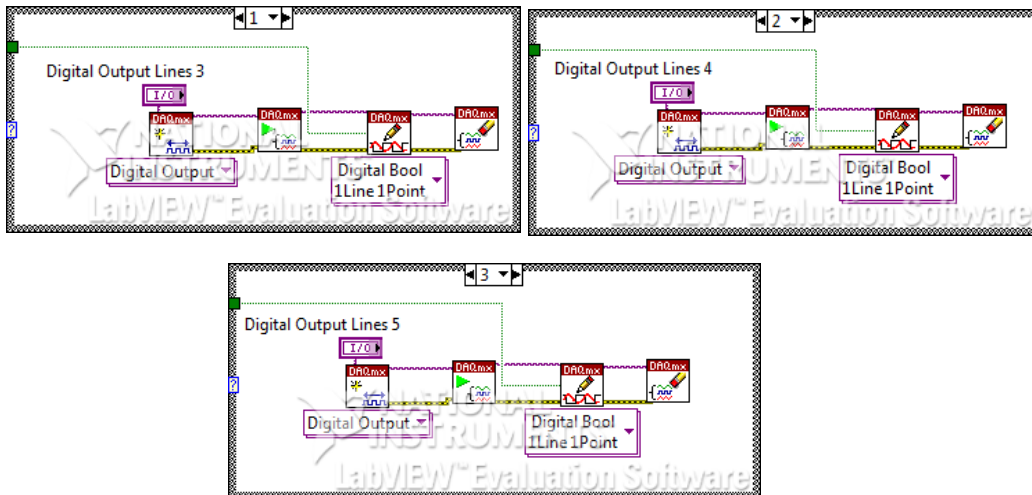
APPENDIX II

 <p>String To Path</p>	<p>Convert the string that sent by the Concatenate Strings.vi to path and send it Write To Spreadsheet File.vi</p>
 <p>DAQ Assistant</p> <p>data</p>	<p>DAQ assistant was placed to continuous acquire measurements from the dissolved oxygen sensor and insert the name of the scale that established before as shown in the section ().</p>
 <p>Time Delay2</p> <p>Delay Time (s)</p>	
 <p>Greater Or Equal?</p>	<p>Greater Or Equal?.vi was used to return TRUE if the measured data is greater than or equal to 4 ppm. Otherwise, this function returns FALSE.</p>
 <p>Less Or Equal?</p>	<p>Less Or Equal?.vi was used to return TRUE if the measured data is less than or equal to 3 ppm. Otherwise, this function returns FALSE.</p>
<p> Convert from Dynamic Data</p> <p>Configure Convert from Dynamic Data.vi to convert the dynamic data to floating point number (double)</p> 	
<p> Convert from Dynamic Data3</p> <p>Configure Convert from Dynamic Data.vi to convert the dynamic data to Boolean number (True or False)</p>	

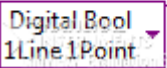
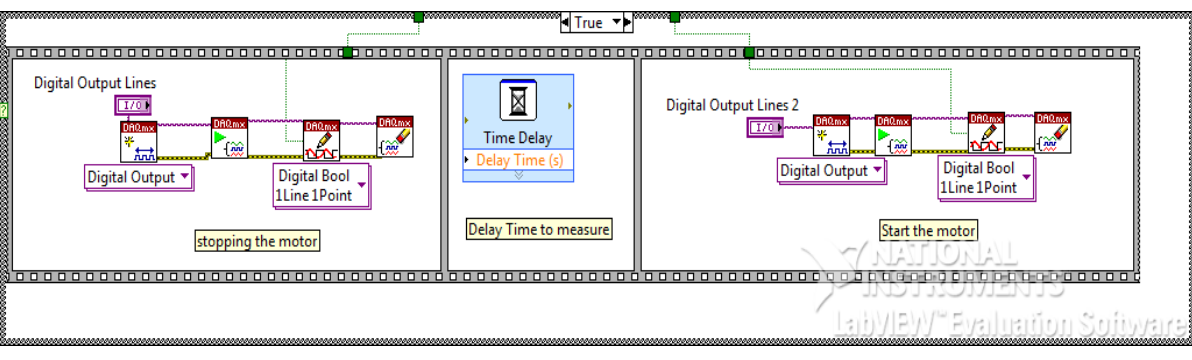


<p>Boolean To (0,1)</p>	<p>Boolean To (0,1).vi was used to convert the Boolean number to 0 or 1 to send it to the Formula Node.vi</p>
<p>Formula Node</p> <pre> x if (x==1&&ty==0) {Z=1; } y else if(x==0&&ty==1) {Z=2;} </pre>	<p>The Formula Node.vi was programmed by C to send 1 or 2 to case structure</p>
	<p>The case structure was set to send TRUE or FALSE to DAQmx write.vi depending the number received (1 or 2)</p>

The case structure was used to send TRUE or FALSE to the specified **DAQmx write.vi** that was established for one of three tanks as shown in the following figures



APPENDIX II

 	<p>DAQmx write.vi was used to write to the channel that connected to the water pump of re-circulating tank</p>
	<p>Write To Spreadsheet File.vi was used to write the data to the predetermined archive append to file was activated by TRUE</p>
 <p>Compound Arithmetic.vi or logic between the three inputs of the sensors of photo optical to take time delay of 2 minutes to acquire the data from the valve by first stopping the motor and return start it as shown in the following figure</p> 	

Appendix III

Elsevier Editorial System(tm) for Aquacultural Engineering
Manuscript Draft

Manuscript Number:

Title: Aquaculture intelligent dissolved oxygen system for monitoring, controlling and sensor anti-fouling

Article Type: Full Length Article

Keywords: dissolved oxygen monitoring, system control, auto-calibration, fish feeding, carps

Corresponding Author: Dr Federico F Hahn, PhD

Corresponding Author's Institution: Universidad Autonoma Chapingo

First Author: Federico F Hahn, PhD

Order of Authors: Federico F Hahn, PhD; Wael El-messery, M. Sc.

Abstract: Success in designing affordable automated control systems for aquaculture will be widely applicable as it enhances water management. Intensive recirculation systems have the potential for increasing fish production per volume of water but require of dissolved oxygen monitoring and control. An intelligent LabView dissolved oxygen sensing unit was designed using only one oxygen sensor and its transmitter for monitoring several tanks. Peristaltic pumps extracted water from each tank without adding oxygen to the sample. Measurements were auto-calibrated and statistically diagnosed using air dissolved oxygen measurements. Dissolved oxygen sensor membrane fouling from algal blooms, sediments or suspended droplets was analyzed; the system controlled membrane fouling problems by means of motor vibration and water jets. An experiment monitored dissolved oxygen changes to determine carp digestive and growth respiration hours.

Chapingo, Texcoco, Mexico 5 November 2011

We would like to submit the article:

**Aquaculture intelligent dissolved oxygen system for
monitoring, controlling and sensor anti-fouling**

So that it can be revised and evaluated.

We don't know if the area we chose was the best for this article. We choose chemical sensors as it is a galvanic sensor.

Thanks in advance for your kindness,

Dr. Federico Hahn

REVIEWERS

Suggested Reviewers: Irineo Lopez PhD
Professor, Irrigation, Universidad Autonoma Chapingo
ilopez@correo.chapingo.mx

He is the best model designer for control systems in the University and he is well recognized worldwide

Fedro Zazueta Dr
Professor, Agricult Engineering, UNiversity Florida
fsz@ufl.edu

He has worked in many designs and is one of the main professors worlwide in information tecnology

Brian Boman PhD
Professor, Crop management, University of Florida
BJBoman@mail.ifas.ufl.edu

He is an excellent professional working with sensors and fouling. His opinion will be interesting

Paper Highlights

Dissolved oxygen is a parameter that requires accurate monitoring. Sensors are expensive, so only one sensor and one transmitter was used for monitoring and controlling four tanks

Algae and solids fouling on the sensor membrane were studied and the system provides codes in case of failure.

Antifouling techniques were studied and developed.

An alternative PV system enters under sensor or line faults providing oxygen for fish survival

1 **Aquaculture intelligent dissolved oxygen system for**
2 **monitoring, controlling and sensor anti-fouling**

3 Federico Hahn; Wael El messery

4 Universidad Autónoma Chapingo, km 38.5 Carretera México-Texcoco,

5 Chapingo 56230, México

6 Email: fhahn@correo.chapingo.mx

7 **ABSTRACT**

8 Success in designing affordable automated control systems for aquaculture will be
9 widely applicable as it enhances water management. Intensive recirculation systems
10 have the potential for increasing fish production per volume of water but require of
11 dissolved oxygen monitoring and control. An intelligent LabView dissolved oxygen
12 sensing unit was designed using only one oxygen sensor and its transmitter for
13 monitoring several tanks. Peristaltic pumps extracted water from each tank without
14 adding oxygen to the sample. Measurements were auto-calibrated and statistically
15 diagnosed using air dissolved oxygen measurements. Dissolved oxygen sensor
16 membrane fouling from algal blooms, sediments or suspended droplets was analyzed;
17 the system controlled membrane fouling problems by means of motor vibration and
18 water jets. An experiment monitored dissolved oxygen changes to determine carp
19 digestive and growth respiration hours.

20
21 **Keywords:** dissolved oxygen monitoring, system control, auto-calibration, fish feeding,
22 carps

1
2
3
4
5
6
7
8
9
10
11
12
13
14
15
16
17
18
19
20
21
22
23
24
25
26
27
28
29
30
31
32
33
34
35
36
37
38
39
40
41
42
43
44
45
46
47
48
49
50
51
52
53
54
55
56
57
58
59
60
61
62
63
64
65

32 1. Introduction

33 Automation of aquaculture systems locates the production closer to markets, improve
34 environmental control by minimizing effluents, reduce production costs and improve
35 product quality. Today aquaculture automation has become an alternative to producers
36 with the decrease of computers & software cost, and off-the-shelf monitoring hardware
37 cost. The monitoring required for recirculating aquaculture systems (RAS) depends on
38 system design, fish life stage and fish density.

39 Aquaculture managers need accurate, real time information on system status and
40 performance, in order to maximize their production potential. At high production
41 densities, failure of a circulation pump or aeration system can result in fish severe stress
42 or even significant losses within minutes ([Appelbaum et al., 1999](#)). LabView is a widely
43 used graphical programming environment which allows designing systems in an
44 intuitive block-based manner ([Pereira et al., 2008](#); [Bart, 2002](#)); it could acquire
45 dissolved oxygen (DO) and temperature data, process them to control sophisticated
46 aquaculture systems. Sensors measuring critical factors can be linked to an automatic
47 telephone dialer for remote diagnostic and prevention of catastrophic losses ([Lee, 2000](#)).
48 Fish grow quicker with optimum temperature, achieving improved food conversion
49 ratios; fish feed poorly beneath 16°C and death will occur beneath 12°C ([Chervinski,](#)
50 [1982](#)).

51
52 After meeting fish feed requirements, low concentration of dissolved oxygen is the
53 major variable that limits fish growth and production in intensive aquaculture and
54 should be kept above 5 ppm. Although several dissolved oxygen sensors are used in
55 aquaculture applications, galvanic and luminescence sensors are now-a-days commonly
56 employed. Galvanic cells avoid sulfide poisoning, reduce anode maintenance and use a
57 constant pH electrolyte solution; no external voltage polarization is required and it
58 works quicker as no warm-up time is necessary ([Eutech Instruments, 2006](#)). [Bryan and](#)
59 [Cushman \(1991\)](#) developed a real time on-line system for monitoring dissolved oxygen
60 testing galvanic sensor membrane impedance and studying its response. Luminescence-
61 based devices quantify O₂ nondestructively as color changes with oxygen variations
62 ([Evans and Douglas, 2006](#)).

63
64
65

1
2
3
4
5
6
7
8
9
10
11
12
13
14
15
16
17
18
19
20
21
22
23
24
25
26
27
28
29
30
31
32
33
34
35
36
37
38
39
40
41
42
43
44
45
46
47
48
49
50
51
52
53
54
55
56
57
58
59
60
61
62
63
64
65
66
67
68
69
70
71
72
73

Algae blooms and fine solid particles are identified as water foulants and affect DO measurements; silica and organic matter become part of the sensor membrane (Howe et al., 2002; Schafer et al., 2000; Lander et al., 2010). Algae produce oxygen during photosynthesis and consume oxygen through the process of respiration (Vasile, 2008; Tafangenyasha et al., 2010); fish die on warm summer nights due to algae blooms excessive oxygen consumption (Stone and Daniels, 2006). The sensor membrane and optical path require an effective cleaning system, as the ultrasonic module integrated to the VisoTurb® 700 IQ (Wissenschaftllch-Technische Werkstatten, 2011).

74
75
76
77
78

In this study, dissolved oxygen was monitored and controlled. The controller was interfaced to LabView and used one dissolved oxygen sensor and transmitter to control four fish tanks; the system presented auto-calibration, statistically self-diagnostic and anti-fouling mechanisms. The choice of the system's architecture was based on price performance considering labor, product value, environment and vendor support.

79 **2. Materials and methods**

80
81
82
83
84

The work was divided in four strategic areas: (1) Installation of equipment for DO monitoring from the four tanks; (2) analysis and detection of different membrane antifouling problems; (3) development of an alternative energy system to assure fish survival and (4) development of a LabView program that monitors the data, stores it, control the aerators and diagnostic sensor status.

85 *2.1. Recirculation aquaculture system*

86
87
88
89
90
91
92
93
94
95

The aquaculture recirculation system (Fig. 1) is located at Tlapeaxco, Chapingo, Mexico at the experimental camp of the Universidad Autonoma Chapingo. The system installed within a greenhouse consists of four circular polyethylene tanks having a diameter of 1.1 m and a capacity of 1100 liter. The tanks were positioned within a square area of 10 by 10 m with the monitoring and control unit at the centre. The four tanks were stocked at different time to obtain one harvest every 37 days being the harvest size of 400 g after 5 cultivation months. Stocking density per tank was of 50 organisms per m³, and cultivated carps presented an initial weight of 25 g. The first tank was cultivated in December, the second in January, the third in February, and the fourth in March with mirror carp var. *Cyprinus carpio*.

1
2
3
4
5
6
7
8
9
10
11
12
13
14
15
16
17
18
19
20
21
22
23
24
25
26
27
28
29
30
31
32
33
34
35
36
37
38
39
40
41
42
43
44
45
46
47
48
49
50
51
52
53
54
55
56
57
58
59
60
61
62
63
64
65

96 Carps were fed with Nutripec 3508 at 9:00, 14:00 and 19:00 hr. The water from each
97 culture tank circulated through the solid waste separator before entering to a trickling
98 biofilter having polyethylene bio-strata as media. A spray column aerator oxygenated
99 the water using fine jet sprays (mod. 130327, SURTEK, MEX); the conical water spray
100 increased the oxygenation efficiency as a better contact area between water and air
101 exists. The column aerator employed an air fan driven by a 1/2 hp induction motor.

102 The photovoltaic system (PV) stored energy in the batteries, and an inverter converted
103 DC to AC voltage (Hahn, 2010). Batteries and solar panels were selected considering
104 the day having the highest energy consumption (2076.787 W.h/day). During this day the
105 aerators worked 20 continuous hours oxygenating water for a carp biomass density of
106 25 kg per cubic meter. A line power failure of 14 continuous hours occurred once a
107 month; batteries should recharge every two weeks and last for 14 hours. A line fault
108 was carried out analyzing dissolved oxygen variations for 200 and 400 grams carps.
109 Energy saving of the aerators was studied under three on-off periods: 1 hr on-1 hr off; 1
110 hr on-0.5 hr off and 1.33 hr on-0.75 hr off. As batteries are charged in 14 days by a solar
111 panel having six irradiance hours over 1000 W.m²/day it should provide 57.6 Ah daily;
112 a 200 W solar panel was selected (mod. ES-A-200, EvergreenSolar, USA).

113 114 *2.2. DO monitoring equipment*

115 The monitoring system was designed to measure the four tanks DO using only one
116 sensor and one controller. A galvanic probe (HI 76410/4, Hanna Instruments, USA) was
117 connected to a panel mounted controller (mod. HI 8410, Hanna Instruments, USA). A
118 membrane covered the galvanic probe having a built-in thermistor for temperature
119 compensation; an electrolyte solution (mod. HI 7041S, Hanna Instruments, USA)
120 refilled the membrane cap. The probe provided a 0.1 mg/L O₂ resolution with a
121 temperature accuracy of ±0.2°C. Calibration is performed with HI 7040L zero oxygen
122 solution while 100% calibration is done when the probe contacts the air. The controller
123 4-20 mA recording output was connected to a USB acquisition board (mod DAQ NI-
124 USB 6008, National Instruments, USA) and then introduced to the PC computer.

125
126 Water sampling was provided by 25W@0.356 liter/min peristaltic pumps (mod.
127 41k25GN-AUL-ES, Oriental Motor Co. LTD, Japan). Water samples from each tank
128 are pumped to the 5° slope hydraulic head (Fig. 1) passing by the DO probe before

129 returning to the tank. Peristaltic pump poor suction required to be primed prior
130 pumping; suction hose inlets were placed below the pumping level, (Fig. 1). A black
131 polyethylene U-mounted hose (internal diameter of 0.65 cm) had its input 30 cm
132 beneath the tank water surface. After adding a 50 cm hose, the input was placed 80 cm
133 beneath the water surface.

134

135 As the distance between the sampling tank and the hydraulic head varied DO
136 measurement delay time had to be programmed. The time required for the water sample
137 to arrive from the first tank (3.3 m away) to the DO probe was of 23.5 or 20.1 seconds
138 according whether the hose inside the tank was 80 or 30 cm deep, respectively. The
139 fourth tank (5.2 m away from the hydraulic head) required 33.4 or 37 seconds before the
140 water sample arrived to the DO probe if the hose was 30 or 80 cm deep, respectively.
141 The sample taken from one depth was programmed at the user interface by a toggle
142 switch named *peristaltic pump automatic sampling*.

143

144 The automated monitoring system starts operating when the peristaltic pump sucks a
145 water sample from the first tank. Maximum dissolved oxygen values of 6.4 ppm (rose
146 marks) were measured during the first 20 seconds and within the 100-120 second
147 interval that starts the new reading cycle (Fig. 2). The galvanic probe measurement
148 settles down after 60 seconds; the controller acquires thirteen values (green marks) and
149 stores them in the LabView data logger. The thirteen values are averaged and when the
150 standard deviation exceeds 0.3 ppm, a fault exists within the monitoring system; another
151 thirteen measurements should be taken. When the average dissolved oxygen value is
152 beneath a given set point the first aerator will be turned-on; it could be turned-off after
153 the next measurement but to avoid excessive motor current peaks it will be disconnected
154 ten minutes after. Once the peristaltic pump is turned-off, the water remaining within
155 the hydraulic head returns to the tank and air will fill-up the hydraulic head. This
156 operation is repeated for each tank being each aerator controlled separately.

157

158 2.3. Acquisition system and LabView interface

159 A multifunction DAQ NI-USB 6008 acquisition board acquired the DO values from the
160 controller and its configuration is shown in Table 2. Port 0 turns-on each peristaltic pump and
161 every aerator fan. The dissolved oxygen analyzer HI 8410 provided a 4-20 mA output current
162 connected in single-ended mode between terminals 1 and 2. Digital terminals P1.2

163 monitors the electrical voltage status in the system and P1.3 activates the inverter of the
164 alternative photovoltaic energy during faulty line situations.

165 The LabView data logger was programmed by the user to control when DO monitoring
166 start for each tank due to variable distance to the galvanic probe at the hydraulic head.
167 Data from each tank was saved in a different Excel file and every new reading was
168 appended. The user interface acknowledges which peristaltic pump is operating and
169 recognizes which fish culture tank is being sampled. Maximum and minimum dissolved
170 oxygen set points are introduced at the user interface to control aerator turn-on; leds
171 indicate aerator operation (Fig. 3).

172 After plotting daily DO values sensor operation can be diagnosed. P1.0 and P1.1
173 controlled sensor cleaning during autocalibration when sensor fouling problems were
174 encountered. After diagnosing a sensor problem, cross sampling between different tanks
175 verified that the problem exists. The program automatically codified error messages in
176 the LabView Front panel-User Interface. The code is generated after that the problem
177 subsists after water jet injection or vibration and sent by phone to a desired cellular.

178 LabView was programed to execute an alternative program as a fixed timer under
179 emergency situations when the monitoring system failed. Under a given water
180 temperature and biomass density the program calculates the required aeration time per
181 tank to maintain the dissolved oxygen within 4 and 5 ppm, Table 3. When an
182 intermediate biomass is present, interpolation was used to determine the required
183 aeration time; for example, a biomass of 12 kg@ 19°C per m³ will require 10.1 hr of
184 aeration.

185

186 *2.4. Sensor calibration and fault analysis.*

187

188 The sensor auto-calibration scale equation used the air saturation value (6.3 ppm @ 20
189 °C @ 2400 m above sea level) as the first calibration point; for the second point a zero
190 oxygen solution HI 7040 was used once a month. The scale equation used for
191 calibration depends on the current I given in mA:

$$192 \quad DO = 2533.1I - 9.662 \quad (1)$$

193

194 In recirculation aquaculture systems (RAS) dissolved oxygen sensors encounter
195 periodic problems during carp growth. Solid particle accumulation at the sensor
196 membrane is encountered for very fine particles below 40 μm . Algae blooms also
197 accumulate on the membrane and affect sensor readings; blooming dinoflagellates
198 ranging between 10 and 50 μm in size pass through inlet screens. Sometimes, after
199 evacuating the water sample from the hydraulic head, water droplets remain suspended
200 on the membrane affecting sensor measurements. Another common measurement error
201 occurs after exchanging the electrolyte or the sensor membrane as air bubbles remain
202 within the electrolyte if not properly installed.

203
204 The effect of DO variations under membrane sediment accumulation was studied. DO
205 was measured at air saturation and then 100 ml of distilled water were sprayed to the
206 sensor head storing the water with particles and measuring its turbidity (DRT-15CE, HF
207 Scientific Inc., Ft. Myers, FL). Three different algae blooms (*Scenedesmus sp.*,
208 *Chlorella sp.* and filamentous microalgae) were reproduced over the galvanic sensor
209 membrane measuring DO values under air saturation prior to cleaning the sensor with
210 distilled water to quantify them with the turbidity sensor.

211
212 The hydraulic sensor head was equipped with an automated water spray to clean the
213 sensor membrane. A 100 W submersible pump (mod. 2480, Kairui Electrochemical,
214 China) produced a working pressure and flow of 15 kPa and 500 cm^3/min , respectively;
215 the water spray resulted from passing the water through a nozzle having a diameter of
216 1.7 mm. The water spray operated for 5 seconds to remove algae and suspended solids
217 adhered to the membrane. A vibrating motor (mod 30827 CRA212-ND, Cramer Co.
218 Digi-Key, USA) with an eccentric disc removed the droplets; the 18W@ 12 VDC motor
219 rotated at 60 RPM. The motor turns ten revolutions every five days offering
220 maintenance to the sensor membrane.

221
222 Another antifouling hydraulic head was designed for cleaning the sensor membrane on-
223 line instead of using a spray nozzle. This system is based on backwash solid removal of
224 irrigation system filters (Bucks et al., 1979; Gilbert et al., 1981). Three orthogonal water
225 sample inlets coming from different tanks entered the hydraulic head and left through
226 the fourth hole after passing through the DO probe (Fig. 4). Algae blooms were grown

227 over the membrane and backwash removal was analyzed. Similarly, the membrane was
228 covered with fine particles to observe its removal by this method.

229 *2.5. Oxygen consumption and water temperature for carp growth*

230 The system was tested with an experiment where dissolved oxygen was monitored
231 during all the day to determine digestive and growth respiration hours. During this
232 experiment two daily meals were applied at 11:16 and 18:30 hr with a feed ratio of 6%
233 of fish bio-mass. Temperature was also monitored to determine its effect in fish feeding.

234

235 **3. Results**

236

237 Sampling with peristaltic pumps and dissolved oxygen data management worked as
238 planned; it could work properly for measuring several tanks at different depths.
239 Peristaltic pumps as pressurized equipment are not efficient but for sampling without
240 gaining oxygen are useful. LabView was easy to use, having a simple hardware-
241 software interaction; for example when the sensor fails the aerator timing table gives
242 enormous flexibility to the system.

243

244 Energy consumption by the peristaltic pumps, re-circulating pumps and the aerator was
245 16.8, 907 and 1,153 W.h, respectively. Energy of 807.2 W was consumed per day when
246 the aerator turned-on for periods of 1.33 h in order to oxygenate the tank with 400 g
247 carps. A bank of five 12 V@250 Ah rechargeable LiFePO₄ batteries (Model OPT-200,
248 Optimum Battery Co., Ltd, China) was used together with a current battery charger. A
249 375 W, 12V DC - 120V AC inverter (mod PV-375, Tripp Lite, USA) was selected to
250 provide AC energy to the aerator and re-circulating pumps.

251

252 During lack of energy dissolved oxygen decreased from 5 to 2.3 ppm for carps
253 weighting 400 grams in tank 1. At 21:45 hr, batteries were turned on for 1.33 hour
254 increasing DO to 4.93 ppm. Dissolved oxygen oscillated between 2.3 and 5 ppm until
255 9:25 AM consuming energy for 8 hours. In tank 2, dissolved oxygen in the water
256 presented oscillations ranging between 3.33 and 5.2 ppm for 400 g carps; battery
257 consumption was of 8 hours. For lower size carps (200 grams), dissolved oxygen varied
258 between 3 and 5 ppm being battery energy consumed in 6 hours (Fig. 5).

259

1
2
3
4
5
6
7
8
9
10
11
12
13
14
15
16
17
18
19
20
21
22
23
24
25
26
27
28
29
30
31
32
33
34
35
36
37
38
39
40
41
42
43
44
45
46
47
48
49
50
51
52
53
54
55
56
57
58
59
60
61
62
63
64
65

3.1. DO probe fouling

DO measurement varies as the probe oxidizes (Fig 6a) affecting its response speed; although anode corrosion there is enough anode material for many years of use. Measurement errors are found during algae (Fig 6c) and colloid (Fig 6d) fouling.

As the electrolyte gets consumed, low level measurements with 1.2 ppm peaks are obtained (Fig. 7) requiring the addition of the electrolyte solution (Smith et al., 2007). Membrane is normally replaced twice a year and when damaged a DO saturation value of 4 ppm is measured followed by a peak which decrements its value to zero; afterwards, the DO value returns immediately to the saturation value, as shown in figure 7 by the violet line. The user should gently tap the membrane to guarantee that no air bubbles remain trapped.

Proper DO saturation values (purple marks) range between 6.1 and 6.5 when the probe is in contact with air (Fig. 8). Sediment accumulation (SA) over the membrane presented during DO saturation peaks centered at 5 ± 0.2 ppm. Once the sediments were removed with distilled water a turbidity of 50 NTU was encountered. When the membrane is cleaned (TSA) with the water jet, a DO saturation value of 6.2 ppm is obtained. Algae accumulation (AA) around the membrane produces oxygen increasing its DO value to 7.5 ppm. Analysis of water samples under super-saturation by Woodbury (1941) showed excess DO values ranging from 17.74 ppm to 23.14 ppm. Fish reactions to DO excess were swimming at an angle and then floating up at surface in a helpless manner. When a biofilm of algae covers the sensor membrane oxygen diffusion drops-off decreasing DO measurements. After spraying water (TAA) the probe measured correctly again, and the algae dissolved in water provided a turbidity of 166 NTU. Suspended water droplets (SWD) on the membrane decreased DO values; measurements returned to normal when the vibrator motor (TSWD) removed the droplets.

3.2. Antifouling mechanisms

Self-backwash and nozzle spray for membrane anti-fouling was extremely better than leaving the probe without any treatment. Dissolved oxygen saturation measurements decreased to 5.3 ppm after five weeks of operation when no anti-fouling treatment was employed. The spray nozzle was the most reliable mechanism due to the reduced

1
2
3
4
5
6
7
8
9
10
11
12
13
14
15
16
17
18
19
20
21
22
23
24
25
26
27
28
29
30
31
32
33
34
35
36
37
38
39
40
41
42
43
44
45
46
47
48
49
50
51
52
53
54
55
56
57
58
59
60
61
62
63
64
65

295 peristaltic pump pressure applied to the membrane. A high water flow of 27 l/min
296 (velocity=14 m/s) was applied to remove the solids accumulated over the sensor
297 membrane. In continuous backwash operation, solids and algae were removed from the
298 membrane surface and dissolved oxygen saturation measurements remained within 6-
299 6.5 ppm range, Fig. 9. It is recommended that under backwash treatment a high pressure
300 treatment is applied every six weeks. Air bubbles within the electrolyte were removed
301 by the user meanwhile vibration gets rid of suspended water droplets.

302

303 *3.3. Oxygen consumption and water temperature for carp growth*

304 Feeding is often strongly affected by reduced oxygen (Carlson et al., 1980; Kramer,
305 1987). Search, digestion and assimilation are major components of the energy budget of
306 many fishes (Brett and Groves, 1979). Digestive respiration increased oxygen demand
307 by 0.03 gO₂/kg[BM].h during three hours. Growth respiration was detected between
308 9:16 PM and 3:26 AM, being the maintenance respiration at 17 °C of 0.32
309 gO₂/kg[BM].h. Fish respiration varied during the day and was limited by water
310 temperature decreasing from 0.422 to 0.32 gO₂/kg[BM].h, (Fig. 10). As water
311 temperature decreased from 20 to 17 °C, fish activity decreased as well as oxygen
312 consumption from 4:26 to 11:16 AM.

313

314 **4. Discussion**

315 Pneumatic bladder, submergible pumps or peristaltic pumps are well suited for low-
316 flow purging and sampling. Low stress purging and sampling is a technique being used
317 in wells where the flow rate of water being extracted is less than the one entering the
318 well. However, peristaltic pumps are not suitable for use in wells containing
319 contaminants or suspended solids. Assuming a static lift of 2 m, the pump suction lift
320 will be 5 m, resulting in a maximum hose length of about 50 m (Van Rijn, 1979). Hoses
321 were fixed within the culture tanks in one extreme in order that fishes didn't move its
322 position; total length from the largest hose used was 10.5 m.

323 Output pressure is always an assay on peristaltic pump applications, although some are
324 used only for sampling. Under different output pressure of two peristaltic pumps the
325 volume metered per pump revolution remained almost constant, Way et al, 1990.
326 Temperature was not a factor within the black hoses avoiding algae formation.

1
2
3
4
5
6
7
8
9
10
11
12
13
14
15
16
17
18
19
20
21
22
23
24
25
26
27
28
29
30
31
32
33
34
35
36
37
38
39
40
41
42
43
44
45
46
47
48
49
50
51
52
53
54
55
56
57
58
59
60
61
62
63
64
65

327 Dissolved oxygen at the water kept within the hose at the middle of the day varied by
328 3% as water temperature increased by 2°C. It is recommended to clean the hoses with a
329 pressurized pump every two weeks to avoid solid deposition inside them.

330
331 A future design should consider a multi-pump module (mod. MD4, DASGIP AG,
332 Jülich, Germany) where the speed of each peristaltic pump can be controlled
333 electronically and adjusted individually. The built-in microprocessor and the serial
334 interface allow straightforward PC support and can be easily managed by the LabView
335 interface. If the MD4 is fixed at the hydraulic head the variable distances from the tanks
336 become irrelevant for timing the DO acquisition routine; this operation is possible as
337 each pump can work at a different speed using the same delay for the four tanks.

338
339 Once that proper maintenance is given to the galvanic probe it sensed accurately with a
340 good speed response. A galvanic probe let in a pond without care accumulates algae or
341 solids over the membrane; erroneous measurements are obtained as oxygen diffusion
342 through the membrane disappears. As a result, the response time is unaffected, but
343 dissolved oxygen magnitude changes. Very fine particles below 40 µm ([Glasspool and](#)
344 [Atkinson, 1998](#)) are difficult to extract and accumulate at the sensor. Adhesion forces
345 attract fine solid particles to the sensor membrane, and after long accumulation time,
346 nitrification bacteria grow on the membrane affecting measurement readouts ([Whelan](#)
347 [and Regan, 2006](#)). Calcium appears to form a bridge between the membrane surface and
348 the organic foulants ([Ahn et al., 2008](#)).

349
350 Algae blooms can accumulate over the sensor membrane and affect sensor readings;
351 blooming dinoflagellates in a size ranging between 10 and 50 µm pass through the inlet
352 screens. Their neutral buoyancy and ability to swim make them a settling material
353 ([Pierce et al., 2004](#)). As algal bloom life cycle peaks and decays, a significant amount of
354 organic material is released upon cell death ([Whipple et al., 2005](#)). Bacteria feed on the
355 decaying material and release their own extracellular polymeric substance (EPS) that
356 has the potential to foul pretreatment and RO membranes ([Asatekin et al., 2006](#);
357 [Rosenberger et al., 2006](#)). It is possible that the material from decomposition fouls the
358 membrane more than the algal cells themselves.

359

360 Self-contained air blast cleaning systems clean automatically DO sensors membranes
361 with a pressurized air jet of 300 kPa (GLI, 2008). Oxyferm, Oxygold and Clark model
362 5500 DO probes (GLI, 2008) withstand maximum pressures of 400, 1200 and 1000 kPa,
363 respectively. The backwash cleaner was efficient maintaining a constant value during
364 five weeks. If a non-maintenance equipment is requested the vibrating motor and the
365 pressure jet should be applied.

366
367 LabView has become a very useful instrumentation tool, being able to acquire, analyze,
368 control and activate different fans and pumps. Its application in aquaculture as an
369 intelligent DO sensor fault detector, can advice the producer when a failure is present
370 meanwhile it can still oxygenate the tanks. In case that a power failure exists, it is
371 necessary to optimize the energy saved in the PV batteries; the LabView interface
372 indicates the amount of energy being available. Two power failures were present one of
373 5 hours and another of twelve hours one per month and the carps survived with the
374 alternative energy. During line loss energy an alternative PV system was used and
375 dissolved oxygen was maintained between set levels allowing fish survival under
376 optimum energy consumption. For the experiment with longest turn-on time (ton:1.33
377 hr, toff: 0.75 hr & 400 g carps) only 40% of the time dissolved oxygen was below 3.5
378 ppm, being its minimum value 2.3 ppm. At this time carps were at the top searching for
379 air in the atmosphere.

380 One of the most common sensor errors occurred during membrane exchange when the
381 user did not take care of air bubble formation within the electrolyte; high peaks were
382 detected by the LabView program sending a 2-0041 message code, Table 4. Three
383 additional codes informed about the battery remaining charge to the producer. As the
384 alternative energy system works, battery gets discharged by 30, 60 or 90% generating
385 and transmitting 2-0071, 2-0081 and 2-0091 codes, respectively.

386

387 **5. Conclusions**

388 Dissolved oxygen in fish production systems should be monitored and controlled as it is
389 a vital factor for fish production and survival. One galvanic sensor and its controller
390 were used for managing four culture tanks. The sensor was checked previous to each
391 measurement when it was in contact with the air. An intelligent instrumentation system
392 monitored the tanks, predicted oxygen sensor failures, sending codes to the producer,
393 controlled the aerators and introduced a PV alternative system in case of a power line

1
2
3
4
5
6
7
8
9
10
11
12
13
14
15
16
17
18
19
20
21
22
23
24
25
26
27
28
29
30
31
32
33
34
35
36
37
38
39
40
41
42
43
44
45
46
47
48
49
50
51
52
53
54
55
56
57
58
59
60
61
62
63
64
65

394 interruption. The system was capable of detecting algae or solids adhered to the
395 membrane and could remove them using a water jet or by means of backwashing. The
396 latter one worked as well as the water jet during one month, but consumed less energy.
397 The system proposes an alternative timing routine based on biomass and water
398 temperature to turn on the aerators in case of a sensor failure.

399

400 **References**

- 401 Ahn,W.Y., Kalinichev A.G., Clark, M. 2008. Effects of background cations on the
402 fouling of polyethersulfone membranes by natural organic matter: Experimental
403 and molecular modeling study. *Journal of Membrane Science* 309, 128-140.
- 404 Appelbaum, S., Parilutsky, A., Birkan, V. 1999. An emergency aeration system for use
405 in aquaculture. *Aquacult. Eng.* 20, 17-20.
- 406 Asatekin, A., Menniti, A., Kang, S.T., Elimelech, M., Morgenroth, E., Mays, M. 2006.
407 Antifouling nanofiltration membranes for membrane bioreactors from self-
408 assembling graft copolymers. *Journal of Membrane Science* 285(1-2), 81-89.
- 409 Bart, Q.J. 2002. An investigation into using fuzzy logic techniques to control a real
410 world application. *PeninsulaTechnikon. Theses & Dissertations.*
- 411 Brett, J.R., Groves, T.D.D. 1979. Physiological energetics. In: Hoar, W.S., Randall D.J.,
412 Brett, J.R. (eds.) *Fish Physiology*, Vol. 8, Academic Press, New York, pp. 279-352.
- 413 Bryan, A.; Cushman, M. 1992. Dissolved oxygen sensor calibration, monitoring and
414 reporting system. United States Patent No. 5,098,547. Mar 24, 1992.
- 415 Bucks, D.A., Nakayama, F.S., Gilbert, R.G. 1979. Trickle irrigation water quality and
416 preventive maintenance. *Agricultural Water Management* 2(2), 149-162.
- 417 Carlson, A.R., Blocher, J., Herman, L.J. 1980. Growth and survival of channel catfish
418 and yellow perch exposed to lowered constant and diurnally fluctuating dissolved
419 oxygen concentrations. *Progress Fish Culturist* 42, 73-78.
- 420 Chervinski, J. 1982. Environmental physiology of tilapias. In: Pullin, R.S.V., Lowe-
421 McConnell, R.H. (Eds.), *The Biology and Culture of Tilapias*. ICLARM
422 Conference Proceedings 7, International Center for Living Aquatic Resources
423 Management, Manila, Philippines, 119–128.
- 424 EUTECH INSTRUMENTS. 2006. Solutions for water analysis. Catalogue, pp 44-46,
425 Singapore.

- 1
2
3
4
5
6
7
8
9
10
11
12
13
14
15
16
17
18
19
20
21
22
23
24
25
26
27
28
29
30
31
32
33
34
35
36
37
38
39
40
41
42
43
44
45
46
47
48
49
50
51
52
53
54
55
56
57
58
59
60
61
62
63
64
65
- 426 Evans, R.C., Douglas, P. 2006. Controlling the color space response of colorimetric
427 luminescent oxygen sensors. *Analytical Chemistry* 78(16), 5645-5652.
- 428 Gilbert, R.G., Nakayama, F.S., Bucks, D.A., French, O.F., Adamson, K.C. 1981.
429 Trickle irrigation: Emitter clogging and other flow problems. *Agricultural Water*
430 *Management* 3(3), 159-178.
- 431 Glasspool W., Atkinson, J. K. 1998. A screen-printed amperometric dissolved oxygen sensor
432 utilising an immobilised electrolyte gel and membrane. *Sens. Actuators B.* 48, 308-317.
- 433 GLI. 2008. Model 5500-series Clark Technology Membrane Dissolved Oxygen Sensor.
434 Datasheet 5500, GLI International, Wisconsin, USA.
- 435 Hahn, F. 2010. Self Powered Instrumentation Equipment and Machinery using Solar
436 Panels, In: Ochieng, R.M. (ed.), *Solar collectors and panels, Theory and*
437 *Applications*. Sciyo International, Vienna, Austria. Pp: 293-314.
- 438 Hahn, F. 2011. On-line detector sorts four types of coconut water efficiently.
439 *Biosystems Engineering (IN PRESS)*
- 440 Howe, K.J., Ishida, K.P., Clark, M.M. 2002. Use of ATR/FTIR spectrometry to study
441 fouling of microfiltration membranes by natural waters. *Desalination* 147, 251-255.
- 442 Kramer, D.L. 1987. Dissolved oxygen and fish behavior. *Environmental Biology of*
443 *Fishes* 18 (2), 81-92.
- 444 Lander, D.A., Vardon, D.R., Clark, M.M. 2010. Effects of shear on microfiltration and
445 ultrafiltration fouling by marine bloom-forming algae. *Journal of Membrane*
446 *Science* 356, 33-43.
- 447 Lee, P.G. 2000. Process control and artificial intelligence software for aquaculture.
448 *Aquacultural Engineering* 23, 13-36.
- 449 Pereira, D.G., Tonso, A., Kilikian, B.V. 2008. Effect of dissolved oxygen concentration
450 on red pigment and citrinin production by *Monascus purpureus* ATCC 36928.
451 *Brazilian Journal of Chemical Engineering* 25(2), 247 - 253.
- 452 Pierce, R.H., Henery, M.S., Higham, C.J., Blum, P., Sengco, M.R., Anderson, D.M.
453 2004. Removal of harmful algal cells (*Karenia brevis*) and toxins from seawater
454 culture by clay flocculation. *Harmful Algae* 3(2), 141-148.
- 455 Rijn, L.C. van. 1979. Pump Filter Sampler. Delft Hydraulics Laboratory, Report S404,
456 The Netherlands
- 457 Rosenberger, S., Laabs, C., Lesjean, B., Gnirss, R., Amy, G., Jekel, M., Schrotter, J.C.
458 2006. Impact of colloidal and soluble organic material on membrane performance

1
2
3
4
5
6
7
8
9
10
11
12
13
14
15
16
17
18
19
20
21
22
23
24
25
26
27
28
29
30
31
32
33
34
35
36
37
38
39
40
41
42
43
44
45
46
47
48
49
50
51
52
53
54
55
56
57
58
59
60
61
62
63
64
65

459 in membrane bioreactors for municipal wastewater treatment. *Water Research*
460 40(4), 710-720.

461 Schafer, A.I., Schwicker U., Fischer M.M., Fane, A.G., Waite, T.D. 2000.
462 Microfiltration of colloids and natural organic matter. *Journal of Membrane*
463 *Science* 171(2), 151-172.

464 Smith, M.J., Kerr, A., Cowling, M.J. 2007. Effects of marine biofouling on gas sensor
465 membrane materials. *Journal of Environmental Monitoring* 9, 1378–1386.

466 Stone, N., Daniels, M. 2006. Algal Blooms, Scums and Mats in Ponds. Report No.
467 FSA9094. University of Arkansas.

468 Tafangenyasha, C., Marshall, B.E., Dube, L.T. 2010. The diurnal variation of the
469 physico-chemical parameters of a lowland river flow in a semi-arid landscape with
470 human interferences in Zimbabwe. *International Journal of Water Resources and*
471 *Environmental Engineering* 2(6), 148-163.

472 Vasile, A. 2008. The implications of water chemical properties from the breeding
473 nursery pond on the fish pathological state. *Innovative Romanian Food*
474 *Biotechnology* 2, 25 – 29.

475 Way, T.R., Bashford, L.L., VonBargen, K. Grisso, R.D. 1990. Peristaltic pump
476 accuracy in metering herbicides. *Applied Engineering in Agriculture*, 6(3), 273-
477 276.

478 Whelan, A., Regan, F. 2006. Antifouling strategies for marine and riverine sensors.
479 *Journal of Environmental Monitoring* 8, 880–886.

480 Whipple, S.J., Patten, B.C., Verity P.G. 2005. Life cycle of the marine alga *Phaeocystis*:
481 A conceptual model to summarize literature and guide research. *J Mar Syst.*, 57,
482 83-110.

483 Wissenschaftllch-Technische Werkstätten GmbH (WTW). 2011. Online
484 instrumentation. Catalogue 32-37, Germany.

485 Woodbury, L.A. 1941. A sudden mortality of fishes accompanying a supersaturation of
486 oxygen in lake Waubesa, Wisconsin. *Tans. Amer. Fish. Soc.*, 71, 112-117.

487 YSI. 2009. *The Dissolved Oxygen Handbook*. YSI Incorporated, pp: 76.

488 .

489

490 **FIGURES AND TABLES**

1
2 491 **Fig.1.** Lateral view showing two column aerators, two fish tanks, the hydraulic head,
3
4 492 the PV system and the instrumentation system.

5
6 493 **Fig. 2.** Dissolved oxygen measurements of the first three tanks being AM (air
7
8 494 measurement) and WM (water measurement).

9 495 **Fig.3.** Front panel-User Interface with dissolved oxygen control.

10
11 496 **Fig. 4.** Backwash mechanism.

12
13 497 **Fig. 5** Dissolved oxygen control with the alternative program for three different aeration
14
15 498 periods during the night.

16
17 499 **Fig. 6.** Probe with (a) oxidized anode, (b) clean membrane, (c) algae fouling, (D)
18
19 500 colloids fouling (E) and suspended water droplets.

20 501 **Fig.7.** Dissolved oxygen measurement under membrane damage or faulty electrolyte.

21
22 502 **Fig. 8.** Dissolved oxygen measuring different sensing anomalies.

23
24
25 503 **Fig. 9.** DO saturation measurements with nozzle jet spray, backwash and without any
26
27 504 antifouling treatment.

28 505 **Fig. 10.** Dissolved oxygen and temperature measurements during digestive and growth
29
30 506 respiration hours

31 507

32
33 508

34 509 **Table 1.**

35
36 510 Time delay required to obtain the DO measurements according to the distance from the
37
38 511 tanks.

39
40 512

41 513 **Table 2.**

42
43 514 Port configuration

44
45 515

46 516 **Table 3.**

47
48 517 Aeration required for different fish stocking densities (kg biomass) per cubic meter of
49
50 518 water at different water temperatures.

51
52 519

53
54 520 **Table 4.**

55 521 LabView interface message codes.

56
57 522

58

59

60

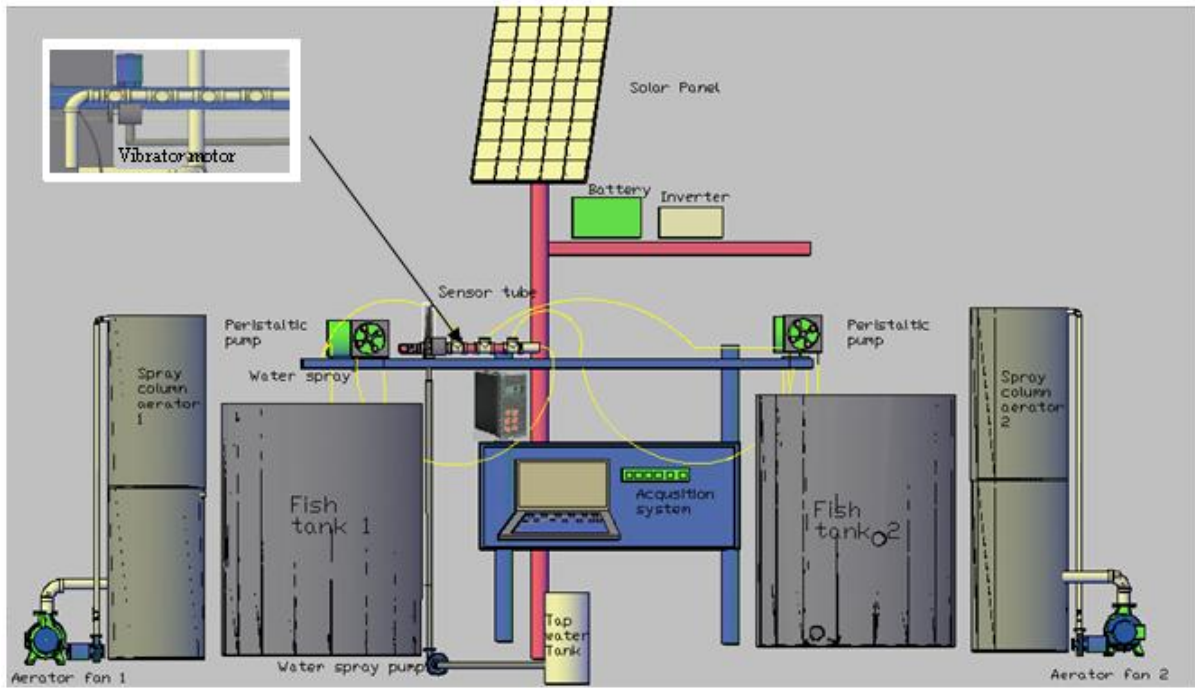
61

62

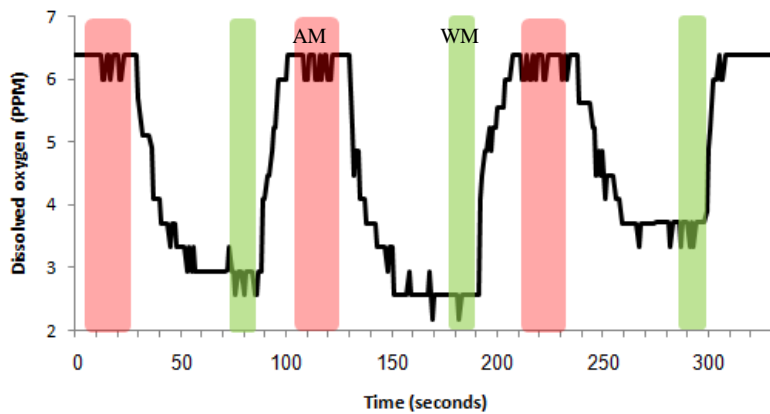
63

64

65

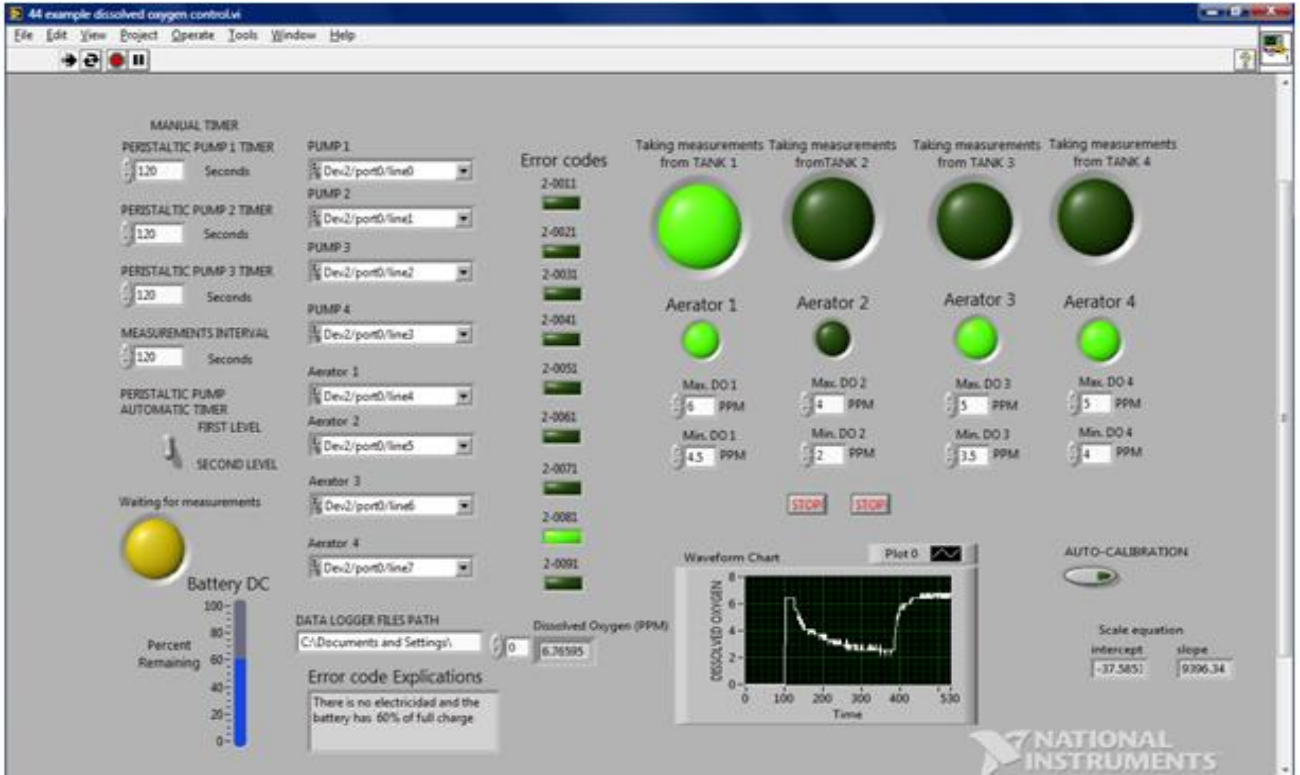


523
 524 **Fig.1.** Lateral view showing two column aerators, two fish tanks, the hydraulic head,
 525 the PV system and the instrumentation system.



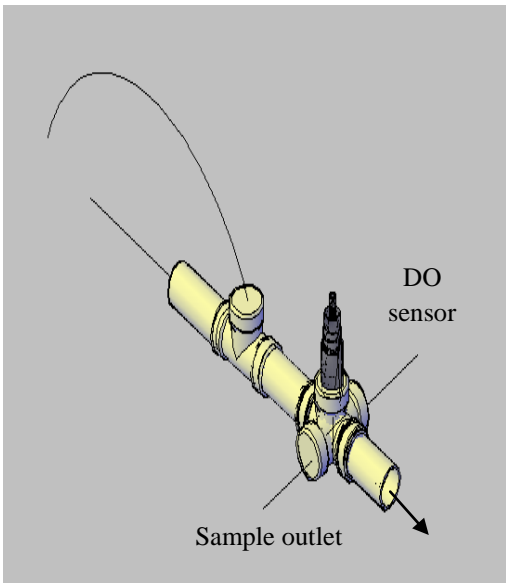
527
 528 **Fig. 2.** Dissolved oxygen measurements of the first three tanks being AM (air
 529 measurement) and WM (water measurement).

1
2
3
4
5
6
7
8
9
10
11
12
13
14
15
16
17
18
19
20
21
22
23
24
25
26
27
28
29
30
31
32
33
34
35
36
37
38
39
40
41
42
43
44
45
46
47
48
49
50
51
52
53
54
55
56
57
58
59
60
61
62
63
64
65



537

538 **Fig.3.** Front panel-User Interface with dissolved oxygen control.



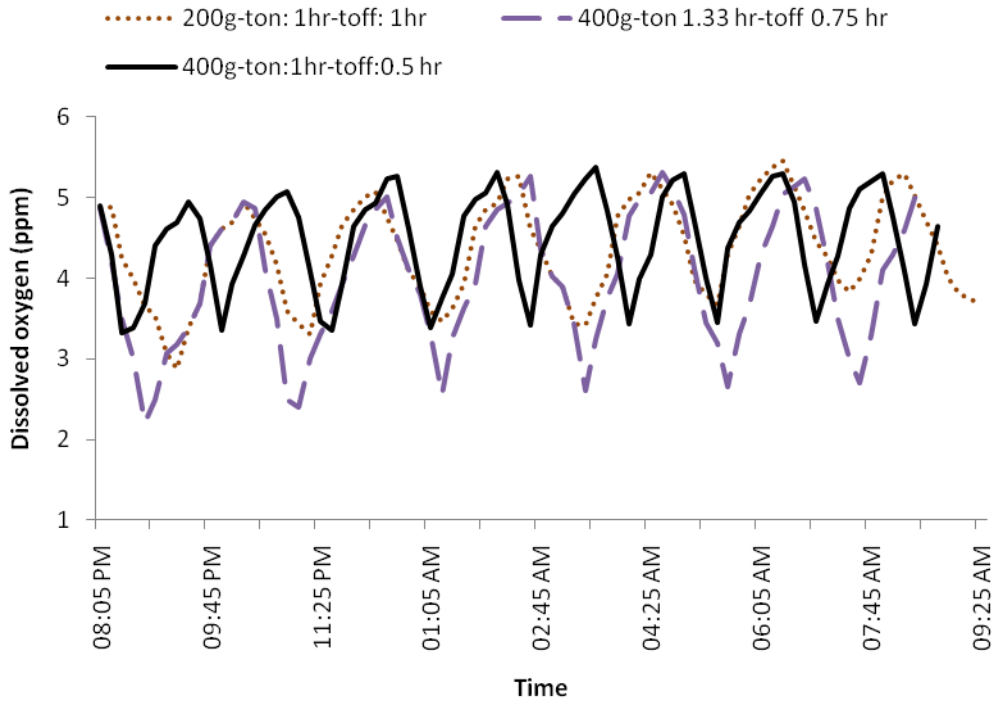
539

540 **Fig. 4.** Backwash mechanism.

541

542

543



544

545 **Fig. 5** Dissolved oxygen control with the alternative program for three different aeration
 546 periods during the night.

547



548

549

550

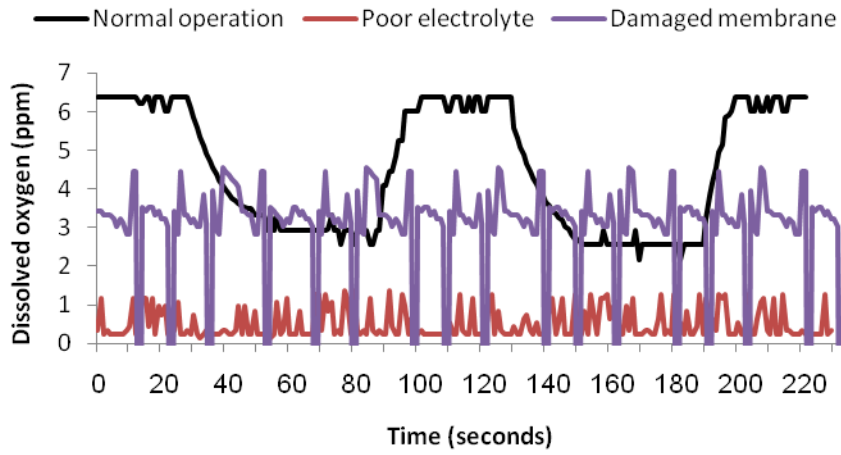
551 **Fig. 6.** Probe with (a) oxidized anode, (b) clean membrane, (c) algae fouling, (D)
 552 colloids fouling (E) and suspended water droplets.

553

554

555

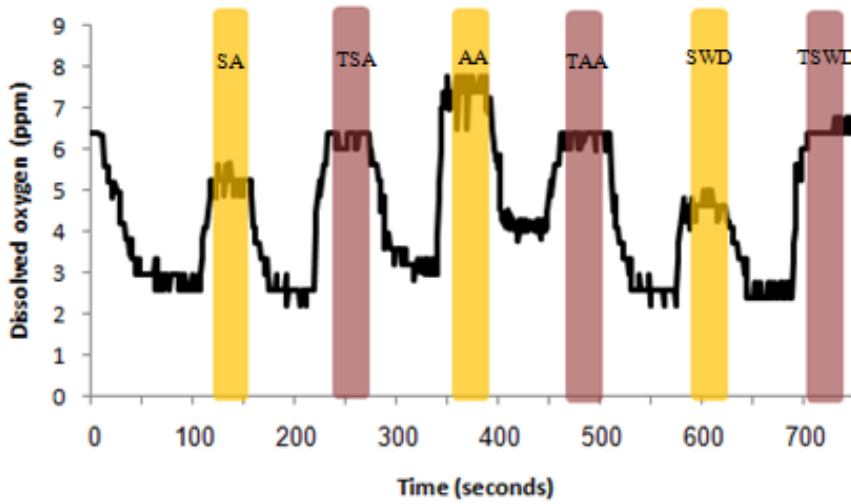
556



557

558 **Fig.7.** Dissolved oxygen measurement under membrane damage or faulty electrolyte.

559



560

561 **Fig. 8.** Dissolved oxygen measuring different sensing anomalies.

562

563

564

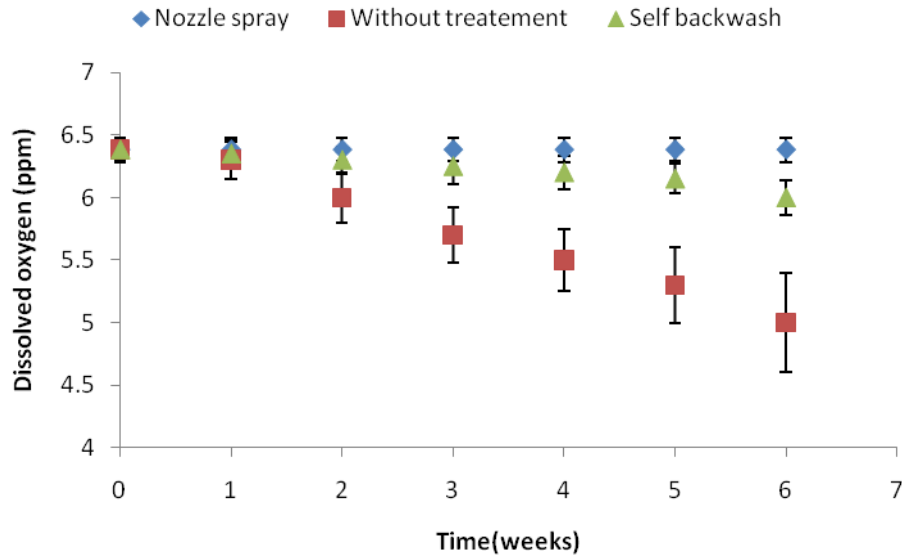
565

566

567

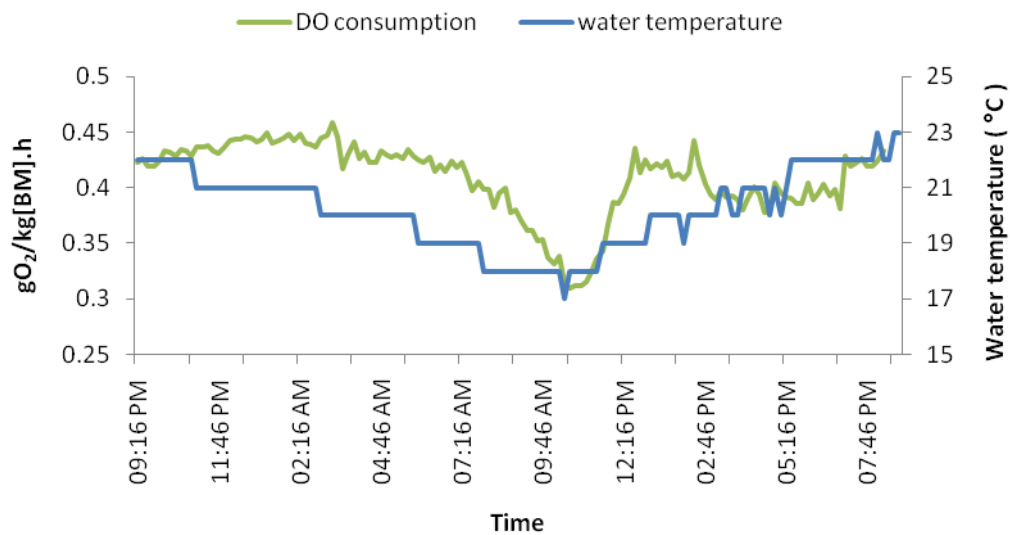
568

1
2
3
4
5
6
7
8
9
10
11
12
13
14
15
16
17
18
19
20
21
22
23
24
25
26
27
28
29
30
31
32
33
34
35
36
37
38
39
40
41
42
43
44
45
46
47
48
49
50
51
52
53
54
55
56
57
58
59
60
61
62
63
64
65



569

570 **Fig. 9.** DO saturation measurements with nozzle jet spray, backwash and without any
 571 antifouling treatment.



572

573 **Fig. 10.** Dissolved oxygen and temperature measurements during digestive and growth
 574 respiration hours

1
2
3
4
5
6
7
8
9
10
11
12
13
14
15
16
17
18
19
20
21
22
23
24
25
26
27
28
29
30
31
32
33
34
35
36
37
38
39
40
41
42
43
44
45
46
47
48
49
50
51
52
53
54
55
56
57
58
59
60
61
62
63
64
65

575 **Table 1.**

576 Time delay required to obtain the DO measurements according to the distance from the
577 tanks.

	Distance		Delay time from hose at	
	from tank, m		30 cm, sec	80 cm, sec
Tank 1	3.3		20.1	23.5
Tank 2	6.1		40	43.6
Tank 3	8		53.5	56.5
Tank 4	5.2		33.4	37

578

579 **Table 2.**

580 Port configuration

Port configuration								
Digital Signal	P0.0	P0.1	P0.2	P0.3	P0.4	P0.5	P0.6	P0.7
Terminal	17	18	19	20	21	22	23	24
Define	1 st peristaltic pump	2 nd peristaltic pump	3 rd peristaltic pump	4 th peristaltic pump	1 st aerator	2 nd aerator	3 rd aerator	4 th aerator
Signal Terminal	GND 1	AI 0 2	P1.0 25	P1.1 26	P1.2 27	P1.3 28	GND 4	AI1 5
Defin	Single-Ended Mode DO sensor		digital			Single-Ended Mode Thermopare		
	Analog current input -ve	Analog current input +ve	Water spray Pump	Vibrator Motor	Electrical voltage state	Photo- voltaic system	Analog voltage	Analog voltage

581

582 **Table 3.**

583 Aeration required for different fish stocking densities (kg biomass) per cubic meter of
584 water at different water temperatures.

Kg biomass per m ³ water	Aeration in hours for different water temperatures °C								
	17	18	19	20	21	22	23	24	
2	1.83	1.94	2.12	2.25	2.38	2.51	2.63	2.76	
6	5.00	5.30	5.77	6.11	6.51	6.90	7.20	7.60	
10	7.68	8.16	8.85	9.33	10.00	10.64	11.06	11.73	
14	9.87	10.52	11.36	11.92	12.85	13.75	14.21	15.15	
18	11.56	12.38	13.30	13.86	15.06	16.22	16.65	17.85	
22	12.75	13.75	14.68	15.17	16.63	18.04	18.39	19.85	
24	13.15	14.25	15.15	15.58	17.18	18.72	18.99	20.58	

585

586 **Table 4.**
 587 LabView interface message codes.
 588

Error source	Values when contacts air	Behavior	Cleaning action	LabView codes
Algae	Higher values during day (super-saturation)	Higher peaks	Water-Jet	2-0011
Solids	Lower value than 5.5	Smooth peaks	Water-Jet	2-0021
Electrolyte membrane	Lower value than 1.3 ppm Values arriving zero	High frequency Low signal with negative peaks	Change Change	2-0031 2-0051
Air Bubbles	Values above 15 ppm	higher frequency peaks	Remove air bubbles	2-0041
Suspended droplets	Values lower than the saturation (in air measurements)	Smooth peaks	Motor	2-0062

- 589
- 590
- 591
- 592
- 593
- 594
- 595
- 596
- 597
- 598
- 599
- 600
- 601
- 602
- 603

1
2
3
4
5
6
7
8
9
10
11
12
13
14
15
16
17
18
19
20
21
22
23
24
25
26
27
28
29
30
31
32
33
34
35
36
37
38
39
40
41
42
43
44
45
46
47
48
49
50
51
52
53
54
55
56
57
58
59
60
61
62
63
64
65

Manuscript Number: COMPAG-D-11-00209R1

Title: Photovoltaic automatic dosing of tilapia tanks

Article Type: Original Research Paper

Keywords: tilapia feeder, weighting mechanism, PV system, pneumatic conveying

Corresponding Author: Dr Frederico F Hahn, PhD

Corresponding Author's Institution: Universidad Autonoma Chapingo

First Author: Frederico F Hahn, PhD

Order of Authors: Frederico F Hahn, PhD; Wael Elmessery, MC

Abstract: Overfeeding results in uneaten feed, poorer water quality, lower economic profit and additional environmental pollution. Market feeders are unable to feed multiple tanks with one feeder, especially if tanks had different fish growth stages. Energy saving and food spreading over the water surface are two essential points that new automatic feeders should optimize. An automatic solar feeder was constructed and its conveying performance analyzed to provide food to four 9.5 m diameter rearing tanks stocked with 7000 organisms. Producers can overcome fish aggressive behavior when feed is applied efficiently, so a better food distribution was obtained using three gates; two of them automatically controlled. The system used a hopper capable of feeding the four tanks during one week being its precision dependant on the weighting mechanism. An embedded system based on the ATM 89C51 microcontroller controlled dosage of tanks according to the tilapia growth stage. Two fans per distribution line conveyed floating pellets with an airspeed exceeding 23 m/s. Energy consumption decreased by 83% when two fans were used, as food was dosed in 41.66% less time. Turbulence and pellet occupied space area were studied to optimize food distribution; the vision software showed that 90% of the tube transported food with the turbulent airflow; only 40% with laminar flow.

Chapingo, Texcoco, Mexico 5 November 2011

We would like to submit the article:

Photovoltaic automatic dosing of tilapia tanks

The article has been modified to answer all the reviewers' comments.

Thanks in advance for your kindness,

Dr. Federico Hahn

Paper Highlights

> Automatic system fed multiple tanks at different fish growth stages. > Airspeed flow from two fans make pellets float avoiding wall collisions. > The 400 gram weighting mechanism proved to be energy efficient. > Airflow turbulence increases occupation area and reduces energy consumption. >

RESPONSE TO REVIEWERS

As the reviewers indicated the paper required a better structure. With the help of an English professor we worked in the paper for two weeks. All the comments and points addressed by both reviewers were addressed and some of the questions are now included in the paper as it is easier to understand.

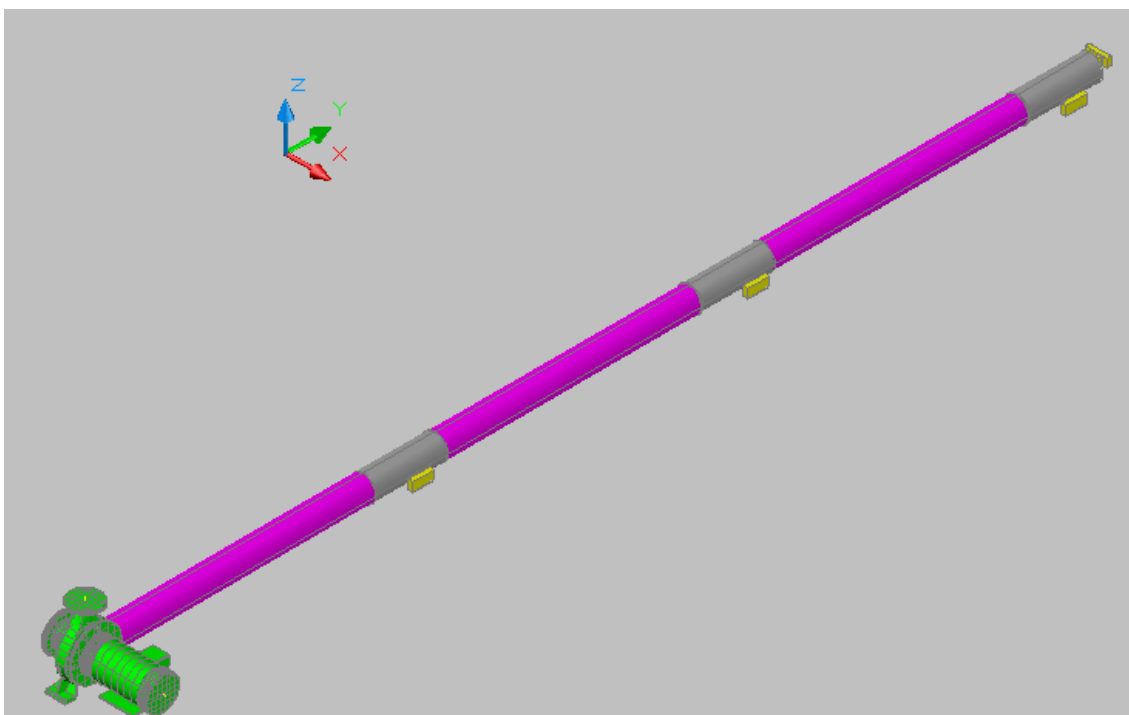
As proposed by the second reviewer the mechanical and control operation were separated and a unit was used for the food particle analysis.

Results of the automated feeder are shown giving the real importance to the paper. Nevertheless, turbulence and airspeed analysis were important to know how the system operates, and to analyze its energy optimization.

Two new tables were added, one about dosing results, which simplify greatly the text. The second one takes away figure 9 and gives the exact values of energy consumed with one and two fans.

Cost, flexibility and accuracy are addressed in the text.

The figure proposed by reviewer one is sent in this paper but it is not of great help and it is not completely necessary.



Figures 6 and 7 had their axes fixed so that can they can be compared. However I find that figure 6 is not well appreciated.

The contribution of this work:

All the previous automatic feeders did not concern to spread food well over the water surface and cannot feed multiple tanks with one feeder, feeding fish tanks that have different purposes; one of them was used as nursing tank and the others were for rearing tanks.

Heat transfer was measured by an infrared thermometer. The temperature of food particles was measured after the fans and at the gates (Δt), the specific heat for fish food calculated based on food components for both types of food (C) and the amount of food delivered (m), using the following equation

$$Q = m * c * \Delta t$$

M is the amount of food delivered (kg)

C is food pellets specific heat (KJ/kg.°C)

Δt is temperature difference ($T_F - T_0$) in °C.

T_F final food temperature

T_0 Initial food temperature

Q is the amount of heat transferred in kJ.

Some other useful comments on questions related:

Lasers were used as the distance is short and laser pointers are very cheap in Mexico. Also it avoids a problematic wiring if many tanks are fed. As well cables must be placed over the tubes and can become wet, and have problems with water evaporation after 2 years.

The condensed analysis of food particle dynamics was placed in the second paragraph of the conclusions.

The weighting mechanism do not contact the spring with the microswitch. As it goes down due to the weight it will activate the microswitch.

All the word rods were substituted by inner tube as it is clearer.

The pneumatic transport analysis was done with images. From the video images were taken out in order to obtain a value of the occupied space. As a vertical image and a horizontal image are present it can be reconstructed. The two fans were used to induce turbulence.

Calibration of the weighting system is only needed when dosing is not correct. Dosing errors are due to lack of spring force or by microswitch damage.

The important of feeding duration is due to energy optimization. Two fans were used and the 400 g weighting system.

Heat transfer is important to understand if food is being heated. This can increased swelling power.

The distribution of the food is important so that fish do not compete for food.

Photovoltaic automatic dosing of tilapia tanks

F. Hahn; W. El messery

Posgrado en Ingeniería Agrícola y Uso Integral del Agua, Universidad Autónoma
Chapingo, km 38.5 Carr México Texcoco, Estado de México, México

Email: fhahn@correo.chapingo.mx

Abstract

Overfeeding results in uneaten feed, poorer water quality, lower economic profit and additional environmental pollution. Market feeders are unable to feed multiple tanks with one feeder, especially if tanks had different fish growth stages. Energy saving and food spreading over the water surface are two essential points that new automatic feeders should optimize. An automatic solar feeder was constructed and its conveying performance analyzed to provide food to four 9.5 m diameter rearing tanks stocked with 7000 organisms. Producers can overcome fish aggressive behavior when feed is applied efficiently, so a better food distribution was obtained using three gates; two of them automatically controlled. The system used a hopper capable of feeding the four tanks during one week being its precision dependent on the weighting mechanism. An embedded system based on the ATM 89C51 microcontroller controlled dosage of tanks according to the tilapia growth stage. Two fans per distribution line conveyed floating pellets with an airspeed exceeding 23 m/s. Energy consumption decreased by 83% when two fans were used, as food was dosed in 41.66% less time. Turbulence and pellet occupied space area were studied to optimize food distribution; the vision software showed that 90% of the tube transported food with the turbulent airflow; only 40% with laminar flow.

Keywords: tilapia feeder, weighting mechanism, PV system, pneumatic conveying

30 **1. Introduction**

31

32 Aquaculture systems represent an important food production system with high-quality protein for
33 human consumption. Increasing productivity and optimizing energy use are two fundamental
34 aspects for successful aquaculture. Fish have a low feed conversion rate and in intensive
35 aquaculture systems food represents approximately 40% of total production costs (Chang et al.,
36 2005). Excess food drops to the tank floor and its decomposition consumes oxygen and produces
37 ammonia-nitrogen (Chang et al., 2005).

38

39 Pond cultivated fishes consume food in 5-10 minutes; but timer control can lead to overfeeding
40 (Masser et al., 1999). Feeding rates vary with fish size and water temperature. Fish fed in 2–3 hour
41 intervals eat more food than their stomachs can hold, resulting in food wastage and an increase of
42 the production cost. Overfeeding wastes, degrades water quality, and can overload the biofilter. Fish
43 fed every 4–5 hours eat the feed needed to refill their stomachs (Riche and Garling, 2003).
44 Ultrasound for monitoring uneaten pellets has shown to be a useful mean to reduce feed wastage
45 (Summerfelt et al., 1995) increasing by 60% fish growth compared with ration feeding.

46

47 Maximum fish growth cannot be achieved by personnel due to human and logistic limitations as
48 lack of night-shift workers. Some automatic feeders use belt feeders working on wind-up springs
49 can employ electric vibrating equipments (Saravanan and Santhanam, 2008). Automatic feeding
50 systems controlled by predetermined time schedules have been extensively reported in the literature
51 (Juell et al., 1993; Fast et al., 1997; Fang and Chang, 1999; Fang et al., 2002; Yeoh et al., 2010). An
52 automatic feeder cultivated eel using a rotating plate and scrubber (Chang et al., 2005). Commercial
53 fish farming use flexible and simple pneumatic feeding systems (Chapelle et al., 2004).

54

55 On demand self-feeders depend upon the ability of fish to press a lever to obtain food and can be
56 manually or electronically controlled. Manual self-feeders are simple and cheap, but the gate
57 mechanism often gets jammed; feeding can be induced by accident, by fish swimming through the
58 gate or by wave action (Shepherd and Bromage, 1989). Food portions are difficult to adjust, and it
59 is not possible to spread food over the water surface (Alanärä, 1996). An electronically controlled
60 self-feeding system was built with a trigger rubber knob, a control unit and a feeder (Noble et al.,
61 2007). As the fish stretches the knob to eat it, pressure changes are detected by a microphone which
62 sends a signal to the control unit. However, the majority of the fish do not trigger the mechanism
63 and food delivery is lost (Alanärä, 1992). Chang et al., (2005) used an infrared photoelectric sensor

64 for feeding depending on fish gathering behavior, but do not work properly with intensive fish
65 tanks. [Papandroulakis et al., \(2002\)](#) provided plankton organisms to feed larvae according to tables
66 stored in the memory of a programmable logic controller (PLC); food was distributed to the tanks
67 by peristaltic pumps and solenoid valves.

68
69 Fish ponds in Mexico are located in remote areas where electricity is not available so alternative
70 energies are required; machines can be driven by photovoltaic systems with daily radiation of 4-6
71 kWh/m². [Fullerton et al., \(2004\)](#) designed a feeding mechanism which uses a small electrical
72 powered pump to force feed slurry down to a cage. A wind generator and solar panels provided
73 energy for pumping; the electric power system operation was monitored.

74
75 The present work describes the operation of a PV solar driven automatic feeder for three
76 commercial rearing tanks growing 7000 tilapias each and one nursing tank. Wireless transmission,
77 solar energy and precise dosing were used by the automated feeder with optimum energy
78 consumption. Three feeding gates distributed more evenly the food in the tanks, reducing fish
79 competition for food. Air-food transport was analyzed with a vision algorithm optimizing pellet
80 occupation area, floating movement and food degradation.

81 82 **2. Materials and methods**

83
84 The automatic feeder presents a food hopper, a weighting mechanism and 9 m distribution tubes to
85 deliver food to the tanks; it was implemented for feeding fishes during one week. An embedded
86 system controlled accurate tank feeding and its distribution along each tank avoiding fish
87 competition for food. Air-food particle movement has to be perfectly understood so that turbulence,
88 temperature and pellet occupation area can be used to optimize food conveying to the tanks with
89 energy saving. Laminar food-air flow resulted when one fan worked; meanwhile two fans conveyed
90 and rotated food at high speed following a turbulent flow. Energy consumption during feeding was
91 important during the photovoltaic system (PV) operation driving motors, solenoids and controls.

92 93 2.1. Tilapia growing tanks

94 Tilapia can be produced in four tanks (A, B, C and D in [Fig. 1](#)) between March and October. The 9
95 m diameter concrete tanks located at Atoyac (17°58' N and 101°45' W) in the Pacific coast of
96 Mexico have a height of 1.5 m. Nursing tank (A) fed 21,000 juveniles during March increasing their
97 weight from 3 to 40 g; tilapias were then transplanted in April to rearing tanks B, C, and D. Each

98 rearing tank stocked 7,000 organisms for three months until each tilapia weighted 300 g. The
99 nursing tank was stocked with other 28,000 organisms in June starting the second growing cycle.
100 With both growing cycles a double quantity of fish was produced.

101 Nutripec 4418 C and Nutripec 3508 commercial fish food were dosed by the automatic feeder to
102 nursing and rearing tanks, respectively. Nutripec 4418 C is a floating food formed by particles
103 having 1.7 mm diameter and consists of 44% protein and 18% fat with an apparent density of 540
104 kg/m³. Nutripec 3508 is a 3.5 mm diameter floating pellet with 35% protein and 8% fat having an
105 apparent density of 415 kg/m³.

106 Three and six food sessions were applied per tank at the rearing and nursing tank, respectively;
107 three gates allowed better food dispersion. The three feeding sessions were applied at 9:00, 14:00
108 and 19:00 hr meanwhile the six sessions were applied at 7:00, 10:00, 13:00, 16:00, 19:00 and 22:00
109 hr. The food feeder installed at the center of the four tanks distributed food to the nursing or rearing
110 tank's gate according to [Tables 1 & 2](#). The food delivered per week was of 495.6 kg during the first
111 month ([Table 1](#) and [Table 2](#)), and increased to a maximum of 772.8 kg on the last month when the
112 four rearing tanks fed tilapias five month old, [Table 1](#).

113

114 2.2 Feeder mechanical operation

115 The 1.5 m³ food hopper fed the fishes during one week and its main components are shown in [figure](#)
116 2.a. Food stored in the hopper has to be introduced to the distribution tubes through the weighting
117 mechanism; a bottom plate is turned 3 cm beneath a fixed surface that avoids excessive loading.
118 The bottom plate is turned by a 24 V DC direct current motor of 17.8 W (mod. AST-G002DC,
119 Geared Motor, USA); the motor rotates at 5 RPM and has a torque of 34 N-m. When the holes of
120 both plates match, food fills the weighting mechanism, [Fig. 2. b](#). The feeder motor turns the bottom
121 plate until micro switch one acknowledges the first hole and gets synchronized with the top plate
122 orifice (sync position). The inner tube of the weighting mechanism starts collecting food and the
123 load causes it to move downwards. The three holes for feeding the other tanks are displaced 90°,
124 180° and 270° from the sync position; orifice synchrony allows tube filling if the bottom plate is
125 properly moved. The sync position orifice will dose tank A again.

126

127 The weighting mechanism presents two overlapping PVC (Polyvinyl Chloride) tubes being the
128 inner tube filled with 100 g of food in 12 seconds; food dosed to each tank will be proportional to
129 multiples of 100 g, [Fig. 3](#). The internal PVC tube (30 cm long) presented a fixed lever where a
130 spring having a force of 0.1N/mm was connected; the other side of the spring was fixed to the

131 external PVC tube. As food fills the inner tube the lever descends until the weight micro switch
132 (WMS) is activated; food entering the tube is restricted when the motor turns clockwise 10°, Fig. 3.
133 b. The diameter of the filling tube was studied to optimize the weighting mechanism operation.

134

135 A 24 VDC electromagnetic coil (mod MAGMAX, ALCO, USA) attracts a steel plate attached to
136 the bottom of the inner PVC tube preventing the inner tube to return until it is empty, Fig. 3. c. Four
137 air extractors supplied by 24V DC (model KZFF263, Guangzhou Keao Electrical Co., Ltd, China)
138 were turned-on; one fan applied food to nursing tank A (Fig. 3. d) and three fans fed the rearing
139 tanks simultaneously.

140

141 2.3 Feeder control

142 The automated feeder was controlled by an embedded system based on the ATM89C51 (ATMEL
143 Inc, San Jose, California) microcontroller. The microcontroller port configuration is depicted in
144 Table 3, and a LUT (look up table) stores the information for monthly food dosing per gate during
145 fish growth, Tables 1 & 2. Each of the four microcontroller ports have eight digital outputs (eg. Port
146 2.1, Port 1.3) having the ability to control external devices as solenoids, relays, motors, etc.
147 Microcontroller port 1 turns on the fan, turns on-off the laser (Port 1.5 and Port 1.6) and controls the
148 motor that turns the plate. When the weighting limit switch contact closes, the microcontroller port
149 1.3 gets activated and fires the electromagnetic coil to assure that the 100 grams of food are
150 completely dosed. Simultaneously the microcontroller turns on the air extractors, conveying the
151 food to the nursing and rearing tanks using port 1.0 and port 1.4, respectively.

152

153 Instructions for manual feeding of the tanks are provided by the external switches of Port 2. When
154 all the fishes present the same growth stage, the system can run automatically after setting Port 2.7
155 to one. Nursing tank A can feed 21,000 or 28,000 fingerlings by switching T1 or T2. If tank A is
156 converted to a rearing tank and fed 7000 juveniles T3 will be triggered. Manual control of T4 will
157 feed rearing tanks B, C or D depending if fishes are three, four or five month old.

158

159 The diameter of the distribution tubes were analyzed for proper operation. Three output gates
160 deliver the food to each tank being the first two automated, Fig. 1. A thin circular plate is rotated
161 inside the gate by a 12 VDC gear motor (model EMG30, Technobots Ltd. UK); a 12 V rechargeable
162 battery supplied the motor (model LC-R121R3P, Panasonic, USA) energy. The first two gates stay
163 normally open allowing food application by gate 3. The accuracy of the dosed food at every gate
164 was obtained as well as the spreading area over the water surface.

165

166 Four green and four red lasers were fixed at the food distribution tubes establishing wireless
167 communication between the microcontroller and the gate motor drivers, [Fig. 1 & 2. a](#). Lasers were
168 activated by microcontroller port 1.5 and port 1.6; the red laser closes gate 1 meanwhile the green
169 laser closes gate 2. Photo detectors receive the laser light at opposite sides of distribution tubes at
170 gate 1 and gate 2, avoiding green laser interference on gate1. Twelve seconds after the photo
171 detector senses the laser light, the gate closes; all the food within the inner tube of the weighting
172 mechanism will be applied to the tank.

173

174 2.4 Feed conveying performance.

175 Pipe air flow was analyzed to optime feeding with the lowest energy consumption; two fans were
176 coupled by a Y- PVC connector introducing different air velocities to the distribution tubes.
177 Pressure drop between the air flow after the fan and before it exits the gate was measured with a
178 pair of manometers. The Reynolds number (Re) for laminar or turbulent air flow during food
179 transport was calculated by [Eqn. 1](#) which depends of air density (ρ) and air dynamic viscosity (μ)
180 expressed in Pa.s. Air turbulance varies with pipe diameter (D) and mean air velocity (V).

181

$$182 \quad \text{Re} = \rho V D / \mu \quad (1)$$

183

184 Food particles temperature in different sections of the distribution tube was measured with an
185 infrared thermometer. Heat transfer was calculated by multiplying the temperature difference
186 between two consecutive sections by the specific heat of the fish food; the result has still to be
187 multiplied by the amount of food (mass) delivered. The solubility of the food applied to the fishes
188 tends to increase with temperature as well as it swelling power ([Adebowale et al, 2005](#)).
189 Temperature data was acquired with three thermocouples fixed at the gates and the values were
190 stored in a datalogger (LabPro, VERNIER, USA). The acrylic tube surface temperature was
191 measured with an infrared temperature probe (mod. 80T-IR, FLUKE, Germany). Particles rotate
192 while drifting radially hitting the pipe wall at different locations ([Shapiro and Galperin, 2005](#)). Food
193 particles collisions were monitored by a sound detector (mod. DIGITAL SOUND METER, Radio
194 Shack, USA).

195

196 Two 10 Megapixel camaras (mod. Cannon Powershot, Cannon, USA) with high focal length and
197 sensitivity were installed ortogonally over three 0.5 m long acrylic transparent tubes which replaced
198 the distribution tubes at the three output gates. The videos acquired simultaneously by the two

199 camaras were converted to digital photos every 0.2 second by the RealPlayer software. Images were
200 segmented and transformed to black and white ones to eliminate tube background and enhanced
201 pellet positioning using the *ImageJ* software, [Fig. 4](#). The food conveying videos were taken five
202 times at 10:00 AM when the air temperature was of 19.5°C; food occupied space values were
203 averaged.

204

205 **3. Results**

206

207 As tilapia does not eat at the tank floor, food should be maintained in suspension as long as
208 possible. The nursing tank was fed every 3 hours from 7:00 to 22:00 hr, finding condensation as the
209 last application remained floating until the next morning. Therefore, food was applied to the nursing
210 tank every two hours, starting at 9:00 AM (9:00, 11:00, 13:00, 15:00, 17:00 and 19:00). The optimal
211 interval used in tilapia rearing tanks was of 5 hours.

212

213 3.1 Automated feeder performance

214 The inner tube of the 100 gram weighting mechanism provided the best feeding precision for
215 Nutripec 3508 and 4418C when its diameter was of 5.08 cm; for the 400 gram weighting
216 mechanism the same precision was achieved with an inner tube having a diameter of 7.62 cm. As a
217 thicker tube (7.62 cm diameter) was used by the 100 weighting mechanism precision decreased; the
218 lever vertical movement was smaller. Nutripec 3508 deposition over the tank surface decreased
219 5.8%; 4.3 % less Nutripec 4418C was deposited to the tank. The inner tube of the weighting
220 mechanism was filled more efficiently with powder food (Nutripec 4418C) than with pellets, as air
221 spaces between particles disappeared. The food was accurately applied to the tanks through each
222 gate presenting R^2 values over 94%, [Table 4](#). In a Bayesian distribution, 95% of Nutripec 3508
223 weighted outputs occurred between 99.1 and 100.5 g. At slow air speed, conveying particles
224 remained trapped at the gate throats and settled at the gate edges.

225

226 If one of the three tanks B,C and D did not grow fishes, the coresponding fan was disconnected
227 after closing the orifice that fills the weighting tube. Microcontroller port 2 was configured
228 monthly and the appropriate signals sent to the feeder through port1. Feeder reliability was studied
229 based on mean time between failures (MTBF) being the predicted life cycle of 5 years. Micro
230 switches and springs failed after 20,000 operations; electromagnetic coil, feeder motor and fans
231 failed after 100,000 operations. The prototype can be constructed with 3,500 US dollars and PVC
232 tubes exposed to the sun need to be exchanged every two years.

233

234 Time of feeding is important as energy consumption decreases, but feeding location affect both the
235 quantity of wasted solids and their distribution within the tanks. The inner tubes for weighting
236 capacities of 400 and 100 gr were compared to determine the dosing time required for the daily
237 ration. In March the feeder delivered 16.8 kg of daily food to the nursing tank in 59.5 minutes with
238 the 400 gr weighting system and consumed 54.2 W.h of energy. The weighting system of 100 gr
239 dosed the same amount of food in 98 minutes with an energy consumption of 59.3 W.h. In May
240 each of the three rearing tanks were fed during 63.75 minutes to dose 54 kg with the 400 gram
241 weighting system; energy consumed per day was 154.11 W.h W.h. The 100 gram weighting system
242 applied food during 105 minutes along the day, consuming 171.45 W.h of energy. The 400 gram
243 weighting system is proper for commercial tanks, meanwhile a 100 gram weighting system is ideal
244 for research purposes were 1000 lt tanks are used. The 400 weighting system was used decreasing
245 feeding time and energy consumption. Total feeding time for a 4 m³ tank ranged from 41-49 min for
246 stocked eels whose size ranged from 45 to 250 grams (Chang et al., 2005).

247

248 Food dosed with two fans at a gate height of 40 cm fell within a 27 cm diameter circle at the tank
249 surface. As the gate was positioned at a height of 80 cm, pellets fell inside a 50 cm diameter circle;
250 this was the height employed by the distribution tubes. The food dosed area decreased by 80%
251 when only one fan was turned-on.

252

253 The distribution tubes length is short enough to use wired communication, but small photovoltaic
254 systems can be added for gate control; electric cables should be waterproof and become expensive.
255 Cheap pointer lasers are reliable communication systems that increase its life cycle with 10 khz
256 pulse modulation. A RC filter circuit detected the pulse modulated signal and activated the photo
257 detector. Twelve seconds after the gate was closed, the capacitor was discharged automatically with
258 a limit switch. PVC tubes bent with heat so laser had to be aligned with the photo detector; both
259 laser diode and photo detector circuits were fixed to the PTR that hold the PVC tube, eliminating
260 gate opening problems.

261

262 3.2. Food conveying

263 Food distribution depends on tube diameter for a given airflow, and as the tube diameter doubles to
264 5.08 cm outlet air velocity decreases by 56.5%. One fan moved the air inside the distribution tube
265 (diameter=5.08 cm) at a speed of 14 with a volumetric rate of 0.0097 m³/s; after 12 seconds food
266 was completely delivered to the tank. Two fans increased airflow to 21 m/s and food dosing lasted 5
267 seconds. Nutripec 3508 pellets arrived at the first gate 0.45 seconds after turning on both fans,

268 meanwhile it took 2.4 seconds using only one fan. Nutripec 4418C powder was deposited 2.6
269 seconds after turning-on one fan at the first gate. As each delay corresponds to an application of 100
270 g, a lower time delay will save energy; the delay does not affect final fish weight or fish eating
271 behavior.

272 A Reynolds number (Re) of 55,200 was achieved with the airflow provide by both fans; the Re
273 number decreased when only one fan was used. Air pressure drops as the air flow impedance
274 through the tube raises with a higher occupied space percentage. For a Reynolds number of 27,551,
275 a 10 Pa pressure drop was measured resulting in a laminar food movement, Fig. 5. Food movement
276 became turbulent at Re=36,800 when air pressure drop increased to 19.6 Pa; with a Reynolds
277 number to 55,200 the pressure drop increased to 49 Pa.

278

279 Too high airspeed generates turbulent flow, degradates pellets and wears out the pipeline (Aarseth,
280 2004). Feeding rate control can maintain floating food without excessive pellet damage, so
281 collisions were analyzed. Air speed of 28 m/s using both fans fed 1.2 kg/min of pellets to the tilapia
282 tanks without being damaged. With only one fan in operation and gates 1 and 2 open, 72 db
283 collisions were detected at the first gate; collisions decreased at the third gate with a maximum
284 sound intensity of 65 db. With both fans working collisions reached 82 db, but impacts were
285 sporadic. Continuous impacts caused by an excessive turbulence are more dangerous than unitary
286 collisions of high magnitudes.

287

288 Food particle flow is affected by heat, as particles transfer heat energy in the pipe, Fig. 6.a. Surface
289 temperature at the acrylic tubes was 5°C hotter than the 19.5°C ambient air temperature; 25.8, 26.5
290 and 24.8°C were measured at the first, second and third tube surface, respectively. As food particles
291 were conveyed from the first to the second gate (interval between blue marks) 0.41652 kJ of heat
292 was transferred, Fig. 6.a. The temperature within the second tube decreased when the fan was
293 brought to standstill (after the second mark), Fig. 6.a. The highest temperature measured inside the
294 tubes with both fans working was 21.3°C, being hotter in tube 3 than in tube 2, Fig. 6.b; air speed
295 increased twice and the Reynolds shear stress was doubled. Food particles transported from the first
296 to the second gate by the airflow induced by both fans presented a lower heat transfer of 0.4137 kJ.
297 A heat gain of 0.51195 kJ explains the temperature raise at the third gate. Food became hotter as the
298 Reynold number increased; for Re=55,200, Nutripec 4418C powder and Nutripec 3508 pellets
299 raised their temperature by 1.5 and 2°C, respectively.

300

301 Every pair of orthogonal images were analyzed by the the vision algorithm to obtain the percentage
302 of occupied space as food was conveyed. The top image shows spread food when one fan works,
303 [Fig. 7.a](#). Pellets occupied only 30% of the area carrying dust and residuals ([Fig. 7.e.](#)); at the bottom
304 of the tube pellets moved, [Fig. 7.c](#). Gate 2 occupied space for pellets (Nutripec 3508) was 44.17%
305 and decreased to 40.09% in gate 3, [Fig. 8.a](#). As turbulence increased to $Re = 55, 200$ food occupied
306 more than 80% of the tube area, [Fig. 7.e](#); pellet images prove that food floats, [Fig. 7.b](#) & [Fig. 7.d](#). A
307 higher cross section occupied space of 86.29 and 91.93% was obtained at gates 2 and 3,
308 respectively, when both fans were turned on, [Fig. 8.b](#).

309

310 3.2. Energy consumption and solar and photovoltaic system

311 Energy consumption for feeding tanks was analyzed when one or two fans functioned, [Table 5](#). Fan
312 energy consumption was 15 times higher than the hopper DC motor, and 30 times higher than coil
313 power consumption. Energy consumption decreased by 83% when the two fans were turned-on, as
314 the time required to dose the food decreased by 41.66%. July and October were the months with
315 more daily energy consumption using one fan with 448.73 and 424.58 W.hr; the use of two fans the
316 energy used decreased to 369.025 and 345.469 W.hr. On March only the nursing tank A was fed
317 with a power consumption of 67.99 W.hr.

318

319 A photovoltaic system capable of supplying energy during three cloudy days was installed. A 24 V
320 battery bank discharging 30% should manage 100 Ah for the highest energy consumption (448.73
321 W.h/day). Two 24 V@50 Ah rechargeable LiFePO₄ batteries (Model LF2450, Optimum Battery
322 Co., Ltd, USA) were used together with a current battery charger. The determination of the
323 photovoltaic cells was obtained for six irradiance hours over 1000 W.m²/day; a 150 W solar panel
324 (mod. TE1700, GmbH, Germany) provided the energy. When two fans worked simultaneously and
325 if battery charging is monitored during July cloudy days, a 100W solar panel was able to provide
326 the required energy.

327

328 **4. Discussion**

329

330 This pneumatic conveying system used positive pressure with large amounts of transport air and
331 little quantity of solids conveyed in the suspension ([Klinzing, 2001](#)). Pellets pushed by the air
332 stream in this prototype advanced horizontally but turned around the tube area following a screw
333 type movement. Nutripec 3508 laminar flow resembles silica particles showing 50 times greater
334 mass flux at the bottom of the pipe than at the top at $Re = 5.4 \times 10^4$; with $Re = 1.91 \times 10^5$ particle mass

335 flux at the bottom of the pipe is only 4 times greater than at the top (Fouad et al., 2010). Air- solid
336 particle flow turbulence varied greatly with particle size and 3.4 mm plastic particles presented a
337 higher turbulence than 0-2 mm particles (Tsuji and Morikawa, 1982); a similar behavior was
338 encountered between Nutripec 4418C particles and Nutripec 3508 pellets.

339

340 Regulated air speed ensures optimal pellet flow; if it is too low the risk for pellet blockage increases
341 (Sorensen et al., 2008). Nutripec 3508 pellets quality at the tank surface did not show particle
342 degradation at maximum airspeed (30 m/s) and produced minimum dust. This airspeed was
343 compared against the maximum airspeed of 35 m/s used by AkvaMarina Feed System (Sorensen et
344 al., 2008). Pipe blockage can occur under very low conveying airspeed, which never occurred as the
345 inner tube of the weighting system controlled food dosage. Pellets were not transported at an
346 airspeed of 5 m/s and began to move with a laminar flow at 10 m/s, Fig. 7.c.; pellets float when
347 airspeed flow exceeds 23 m/s.

348

349 One hundred grams were fed in 12 seconds by the system, similar to the time interval response for
350 self feeders, which varied from 3 s (Yamamoto et al., 2000; Shima et al., 2001) to 15 s (Alanärä,
351 1992, 1996) and 1 minute (Gélineau et al., 1998). These response intervals reflect either the time
352 required for single feeder activation (Yamamoto et al., 2000; Shima et al., 2001) or intervals chosen
353 to avoid trigger activation during food release by tilapias (Alanärä, 1992, 1996). Maximum weight
354 at the gate of 103 gram resulted from accumulated food along the tube during previous dosing, Fig.
355 7.c. The lowest dosage of 95.9 gram only happened once at the third gate of tank A and three grams
356 remained adhered to the gate circular plates.

357

358 The algorithm informs the user whether the food is floating when pixels nearby the borders
359 presented zero gray values. As the acrylic tube is thick, transparency was lost using vision software
360 processing filters; histograms determined the gray value for segmenting the tube contour. Once
361 segmented the tube, the background was eliminated with exponential enhancement increasing the
362 color contrast of the pellets. High airspeed blurred the food image but the occupied area was
363 obtained with a 3.8% maximum error. The vision algorithm provided a higher value than the real
364 one, when a row containing few pixels was under a row having many pixels. The nearest neighbor
365 applied to five columns helped to identify profundity with respect to tube span.

366

367 Energy consumption decreased by 11% using the 400 gram weighting mechanism as 25% less
368 feeding cycles were required; fans consumed 90.5% of the energy. The dosed area by the three

369 gates was 0.59 m² and should be increased to 9 gates to reduce fish competition for food. In June
370 during the rainy season four continuous days were cloudy, so two batteries were removed and
371 charged from the main line during the second night; enough energy was stored for the next two
372 days. Gate motors consumed energy from batteries before discharging below 70% of its nominal
373 voltage. When the gate motors were supplied with 7 V batteries recharge was done after 34 days.

374

375 **5. Conclusion**

376

377 A \$3,500 US automatic feeder used a pneumatic conveying system to dose dry pellets to four tilapia
378 tanks. The system considered time of feeding and feeding location in order to reduce wasted solids
379 and fish competition for food. An embedded system based on the AT 89C51 controlled the
380 weighting mechanism and the motorized gates using laser wireless control; it also provided the
381 monthly food dosed per tank. The photovoltaic system provided three days of autonomy and used a
382 150 W solar panel to manage 450 W.h per day.

383

384 The dynamics of food particles through pipes analyzed fan energy consumption as airflow became
385 turbulent, food heat transfer and occupied space. Food discharge time decreased from 12 to 5
386 seconds with the use of two fans reducing energy consumption by 86%; tube occupation area was of
387 91.93%. Energy consumption decreased also with the 400 gram weighting mechanism as 25% less
388 dosing cycles were required. Pellets screw-type conveying allowed food particles to float avoiding
389 dust production; powder (Nutripec 4418C) and pellets (Nutripec 3508) occupied more space area
390 under turbulent airflow. Two fans generated turbulent flow at airspeeds exceeding 23 m/s and food
391 floated during its transport; sporadic pellet collisions were detected resulting in minimum pellet
392 degradation and wear out of the pipeline. Heat transfer of food particles during transport increases
393 food swelling power and solubility; as temperature within tubes should exceed 50°C heating coils
394 will be used in future works.

395

396 **References**

397

398 Adebowale, K.O., Olu-Owolabi, B.I., Olayinka, O.O., Olayide, O.S. 2005. Effect of heat moist
399 treatment and annealing on the physicochemical properties of red sorghum. *Afr. J.*
400 *Biotechnol.*, 4: 928-933.

401 Alanärä, A. 1992. The effect of time-restricted demand feeding on feeding activity, growth and feed
402 conversion in rainbow trout (*Oncorhynchus mykiss*). *Aquaculture* 108, 357– 368.

403 Alanärä, A. 1996. The use of self-feeder in rainbow trout (*Oncorhynchus mykiss*) production.
404 *Aquaculture* 145, 1– 20.

405 Aarseth, K.A. 2004. Attrition of feed pellets during pneumatic conveying: the influence of velocity
406 and bend radius. *Biosystems Engineering* 89, 197-213.

407 Chang, C.M., Fang, W., Jao, R.C., Shyu, C.Z., Liao, I.C. 2005. Development of an intelligent
408 feeding controller for indoor intensive culturing of eel. *Aquaculture Engineering* 32, 343-353.

409 Chapelle, P., Abou-Chakra, H., Christakis, N., Bridle, I., Patel, M.K., Baxter, J., Tuzun, U., Cross,
410 M. 2004. Numerical predictions of particle degradation in industrial-scale pneumatic
411 conveyors. *Powder Technology* 143, 321-330.

412 Fang, W., Chang, C.M. 1999. Development of an automatic feeder with the capability of knowing
413 when to stop feeding. In: Proceedings of the Annual International Conference and Exposition
414 of the World Aquaculture society, Australia, 26 April–2 May, 251.

415 Fang, W., Chang, C.M., Shyu, C.Z., Liao, I.C. 2002. Development of an intelligent feeding system
416 for indoor intensive culturing of eel. *World Aquaculture*, Beijing, China, 23–April 27.

417 Fast, A.W., Qin, T., Szyper, J.P. 1997. A new method for assessing fish feeding rhythms using
418 demand feeders and automated data acquisition. *Aquaculture Engineering* 16, 213–220.

419 Fouad, M.A., Elsallak, M.A., Rahman, Y.I. 2010. Experimental study of dilute gas-solid flow in a
420 horizontal pipe. Proceedings of the Tenth International Congress of Fluid Dynamics, ICFD
421 10-EG-3157, Ain Soukhna, Egypt.

422 Fullerton, B., Swift, M.R., Boduch, S., Eroshkin, O., Rice, G. 2004. Design and analysis of an
423 automated feed-buoy for submerged cages. *Aquaculture Engineering* 32, 95-111.

424 Gelineau, A., Corraze, G., Boujard, T. 1998. Effect of restricted ration, time-restricted access and
425 reward level on voluntary food intake, growth and growth heterogeneity of rainbow trout
426 (*Oncorhynchus mykiss*) fed on demand with self-feeder. *Aquaculture* 167, 247– 258.

427 Juell, J.E., Furevik, D.M., Bjordal, A. 1993. Demand feeding in salmon farming by hydroacoustic
428 food detection. *Aquaculture Engineering* 12, 155–167.

429 Klinzing, G.E. 2001. Pneumatic conveying: transport solutions, pitfalls, and measurements.
430 *Handbook of Conveying and Handling of Particulate solids*. Levy, A and Kalman, H. (Eds),
431 Elsevier Science B.V., 291-301.

432 Masser, M.P., Rakocy, J., Losordo, T. M. 1999. *Recirculating Aquaculture Tank Production*
433 *Systems, Management of Recirculating Systems*. SRAC Publication No. 452.

434 Noble, C., Mizusawa, K., Tabata, M. 2007. The effect of trigger depth on self-feeder utilisation,
435 growth and the vertical distribution of tank-held rainbow trout *Oncorhynchus mykiss*
436 (Walbaum). *Aquaculture* 273, 64-70.

- 437 Papandroulakis, N., Dimitris, P., Pascal, D. 2002. An automated feeding system for intensive
438 hatcheries. *Aquaculture Engineering* 26, 13-26.
- 439 Riche, M., Garling, D. 2003. *Feeding Tilapia in Intensive Recirculating Systems*, North Central
440 Regional Aquaculture Center, UK.
- 441 Saravanan, M.R., Santhanam, K.L. 2008. International encyclopedia of fishery science and
442 technology: fish nutrition and biochemistry, volume two. International Scientific Publishing
443 Academy, India.
- 444 Shapiro, M., Galperin, V. 2005. Air Classification of Solid Particles: a Review. *Chemical*
445 *Engineering and Processing* 44(2), 279-285.
- 446 Shepherd, J., Bromage, N. 1989. *Intensive Fish Farming*. Blackwell, Oxford, pp. 78-83.
- 447 Shima, T., Suzuki, N., Yamamoto, T., Furuita, H. 2001. A comparative study of self-feeders and
448 automatic feeders on the growth performance of rainbow trout fry. *Aquaculture Research* 32,
449 142–146.
- 450 Sorensen, M., He, G., Oehme, M., Asgard, T., Storebakken, T., Aas, T.S. 2008. Feed pellet
451 durability in pneumatic conveying systems for fish farming. Report No. 11/2008. Nofima
452 Marine, Tromso, Norway.
- 453 Summerfelt, S.T., Holland, K.H., Hankins, J.A., Durant, M.D. 1995. A hydroacoustic waste feed
454 controller for tank systems. *Water Science Technology* 31, 123–129.
- 455 Tsuji, Y., Morikawa, Y. 1982. LVD measurements of an air-solid two-phase flow in a horizontal
456 pipe. *Journal of Fluid Mechanics* 120, 385-409.
- 457 Yamamoto, T., Shima, T., Unuma, T., Shiraishi, M., Akiyama, T., Tabata, M. 2000. Voluntary
458 intake of diets with varying digestible energy contents and energy sources, by juvenile
459 rainbow trout *Oncorhynchus mykiss*, using self-feeders. *Fish Science* 66, 528– 534.
- 460 Yeoh, S.J., Taip, F.S., Endan, J., Talib, R.A., Siti Mazlina. M.K. 2010. Development of automatic
461 feeding machine for aquaculture industry. *Pertanika J. Sci. & Technology* 18(1), 105-110.

462

463

464

465

466

467

468

469

470 Figures and Tables

471 Fig.1. Automatic feeder and tilapia tanks

472 Fig. 2. Automatic feeder shows (a) its lateral view, (b) orifices in the bottom plate and (c) its
473 internal shaft system.

474

475 Fig.3. Weighting mechanism show a) initial position, b) after one hundred grams, c)
476 electromagnetic coil firing and d) fan configuration.

477

478 Fig.4. Algorithm to obtain the cross section occupied space percentage of the pellets.

479

480 Fig. 5. Air Reynolds number effect on fan operation time and energy consumption for laminar (A)
481 and turbulent (B) Nutripec 3508 movement.

482

483 Fig. 6 Air temperature measured at the three acrylic tube for fish food Nutripec 3508 transportation
484 (a) by one fan and (b) by two fans.

485

486 Fig. 7. Effect of using one fan (a, c) and two fans (b, d) on particles movement and flux distribution,
487 together with cross section images (e, f).

488

489 Fig.8. Food particle distribution along the pipe cross section given as percentage for Nutripec
490 4418C at each gate using (a) one and (b) two fans.

491

492

493 Table 1. Monthly feeding for each tank containing 7000 organisms with three meals daily

494 Table 2. Monthly feeding for the nursing tank with six meals daily.

495

496 Table 3. Port configuration

497

498 Table 4. Output food range and R^2 between food inlet and output obtained per gate using Nutripec
499 4418C and 3508.

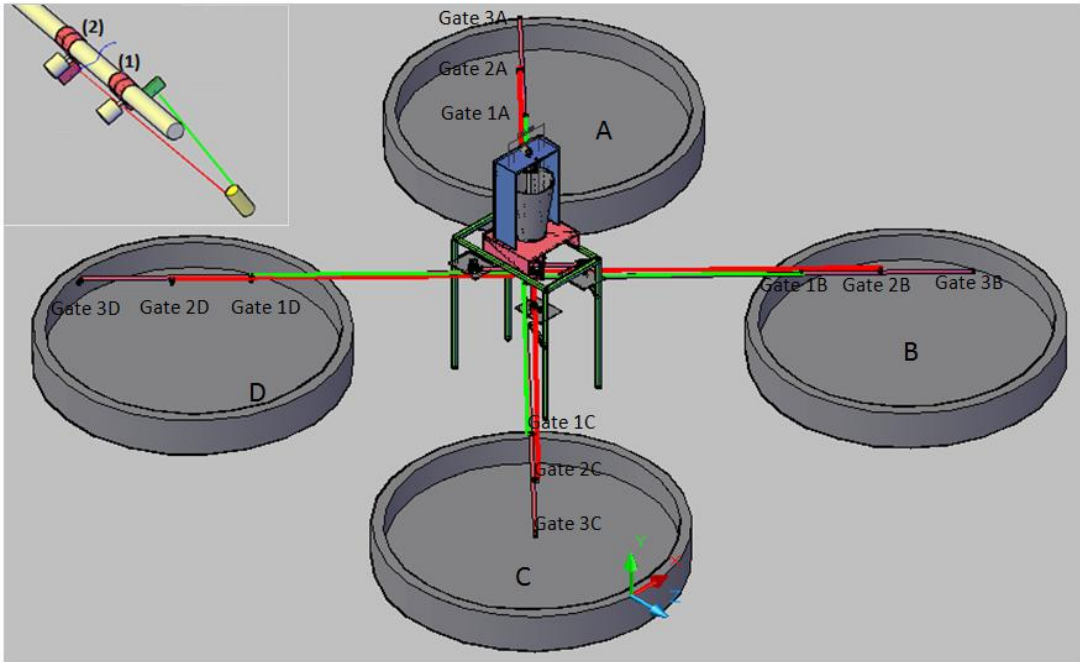
500 Table 5. Daily energy consumed per month using one or two fans.

501

502

503

504



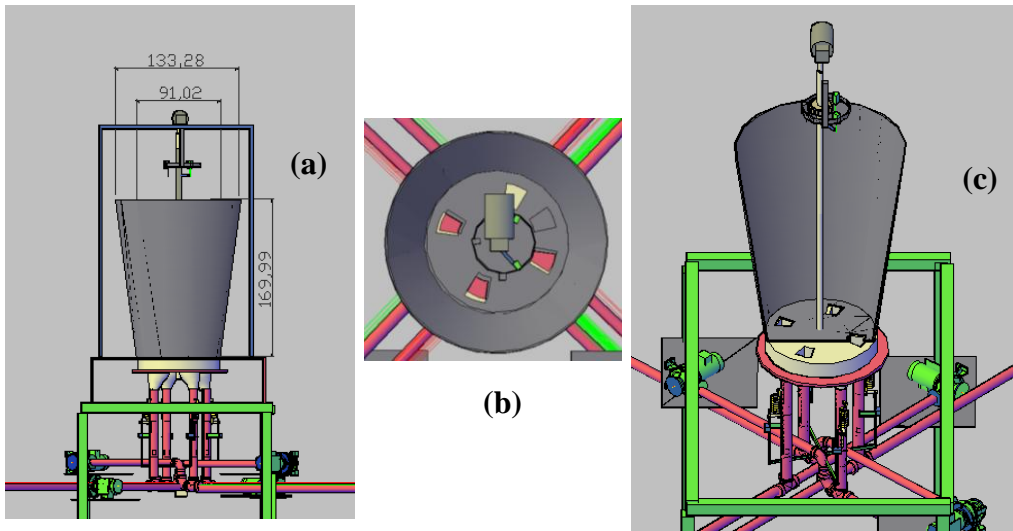
505

506 Fig.1. Automatic feeder and tilapia tanks

507

508

509



510

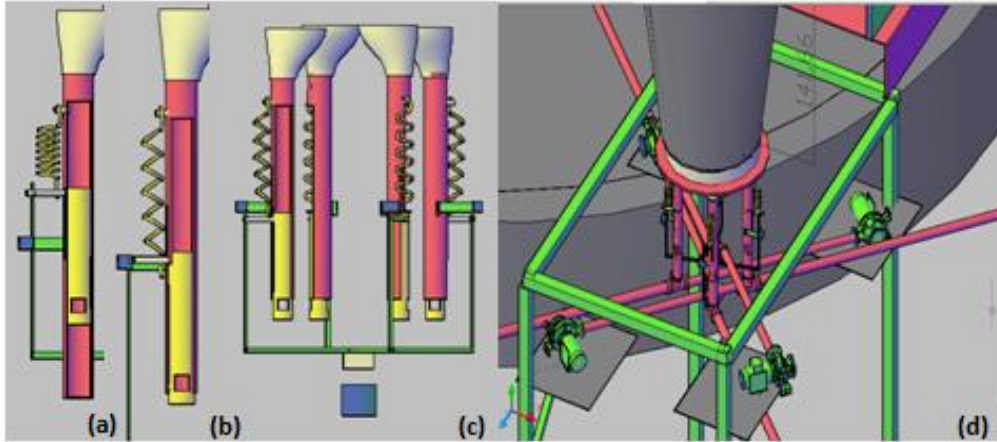
511

512 Fig. 2. Automatic feeder shows (a) its lateral view, (b) orifices in the bottom plate and (c) its
513 internal shaft system.

514

515

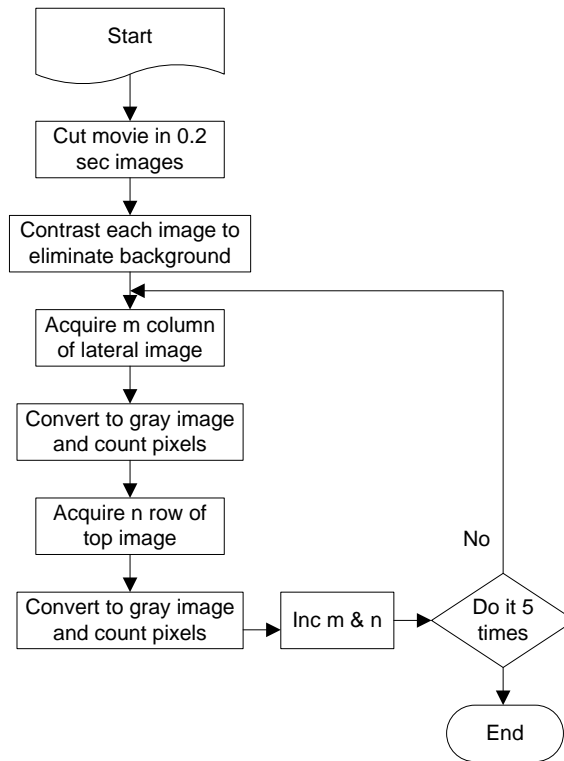
516



517

518 Fig.3. Weighting mechanism show a) initial position, b) after one hundred grams, c)

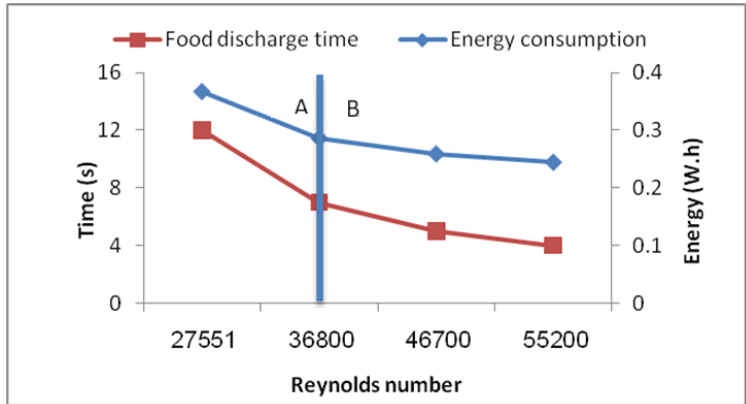
519 electromagnetic coil firing and d) fan configuration.



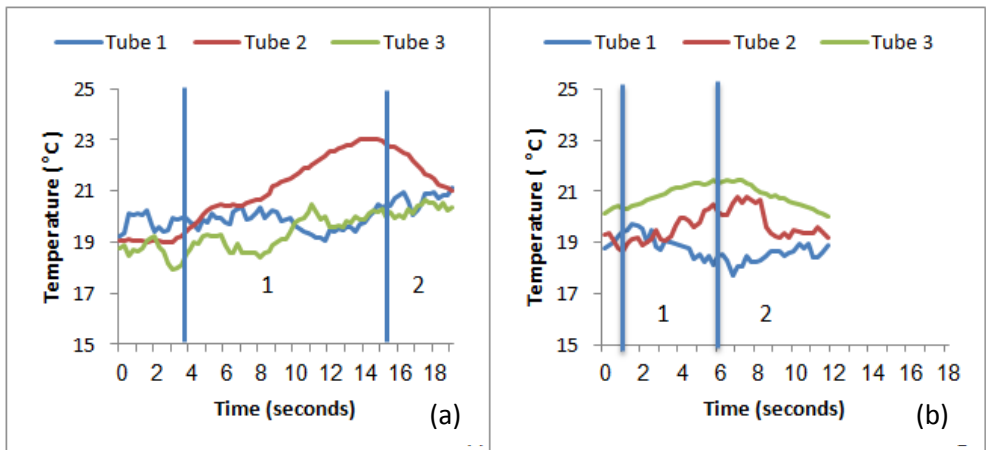
520

521 Fig.4. Algorithm to obtain the cross section occupied space percentage of the pellets

522



523
 524 Fig. 5. Air Reynolds number effect on fan operation time and energy consumption for laminar (A)
 525 and turbulent (B) Nutripec 3508 movement.



526
 527 Fig. 6 Air temperature measured at the three acrylic tube for fish food Nutripec 3508 transportation
 528 (a) by one fan and (b) by two fans.

529



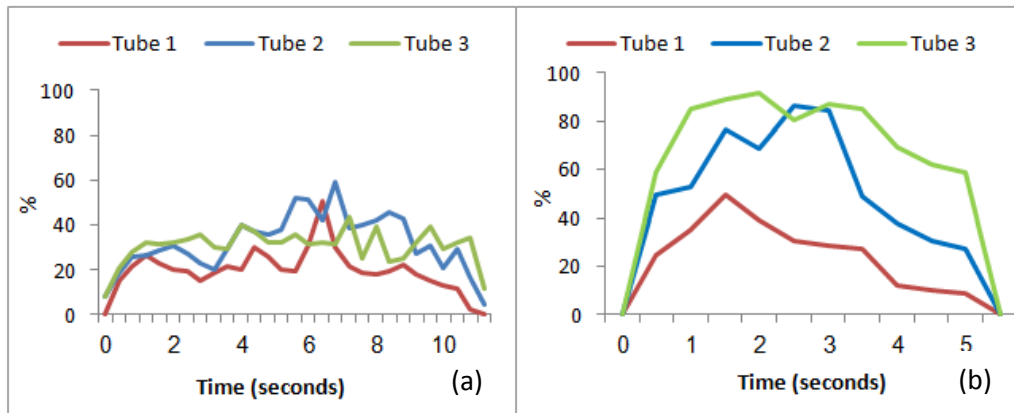
530
 531 Fig. 7. Effect of using one fan (a, c) and two fans (b, d) on particles movement and flux distribution,
 532 together with cross section images (e, f).

533

534

535

536



537

538 Fig.8. Food particle distribution along the pipe cross section given as percentage for Nutripec
 539 4418C at each gate using (a) one and (b) two fans.

540

541 Table 1. Monthly feeding for each tank containing 7000 organisms with three meals daily

Time	Daily feeding weight(g) per tank	Meal weight (g)	Feeding (g) per every doses per tank		
			1 st gate	2 nd gate	3 rd gate
Third month	18000	6000	2000	2000	2000
Fourth month	18000	6000	2000	2000	2000
Fifth month	27600	9200	2800	3200	3200

542

543

544 Table 2. Monthly feeding for the nursing tank with six meals daily

Fish numbers in the tank	Time	Daily feeding weight(g) per tank	Meal weight (g)	Daily feeding weight(g) per tank	Feeding (g) per every doses per tank		
					1er gate	2nd gate	3rd gate
21,000	First month	16800	2800	16800	900	1000	900
	Second month	25200	4200	25200	1400	1400	1400
28,000	First month	22800	3800	22800	1200	1400	1200
	Second month	33600	5600	33600	1800	2000	1800

545

546

547

548

549

550

551

552

553

554

555

556 Table 3. Port configuration

Port configuration								
Port 1	P1.0	P1.1	P1.2	P1.3	P1.4	P1.5	P1.6	P1.7
Name	NTF	M1	MS	WMS	RTF	Laser control	Laser control	
Defin	0-Nurse fan cont 1-coil turn off	Motor Feeder 0-cw 1-ccw	Micro Switch	Weight Micro Switch	0-Rear fan cont 1-coil turn off	Green laser	Red laser	
Port 2	P2.0	P2.1	P2.2	P2.3	P2.4	P2.5	P2.6	P2.7
Name	T1	T1	T2	T2	T3	T3	T4	T4
Defin	0-finish 1-1st month 21,000	0-finish 1-2nd month 21,000	0-finish 1-1st month 28,000	0- finish 1-2nd month 28,000	0-3rd month 1-4th Month 7,000	0-5th month 7,000 1- aut.	0-3rd month 1-4th Month 7,000	0-5th month 7,000 1- aut.

557

558

559

560

561 Table 4. Output food range and R² between food inlet and output obtained per gate using Nutripec
562 4418C and 3508.

	Gate 1		Gate 2		Gate 3	
	Output food (g)	R ²	Output food (g)	R ²	Output food (g)	R ²
4418C	99.545±3.241	0.9614	99.394±3.239	0.9572	99.33±3.4248	0.9456
3508	97.35±5.5275	0.9812	96.56±5.606	0.9733	96.298±5.68	0.9816

563

564

565

566

567

568

569

570 Table 5. Daily energy consumption per month using one or two fans

Month	Energy consumption W.h	
	One fan	Two fans
March	57.353	67.62
April	86.03	101.43
May	171.45	204.45
June	249.287	296.22
July	369.025	448.73
August	232.9	276.9
September	232.9	276.9
October	435.469	4214.58

571

572

573

574